# Examining Mechanisms of Sensitivity and Resistance to Phosphatidylinositol 3-kinase Inhibitors in Head and Neck Squamous Cell Carcinoma

by

Nicole Michmerhuizen

A dissertation submitted in partial fulfillment
of the requirements for the degree of
Doctor of Philosophy
(Pharmacology)
in the University of Michigan
2019

Doctoral Committee:

Assistant Professor J. Chad Brenner, Chair
Professor Thomas E. Carey
Dr. Vincent Groppi
Associate Professor Hui Jiang
Associate Professor Sunny Wong

Nicole Michmerhuizen

nmich@umich.edu

ORCID iD: 0000-0002-9960-5119

## Acknowledgements

In spite of the challenges of each phase of graduate school, I will remember fondly my time as a PhD student—and for that I am indebted to the advisors, colleagues, family and friends who have made my five years in Ann Arbor such a positive experience.

To begin, I would like to acknowledge Chad. Thank you for the discussions we've had, scientific and otherwise, beginning on the November day when I came to your office for the first time and continuing into Monday mornings over the last few months. Thank you for reading and answering my e-mails, no matter when I sent them and how frequent they were. Thank you for always being optimistic, even and especially when I was on the verge of giving up hope on an experiment or project. Thank you for never running out of ideas and for letting me contribute my ideas, too. Most notably, thank you for setting me up to succeed, but also for letting me try again on the many occasions that I failed.

Next, I would like to thank my thesis committee for their feedback on my project and support of me, as a PhD student and as a person. Dr. Carey, thank you for being my co-mentor and for your encouragement and advice throughout graduate school. Dr. Jiang, thank you for your consistent willingness to address with statistical concerns of all kinds—I deeply appreciate the time you spent writing and troubleshooting R scripts and ensuring that appropriate and important comparisons were being made in the analyses for my thesis project. Dr. Wong, thank you for your collaboration on our *in vivo* studies and your informative perspectives on all aspects of my thesis research. Dr. Groppi, thank you for sharing so much input on my work in the

context of your scientific experiences and broad professional network. Collectively, your comments at my thesis committee meetings and elsewhere have been very beneficial, providing ideas to push me in new and exciting directions.

Thank you to the Pharmacology Department for being interested in my development as a scientist and as an individual. Thank you for hosting seminars, professional development events, retreats, and symposia; these activities have provided a rich training environment for me. Thank you Dr. Isom for your leadership, and to the administrative staff for making everything run so seamlessly. Thank you also to the Department of Otolaryngology – Head and Neck Surgery for letting me be part of your translational research team.

Thank you, next, to the many members of the Brenner and Carey labs that I have been privileged to work alongside of over the past few years. Thank you for your contributions to my projects and for allowing me to participate in yours as well. Thank you Megan, Jackie, and Elizabeth for offering input and ideas and for traversing the ups and downs of graduate school with me. Thank you Brittany for teaching me the fundamentals of working with xenografts and for keeping things in the lab running as smoothly as possible. Thank you Sue for teaching me how to use the liquid handling robot and for patiently helping troubleshoot any and all malfunctioning pieces of equipment. Thank you to Aditi and Apurva for your bioinformatic analyses, to Collin for your assistance with histology, and to Jingyi for graciously running statistical tests of all kinds on my behalf. Thank you Andrew, Becky, Kevin, Molly, and Josh for providing personal perspective on what it means to bring the bench to the bedside. Thank you to the students I've had the opportunity to mentor throughout my time in the Brenner lab: Elizabeth Leonard, Danielle Pallas, Eric Desjarlais, Micah Harris, Chloe Matovina, Gabrielle Herbst, Caitlin Heenan, Vivek Nair, Daniel Kim, Amanda Bachand, and Jiayu Wang. I appreciate your

patience with me and your willingness to learn alongside of me, teaching me more than all the knowledge I could ever hope to impart to you. This thesis would look much different without your positive contributions, and I am eager to see your hard work and bright minds propel you into successful futures. To all my labmates—your scientific efforts on my behalf have been noteworthy, but I will always value your friendship most.

I would also like to thank my early scientific mentors for steering me toward my doctoral degree. Thank you to my teachers at Holland Christian, particularly those who opened my eyes to the world of science while I was a high school student. Thank you to my professors at Calvin College, who introduced me to research and helped me realize that this path was one I could and should pursue. I would especially like to thank Dr. Kumar Sinniah for giving the opportunity to work in his laboratory as an undergraduate. As a result of Dr. Sinniah's mentorship I learned how exciting research could be and gained the much of the experience and confidence necessary to enter graduate school.

Thank you to my friends, who helped make Ann Arbor my home since September 2014. The early morning runs, board games, Tuesday night dinners, camping trips, and conversations we have shared have meant so much to me. And thank you to the members of Ann Arbor Christian Reformed Church; it has been a blessing to be part of your congregation over the last five years and to contribute to the life of the church together.

Thank you to my family for their endless support and for always making the most of our times together, even if they were less frequent than we may have liked. I wouldn't have made it to this point without you. Thank you Anna for being an amazing sister but an even better friend—the years we've spent in graduate school together hold some of our most special memories. Seth, thank you for providing technical assistance of all kinds and ensuring that my

car would always be ready for a trek across the state. Luke, thanks for keeping my mind sharp with Rubik's cubes and for saving the world with me, one game of Pandemic at a time. Thank you to my parents for teaching me the value of hard work and for believing in me always. Thanks for running the errands that I should be able to do myself and for always encouraging my goals, no matter how far-reaching they are.

Finally, and most importantly, thank you to God for bringing me to and through graduate school at the University of Michigan. Thank you for leading me through each choice, over each obstacle, and into the future in a way that only You could have planned.

# Table of Contents

## List of Figures

## List of Tables

## Abstract

Head and neck squamous cell carcinoma (HNSCC) is a common and debilitating form of cancer with few effective treatment options. HNSCC tumors display a complex array of molecular changes, and sequencing studies have identified the phosphatidylinositol 3-kinase pathway (PI3K) as the most frequently mutated oncogenic and targetable pathway in this cancer type. PI3K signaling contributes to cell growth and survival and is most commonly dysregulated by alterations in the gene *PIK3CA*, which encodes the catalytic subunit and alpha isoform of PI3K. In spite of this, PI3K inhibition has shown underwhelming efficacy in HNSCC clinical trials to date. Thus, my thesis seeks to evaluate the hypothesis that resistance to PI3K targeting therapies is the result of compensatory signals, which are activated in the presence of PI3K inhibitors. To test this, I examined how aberrant PI3K signaling was influenced by co-expression of EGFR, co-alteration of *NOTCH1*, and co-dependence of multiple RTKs, including ALK and IGF-1R.

EGFR is overexpressed in most HNSCCs and its signaling is a widely studied means by which HNSCC cells evade death in the presence of PI3K inhibition. Consistent with previous studies, I demonstrated activation of the Ras-MEK-ERK pathway, downstream of EGFR, following treatment with PI3K inhibitor monotherapy in multiple *PIK3CA* amplified UM-SCC cell lines. I also showed that co-inhibition of PI3K with MEK or EGFR was synergistic in a further subset of these cell lines. I then tested several PI3K and EGFR inhibitor combinations in

additional *in vitro* models. My pharmacologic analysis revealed that combinations including irreversible EGFR inhibitors were more effective than those utilizing reversible EGFR inhibitors.

In HNSCC, *NOTCH1* acts as a tumor suppressor, and inactivating alteration in this gene is observed in nearly 20% of tumors. Emerging data suggests interplay between PI3K and NOTCH signaling in this cancer type. Our CRISPR/Cas9 partial knockout model of *PIK3CA* in UM-SCC-47, reveal the cooperativity between the PI3K and NOTCH pathways. We confirmed this relationship and its potential importance using a transgenic mouse model: following treatment with 4-nitroquinoline N-oxide, mice with overexpression of mutant *Pik3ca* and knockout of *Notch1* reach endpoint faster than animals with alterations in just one of these genes.

Finally, in order to characterize additional signaling pathways driving compensatory PI3K inhibitor resistance, we developed and optimized an unbiased, high-throughput screening approach. We used this assay to test ~1400 inhibitors as monotherapies and in combination with PI3K inhibitors HS-173 and BKM120 in ten HNSCC cell lines. Our initial screening data suggested that combinations of PI3K inhibitors and ALK/IGF-1R inhibitors were among the most effective drug pairs. Using viability, apoptosis and cell cycle assays to test single-agent and combined treatments, we validated the combinatory effects of FDA-approved agents PI3K inhibitor pictilisib and ALK inhibitor brigatinib in a subset of cell lines. These inhibitors were similarly effective in a xenograft model. Furthermore, we identified additional synergistic dual-therapies; many of these inhibited PI3K in combination with upstream receptor tyrosine kinases, while combining PI3K inhibition with inhibition of downstream pathway members did not display synergy.

Collectively, these data deepen our understanding of the combined effects of PI3K activation and aberration of an additional signaling pathway in HNSCC. In doing so, they inform

the use of targeted PI3K inhibitors, motivate further analyses of PI3K combination treatments and suggest dual-therapies that may result in improved prognoses for HNSCC patients.

# Chapter 1 : Genetic Determinants in Head and Neck Squamous Cell Carcinoma and Their Influence on Global Personalized Medicine[1]


## Abstract

While sequencing studies have provided an improved understanding of the genetic landscape of head and neck squamous cell carcinomas (HNSCC), there remains a significant lack of genetic data derived from non-Caucasian cohorts. Additionally, there is wide variation in HNSCC incidence and mortality worldwide both between and within various geographic regions. These epidemiologic differences are in part accounted for by varying exposure to environmental risk factors such as tobacco, alcohol, high risk human papilloma viruses and betel quid. However, inherent genetic factors may also play an important role in this variability. As limited sequencing data is available for many populations, the involvement of unique genetic factors in HNSCC pathogenesis from epidemiologically diverse groups is unknown. Here, we review current knowledge about the epidemiologic, environmental, and genetic variation in HNSCC cohorts globally and discuss future studies necessary to further our understanding of these differences. Long-term, a more complete understanding of the genetic drivers found in diverse HNSCC cohorts may help the development of personalized medicine protocols for patients with rare or complex genetic events.


[1] This chapter was published in *Genes and Cancer* and completed in collaboration with the following authors: Andrew Birkeland, Carol R. Bradford, and J. Chad Brenner.

## Introduction

Recent next generation sequencing (NGS) studies of head and neck squamous cell carcinomas (HNSCC) have shed light onto the underlying genetic profiles for this aggressive disease (1, 2) and enabled a move towards personalized medicine, in which therapy is guided by tumor genetics. Notably, however, the vast majority of patients sequenced thus far have been restricted to a single epidemiologic population—human papillomavirus (HPV) negative, Caucasian, and high tobacco and/or alcohol use. There has been little information on the genetic profiles in other epidemiologic cohorts; thus, the genomic events driving pathogenesis in these patients remain poorly understood. The rationale to overcome this void is clear and detailed below.

In the US and other high-income countries, personalized medicine approaches are increasingly being applied for many advanced cancers including HNSCC (2-4). Personalized medicine protocols, such as the National Cancer Institute-Molecular Analysis for Therapy Choice (NCI-MATCH) trial, seek to test molecularly targeted therapies in patients with corresponding mutations (5). However, these protocols often rely on targeted NGS approaches, which are resource intensive and unlikely to be implemented in low- or middle-income countries in the near future. Thus, the idea of targeted and personalized therapy may need to be adjusted in areas where sequencing-based medicine is not yet achievable. One way to do this is to understand the genetic events common to different epidemiologic populations and guide biomarker-based research and medicine towards the most frequent and tractable biomarkers in the region.

Genetic studies comparing ethnic and epidemiologic sub-groups have also been very informative in generally understanding oncogenes and tumor suppressors in cancer. As an

example of differential distributions of genetic events based on ethnicity, the TMPRSS2:ETS gene fusions are found in approximately 50% of prostate cancers in the US, but only 10% of prostate cancers in China. As a result, focused deep sequencing of TMPRSS2:ETS gene fusion negative Chinese prostate cancers identified high frequency and previously unrecognized genomic events in alternative pathways (6, 7). Similarly, we recently performed NGS analysis of an epidemiologically low risk HNSCC (from a young, non-smoker/drinker, HPV-negative patient) with the hypothesis that the tumor would have relatively few mutations compared to a tobacco-related HNSCC. Indeed, our analysis found a potential driver amplification of the tyrosine kinase receptor FGFR1. Extending the discovery to The Cancer Genome Atlas (TCGA) HNSCC cohort, we demonstrated that the FGF/FGFR pathway is dysregulated in >30% of HNSCCs and likely represents a previously unrecognized aberration driving disease pathogenesis (8). Consequently, carefully designed studies focusing on the genetics of under-studied epidemiologic populations can be very informative.

In this review, we will discuss current knowledge of the variations in prevalence, environmental factors, and genetic factors in HNSCC across different regions from around the world. We also include discussion of the variation in HNSCC incidence and severity evidenced in black and white American cohorts (9-12). (In this review, we will use the New England Journal of Medicine convention of black as opposed to African American (13).) It is evident from these early studies that different epidemiologic subsets of HNSCC may associate with different tumor genetics and unique outcomes, and thus may be responsive to different targeted therapies.

## HNSCC Rates Globally

Historically, different rates of HNSCC have been evidenced in different epidemiologic populations (**Figure 1-1**, **Table 1-1**). While environmental factors are thought to be a major contributor to this variability, it is unclear if the underlying acquired genetic events are similar across cohorts. Furthermore, the mutational effects of other factors associated with HNSCC globally (most notably high risk HPV, but also betel nut in Southeast Asia, nitrosamines in Asia, Epstein-Barr virus (EBV) in Africa and Asia) have not been identified. Here, we will review what is known about HNSCC incidence and mortality in representative countries from around the world.

*Developed Countries: United States, Canada, and Europe*

Two thirds of HNSCC cases occur in developed countries, where the use of tobacco and alcohol is prevalent (14). Odds ratios for developing HNSCC due to tobacco and/or alcohol use are 3-4 times higher in Europe and Latin America, where the use of both substances is more widespread, than in North America (15). In general, between 1983 and 2002, incidence rates for oral cavity cancers (for which increased risk is particularly noted in smokers) increased in Europe and decreased in the US and Canada (16). During this time period, incidence of oropharyngeal cancer also increased in eastern and northern Europe. These trends may reflect changes in the proportion of the population using tobacco and/or alcohol.

Tobacco use alone, however, does not account for variation in HNSCC throughout Europe. Based on rates reported by Simard et al., HNSCC incidence in all anatomic subsites is somewhat increased in France compared to eastern European countries and is markedly higher in France compared to other European nations (such as the UK and Italy) (16). Of the representative European countries in **Figure 1-1**, however, smoking rates are similar in France,

Italy, and the UK. Increased tobacco use, then, cannot completely explain the increased rate of oral cavity cancers between France and other European nations or the higher incidence of cancers of other sites in men from Italy as compared to the UK (16). While HNSCC in France may be driven somewhat by elevated levels of tobacco use, other factors, including biological differences, may also be crucial for tumorigenesis.

*Asia*

Increased rates of HNSCC, particularly oral squamous cell carcinoma, in southern and southeastern Asian countries are often attributed to betel quid exposure (17). Head and neck tumors are one of the most common malignancies in males in some parts of south central Asia. Parkin et al. identified the highest incidence of oral cancer in Melanesia (31.5 per 100,000 in men, 21.2 per 100,000 in women) (18). While nasopharyngeal tumors also have greatest incidence in southeastern Asia, trends in oropharynx cancer vary by specific country (18).

Fewer oral cancer cases are observed in Chinese and Middle Eastern cohorts, where betel quid is used more rarely, as compared to other Asian countries (19). High rates of laryngeal and other types of HNSCC in China may be due in part to increased tobacco use in this country. Lower incidences of HNSCC at all sites in the Middle East are possible for a variety of reasons, including, but not limited to, the lower use of betel quid, tobacco, and alcohol in this region.

*Africa*

There is relatively little data available on HNSCC in African cohorts; nevertheless, tumor epidemiologic differences may exist. A systematic review of the literature since 1990 by Faggons et al. found that 7750/8861 (87.5%) patients with HNSCC in sub-Saharan Africa presented with cancer of the oral cavity or oropharynx (20). Subsite specificity may vary significantly between countries; the nasopharynx was the most common site identified in a

review of the literature on head and neck cancer in Nigeria (21), but there were much less frequent reports of tumors of the nasopharynx, nasal cavity, or paranasal sinuses (410/8861, 4.8%), larynx (385/8861, 4.5%), or hypopharynx (66/8861, 0.8%) in sub-Saharan Africa (20). These differences may be due to difficulties in screening for cancers in these subsites. Consistent with prevalences in the sub-Saharan cohort, oral cavity and oropharyngeal tumors accounted for 27/46 (58.7%) cases in black TCGA patients while larynx cancer was also common (18/46, 39.1%) and hypopharynx tumors were infrequent (1/46, 2.2%).

Within Africa, reports of HNSCC incidence vary widely, from 0.8/100,000 in Ghana (22) to 11.1/100,000 in South Africa (18). Tumors of the pharynx and larynx are the second and seventh most common types of cancer seen at the Korle Bu teaching hospital in Ghana, representing 7.4% and 3.5% of all malignancies, respectively (23). Furthermore, age at tumor presentation in African patients was approximately 20 years younger than in American populations, which may be explained by biological, exposure and/or other differences between these populations (20). Several epidemiologic factors may contribute to differences in African HNSCC including HIV infection, which has been shown to increase the risk of HNSCC by two to three times in the US (24). Despite this fact, the role of HIV in African HNSCCs is unclear due to a lack of studies comparing HIV positive and negative patients; anecdotal evidence suggests that HIV positive patients have poorer clinical outcomes but further comparison is necessary (20).

*Variation within Geographic Regions*

Variation in HNSCC rates are also observed within different ethnic groups within specific geographic regions (25). For example, Ho et al. considered head and neck cancer incidence and mortality rates in three Taiwanese tribal groups (Fukkien, Hakkas, and Aboriginal)

(26). Between 1979 and 1997, compared to Fukkien groups, HNSCC mortality rates decreased in Hakka and increased in Aboriginal tribes. Incidence trends between 1979 and 1996 were similar, particularly in Aboriginals with high chewing prevalence for betel quid. While environmental and socioeconomic factors vary between groups, these differences alone may not explain the observed variation in incidence of and mortality from HNSCC. Interestingly, genetic differences have been noted between Fukkiens and Aboriginal in alleles responsible for metabolic activation of carcinogenic nitrosamines (27).

Additionally, significant differences in HNSCC incidence, particularly for larynx cancer, have been noted between black and white Americans. In a study by DeSantis et al., there was a higher incidence of laryngeal cancer in black (10.4/100,000) compared to white males (6.6/100,000); differences were not noted in the incidence of tumors at other HNSCC subsites (9). Goodwin et al. evidenced 15% and 77% increased incidence of oral cavity/pharynx and larynx tumors, respectively, in black as compared to white male Americans. These authors also observed increased incidence of larynx cancer (but not other sites) in black females (10). The differences in this study were observed to the greatest degree in patients under the age of 65, suggesting that hereditary or early onset factors may be involved. Furthermore, black women displayed higher rates of non-oral cavity, non-oropharyngeal HNSCCs compared to white and other ethnic female cohorts worldwide (16).

HNSCC incidence varies not only by subsite but also by severity and survival rates. Black patients are more likely to present with late stage, poor prognosis HNSCC than whites (10, 11). Regardless of cancer site, mortality for black males is on the order of two times higher when compared to that of similar white patients (10). Furthermore, independent of cancer stage, 63% of whites and only 42% of blacks survive five years of HNSCC diagnosis (9). Because

differences in survival are most significant in patients under the age of 60 (12), cancer growth may be driven by biological factors rather than exposure to environmental toxins or socioeconomic influences. Further investigation is necessary to determine these potential hereditary factors and how they may diverge between ethnic cohorts to cause more aggressive disease phenotypes.

## High Risk Human Papillomavirus is Changing HNSCC Epidemiology

Infection with high risk is a major risk factor for head and neck cancers, particularly in the oropharynx (28-35), and the recent HPV epidemic is contributing to a rapid change in the epidemiologic distribution of HNSCC globally. To place this in perspective, HPV-positive oropharyngeal squamous cell carcinoma incidence surpassed that of invasive cervical cancer in 2013 (36). While cervical lesions are often diagnosed early and treated pre-neoplastically to avoid disease progression (37, 38), most oropharyngeal cancer patients present with advanced stage III/IV disease (34). 70-80% of HPV-positive oropharynx cancers respond to intensive therapy consisting of chemoradiation or surgery in most series (39, 40). The remaining 20-30% of patients' tumors progress to lethal recurrent or metastatic disease, indicating the need to define biomarkers that will predict the subset of patients that would benefit from more aggressive therapy and minimize morbidity in less difficult cases.

In the face of the HPV epidemic, high risk viral infection has been associated with oropharyngeal cancers in studies from across the world. A systematic review by Stein et al. compared the prevalence of HPV-positive oropharynx cancer in 23 countries worldwide (41). Taiwan, Canada, and the Czech Republic had the highest prevalence of HPV-positive oropharyngeal cancer, with much lower HPV burdens in the Netherlands, Brazil, and Spain.

Overall, the results of this analysis suggest that HPV-positive tumors may be more common in developed countries. In another systematic review, Mehanna et al. identified HPV-positive cancers of the oropharynx in 59.9% of 2550 North American patients, but only 39.7% of 2278 European patients and 32.5% of 568 patients from other regions (42). An additional cohort of 31/67 (46.2%) Australian patients also displayed high prevalence of HPV-positive oropharyngeal cancer (43). Chinese patients displayed lower infection rates with 43/207 (20.8%) HPV-positive oropharyngeal tumors and 36/124 (29.4%) HPV-positive tonsil lesions (44). The prevalence of oral and oropharyngeal HPV was also lower across Africa as compared to many developed countries. 5/125 (4%) South African men were identified with HPV-positive oropharyngeal cancer, and only two of these cases were high risk HPV (45). Similarly, 0/22 (0%) oropharyngeal cancer and 2/29 (6.9%) oral tongue cancer patients in Mozambique tested positive for HPV infection (46). In Senegal, only 4/117 (3.4%) HNSCC patients had HPV-related tumors and none of these were located in the oropharynx (47).

Of note, the use of numerous testing methodologies to access a diverse array of HPV variants may introduce inconsistency in HPV detection outcomes. HPV16 accounts for over 90% of HPV-positive HNSCC cases (48) and can be detected by accessing HPV DNA, HPV RNA, viral oncoprotein, cellular protein and/or HPV-specific serum antibody levels (49). The most sensitive and reliable method of detecting HPV-related HNSCC has been strong staining for p16 by immunohistochemistry (IHC), although reverse transcriptase (RT)-PCR, PCR-mass spectrometry and in situ hybridization (ISH)-based protocols are also used in some cases (50, 51). Thus, consideration of further studies with controlled testing of the global prevalence of HPV-positive oropharyngeal cancer will be important, particularly in Africa given the

discordance between high cervical and low oropharyngeal HPV-positive cancer rates in this region.

While rates of HPV infection worldwide are not fully realized, evidence does indicate that prevalence may be rising globally and may drive increased incidence of HNSCC. Considering the large proportion of the population that is infected with HPV (52), malignant transformation is comparatively rare as HPV infections are usually cleared quickly (53). In rare cases, however, genomic instability and unrestricted proliferation caused by viral oncogene activity lead to tumorigenesis. Cervical infection with HPV, if not cleared, can lead to precancers in the genital area as well as the head and neck region through sexual contact. Thus, as a high-level surrogate for oropharyngeal cancer prevalence, we can analyze the reports of HPV prevalence in women, noting a wide range of cervical infection rates in cohorts worldwide (54-56). Based on a meta-analysis of women with normal cytology, Bruni et al. estimated that the regionally-adjusted prevalence of high risk HPV infection, as detected by polymerase chain reaction (PCR) or Hybrid Capture 2 (a DNA hybridization assay for detecting HPV strains with a fluorescent readout), in females is 47,271/851,901 (5.0%) worldwide. The prevalence of both low and high-risk HPV strains is 73,019/1,016,719 (11.7%), which varies between rates as high as 75/225 (35.4%) in the Caribbean to those as low as 31/1,435 (1.7%) in Western Asia (56). Of all viral strains, HPV16 was the most commonly detected in this study but tended to correlate inversely with overall HPV prevalence. In the more limited analysis of data from male patients, an important population given the increased prevalence of HNSCC in this group, a similar overall prevalence (182/1139, 16%) and even more significant amount of variation was observed, particularly when separating low- and high-risk groups (57, 58). We compared adjusted HPV infection prevalence with oropharyngeal cancer incidence in cohorts worldwide to

consider possible associations between these two variables (**Figure 1-2**). In a subset of countries, both increased HPV prevalence and oropharyngeal cancer incidence were observed. (For example, women in Eastern Europe have high prevalence of cervical HPV infection (904/4053, 21.4%), and the oropharyngeal cancer incidence in Slovakian men is also elevated (15.4/100,000).) Alternatively, in other regions, decreased HPV prevalence and increased oropharyngeal cancer incidence were noted. (In India, only 1816/23,061 (7.1%) women tested positive for HPV infection, but 9.1/100,000 men develop oropharyngeal tumors (56, 59).) These findings may be explained by regional differences in HPV infection rates; however, developing a more complete understanding of this relationship is additional motivation for controlled HPV testing in global cohorts.

Sexual activity, particularly oral sex with multiple partners, increases HPV-positive cancer risk at all sites. As is the case with other risk factors, sexual practices are widely divergent across populations globally. For instance, 78% of American, but only 9% of Indian men reported ever having oral sex, and individuals born after 1960 have more commonly engaged in this activity (60). Men are also more likely to have multiple partners than women (61-63) and the prevalence of HPV infection was much higher in high-risk populations of males as compared to females with similar numbers of sexual partners (64). Given these differences, it stands to reason that HPV-positive HNSCC rates will vary widely between cohorts globally.

Similarly, variation between HPV-positive head and neck cancer rates has already been observed in whites and blacks in the US and may explain racial disparity in survival rates at least partially. Settle et al. found that differences in the median overall survival (OS) of an American cohort were driven primarily by differences in tumors of the oropharynx (white 69.4 months, black 25.2 months, $p = 0.0006$) and not by tumors at other sites (white 17.1 months, black 17.5

months, difference n.s.) (65). In a separate analysis of OS for black and white Americans with HPV-positive or HPV-negative HNSCC, Jiron et al. determined that the hazard ratio was greatest for black patients with tumors of the oropharynx but that adjustment for HPV status drastically reduced this ratio to a value close to unity (66). These results suggest that the poorer prognosis of black patients in the US may be due to the reduced rate of HPV-positive oropharyngeal cancers in this group. Nevertheless, further studies are necessary to more fully evaluate this hypothesis.

## Variation in Genetic Landscape between Epidemiologic Sub-Groups

Despite the majority of HNSCCs occurring in non-American populations (incidence rate of 60,000 annually in US vs 490,000 annually in rest of world), NGS studies have been limited to cohorts of primarily European ancestry and not other ethnic groups or epidemiologic populations. TCGA and the International Cancer Genome Consortium (ICGC) reported sequencing for cohorts of HNSCC patients in the United States and India, respectively (1, 67). In the TCGA cohort, the majority of these patients were white (242/279, 86.7%), with only 25/279 (9.0%) black. Different mutational profiles were evidenced between black and white HPV-negative patients (**Figure 1-3**). For instance, black patients have significantly higher rates of BIRC2/3 amplification compared to white HNSCC patients in this study (25.0% vs 4.3%, $p < 0.001$). Although they do not reach statistical significance, blacks also trend toward decreased *EGFR* (4.2% vs 13.5%, $p = 0.19$) and increased *FGFR1* (16.7% vs 9.1%, $p = 0.24$) amplification. Other genetic aberrations were similar between ethnic groups (68, 69).

ICGC data also noted distinct differences in genomic aberrations in Indian patients with oral cancer of the gingivo-buccal region (67). When compared to white American HNSCC TCGA patients, Indian patients display significantly lower rates of *EGFR* ($p = 0.0365$) and *MYC*

(p = 0.0365) amplification, *PIK3CA* activation by mutation or amplification (p = 0.0027) and *CDKN2A* deletion (p = 0.0045) (**Figure 1-3**). As identified in previous studies of HNSCC, the authors observed frequent copy number alterations or mutations in *TP53*, *FAT1*, *CASP8*, *HRAS* and *NOTCH1* in the Indian HNSCC patients (70). Interestingly, the ICGC study also identified five genes (*USP9X*, *MLL4*, *ARID2*, *UNC13C* and *TRPM3*) and three pathways (Wnt signaling, dorso-ventral axis formation and axon guidance) previously not associated with HNSCC in TCGA. These events may be specific to this epidemiologic sub-group. For example, mutations in TRPM3 were identified in 5/50 (10%) Indian ICGC patients, but only 4/208 (1.9%) white and 1/25 (4%) black HPV-negative TCGA patients. *USP9X* was more frequently mutated or deleted in Indian (7/37, 18.9%) than in white (23/208, 11.1%) or black (1/25, 4%) HPV-negative patients (68, 69) although this difference did not reach significance using the Chi-square test with Yate's correction (p = 0.2837). Furthermore, the frequency of copy number alteration or mutation of *FAT1*, *FAT3*, and *FAT4* were increased in the Indian ICGC cohort (67).

While there have been few other in-depth genomic studies of large ethnic or epidemiologic cohorts, unique mutational profiles are likely to exist in other global populations. Vettore et al. recently performed targeted deep sequencing on a cohort of 60 patients treated in Singapore and found that mutation frequencies for *TP53*, *CDKN2A*, and *NOTCH1* were infrequent compared to other studies. While *TP53* and *CDKN2A* represent the first and third most commonly mutated genes in the overall TCGA HNSCC cohort, mutations in these genes, respectively, were present in only 23/60 (38.3%) and 3/60 (5%) of Asian patients. Furthermore, *NOTCH1* mutation was identified in significantly fewer Asian patients (3/60, 5%) than white HPV-negative TCGA patients (41/208, 14.6%) (p = 0.012). Conversely, *DST*, *RNF213*, *COL6A6* and *ZFHSX4* mutations were observed much more commonly in Asian patients. Similar studies

that could reveal additional trends in other epidemiologic populations, therefore, are clearly warranted.

The mutational loads were similar between white and black cohorts in TCGA (**Figure 1-4**) and Indian patients in ICGC data (mean total number of mutations: 112.79 +/- 19.25) (67). Copy number alterations, however, were increased in black as compared to white patients (0.3342 vs 0.2560, p = 0.0443) (**Figure 1-5**). When subsites were considered individually, trends between ethnic cohorts were apparent for copy number alterations in oropharyngeal tumors (however only 2 black patients compared to 8 white) and were also observed for tumors of the oral cavity (0.2884 vs 0.2174, p = 0.17). These comparisons are limited by the small number of black patients included in this analysis and may be due to sample bias.

## Worldwide rates of established HNSCC molecular events

Currently, EGFR, PIK3CA, NOTCH pathway and *TP53* genes are among the most frequently mutated in HNSCC. As these genes have long been associated with HNSCC pathogenesis, several smaller cohort studies have been published assessing the rates of genomic events for these genes in various ethnic and epidemiologic populations. Understanding which populations have unique genetic landscapes may aid in selecting the most informative populations for immediate NGS analysis. Unfortunately, a relatively small number of studies have sequenced HPV-positive HNSCCs in international studies. Thus, we will separately address worldwide genomic event frequencies in HPV-negative and HPV-positive disease when possible.

*Epidermal Growth Factor Receptor (EGFR)*

It has been recognized for nearly 30 years that EGFR is overexpressed in the majority of HNSCC tumors (71). The effects of EGFR activation in squamous cells may be pleiotropic: not only can changes in receptor signaling affect the Ras-MAPK, PI3K-AKT-PTEN, and/or phospholipase C pathways, but they may also activate other receptors by ligand-independent dimerization. Consistent with the prevalence of EGFR protein overexpression and demonstrating its importance, EGFR-targeted antibody, cetuximab, is currently the only FDA-approved targeted therapy for HNSCC and has been shown to improve overall survival of patients (72, 73). A meta-analysis of 37 studies by Keren et al. examined EGFR levels in surgically resected primary tumor samples and identified 1948/3346 (57.8%) cases with high protein expression. The majority of patients were from Europe, with some cohorts also from the US and east Asia; overexpression was frequently and consistently noted in Austrian, Spanish, and Dutch cohorts, while it was infrequent in Swedish, French, and Italian populations (74). High levels of EGFR expression may also be more common in Sudan, where 126/150 (84%) head and neck cancer cases displayed overexpression by IHC analysis (75).

Despite frequent overexpression of EGFR, rates of genetic aberration (by amplification or mutation) are relatively low (14.3% in TCGA) (1) and a small number of studies have assessed EGFR genomic aberrations in individual populations. For example, 3/41 (7.3%) Korean patients, most of whom had larynx cancer, displayed a mutation in the kinase domain of EGFR (76), but similar mutations were much less commonly observed in Caucasian or Spanish patients (77-79). One TCGA patient displayed truncating EGFRvIII mutation, which was previously detected by Sok et al. in 14/33 (42.4%) HNSCCs along with wild type EGFR and was correlated with resistance to targeted EGFR therapy (80). While mutations of EGFR in particular may be

somewhat infrequent, this pathway as a whole is often aberrantly expressed. For example, 31/60 (52%) Indian patients with buccal-gingival cancer displayed mutations in the EGFR pathway, and 46/208 (22.1%) of the TCGA cohort displayed amplification of EGFR family members (*EGFR*, *ERBB2-4*, *EGF*, *NRG1-4*, *EREG*, *AREG*, *TFGA*, *BTC*, and *HBEGF*) (1, 81). An improved understanding of the genetic and/or biochemical mechanisms driving EGFR overexpression in HNSCC will be necessary before extending the assessment of EGFR mechanisms globally. However, as global cohorts are being prioritized for genetic studies, populations such as Swedish and Italian, which have been associated with lower overall rates of EGFR overexpression, may show the largest variation in genomic landscape to those HNSCCs already sequenced.

*Catalytic Subunit of Phosphotidylinositol 3-kinase (*PIK3CA*)*

The PI3K-AKT-PTEN pathway has been identified as the most frequently mutated or amplified oncogenic pathway in HNSCCs in the TCGA cohort (1, 82). Mutations and/or amplifications in *PIK3CA*, the gene encoding the catalytic subunit of phosphotidylinositol 3-kinase (PI3K), are the most common alterations in this pathway and are observed in 36.9% of the TCGA HNSCC cohort (68, 69). These aberrations lead to increased cell growth and viability, may drive tumor progression, and are more commonly observed in advanced stage disease as reviewed elsewhere (83, 84). *PIK3CA* mutation or amplification is also more frequent in HPV-positive tumors, including in the TCGA cohort (56% HPV-positive vs 34% HPV-negative) (1, 82, 85). Loss of function of *PTEN* also results in failure to "turn off" PI3K signaling and is observed in an additional 10% of HNSCC patients (86).

Rates of *PIK3CA* aberration have been assessed in various global cohorts (87-92) and are shown in **Figure 1-1**. Low frequencies of gene amplification were observed in 3/33 (9%)

patients in a German HNSCC cohort as well as 3/115 (2.3%) and 6/50 (12%) individuals in two independent Japanese groups (88, 90, 93). Alternatively, Redon et al. noted 6/9 (66.6%) of French HNSCC patients have increased copy number (94). PIK3CA mutation is generally less common than gene amplification. Somatic mutations, commonly including "hotspot" amino acid changes to the kinase (H1047R) or helical (E545K, E542K) domains, occur in 20.8% of the TCGA cohort, which is consistent with rates of ~10-20% in other studies (87-89). *PIK3CA* mutation rates greater than 10% were noted in cohorts from Thailand (6/58), India (2/19), and Israel (4/37) (88, 89, 92). Surprisingly, a complete lack of *PIK3CA* mutations in the helical or kinase domains (exons 9 and 20) were observed in populations of 18 Vietnamese, 33 German, and 86 Greek patients as detected by PCR (89-91). This may be due to increased activation of *HRAS*, which signals upstream of *PIK3CA*, in these epidemiologic sub-groups (95). Due to the variation in *PIK3CA* mutation rates between 1/35 (2.9%) and 5/24 (20.8%) in US patient populations (87, 96) and the relatively small number of HNSCC tumor samples that have been sequenced worldwide, additional cohort studies are warranted to further consider potential associations between rates of genetic aberration and patient ethnicity or epidemiologic-risk.

*NOTCH pathway genes*

In 2011, sequencing-based analysis of HNSCC tumors led to the discovery of inactivating NOTCH pathway alterations as the third most common molecular event in the disease (1, 68, 70, 96). In fact, mutations in one gene from this pathway, NOTCH1, were observed in ~15% of samples in addition to less frequent mutations of the NOTCH2 (~5%) and NOTCH3 (~4%) genes, with rare copy number alterations reported. Soon after these reports were published, and in contrast to the prevalent loss-of-function mutations, copy number increases and overexpression of the NOTCH ligands JAG1 and JAG2 and the receptor NOTCH3 were found in

a small subset of predominantly white HNSCCs (97). Importantly, the functional role of both the activating and inactivating alterations have yet to be fully characterized. These alterations have been reviewed elsewhere (98), but they are suggested to regulate squamous cell differentiation in multiple model systems. Consistent with this notion, many HNSCCs are characterized by recurrent mutations in the *TP63*, *IRF6* or *MED1* genes, which have also been suggested to regulate squamous differentiation, supporting a functional importance of this pathway for HNSCC pathogenesis (70).

While the discovery of NOTCH pathway alterations is still relatively new, several studies have assessed the frequencies of molecular events globally. These have demonstrated that 22/51 (43.1%) Chinese oral cavity HNSCC tumors harbored *NOTCH1* alterations, with at least half predicted to activate function (99), while only 8/84 (9.5%) Japanese oral cavity HNSCCs had mutations that were all predicted to inactivate *NOTCH1* activity (100). In another cohort of Asian patients with tongue cancer, *NOTCH1* mutations occurred infrequently but alterations in other NOTCH pathway genes (i.e. *AR*, *ARNT*, *EP300*, *CREBBP*, *JAK2*, *JAK3*, *NCOA1*, *NOTCH2*, *NOTCH3*, and *PARP1*) were common (19/60, 32%) and correlated with disease survival (81). While much larger cohort studies are needed, the preliminary published data indicates that activating NOTCH pathway alterations may be much more common in Chinese HNSCCs than in patients represented in the Indian ICGC and TCGA HNSCC projects.

*The Tumor Suppressor Protein,* TP53

The p53 protein functions as a master regulator of the interplay between the cell cycle and apoptosis and is the most frequently deregulated tumor suppressor in HNSCC. In fact, the function and role of p53 in HNSCC have been reviewed extensively due to the high frequency of genetic or biochemical inactivation in the disease (101, 102). In HPV-negative HNSCC, *TP53* is

commonly inactivated by mutation or deletion (103), while the HPV oncoproteins inactivate p53 by biochemical mechanisms in HPV-positive HNSCC. Thus, because *TP53* is usually wild type in HPV-positive HNSCCs, we will restrict the review of genetic events for this gene to oral cavity and larynx HNSCCs, which are historically largely HPV-negative. At these organ sites, TP53 mutation often correlates with poorer survival (104) and has been associated with exposure to tobacco or betel quid (103). Consequently, we may expect to find different rates of *TP53* disruption in different epidemiologic subgroups if the gene is related to these risk factors, or may observe high rates across all populations if inactivation is generally required for squamous pathogenesis.

In the TCGA data set, TP53 mutation was observed in 129/160 (80.6%) HPV-negative tumors of the oral cavity (1, 68, 69). In tongue cancer samples from an Asian cohort, TP53 was the most frequently mutated gene (as in TCGA), but was mutated in only 23/60 (38.3%) cases. Relatively low rates of TP53 mutation are consistent across multiple studies of oral cavity cancer in Asian patients (81, 105, 106). Cohorts of Icelandic and American never-smokers also displayed lower oral cancer TP53 mutation rates (107, 108), while rates in Brazil and India were more consistent with those in the HPV-negative TCGA cohort (67, 109, 110). Global mutation rates for oral cavity and larynx HNSCC are summarized in **Table 1-2** and **Table 1-3**, respectively. In the studies published thus far, *TP53* mutation rates for laryngeal cancers are generally moderately higher than those in oral cavity cancer and also vary by geographic region. For example, in the TCGA cohort, 64/72 (88.9%) HPV-negative patients with laryngeal cancer display *TP53* mutation (1, 68, 69). Most other countries also have mutation rates of 50% or higher with the exception of China, South Africa, and Argentina (111-113). Overall, however,

these metadata are indicative of a relationship between inactivation and carcinogen exposure as opposed to specific pathogenic requirements.

Consistent with this observation, several groups have attempted to model the predictive value of individual *TP53* mutations in different epidemiologic populations. For example, Ren et al. performed a meta-analysis to assess HNSCC risk and Arg72Pro *TP53* mutation across various tumor sites in Asian and Caucasian cohorts. They found that this mutation was associated with increased risk of nasopharyngeal cancer, but not oral cancer, for homozygous, heterozygous and dominant model mutation comparisons in Caucasian cohorts but only homozygous mutations in Asian patients (114). Given the frequency and complexity of *TP53* aberration, further studies on the distinct role of this gene in specific epidemiological populations will be critical to developing an improved understanding of HNSCC pathogenesis.

## Future Directions

Ultimately, additional sequencing of various epidemiologic sub-groups will need to be performed to understand the distribution of molecular events on a global scale. This work should also assess the correlations of disruptive genomic events with worldwide incidence, mortality, and particularly survival differences, which have not previously been taken into account. There is also a significant void of sequencing data in African populations in particular. Sequencing of these groups may identify both common and unique drivers for HNSCC between various cohorts. Studies of African populations are extremely important due to the high rate of HIV/AIDS patients in the region. We still have very limited knowledge of the pathogenesis or molecular distribution of HNSCCs in immunocompromised patients such as those who have HIV/AIDS or have undergone organ transplant. Additionally, analysis of cohorts worldwide will

be necessary to determine the extent to which other environmental and genetic factors affect the incidence and severity of HNSCC both between and within epidemiologic sub-groups.

HPV-positive oropharyngeal squamous cell carcinoma now displays greater incidence than invasive cervical cancer (36). While HPV vaccines have the potential to reduce the overall number of tumors caused by this virus, many populations around the world are incompletely vaccinated and it is unknown how many people encountered HPV before having the opportunity to be vaccinated. Thus, given the increasing rates of HPV in the US and abroad as well as wide variation between cohorts, there is a clear and urgent need for both epidemiologic data and sequencing analysis on HPV-positive tumors, especially those that are associated with additional risk factors. Fortunately, patients in the US with HPV-positive tumors are generally younger and have improved prognosis since HPV-positive tumors are more sensitive to chemoradiation (115). Despite this fact, some HPV-positive tumors are highly aggressive and rapidly lethal, and there are no established biomarkers that can identify patients that would respond to more aggressive therapy. Future studies are needed to more fully elucidate the specific differences between HPV-positive patients from different geographic regions, cultural backgrounds, and genders using careful genetic analysis in the context of understanding the lethality of each tumor. These efforts are important as they may enable the development of biomarkers for the most aggressive forms of this epidemic subset of HNSCCs.

The heterogeneity of HNSCC has been clearly observed in previous studies and is dependent on tumor genetics and exposure to various risk factors including the use of tobacco, alcohol, and betel quid, HPV infection, and others. This variation is noted between not only between patients but also within individual tumors and between local, nodal, and distant tumor sites. Understanding the broad and underappreciated heterogeneity of HNSCC using comparative

genetics will be valuable in establishing personalized medicine protocols first for clinical trials and then for individualized treatment plans. At this point, however, studies have not assessed the genetic heterogeneity found in individual tumors on a large scale. It is possible that different causal or associated factors driving HNSCC pathogenesis will lead to different levels of genetic heterogeneity within a tumor. As recurrence from targeted therapy can arise from individual cells with pre-existing resistant mutations, understanding the degree of heterogeneity in tumors from different epidemiologic subgroups may have a substantial impact on the choice of targeted therapy in each population.

Consequently, further sequencing analysis of patients will likely allow for more effective use of targeted therapies in countries where NGS analysis is readily available. Unfortunately, while precision-guided targeted antibodies and small molecule inhibitors display great promise in the future of cancer treatment, their use is currently limited by several disadvantages, including high cost and complex infusion regimens. Thus, while genetic studies are perhaps most feasible in high income countries, understanding the contribution of epidemiological factors to HNSCC development and progression through various genetic pathways may enable treatments to be more effectively selected for patients. For example, understanding the high frequency genetic events in each region may restrict the number of biomarker tests needed to identify tumor drivers, and may enable clinicians to predict whether more or less aggressive therapy is needed based on those markers.

In the future, the hope is that access to healthcare resources and infrastructure will be enhanced globally so that patients have access to the best possible personalized therapy. In the meantime, we must think critically about the cost-benefit of biomarker-guided medicine in different epidemiologic subgroups of HNSCC in order to maximize the return on the high cost of

NGS. Analyzing populations with unique epidemiologic and/or biomarker characteristics may be the first step to both enhancing our understanding globally and designing interventional protocols adapted to regional differences in health care resources and tumor genetics. We are in an exciting era of sequencing-guided personalized medicine in the US, and our challenge moving forward is to take the discoveries and lessons from these early personalized medicine trials, incorporate global sequencing information, and improve HNSCC therapy worldwide.

**Conflict of Interest:** Dr. Brenner has previously collaborated with Novartis on the development of WNT974 for NOTCH-deficient HNSCC. The other authors have no conflicts of interest to disclose.

**Acknowledgements**

We acknowledge Elizabeth Leonard for reviewing this manuscript.

## Figures

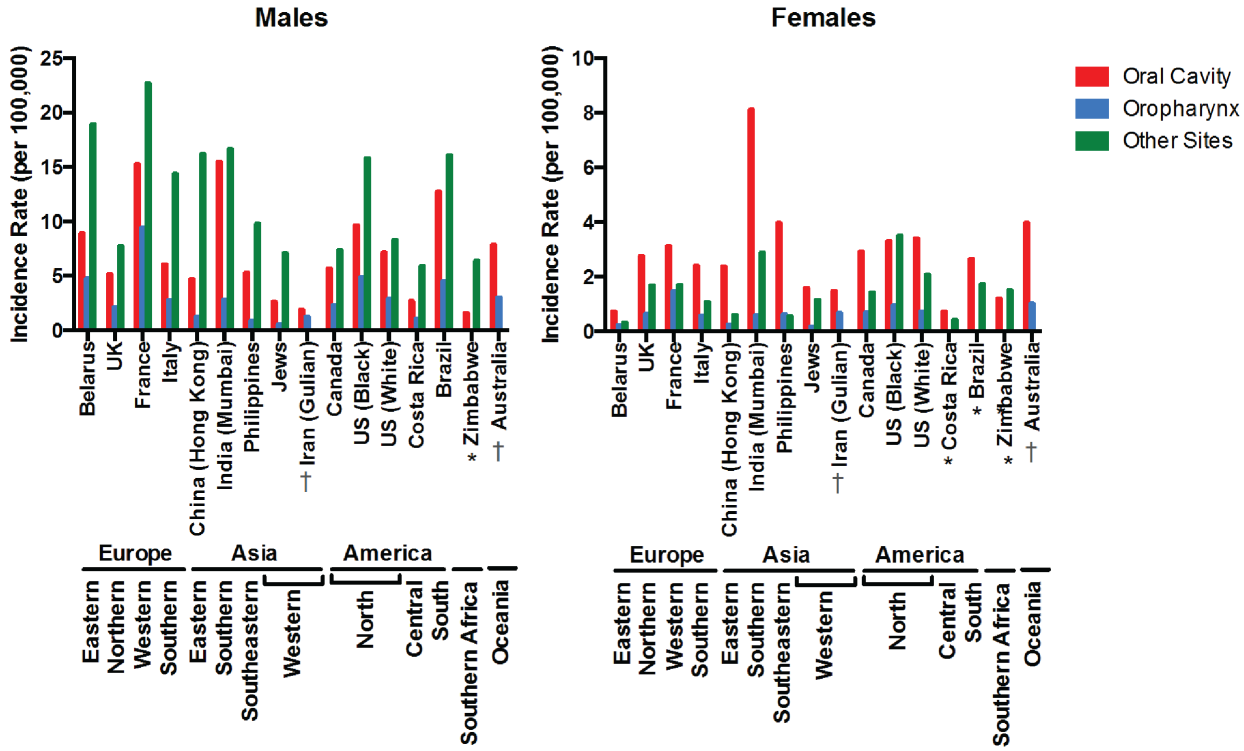


**Figure 1-1. Age-standardized head and neck cancer incidence rates by sex and subsite for various global cohorts**

Incidence rates per 100,000 for males and females in various global cohorts with cancers of the oral cavity, oropharynx, or other head and neck sites. Raw incidences, references, and more detailed descriptions of each study can be found in **Table 1-1**.
* indicates that incidence for oropharyngeal cancer was not reported. † indicates that incidence for cancer of other sites was not reported.

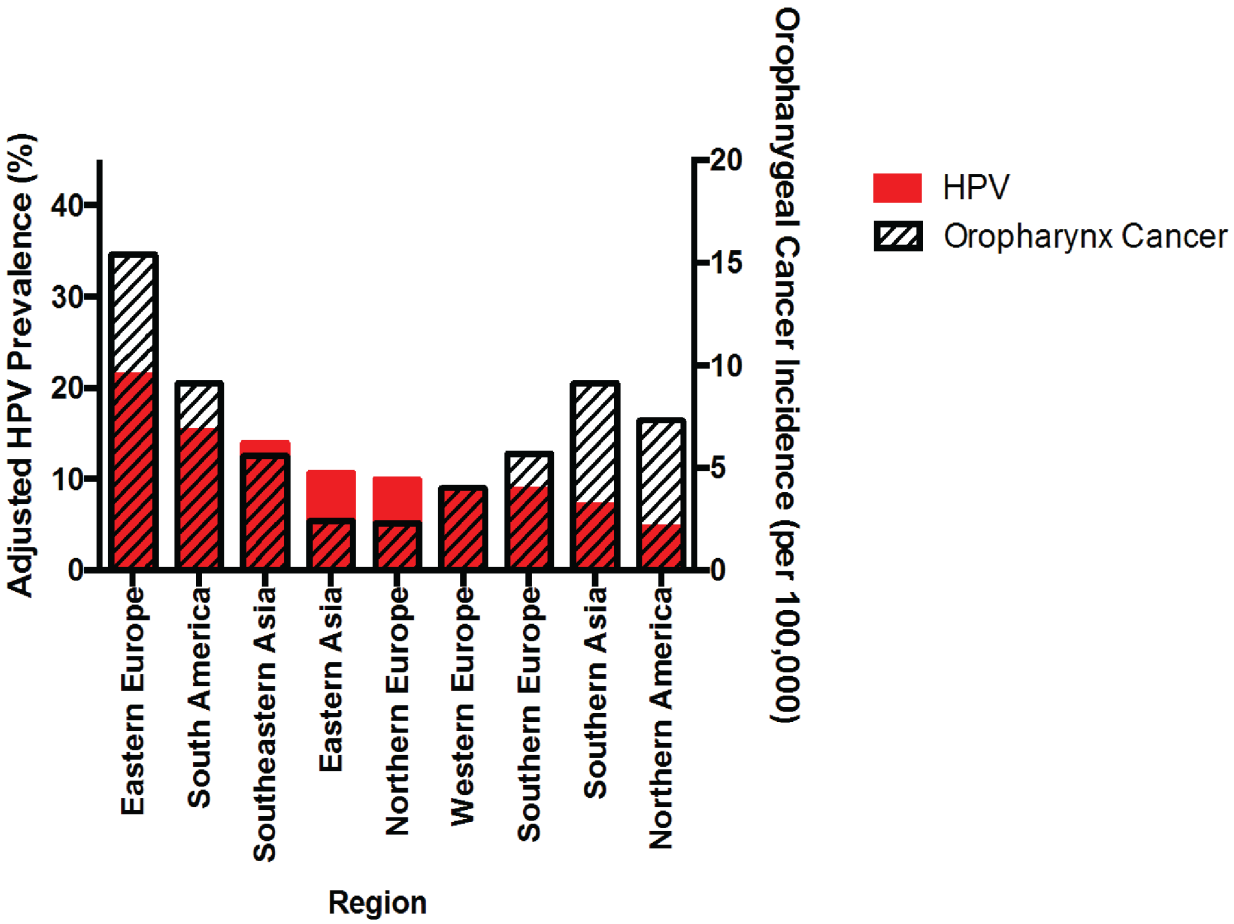


**Figure 1-2. Adjusted cervical HPV infection prevalence among women with normal cytology and oropharyngeal cancer incidence among men by geographic region (55, 58)**

HPV prevalence includes infection with both low and high risk viral strains and was adjusted based on patient age, year of study, sample type, HPV screening method, and viral strain(s). Oropharyngeal cancer incidence given for a representative country within each region: Slovakia (Eastern Europe), Brazil (South America), Thailand (Southeastern Asia), Japan (Eastern Asia), Denmark (Northern Europe), Netherlands (Western Europe), Spain (Southern Europe), India (Southern Asia), and United States (North America).

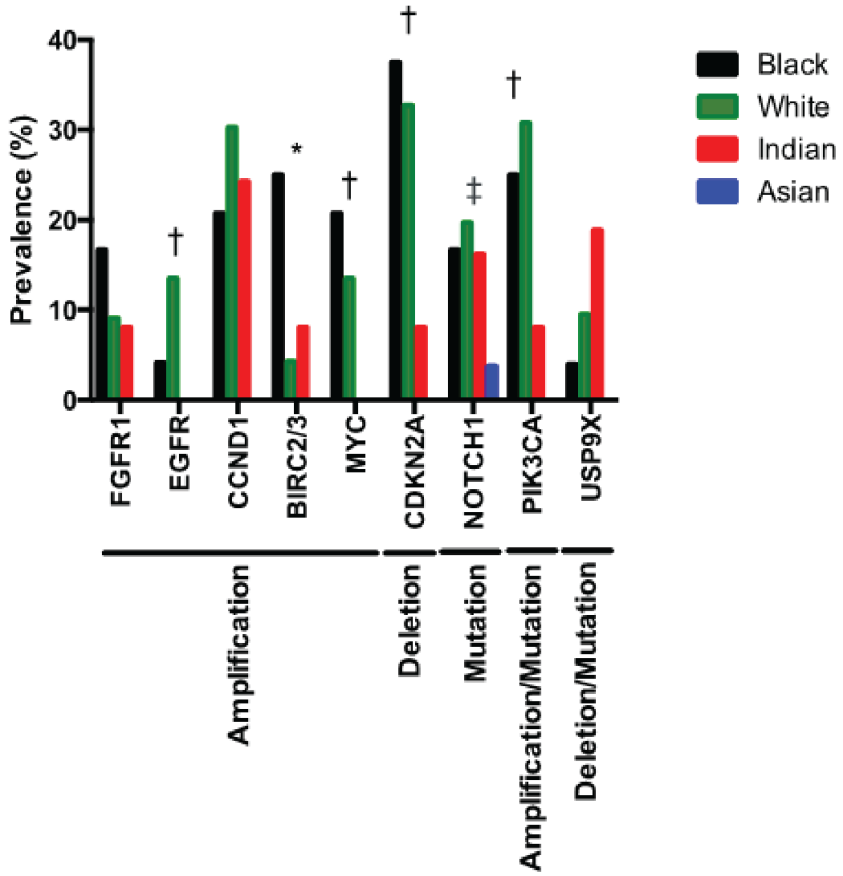


**Figure 1-3. Prevalence of copy number alterations and/or mutation for various genes in HPV-negative black and white patients in the TCGA HNSCC cohort, Indian patients in the ICGC HNSCC cohort, and Asian patients in the Vettore cohort (1, 66, 80)**

Prevalence of key genetic aberrations in 24 black and 208 white HPV-negative patients (TCGA HNSCC cohort), 37 HPV-negative Indian patients (ICGC HNSCC cohort), and 60 Asian patients of unidentified HPV status (Vettore cohort). NOTCH1 mutation prevalence only is reported for the Asian cohort.
* indicates significant differences between white and black TCGA cohorts. † indicates significant differences between white TCGA and Indian ICGC cohorts. ‡ indicates significant differences between white TCGA and Asian cohorts.

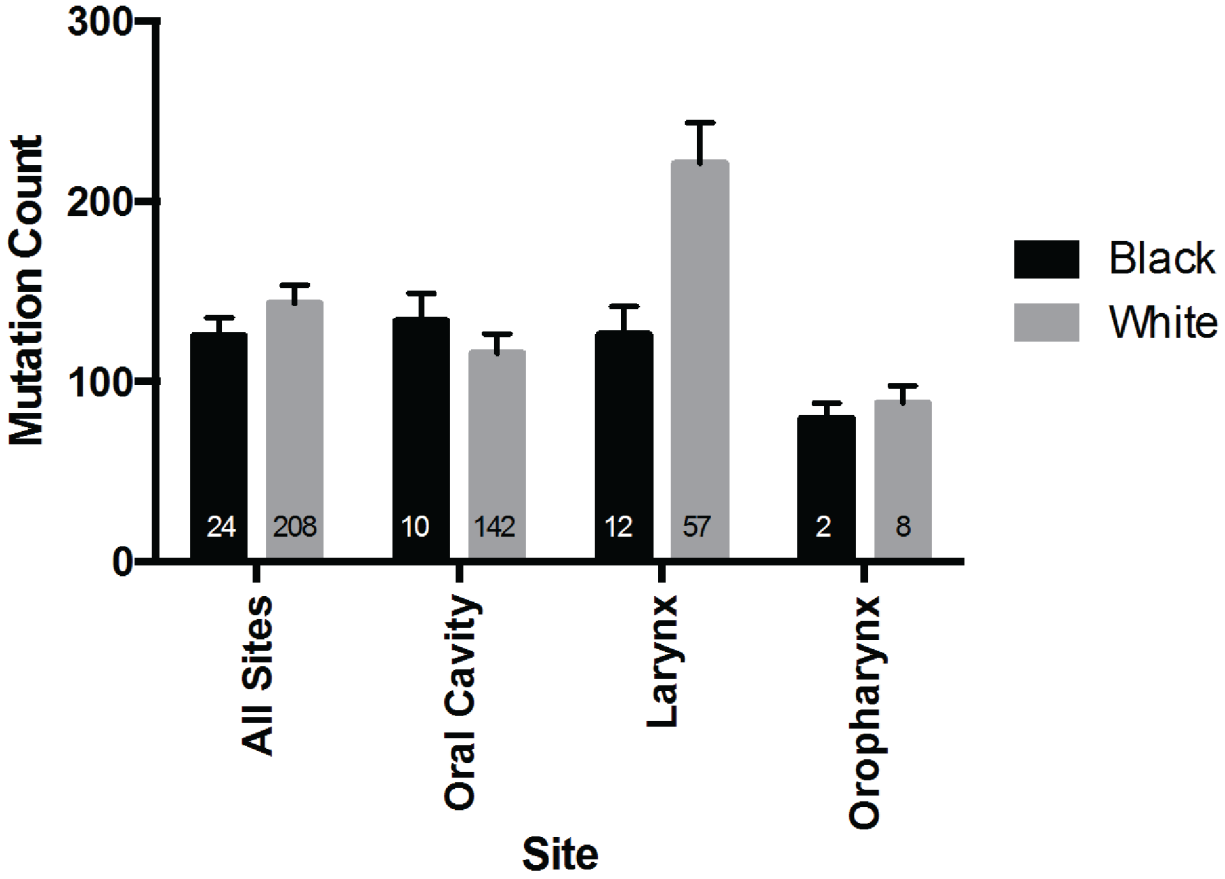


**Figure 1-4. Total mutation load in black and white patients in the TCGA HNSCC cohort**

Mutation rates were determined based on data from 24 black and 208 white HPV-negative HNSCC patients assessed as part of TCGA.

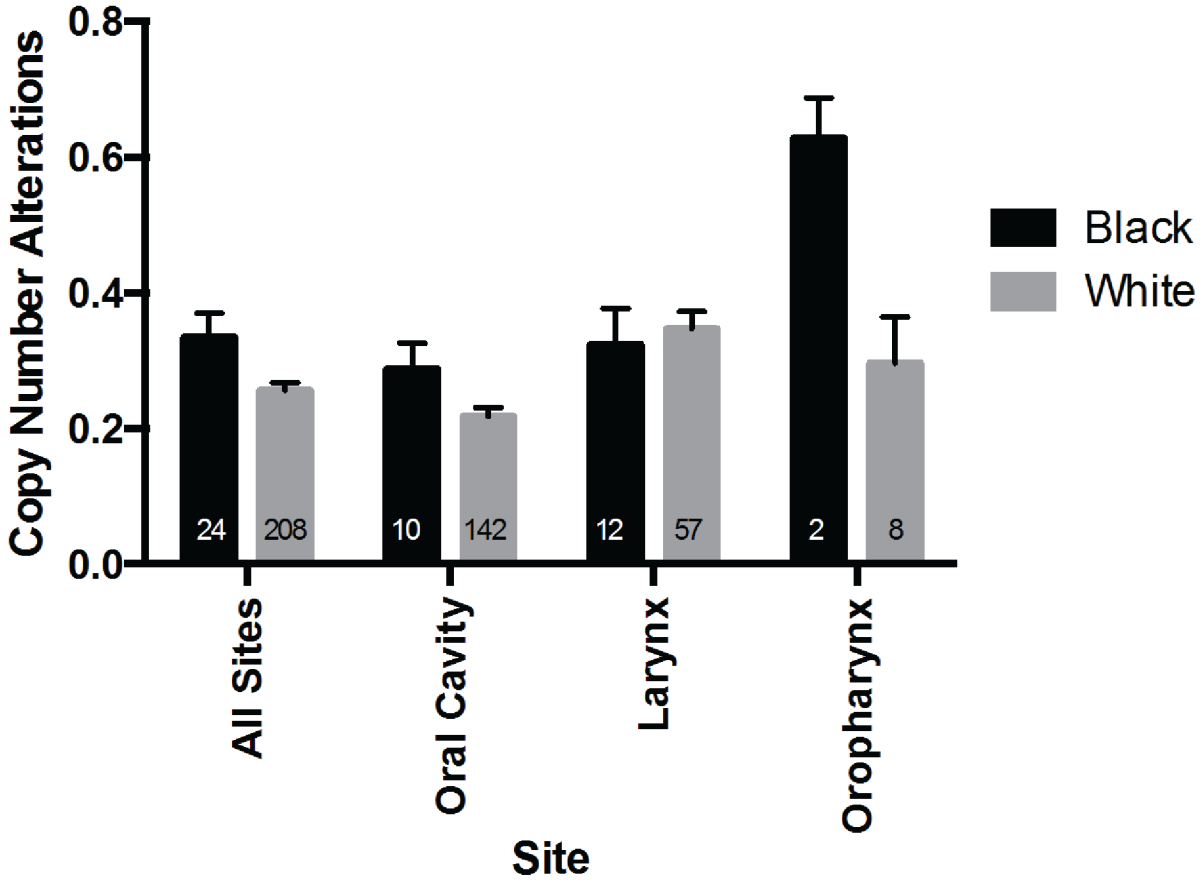


**Figure 1-5. Copy number alterations in black and white patients in the TCGA HNSCC cohort**

Aberration rates were determined based on data from 24 black and 208 white HPV-negative HNSCC patients assessed as part of TCGA.

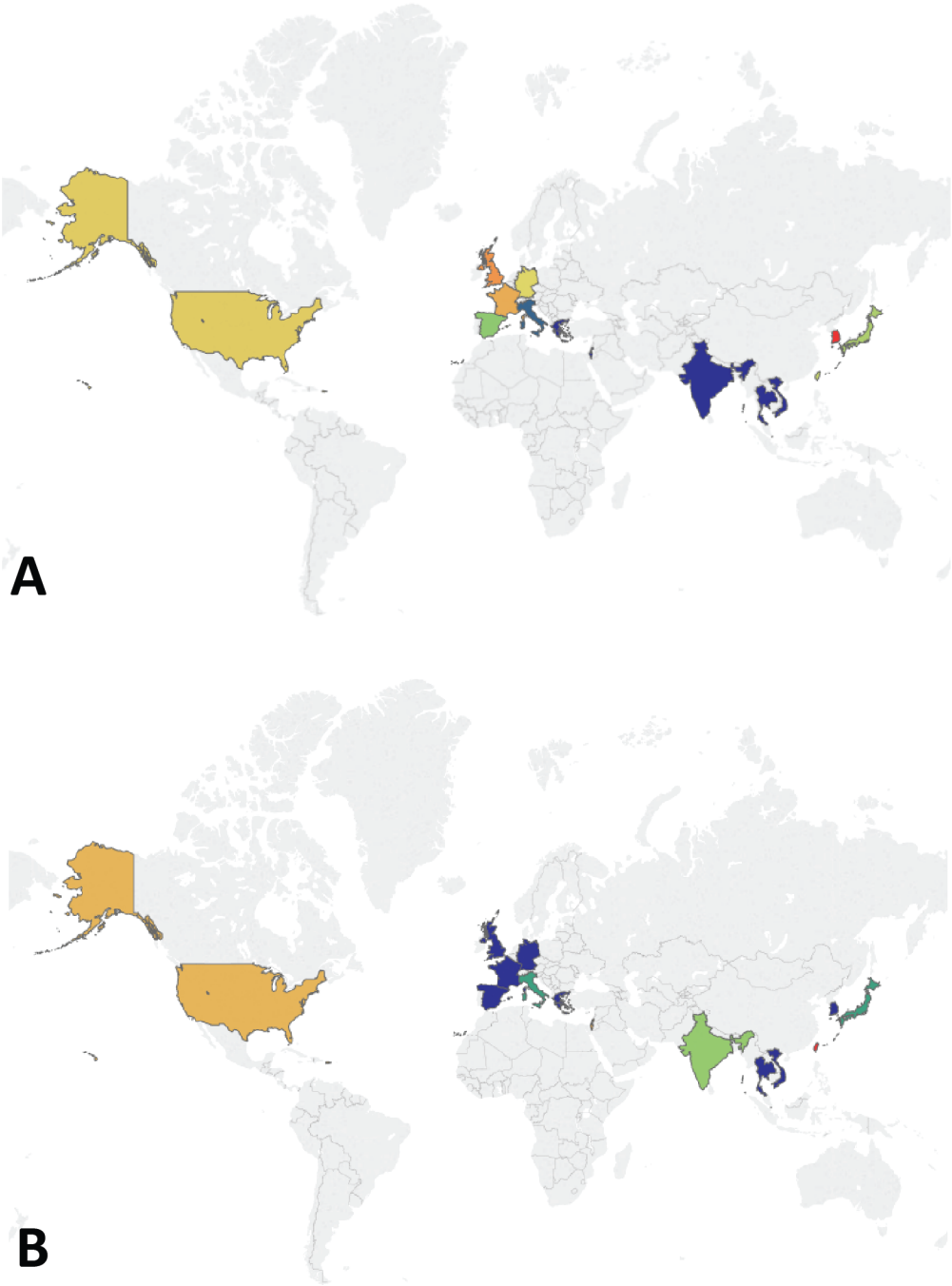


**Figure 1-6. Global variation in frequency of *PIK3CA* aberration in oral cancer**

Frequency of *PIK3CA* amplification (**A**) and mutation (**B**) in oral cancer cohorts from countries worldwide. Based on data from Murugan *et al.* (*94*) and review of more recent literature, as detailed in **Table 1-4**.

## Tables

### Table 1-1. Age-standardized head and neck cancer incidence rates by sex and subsite for various global cohorts

(*16*) Incidence rates per 100,000 for adult (age > 15 years) males and females in various global cohorts with cancers of the oral cavity, oropharynx, or other head and neck sites from 1998-2002. Other HNSCC sites include the pyriform sinus, hypopharnyx, lip/oral cavity/pharynx not otherwise specified, and larynx.
(*118*) Incidence rates per 100,000 for adult males and females in Zimbabwe from 1996-2000. Other HNSCC site incidence is the sum of the nasopharyngeal and laryngeal cancer incidence.
(*119*) Incidence rates per 100,000 for males and females of all ages in Australia with cancer of the lip and oral cavity or oropharynx from 1982-2008.
(*120*) Incidence rates per 100,000 for males and females of all ages in Guilan, Iran from 2008-2009 with cancers of the lip and oral cavity or pharynx and tonsil from 2008-2009.
* indicates incidence not available

| | **Oral Cavity** | | **Oropharynx** | | **Other Sites** | | |
|---|---|---|---|---|---|---|---|
| **Country** | ***Male*** | ***Female*** | ***Male*** | ***Female*** | ***Male*** | ***Female*** | **Reference** |
| ***Belarus*** | 8.93 | 0.73 | 4.75 | 0.23 | 18.93 | 0.34 | (*16*) |
| ***UK*** | 5.18 | 2.75 | 2.13 | 0.65 | 7.74 | 1.69 | (*16*) |
| ***France*** | 15.25 | 3.12 | 9.43 | 1.48 | 22.69 | 1.7 | (*16*) |
| ***Italy*** | 6.08 | 2.41 | 2.8 | 0.57 | 14.36 | 1.08 | (*16*) |
| ***China (Hong Kong)*** | 4.72 | 2.38 | 1.25 | 0.26 | 16.19 | 0.61 | (*16*) |
| ***India (Mumbai)*** | 15.49 | 8.12 | 2.82 | 0.61 | 16.66 | 2.89 | (*16*) |
| ***Philippines*** | 5.3 | 3.97 | 0.93 | 0.62 | 9.81 | 0.55 | (*16*) |
| ***Iran (Guilan)*** | 1.91 | 1.25 | 1.49 | 0.67 | * | * | (*120*) |
| ***Jews*** | 2.64 | 1.59 | 0.57 | 0.18 | 7.09 | 1.16 | (*16*) |
| ***Canada*** | 5.7 | 2.92 | 2.36 | 0.7 | 7.39 | 1.44 | (*16*) |
| ***US (Black)*** | 9.65 | 3.31 | 4.93 | 0.95 | 15.81 | 3.5 | (*16*) |
| ***US (White)*** | 7.16 | 3.41 | 2.9 | 0.73 | 8.31 | 2.07 | (*16*) |
| ***Costa Rica*** | 2.69 | 0.73 | 1.07 | * | 5.95 | 0.42 | (*16*) |
| ***Brazil*** | 12.73 | 2.66 | 4.56 | * | 16.12 | 1.73 | (*16*) |
| ***Zimbabwe*** | 6.4 | 1.2 | * | * | 1.6 | 1.5 | (*118*) |
| ***Australia*** | 7.84 | 3.06 | 3.97 | 1.01 | * | * | (*119*) |

**Table 1-2. *TP53* mutation rates in geographical cohorts with oral cavity cancer**

| Country | Site | *TP53* Mutation Frequency | Reference |
|---|---|---|---|
| US (TCGA) | Oral cavity | 129/160 (80.6%) | (*67*) |
| Asia | Tongue | 23/60 (38.3%) | (*80*) |
| Asia | Tongue | 7/66 (10.6%) | (*104*) |
| Asia | Oral cavity | 31/112 (27.7%) | (*105*) |
| Taiwan | Oral cavity | 26/79 (32.9%) | (*103*) |
| India | Gingivo-buccal | 31/50 (62%) | (*66*) |
| US (never-smoker) | Oral cavity | 10/61 (16.4%) | (*107*) |
| Iceland | Oral cavity | 11/52 (21.1%) | (*106*) |
| Brazil | Oral cavity | 15/30 (15%) | (*108*) |
| Brazil | Oral cavity | (40%) | (*109*) |

**Table 1-3. *TP53* mutation rates in geographical cohorts with larynx cancer**

| Country | Site | *TP53* Mutation Frequency | Reference |
|---|---|---|---|
| US HPV-negative (TCGA) | Larynx | 64/72 (88.9%) | (*67*) |
| China | Larynx | 22/64 (34.4%) | (*110*) |
| Italy | Larynx | 62/82 (75.6%) | (*115*) |
| Italy | Larynx | 36/81 (44.4%) | (*116*) |
| Denmark | Larynx (supraglottic) | 87/158 (55.1%) | (*117*) |
| South Africa | Larynx | 11/44 (25%) | (*111*) |
| Brazil | Larynx | 3/7 (42.9%) | (*108*) |
| Brazil | Larynx/hypopharynx | 49/58 (69.0%) | (*112*) |
| Argentina (Buenos Aires) | Larynx/hypopharynx | 2/15 (13.3%) | (*112*) |

**Table 1-4. Raw data for frequency of *PIK3CA* aberration in oral cancer used to generate Figure 1-6**

Bold text indicates amplification of chromosomal locus 3q26 (as opposed to *PIK3CA*)
* indicates that both amplification of *PIK3CA* and chromosomal locus 3q26 were reported (*PIK3CA* amplification rate was used to generate **Figure 1-6**.)
For countries with more than one value for *PIK3CA* mutation or amplification, an average was used to generate the **Figure 1-6**.

| | **Amplification** | | | | **Mutation** | | | |
|---|---|---|---|---|---|---|---|---|
| ***Country*** | **No. amp** | **Total** | **%** | ***** | **No. mut** | **Total** | **%** | **Ref** |
| ***Japan*** | 3 | 115 | 2.6% | | 3 | 115 | 2.6% | (*94*) |
| ***US*** | 14 | 31 | **45.2%** | | 2 | 31 | 6.5% | (*94*) |
| ***Israel*** | | | | | 4 | 37 | 10.8% | (*94*) |
| ***US*** | | | | | 6 | 74 | 8.1% | (*94*) |
| ***US*** | | | | | 3 | 120 | 2.5% | (*94*) |
| ***Taiwan*** | 40 | 82 | 48.8% | | | | | (*94*) |
| ***US*** | | | | | 1 | 35 | 2.9% | (*94*) |
| ***Greece*** | | | | | 0 | 86 | 0% | (*94*) |
| ***Spain*** | 9 | 24 | 37.5% | | | | | (*94*) |
| ***Vietnam*** | | | | | 0 | 18 | 0% | (*94*) |
| ***India*** | | | | | 2 | 19 | 10.5% | (*94*) |
| ***US*** | | | | | 5 | 24 | 20.8% | (*94*) |
| ***UK*** | 56 | 68 | **82.4%** | | | | | (*94*) |
| ***Germany*** | 7 | 12 | **58.3%** | | | | | (*94*) |
| ***Germany*** | 3 | 33 | 9.1% | * | 0 | 33 | 0% | (*94*) |
| ***Japan*** | 6 | 50 | 12% | | 2 | 50 | 4% | (*94*) |
| ***Thailand*** | 12 | 58 | 20.7% | | 6 | 58 | 10.3% | (*94*) |
| ***US*** | | | | | 4 | 38 | 10.5% | (*94*) |
| ***Taiwan*** | 21 | 25 | **84%** | | | | | (*94*) |
| ***Germany*** | 85 | 280 | **30.4%** | | | | | (*94*) |
| ***Spain*** | 43 | 117 | 36.8% | | | | | (*94*) |
| ***UK*** | 34 | 45 | **75.6%** | | | | | (*94*) |
| ***US*** | 34 | 49 | **69.4%** | | | | | (*94*) |
| ***Germany*** | 4 | 7 | **57.1%** | | | | | (*94*) |
| ***US*** | 50 | 75 | **66.7%** | | | | | (*94*) |
| ***Germany*** | 26 | 44 | **59.1%** | | | | | (*94*) |
| ***France*** | 6 | 9 | 66.7% | * | | | | (*94*) |
| ***Japan*** | 29 | 32 | **90.6%** | | | | | (*94*) |
| ***Japan*** | 7 | 11 | **63.6%** | | | | | (*94*) |
| ***Germany*** | 26 | 30 | **86.7%** | | | | | (*94*) |
| ***US*** | 5 | 10 | **50%** | | | | | (*94*) |

| | | | | | | | | |
|---|---|---|---|---|---|---|---|---|
| ***US*** | 10 | 13 | **76.9%** | | | | | (*94*) |
| ***India*** | | | | | 2 | 50 | 4.0% | (*121*) |
| ***Taiwan*** | | | | | 9 | 50 | 18% | (*122*) |
| ***Taiwan*** | | | | | 58 | 345 | 16.8% | (*123*) |
| ***US*** | | | | | 45 | 279 | 16.1% | (*124*) |
| ***India*** | | | | | 2 | 50 | 4% | (*66*) |
| ***Italy*** | | | | | 2 | 61 | 3.3% | (*125*) |
| ***Singapore*** | | | | | 3 | 66 | 4.5% | (*104*) |
| ***Asia*** | | | | | 5 | 60 | 8.3% | (*80*) |
| ***Taiwan*** | | | | | 11 | 79 | 13.9% | (*103*) |
| ***Asia*** | | | | | 5 | 123 | 4.1% | (*105*) |
| ***US*** | 44 | 279 | 15.8% | | | | | (*124*) |
| ***Italy*** | 6 | 64 | 9.4% | | | | | (*125*) |
| ***South Korea*** | 7 | 7 | 100% | | | | | (*126*) |
| ***India*** | 0 | 50 | 0% | | | | | (*66*) |
| ***Taiwan*** | 5 | 123 | 4.1% | | | | | (*127*) |

## References


1. Cancer Genome Atlas N. Comprehensive genomic characterization of head and neck squamous cell carcinomas. Nature. 2015;517(7536):576-82. doi: 10.1038/nature14129. PubMed PMID: 25631445; PMCID: 4311405.

2. Birkeland AC, Ludwig ML, Meraj TS, Brenner JC, Prince ME. The Tip of the Iceberg: Clinical Implications of Genomic Sequencing Projects in Head and Neck Cancer. Cancers. 2015;7(4):2094-109. Epub 2015/10/28. doi: 10.3390/cancers7040879. PubMed PMID: 26506389.

3. Birkeland AC, Uhlmann WR, Brenner JC, Shuman AG. Getting personal: Head and neck cancer management in the era of genomic medicine. Head & neck. 2015. Epub 2015/05/23. doi: 10.1002/hed.24132. PubMed PMID: 25995036; PMCID: Pmc4654712.

4. Birkeland AC, Brenner JC. Personalizing medicine in head and neck squamous cell carcinoma: The rationale for combination therapies. . Med Res Arch. 2015;3.

5. McNeil C. NCI-MATCH launch highlights new trial design in precision-medicine era. Journal of the National Cancer Institute. 2015;107(7). Epub 2015/07/05. doi: 10.1093/jnci/djv193. PubMed PMID: 26142446.

6. Mao X, Yu Y, Boyd LK, Ren G, Lin D, Chaplin T, Kudahetti SC, Stankiewicz E, Xue L, Beltran L, Gupta M, Oliver RT, Lemoine NR, Berney DM, Young BD, Lu YJ. Distinct genomic alterations in prostate cancers in Chinese and Western populations suggest alternative pathways of prostate carcinogenesis. Cancer research. 2010;70(13):5207-12. Epub 2010/06/03. doi: 10.1158/0008-5472.can-09-4074. PubMed PMID: 20516122; PMCID: Pmc2896548.

7. Ren S, Peng Z, Mao JH, Yu Y, Yin C, Gao X, Cui Z, Zhang J, Yi K, Xu W, Chen C, Wang F, Guo X, Lu J, Yang J, Wei M, Tian Z, Guan Y, Tang L, Xu C, Wang L, Gao X, Tian W, Wang J, Yang H, Wang J, Sun Y. RNA-seq analysis of prostate cancer in the Chinese population identifies recurrent gene fusions, cancer-associated long noncoding RNAs and aberrant alternative splicings. Cell research. 2012;22(5):806-21. Epub 2012/02/22. doi: 10.1038/cr.2012.30. PubMed PMID: 22349460; PMCID: Pmc3343650.

8. Tillman BN YM, Birkeland AC, Liu C, Hovelson DH, Cani AK, Palanisamy N, Carskadon S, Carey TE, Bradford CR, Tomlins S, McHugh JB, Spector ME, Brenner JC. . Targeted sequencing of an epidemiologically low risk patient defines Fibroblast Growth Factor Receptor family aberrations as a putative driver of head and neck squamous cell carcinoma. . Head Neck (in press). 2015.

9. DeSantis C, Naishadham D, Jemal A. Cancer statistics for African Americans, 2013. CA: a cancer journal for clinicians. 2013;63(3):151-66. Epub 2013/02/07. doi: 10.3322/caac.21173. PubMed PMID: 23386565.

10. Goodwin WJ, Thomas GR, Parker DF, Joseph D, Levis S, Franzmann E, Anello C, Hu JJ. Unequal burden of head and neck cancer in the United States. Head & neck. 2008;30(3):358-71. Epub 2007/11/01. doi: 10.1002/hed.20710. PubMed PMID: 17972309.

11. Morse DE, Kerr AR. Disparities in oral and pharyngeal cancer incidence, mortality and survival among black and white Americans. Journal of the American Dental Association (1939). 2006;137(2):203-12. Epub 2006/03/09. PubMed PMID: 16521387; PMCID: Pmc1398075.

12. Moore RJ, Doherty DA, Do KA, Chamberlain RM, Khuri FR. Racial disparity in survival of patients with squamous cell carcinoma of the oral cavity and pharynx. Ethnicity & health. 2001;6(3-4):165-77. Epub 2001/11/08. doi: 10.1080/13557850120078099. PubMed PMID: 11696928.

13. Berry JD, Dyer A, Cai X, Garside DB, Ning H, Thomas A, Greenland P, Van Horn L, Tracy RP, Lloyd-Jones DM. Lifetime risks of cardiovascular disease. The New England journal of medicine. 2012;366(4):321-9. Epub 2012/01/27. doi: 10.1056/NEJMoa1012848. PubMed PMID: 22276822; PMCID: Pmc3336876.

14. Marur S, Forastiere AA. Head and neck cancer: changing epidemiology, diagnosis, and treatment. Mayo Clinic proceedings. 2008;83(4):489-501. Epub 2008/04/03. doi: 10.4065/83.4.489. PubMed PMID: 18380996.

15. Hashibe M, Brennan P, Chuang SC, Boccia S, Castellsague X, Chen C, Curado MP, Dal Maso L, Daudt AW, Fabianova E, Fernandez L, Wunsch-Filho V, Franceschi S, Hayes RB, Herrero R, Kelsey K, Koifman S, La Vecchia C, Lazarus P, Levi F, Lence JJ, Mates D, Matos E, Menezes A, McClean MD, Muscat J, Eluf-Neto J, Olshan AF, Purdue M, Rudnai P, Schwartz SM, Smith E, Sturgis EM, Szeszenia-Dabrowska N, Talamini R, Wei Q, Winn DM, Shangina O, Pilarska A, Zhang ZF, Ferro G, Berthiller J, Boffetta P. Interaction between tobacco and alcohol use and the risk of head and neck cancer: pooled analysis in the International Head and Neck Cancer Epidemiology Consortium. Cancer epidemiology, biomarkers & prevention : a publication of the American Association for Cancer Research, cosponsored by the American Society of Preventive Oncology. 2009;18(2):541-50. Epub 2009/02/05. doi: 10.1158/1055-9965.epi-08-0347. PubMed PMID: 19190158; PMCID: Pmc3051410.

16. Simard EP, Torre LA, Jemal A. International trends in head and neck cancer incidence rates: differences by country, sex and anatomic site. Oral oncology. 2014;50(5):387-403. Epub 2014/02/18. doi: 10.1016/j.oraloncology.2014.01.016. PubMed PMID: 24530208.

17. Gupta B, Johnson NW. Systematic review and meta-analysis of association of smokeless tobacco and of betel quid without tobacco with incidence of oral cancer in South Asia and the Pacific. PloS one. 2014;9(11):e113385. Epub 2014/11/21. doi: 10.1371/journal.pone.0113385. PubMed PMID: 25411778; PMCID: Pmc4239077.

18. Parkin DM, Bray F, Ferlay J, Pisani P. Global cancer statistics, 2002. CA: a cancer journal for clinicians. 2005;55(2):74-108. Epub 2005/03/12. PubMed PMID: 15761078.

19. Franceschi S, Bidoli E, Herrero R, Munoz N. Comparison of cancers of the oral cavity and pharynx worldwide: etiological clues. Oral oncology. 2000;36(1):106-15. Epub 2000/07/13. PubMed PMID: 10889929.

20. Faggons CE, Mabedi C, Shores CG, Gopal S. Review: Head and neck squamous cell carcinoma in sub-Saharan Africa. Malawi medical journal : the journal of Medical Association of Malawi. 2015;27(3):79-87. Epub 2015/12/31. PubMed PMID: 26715951; PMCID: Pmc4688867.

21. da Lilly-Tariah OB, Somefun AO, Adeyemo WL. Current evidence on the burden of head and neck cancers in Nigeria. Head & neck oncology. 2009;1:14. Epub 2009/05/30. doi: 10.1186/1758-3284-1-14. PubMed PMID: 19476614; PMCID: Pmc2694192.

22. Laryea DO, Awuah B, Amoako YA, Osei-Bonsu E, Dogbe J, Larsen-Reindorf R, Ansong D, Yeboah-Awudzi K, Oppong JK, Konney TO, Boadu KO, Nguah SB, Titiloye NA, Frimpong NO, Awittor FK, Martin IK. Cancer incidence in Ghana, 2012: evidence from a population-based cancer registry. BMC cancer. 2014;14:362. Epub 2014/06/03. doi: 10.1186/1471-2407-14-362. PubMed PMID: 24884730; PMCID: Pmc4046022.

23. Calys-Tagoe BN, Yarney J, Kenu E, Amanhyia NA, Enchill E, Obeng I. Profile of cancer patients' seen at Korle Bu teaching hospital in Ghana (a cancer registry review). BMC research notes. 2014;7:577. Epub 2014/08/29. doi: 10.1186/1756-0500-7-577. PubMed PMID: 25164384; PMCID: Pmc4155104.

24. Patel P, Hanson DL, Sullivan PS, Novak RM, Moorman AC, Tong TC, Holmberg SD, Brooks JT. Incidence of types of cancer among HIV-infected persons compared with the general population in the United States, 1992-2003. Annals of internal medicine. 2008;148(10):728-36. Epub 2008/05/21. PubMed PMID: 18490686.

25. Saman DM. A review of the epidemiology of oral and pharyngeal carcinoma: update. Head & neck oncology. 2012;4:1. Epub 2012/01/17. doi: 10.1186/1758-3284-4-1. PubMed PMID: 22244087; PMCID: Pmc3292826.

26. Ho PS, Yang YH, Shieh TY, Chen CH, Tsai CC, Ko YC. Ethnic differences in the occurrence of oropharyngeal cancer in Taiwan. Public health. 2007;121(10):765-73. Epub 2007/05/15. doi: 10.1016/j.puhe.2007.02.001. PubMed PMID: 17499319.

27. Chen CM, Chang JC, Y.C. K. Ethnic variation in CYP2E1, GSTM1, GSTT1 genes polymorphism analysis: Taiwan aborigines, Thai and Filipino. Mid Taiwan J Med. 2000;5:181-8.

28. D'Souza G, Kreimer AR, Viscidi R, Pawlita M, Fakhry C, Koch WM, Westra WH, Gillison ML. Case-control study of human papillomavirus and oropharyngeal cancer. N Engl J Med. 2007;356(19):1944-56. Epub 2007/05/15. doi: 356/19/1944 [pii] 10.1056/NEJMoa065497. PubMed PMID: 17494927.

29. Fakhry C, Gillison ML. Clinical implications of human papillomavirus in head and neck cancers. J Clin Oncol. 2006;24(17):2606-11. Epub 2006/06/10. doi: 24/17/2606 [pii]

10.1200/JCO.2006.06.1291. PubMed PMID: 16763272

30. Gillison ML, D'Souza G, Westra W, Sugar E, Xiao W, Begum S, Viscidi R. Distinct risk factor profiles for human papillomavirus type 16-positive and human papillomavirus type 16-negative head and neck cancers. J Natl Cancer Inst. 2008;100(6):407-20. Epub 2008/03/13. doi: djn025 [pii]
10.1093/jnci/djn025. PubMed PMID: 18334711.

31. Gillison ML, Koch WM, Capone RB, Spafford M, Westra WH, Wu L, Zahurak ML, Daniel RW, Viglione M, Symer DE, Shah KV, Sidransky D. Evidence for a causal association between human papillomavirus and a subset of head and neck cancers. J Natl Cancer Inst. 2000;92(9):709-20. Epub 2000/05/04. PubMed PMID: 10793107.

32. Kumar B, Cordell KG, Lee JS, Worden FP, Prince ME, Tran HH, Wolf GT, Urba SG, Chepeha DB, Teknos TN, Eisbruch A, Tsien CI, Taylor JM, D'Silva NJ, Yang K, Kurnit DM, Bauer JA, Bradford CR, Carey TE. EGFR, p16, HPV Titer, Bcl-xL and p53, sex, and smoking as indicators of response to therapy and survival in oropharyngeal cancer. J Clin Oncol. 2008;26(19):3128-37. Epub 2008/05/14. doi: JCO.2007.12.7662 [pii]
10.1200/JCO.2007.12.7662. PubMed PMID: 18474878.

33. Licitra L, Bossi P, Locati LD. A multidisciplinary approach to squamous cell carcinomas of the head and neck: what is new? Curr Opin Oncol. 2006;18(3):253-7. Epub 2006/03/23. doi: 10.1097/01.cco.0000219254.53091.35
00001622-200605000-00007 [pii]. PubMed PMID: 16552237.

34. Maxwell JH, Kumar B, Feng FY, Worden FP, Lee JS, Eisbruch A, Wolf GT, Prince ME, Moyer JS, Teknos TN, Chepeha DB, McHugh JB, Urba SG, Stoerker J, Walline HM, Kurnit DM, Cordell KG, Davis SJ, Ward PD, Bradford CR, Carey TE. Tobacco use in human papillomavirus-positive advanced oropharynx cancer patients related to increased risk of distant metastases and tumor recurrence. Clin Cancer Res. 2010;16(4):1226-35. Epub 2010/02/11. doi: 1078-0432.CCR-09-2350 [pii]
10.1158/1078-0432.CCR-09-2350. PubMed PMID: 20145161; PMCID: 2822887.

35. Worden FP, Kumar B, Lee JS, Wolf GT, Cordell KG, Taylor JM, Urba SG, Eisbruch A, Teknos TN, Chepeha DB, Prince ME, Tsien CI, D'Silva NJ, Yang K, Kurnit DM, Mason HL, Miller TH, Wallace NE, Bradford CR, Carey TE. Chemoselection as a strategy for organ preservation in advanced oropharynx cancer: response and survival positively associated with HPV16 copy number. Journal of clinical oncology : official journal of the American Society of Clinical Oncology. 2008;26(19):3138-46. doi: 10.1200/JCO.2007.12.7597. PubMed PMID: 18474879; PMCID: 2742158.

36. Ziegert C, Wentzensen N, Vinokurova S, Kisseljov F, Einenkel J, Hoeckel M, von Knebel Doeberitz M. A comprehensive analysis of HPV integration loci in anogenital lesions combining transcript and genome-based amplification techniques. Oncogene. 2003;22(25):3977-84. Epub 2003/06/19. doi: 10.1038/sj.onc.1206629
1206629 [pii]. PubMed PMID: 12813471.

37. De Marco L, Gillio-Tos A, Bonello L, Ghisetti V, Ronco G, Merletti F. Detection of human papillomavirus type 16 integration in pre-neoplastic cervical lesions and confirmation by DIPS-PCR and sequencing. J Clin Virol. 2007;38(1):7-13. Epub 2006/10/31. doi: S1386-6532(06)00344-1 [pii]
10.1016/j.jcv.2006.09.008. PubMed PMID: 17070101.

38. Schmitt M, Dalstein V, Waterboer T, Clavel C, Gissmann L, Pawlita M. Diagnosing cervical cancer and high-grade precursors by HPV16 transcription patterns. Cancer Res. 2010;70(1):249-56. Epub 2009/12/24. doi: 0008-5472.CAN-09-2514 [pii]
10.1158/0008-5472.CAN-09-2514. PubMed PMID: 20028865.

39. Quon H, Cohen MA, Montone KT, Ziober AF, Wang LP, Weinstein GS, O'Malley BW, Jr. Transoral robotic surgery and adjuvant therapy for oropharyngeal carcinomas and the influence of p16 INK4a on treatment outcomes. Laryngoscope. 2013;123(3):635-40. doi: 10.1002/lary.22172. PubMed PMID: 22588642.

40. Haughey BH, Hinni ML, Salassa JR, Hayden RE, Grant DG, Rich JT, Milov S, Lewis JS, Jr., Krishna M. Transoral laser microsurgery as primary treatment for advanced-stage oropharyngeal cancer: a United States multicenter study. Head Neck. 2011;33(12):1683-94. doi: 10.1002/hed.21669. PubMed PMID: 21284056.

41. Stein AP, Saha S, Kraninger JL, Swick AD, Yu M, Lambert PF, Kimple RJ. Prevalence of Human Papillomavirus in Oropharyngeal Cancer: A Systematic Review. Cancer journal (Sudbury, Mass). 2015;21(3):138-46. Epub 2015/06/08. doi: 10.1097/ppo.0000000000000115. PubMed PMID: 26049691; PMCID: Pmc4459520.

42. Mehanna H, Beech T, Nicholson T, El-Hariry I, McConkey C, Paleri V, Roberts S. Prevalence of human papillomavirus in oropharyngeal and nonoropharyngeal head and neck cancer--systematic review and meta-analysis of trends by time and region. Head & neck. 2013;35(5):747-55. Epub 2012/01/24. doi: 10.1002/hed.22015. PubMed PMID: 22267298.

43. Li W, Thompson CH, O'Brien CJ, McNeil EB, Scolyer RA, Cossart YE, Veness MJ, Walker DM, Morgan GJ, Rose BR. Human papillomavirus positivity predicts favourable outcome for squamous carcinoma of the tonsil. International journal of cancer Journal international du cancer. 2003;106(4):553-8. Epub 2003/07/08. doi: 10.1002/ijc.11261. PubMed PMID: 12845651.

44. Lam EW, Chan JY, Chan AB, Ng CS, Lo ST, Lam VS, Chan MM, Ngai CM, Vlantis AC, Ma RK, Chan PK. Prevalence, Clinicopathological Characteristics, and Outcome of Human Papillomavirus-Associated Oropharyngeal Cancer in Southern Chinese Patients. Cancer epidemiology, biomarkers & prevention : a publication of the American Association for Cancer Research, cosponsored by the American Society of Preventive Oncology. 2015. Epub 2015/11/26. doi: 10.1158/1055-9965.epi-15-0869. PubMed PMID: 26604268.

45. Davidson CL, Richter KL, Van der Linde M, Coetsee J, Boy SC. Prevalence of oral and oropharyngeal human papillomavirus in a sample of South African men: a pilot study. South

African medical journal = Suid-Afrikaanse tydskrif vir geneeskunde. 2014;104(5):358-61. Epub 2014/09/13. doi: 10.7196/samj.7542. PubMed PMID: 25212204.

46. Blumberg J, Monjane L, Prasad M, Carrilho C, Judson BL. Investigation of the presence of HPV related oropharyngeal and oral tongue squamous cell carcinoma in Mozambique. Cancer epidemiology. 2015;39(6):1000-5. Epub 2015/11/22. doi: 10.1016/j.canep.2015.10.015. PubMed PMID: 26590333.

47. Ndiaye C, Alemany L, Diop Y, Ndiaye N, Dieme MJ, Tous S, Klaustermeier JE, Alejo M, Castellsague X, Bosch FX, Trottier H, Sanjose S. The role of human papillomavirus in head and neck cancer in Senegal. Infectious agents and cancer. 2013;8(1):14. Epub 2013/04/19. doi: 10.1186/1750-9378-8-14. PubMed PMID: 23594504; PMCID: Pmc3637397.

48. Mork J, Lie AK, Glattre E, Hallmans G, Jellum E, Koskela P, Moller B, Pukkala E, Schiller JT, Youngman L, Lehtinen M, Dillner J. Human papillomavirus infection as a risk factor for squamous-cell carcinoma of the head and neck. The New England journal of medicine. 2001;344(15):1125-31. Epub 2001/04/12. doi: 10.1056/nejm200104123441503. PubMed PMID: 11297703.

49. Westra WH. Detection of human papillomavirus (HPV) in clinical samples: evolving methods and strategies for the accurate determination of HPV status of head and neck carcinomas. Oral oncology. 2014;50(9):771-9. Epub 2014/06/17. doi: 10.1016/j.oraloncology.2014.05.004. PubMed PMID: 24932529; PMCID: Pmc4318232.

50. Lewis JS, Jr. p16 Immunohistochemistry as a standalone test for risk stratification in oropharyngeal squamous cell carcinoma. Head and neck pathology. 2012;6 Suppl 1:S75-82. Epub 2012/07/13. doi: 10.1007/s12105-012-0369-0. PubMed PMID: 22782226; PMCID: Pmc3394161.

51. Walline HM, Komarck C, McHugh JB, Byrd SA, Spector ME, Hauff SJ, Graham MP, Bellile E, Moyer JS, Prince ME, Wolf GT, Chepeha DB, Worden FP, Stenmark MH, Eisbruch A, Bradford CR, Carey TE. High-risk human papillomavirus detection in oropharyngeal, nasopharyngeal, and oral cavity cancers: comparison of multiple methods. JAMA otolaryngology-- head & neck surgery. 2013;139(12):1320-7. Epub 2013/11/02. doi: 10.1001/jamaoto.2013.5460. PubMed PMID: 24177760; PMCID: Pmc4049419.

52. Gillison ML, Broutian T, Pickard RK, Tong ZY, Xiao W, Kahle L, Graubard BI, Chaturvedi AK. Prevalence of oral HPV infection in the United States, 2009-2010. JAMA. 2012;307(7):693-703. Epub 2012/01/28. doi: jama.2012.101 [pii] 10.1001/jama.2012.101. PubMed PMID: 22282321.

53. Matovina M, Sabol I, Grubisic G, Gasperov NM, Grce M. Identification of human papillomavirus type 16 integration sites in high-grade precancerous cervical lesions. Gynecol Oncol. 2009;113(1):120-7. Epub 2009/01/23. doi: S0090-8258(08)01053-6 [pii] 10.1016/j.ygyno.2008.12.004. PubMed PMID: 19157528.

54. Smith JS, Melendy A, Rana RK, Pimenta JM. Age-specific prevalence of infection with human papillomavirus in females: a global review. The Journal of adolescent health : official publication of the Society for Adolescent Medicine. 2008;43(4 Suppl):S5-25, S.e1-41. Epub 2008/10/01. doi: 10.1016/j.jadohealth.2008.07.009. PubMed PMID: 18809145.

55. Forman D, de Martel C, Lacey CJ, Soerjomataram I, Lortet-Tieulent J, Bruni L, Vignat J, Ferlay J, Bray F, Plummer M, Franceschi S. Global burden of human papillomavirus and related diseases. Vaccine. 2012;30 Suppl 5:F12-23. Epub 2012/12/05. doi: 10.1016/j.vaccine.2012.07.055. PubMed PMID: 23199955.

56. Bruni L, Diaz M, Castellsague X, Ferrer E, Bosch FX, de Sanjose S. Cervical human papillomavirus prevalence in 5 continents: meta-analysis of 1 million women with normal cytological findings. The Journal of infectious diseases. 2010;202(12):1789-99. Epub 2010/11/12. doi: 10.1086/657321. PubMed PMID: 21067372.

57. Smith JS, Gilbert PA, Melendy A, Rana RK, Pimenta JM. Age-specific prevalence of human papillomavirus infection in males: a global review. The Journal of adolescent health : official publication of the Society for Adolescent Medicine. 2011;48(6):540-52. Epub 2011/05/18. doi: 10.1016/j.jadohealth.2011.03.010. PubMed PMID: 21575812.

58. Castellsague X, Bosch FX, Munoz N, Meijer CJ, Shah KV, de Sanjose S, Eluf-Neto J, Ngelangel CA, Chichareon S, Smith JS, Herrero R, Moreno V, Franceschi S. Male circumcision, penile human papillomavirus infection, and cervical cancer in female partners. The New England journal of medicine. 2002;346(15):1105-12. Epub 2002/04/12. doi: 10.1056/NEJMoa011688. PubMed PMID: 11948269.

59. Chaturvedi AK, Anderson WF, Lortet-Tieulent J, Curado MP, Ferlay J, Franceschi S, Rosenberg PS, Bray F, Gillison ML. Worldwide trends in incidence rates for oral cavity and oropharyngeal cancers. Journal of clinical oncology : official journal of the American Society of Clinical Oncology. 2013;31(36):4550-9. Epub 2013/11/20. doi: 10.1200/jco.2013.50.3870. PubMed PMID: 24248688; PMCID: Pmc3865341.

60. Heck JE, Berthiller J, Vaccarella S, Winn DM, Smith EM, Shan'gina O, Schwartz SM, Purdue MP, Pilarska A, Eluf-Neto J, Menezes A, McClean MD, Matos E, Koifman S, Kelsey KT, Herrero R, Hayes RB, Franceschi S, Wunsch-Filho V, Fernandez L, Daudt AW, Curado MP, Chen C, Castellsague X, Ferro G, Brennan P, Boffetta P, Hashibe M. Sexual behaviours and the risk of head and neck cancers: a pooled analysis in the International Head and Neck Cancer Epidemiology (INHANCE) consortium. International journal of epidemiology. 2010;39(1):166-81. Epub 2009/12/22. doi: 10.1093/ije/dyp350. PubMed PMID: 20022926; PMCID: Pmc2817092.

61. Gillison ML, Chaturvedi AK, Anderson WF, Fakhry C. Epidemiology of Human Papillomavirus-Positive Head and Neck Squamous Cell Carcinoma. Journal of clinical oncology : official journal of the American Society of Clinical Oncology. 2015;33(29):3235-42. Epub 2015/09/10. doi: 10.1200/jco.2015.61.6995. PubMed PMID: 26351338.

62. D'Souza G, Cullen K, Bowie J, Thorpe R, Fakhry C. Differences in oral sexual behaviors by gender, age, and race explain observed differences in prevalence of oral human papillomavirus infection. PloS one. 2014;9(1):e86023. Epub 2014/01/30. doi: 10.1371/journal.pone.0086023. PubMed PMID: 24475067; PMCID: Pmc3901667.

63. Chaturvedi AK, Graubard BI, Broutian T, Pickard RK, Tong ZY, Xiao W, Kahle L, Gillison ML. NHANES 2009-2012 Findings: Association of Sexual Behaviors with Higher Prevalence of Oral Oncogenic Human Papillomavirus Infections in U.S. Men. Cancer research. 2015;75(12):2468-77. Epub 2015/04/16. doi: 10.1158/0008-5472.can-14-2843. PubMed PMID: 25873485; PMCID: Pmc4470779.

64. Giuliano AR, Nyitray AG, Kreimer AR, Pierce Campbell CM, Goodman MT, Sudenga SL, Monsonego J, Franceschi S. EUROGIN 2014 roadmap: differences in human papillomavirus infection natural history, transmission and human papillomavirus-related cancer incidence by gender and anatomic site of infection. International journal of cancer Journal international du cancer. 2015;136(12):2752-60. Epub 2014/07/22. doi: 10.1002/ijc.29082. PubMed PMID: 25043222; PMCID: Pmc4297584.

65. Settle K, Posner MR, Schumaker LM, Tan M, Suntharalingam M, Goloubeva O, Strome SE, Haddad RI, Patel SS, Cambell EV, 3rd, Sarlis N, Lorch J, Cullen KJ. Racial survival disparity in head and neck cancer results from low prevalence of human papillomavirus infection in black oropharyngeal cancer patients. Cancer prevention research (Philadelphia, Pa). 2009;2(9):776-81. Epub 2009/07/31. doi: 10.1158/1940-6207.capr-09-0149. PubMed PMID: 19641042; PMCID: Pmc4459126.

66. Jiron J, Sethi S, Ali-Fehmi R, Franceschi S, Struijk L, van Doorn LJ, Quint W, Kato I. Racial disparities in Human Papillomavirus (HPV) associated head and neck cancer. American journal of otolaryngology. 2014;35(2):147-53. Epub 2013/11/12. doi: 10.1016/j.amjoto.2013.09.004. PubMed PMID: 24209992; PMCID: Pmc3947473.

67. Mutational landscape of gingivo-buccal oral squamous cell carcinoma reveals new recurrently-mutated genes and molecular subgroups. Nature communications. 2013;4:2873. Epub 2013/12/03. doi: 10.1038/ncomms3873. PubMed PMID: 24292195; PMCID: Pmc3863896.

68. Cerami E, Gao J, Dogrusoz U, Gross BE, Sumer SO, Aksoy BA, Jacobsen A, Byrne CJ, Heuer ML, Larsson E, Antipin Y, Reva B, Goldberg AP, Sander C, Schultz N. The cBio cancer genomics portal: an open platform for exploring multidimensional cancer genomics data. Cancer discovery. 2012;2(5):401-4. Epub 2012/05/17. doi: 10.1158/2159-8290.cd-12-0095. PubMed PMID: 22588877; PMCID: Pmc3956037.

69. Gao J, Aksoy BA, Dogrusoz U, Dresdner G, Gross B, Sumer SO, Sun Y, Jacobsen A, Sinha R, Larsson E, Cerami E, Sander C, Schultz N. Integrative analysis of complex cancer genomics and clinical profiles using the cBioPortal. Science signaling. 2013;6(269):pl1. Epub 2013/04/04. doi: 10.1126/scisignal.2004088. PubMed PMID: 23550210; PMCID: Pmc4160307.

70. Stransky N, Egloff AM, Tward AD, Kostic AD, Cibulskis K, Sivachenko A, Kryukov GV, Lawrence MS, Sougnez C, McKenna A, Shefler E, Ramos AH, Stojanov P, Carter SL, Voet D, Cortes ML, Auclair D, Berger MF, Saksena G, Guiducci C, Onofrio RC, Parkin M, Romkes M, Weissfeld JL, Seethala RR, Wang L, Rangel-Escareno C, Fernandez-Lopez JC, Hidalgo-Miranda A, Melendez-Zajgla J, Winckler W, Ardlie K, Gabriel SB, Meyerson M, Lander ES, Getz G, Golub TR, Garraway LA, Grandis JR. The mutational landscape of head and neck squamous cell carcinoma. Science (New York, NY). 2011;333(6046):1157-60. Epub 2011/07/30. doi: 10.1126/science.1208130. PubMed PMID: 21798893; PMCID: Pmc3415217.

71. Ozanne B, Richards CS, Hendler F, Burns D, Gusterson B. Over-expression of the EGF receptor is a hallmark of squamous cell carcinomas. The Journal of pathology. 1986;149(1):9-14. Epub 1986/05/01. doi: 10.1002/path.1711490104. PubMed PMID: 2425067.

72. Vermorken JB, Mesia R, Rivera F, Remenar E, Kawecki A, Rottey S, Erfan J, Zabolotnyy D, Kienzer HR, Cupissol D, Peyrade F, Benasso M, Vynnychenko I, De Raucourt D, Bokemeyer C, Schueler A, Amellal N, Hitt R. Platinum-based chemotherapy plus cetuximab in head and neck cancer. The New England journal of medicine. 2008;359(11):1116-27. Epub 2008/09/12. doi: 10.1056/NEJMoa0802656. PubMed PMID: 18784101.

73. Bonner JA, Harari PM, Giralt J, Azarnia N, Shin DM, Cohen RB, Jones CU, Sur R, Raben D, Jassem J, Ove R, Kies MS, Baselga J, Youssoufian H, Amellal N, Rowinsky EK, Ang KK. Radiotherapy plus cetuximab for squamous-cell carcinoma of the head and neck. The New England journal of medicine. 2006;354(6):567-78. Epub 2006/02/10. doi: 10.1056/NEJMoa053422. PubMed PMID: 16467544.

74. Keren S, Shoude Z, Lu Z, Beibei Y. Role of EGFR as a prognostic factor for survival in head and neck cancer: a meta-analysis. Tumour biology : the journal of the International Society for Oncodevelopmental Biology and Medicine. 2014;35(3):2285-95. Epub 2013/11/16. doi: 10.1007/s13277-013-1303-0. PubMed PMID: 24234257.

75. Abusail MS, Dirweesh AM, Salih RA, Gadelkarim AH. Expression of EGFR and p53 in head and neck tumors among Sudanese patients. Asian Pacific journal of cancer prevention : APJCP. 2013;14(11):6415-8. Epub 2014/01/01. PubMed PMID: 24377543.

76. Lee JW, Soung YH, Kim SY, Nam HK, Park WS, Nam SW, Kim MS, Sun DI, Lee YS, Jang JJ, Lee JY, Yoo NJ, Lee SH. Somatic mutations of EGFR gene in squamous cell carcinoma of the head and neck. Clinical cancer research : an official journal of the American Association for Cancer Research. 2005;11(8):2879-82. Epub 2005/04/20. doi: 10.1158/1078-0432.ccr-04-2029. PubMed PMID: 15837736.

77. Loeffler-Ragg J, Witsch-Baumgartner M, Tzankov A, Hilbe W, Schwentner I, Sprinzl GM, Utermann G, Zwierzina H. Low incidence of mutations in EGFR kinase domain in Caucasian patients with head and neck squamous cell carcinoma. European journal of cancer (Oxford, England : 1990). 2006;42(1):109-11. Epub 2005/12/06. doi: 10.1016/j.ejca.2005.08.034. PubMed PMID: 16324836.

78. Schwentner I, Witsch-Baumgartner M, Sprinzl GM, Krugmann J, Tzankov A, Jank S, Zwierzina H, Loeffler-Ragg J. Identification of the rare EGFR mutation p.G796S as somatic and germline mutation in white patients with squamous cell carcinoma of the head and neck. Head & neck. 2008;30(8):1040-4. Epub 2008/06/06. doi: 10.1002/hed.20831. PubMed PMID: 18528899.

79. Lemos-Gonzalez Y, Paez de la Cadena M, Rodriguez-Berrocal FJ, Rodriguez-Pineiro AM, Pallas E, Valverde D. Absence of activating mutations in the EGFR kinase domain in Spanish head and neck cancer patients. Tumour biology : the journal of the International Society for Oncodevelopmental Biology and Medicine. 2007;28(5):273-9. Epub 2007/10/27. doi: 10.1159/000110425. PubMed PMID: 17962724.

80. Sok JC, Coppelli FM, Thomas SM, Lango MN, Xi S, Hunt JL, Freilino ML, Graner MW, Wikstrand CJ, Bigner DD, Gooding WE, Furnari FB, Grandis JR. Mutant epidermal growth factor receptor (EGFRvIII) contributes to head and neck cancer growth and resistance to EGFR targeting. Clinical cancer research : an official journal of the American Association for Cancer Research. 2006;12(17):5064-73. Epub 2006/09/05. doi: 10.1158/1078-0432.ccr-06-0913. PubMed PMID: 16951222.

81. Vettore AL, Ramnarayanan K, Poore G, Lim K, Ong CK, Huang KK, Leong HS, Chong FT, Lim TK, Lim WK, Cutcutache I, McPherson JR, Suzuki Y, Zhang S, Skanthakumar T, Wang W, Tan DS, Cho BC, Teh BT, Rozen S, Tan P, Iyer NG. Mutational landscapes of tongue carcinoma reveal recurrent mutations in genes of therapeutic and prognostic relevance. Genome medicine. 2015;7(1):98. Epub 2015/09/24. doi: 10.1186/s13073-015-0219-2. PubMed PMID: 26395002; PMCID: Pmc4580363.

82. Lui VW, Hedberg ML, Li H, Vangara BS, Pendleton K, Zeng Y, Lu Y, Zhang Q, Du Y, Gilbert BR, Freilino M, Sauerwein S, Peyser ND, Xiao D, Diergaarde B, Wang L, Chiosea S, Seethala R, Johnson JT, Kim S, Duvvuri U, Ferris RL, Romkes M, Nukui T, Kwok-Shing Ng P, Garraway LA, Hammerman PS, Mills GB, Grandis JR. Frequent mutation of the PI3K pathway in head and neck cancer defines predictive biomarkers. Cancer discovery. 2013;3(7):761-9. Epub 2013/04/27. doi: 10.1158/2159-8290.cd-13-0103. PubMed PMID: 23619167; PMCID: Pmc3710532.

83. Osaki M, Oshimura M, Ito H. PI3K-Akt pathway: its functions and alterations in human cancer. Apoptosis : an international journal on programmed cell death. 2004;9(6):667-76. Epub 2004/10/27. doi: 10.1023/B:APPT.0000045801.15585.dd. PubMed PMID: 15505410.

84. Isaacsson Velho PH, Castro G, Jr., Chung CH. Targeting the PI3K Pathway in Head and Neck Squamous Cell Carcinoma. American Society of Clinical Oncology educational book / ASCO American Society of Clinical Oncology Meeting. 2015:123-8. Epub 2015/05/21. doi: 10.14694/EdBook_AM.2015.35.123. PubMed PMID: 25993150.

85. Seiwert TY, Zuo Z, Keck MK, Khattri A, Pedamallu CS, Stricker T, Brown C, Pugh TJ, Stojanov P, Cho J, Lawrence MS, Getz G, Bragelmann J, DeBoer R, Weichselbaum RR, Langerman A, Portugal L, Blair E, Stenson K, Lingen MW, Cohen EE, Vokes EE, White KP, Hammerman PS. Integrative and comparative genomic analysis of HPV-positive and HPV-

negative head and neck squamous cell carcinomas. Clinical cancer research : an official journal of the American Association for Cancer Research. 2015;21(3):632-41. doi: 10.1158/1078-0432.CCR-13-3310. PubMed PMID: 25056374; PMCID: 4305034.

86. Okami K, Wu L, Riggins G, Cairns P, Goggins M, Evron E, Halachmi N, Ahrendt SA, Reed AL, Hilgers W, Kern SE, Koch WM, Sidransky D, Jen J. Analysis of PTEN/MMAC1 alterations in aerodigestive tract tumors. Cancer research. 1998;58(3):509-11. Epub 1998/02/11. PubMed PMID: 9458098.

87. Qiu W, Schonleben F, Li X, Ho DJ, Close LG, Manolidis S, Bennett BP, Su GH. PIK3CA mutations in head and neck squamous cell carcinoma. Clinical cancer research : an official journal of the American Association for Cancer Research. 2006;12(5):1441-6. Epub 2006/03/15. doi: 10.1158/1078-0432.ccr-05-2173. PubMed PMID: 16533766; PMCID: Pmc1780023.

88. Kozaki K, Imoto I, Pimkhaokham A, Hasegawa S, Tsuda H, Omura K, Inazawa J. PIK3CA mutation is an oncogenic aberration at advanced stages of oral squamous cell carcinoma. Cancer science. 2006;97(12):1351-8. Epub 2006/10/21. doi: 10.1111/j.1349-7006.2006.00343.x. PubMed PMID: 17052259.

89. Murugan AK, Hong NT, Fukui Y, Munirajan AK, Tsuchida N. Oncogenic mutations of the PIK3CA gene in head and neck squamous cell carcinomas. International journal of oncology. 2008;32(1):101-11. Epub 2007/12/22. PubMed PMID: 18097548.

90. Fenic I, Steger K, Gruber C, Arens C, Woenckhaus J. Analysis of PIK3CA and Akt/protein kinase B in head and neck squamous cell carcinoma. Oncology reports. 2007;18(1):253-9. Epub 2007/06/06. PubMed PMID: 17549376.

91. Kostakis GC, Papadogeorgakis N, Koumaki V, Kamakari S, Koumaki D, Alexandridis C. Absence of hotspot mutations in exons 9 and 20 of the PIK3CA gene in human oral squamous cell carcinoma in the Greek population. Oral surgery, oral medicine, oral pathology, oral radiology, and endodontics. 2010;109(5):e53-8. Epub 2010/04/27. doi: 10.1016/j.tripleo.2010.01.015. PubMed PMID: 20416519.

92. Cohen Y, Goldenberg-Cohen N, Shalmon B, Shani T, Oren S, Amariglio N, Dratviman-Storobinsky O, Shnaiderman-Shapiro A, Yahalom R, Kaplan I, Hirshberg A. Mutational analysis of PTEN/PIK3CA/AKT pathway in oral squamous cell carcinoma. Oral oncology. 2011;47(10):946-50. Epub 2011/08/10. doi: 10.1016/j.oraloncology.2011.07.013. PubMed PMID: 21824802.

93. Suda T, Hama T, Kondo S, Yuza Y, Yoshikawa M, Urashima M, Kato T, Moriyama H. Copy number amplification of the PIK3CA gene is associated with poor prognosis in non-lymph node metastatic head and neck squamous cell carcinoma. BMC cancer. 2012;12:416. Epub 2012/09/22. doi: 10.1186/1471-2407-12-416. PubMed PMID: 22994622; PMCID: Pmc3518180.

94. Redon R, Muller D, Caulee K, Wanherdrick K, Abecassis J, du Manoir S. A simple specific pattern of chromosomal aberrations at early stages of head and neck squamous cell carcinomas: PIK3CA but not p63 gene as a likely target of 3q26-qter gains. Cancer research. 2001;61(10):4122-9. Epub 2001/05/19. PubMed PMID: 11358835.

95. Murugan AK, Munirajan AK, Tsuchida N. Genetic deregulation of the PIK3CA oncogene in oral cancer. Cancer letters. 2013;338(2):193-203. Epub 2013/04/20. doi: 10.1016/j.canlet.2013.04.005. PubMed PMID: 23597702.

96. Agrawal N, Frederick MJ, Pickering CR, Bettegowda C, Chang K, Li RJ, Fakhry C, Xie TX, Zhang J, Wang J, Zhang N, El-Naggar AK, Jasser SA, Weinstein JN, Trevino L, Drummond JA, Muzny DM, Wu Y, Wood LD, Hruban RH, Westra WH, Koch WM, Califano JA, Gibbs RA, Sidransky D, Vogelstein B, Velculescu VE, Papadopoulos N, Wheeler DA, Kinzler KW, Myers JN. Exome sequencing of head and neck squamous cell carcinoma reveals inactivating mutations in NOTCH1. Science (New York, NY). 2011;333(6046):1154-7. Epub 2011/07/30. doi: 10.1126/science.1206923. PubMed PMID: 21798897; PMCID: Pmc3162986.

97. Sun W, Gaykalova DA, Ochs MF, Mambo E, Arnaoutakis D, Liu Y, Loyo M, Agrawal N, Howard J, Li R, Ahn S, Fertig E, Sidransky D, Houghton J, Buddavarapu K, Sanford T, Choudhary A, Darden W, Adai A, Latham G, Bishop J, Sharma R, Westra WH, Hennessey P, Chung CH, Califano JA. Activation of the NOTCH pathway in head and neck cancer. Cancer research. 2014;74(4):1091-104. doi: 10.1158/0008-5472.CAN-13-1259. PubMed PMID: 24351288; PMCID: 3944644.

98. Yap LF, Lee D, Khairuddin A, Pairan MF, Puspita B, Siar CH, Paterson IC. The opposing roles of NOTCH signalling in head and neck cancer: a mini review. Oral diseases. 2015;21(7):850-7. Epub 2015/01/13. doi: 10.1111/odi.12309. PubMed PMID: 25580884.

99. Song X, Xia R, Li J, Long Z, Ren H, Chen W, Mao L. Common and complex Notch1 mutations in Chinese oral squamous cell carcinoma. Clinical cancer research : an official journal of the American Association for Cancer Research. 2014;20(3):701-10. Epub 2013/11/28. doi: 10.1158/1078-0432.ccr-13-1050. PubMed PMID: 24277457; PMCID: Pmc3946562.

100. Aoyama K, Ota Y, Kajiwara K, Hirayama N, Kimura M. Frequent mutations in NOTCH1 ligand-binding regions in Japanese oral squamous cell carcinoma. Biochemical and biophysical research communications. 2014;452(4):980-5. Epub 2014/09/23. doi: 10.1016/j.bbrc.2014.09.021. PubMed PMID: 25234595.

101. Blons H, Laurent-Puig P. TP53 and head and neck neoplasms. Human mutation. 2003;21(3):252-7. Epub 2003/03/06. doi: 10.1002/humu.10171. PubMed PMID: 12619110.

102. Gasco M, Crook T. The p53 network in head and neck cancer. Oral oncology. 2003;39(3):222-31. Epub 2003/03/06. PubMed PMID: 12618194.

103. Yadav DS, Chattopadhyay I, Verma A, Devi TR, Singh LC, Sharma JD, Kataki A, Saxena S, Kapur S. A pilot study evaluating genetic alterations that drive tobacco- and betel

quid-associated oral cancer in Northeast India. Tumour biology : the journal of the International Society for Oncodevelopmental Biology and Medicine. 2014;35(9):9317-30. Epub 2014/06/20. doi: 10.1007/s13277-014-2222-4. PubMed PMID: 24943687.

104. Chang YS, Hsu HT, Ko YC, Yeh KT, Chang SJ, Lin CY, Chang JG. Combined mutational analysis of RAS, BRAF, PIK3CA, and TP53 genes in Taiwanese patients with oral squamous cell carcinoma. Oral surgery, oral medicine, oral pathology and oral radiology. 2014;118(1):110-6.e1. Epub 2014/06/09. doi: 10.1016/j.oooo.2014.03.016. PubMed PMID: 24908601.

105. Tan DS, Wang W, Leong HS, Sew PH, Lau DP, Chong FT, Krisna SS, Lim TK, Iyer NG. Tongue carcinoma infrequently harbor common actionable genetic alterations. BMC cancer. 2014;14:679. Epub 2014/09/23. doi: 10.1186/1471-2407-14-679. PubMed PMID: 25234657; PMCID: Pmc4177593.

106. Zanaruddin SN, Yee PS, Hor SY, Kong YH, Ghani WM, Mustafa WM, Zain RB, Prime SS, Rahman ZA, Cheong SC. Common oncogenic mutations are infrequent in oral squamous cell carcinoma of Asian origin. PloS one. 2013;8(11):e80229. Epub 2013/11/14. doi: 10.1371/journal.pone.0080229. PubMed PMID: 24224046; PMCID: Pmc3817115.

107. Ogmundsdottir HM, Hilmarsdottir H, Astvaldsdottir A, Johannsson JH, Holbrook WP. Oral lichen planus has a high rate of TP53 mutations. A study of oral mucosa in icelanD. European journal of oral sciences. 2002;110(3):192-8. Epub 2002/07/18. PubMed PMID: 12120703.

108. Heaton CM, Durr ML, Tetsu O, van Zante A, Wang SJ. TP53 and CDKN2a mutations in never-smoker oral tongue squamous cell carcinoma. The Laryngoscope. 2014;124(7):E267-73. Epub 2014/01/17. doi: 10.1002/lary.24595. PubMed PMID: 24431303.

109. Nagai MA, Miracca EC, Yamamoto L, Kowalski LP, Brentani RR. TP53 mutations in upper aerodigestive squamous cell carcinomas from a group of Brazilian patients. American journal of surgery. 1995;170(5):492-4. Epub 1995/11/01. PubMed PMID: 7485740.

110. Chaves AC, Cherubini K, Herter N, Furian R, Santos DS, Squier C, Domann FE. Characterization of p53 gene mutations in a Brazilian population with oral squamous cell carcinomas. International journal of oncology. 2004;24(2):295-303. Epub 2004/01/14. PubMed PMID: 14719105.

111. Shi Q, Xiao K, Wei W, Zhang BY, Chen C, Xu Y, Chen LN, Song YT, Ma X, Zhang NS, Dong XP. Associations of TP53 mutations, codon 72 polymorphism and human papillomavirus in head and neck squamous cell carcinoma patients. Oncology reports. 2013;30(6):2811-9. Epub 2013/09/26. doi: 10.3892/or.2013.2750. PubMed PMID: 24064928.

112. Barnard D, Lehmann K, Hoal EG, van Helden PD, Victor TC. The spectrum of mutations in TP53 in laryngeal cancer patients from a high-incidence population shows similarities to many of the known mutational hotspots. Cancer genetics and cytogenetics. 2003;145(2):126-32. Epub 2003/08/26. PubMed PMID: 12935924.

113. Szymanska K, Levi JE, Menezes A, Wunsch-Filho V, Eluf-Neto J, Koifman S, Matos E, Daudt AW, Curado MP, Villar S, Pawlita M, Waterboer T, Boffetta P, Hainaut P, Brennan P. TP53 and EGFR mutations in combination with lifestyle risk factors in tumours of the upper aerodigestive tract from South America. Carcinogenesis. 2010;31(6):1054-9. Epub 2009/12/04. doi: 10.1093/carcin/bgp212. PubMed PMID: 19955396.

114. Ren WH, Jiang DK, Pei Y, Wang SQ, Yang XM, Yu L. Meta-analysis of associations between the TP53 Arg72Pro polymorphism with risk of head and neck carcinomas based on case-control studies. Genetics and molecular research : GMR. 2014;13(1):103-14. Epub 2014/01/22. doi: 10.4238/2014.January.8.9. PubMed PMID: 24446292.

115. Fakhry C, Westra WH, Li S, Cmelak A, Ridge JA, Pinto H, Forastiere A, Gillison ML. Improved survival of patients with human papillomavirus-positive head and neck squamous cell carcinoma in a prospective clinical trial. Journal of the National Cancer Institute. 2008;100(4):261-9. Epub 2008/02/14. doi: 10.1093/jnci/djn011. PubMed PMID: 18270337.

116. Chokunonga E, Borok MZ, Chirenje ZM, Nyakabau AM, Parkin DM. Trends in the incidence of cancer in the black population of Harare, Zimbabwe 1991-2010. International journal of cancer Journal international du cancer. 2013;133(3):721-9. Epub 2013/02/01. doi: 10.1002/ijc.28063. PubMed PMID: 23364833.

117. Ariyawardana A, Johnson NW. Trends of lip, oral cavity and oropharyngeal cancers in Australia 1982-2008: overall good news but with rising rates in the oropharynx. BMC cancer. 2013;13:333. Epub 2013/07/09. doi: 10.1186/1471-2407-13-333. PubMed PMID: 23829309; PMCID: Pmc3716721.

118. Rabiei M, Basirat M, Rezvani SM. Trends in the incidence of Oral and Pharyngeal Cancer (ICD00-14) in Guilan, North of Iran. Journal of oral pathology & medicine : official publication of the International Association of Oral Pathologists and the American Academy of Oral Pathology. 2015. Epub 2015/10/02. doi: 10.1111/jop.12369. PubMed PMID: 26426284.

119. Marioni G, Agostini M, Bedin C, Blandamura S, Stellini E, Favero G, Lionello M, Giacomelli L, Burti S, D'Angelo E, Nitti D, Staffieri A, De Filippis C. Survivin and laryngeal carcinoma prognosis: nuclear localization and expression of splice variants. Histopathology. 2012;61(2):247-56. Epub 2012/03/16. doi: 10.1111/j.1365-2559.2012.04217.x. PubMed PMID: 22416874.

120. Russo A, Corsale S, Agnese V, Macaluso M, Cascio S, Bruno L, Surmacz E, Dardanoni G, Valerio MR, Vieni S, Restivo S, Fulfaro F, Tomasino RM, Gebbia N, Bazan V. TP53 mutations and S-phase fraction but not DNA-ploidy are independent prognostic indicators in laryngeal squamous cell carcinoma. Journal of cellular physiology. 2006;206(1):181-8. Epub 2005/06/21. doi: 10.1002/jcp.20447. PubMed PMID: 15965904.

121. Eriksen JG, Buffa FM, Alsner J, Steiniche T, Bentzen SM, Overgaard J. Molecular profiles as predictive marker for the effect of overall treatment time of radiotherapy in supraglottic larynx squamous cell carcinomas. Radiotherapy and oncology : journal of the

European Society for Therapeutic Radiology and Oncology. 2004;72(3):275-82. Epub 2004/09/29. doi: 10.1016/j.radonc.2004.07.014. PubMed PMID: 15450725.

122. Shah S, Shah S, Padh H, Kalia K. Genetic alterations of the PIK3CA oncogene in human oral squamous cell carcinoma in an Indian population. Oral surgery, oral medicine, oral pathology and oral radiology. 2015;120(5):628-35. Epub 2015/10/11. doi: 10.1016/j.oooo.2015.08.003. PubMed PMID: 26453385.

123. Er TK, Wang YY, Chen CC, Herreros-Villanueva M, Liu TC, Yuan SS. Molecular characterization of oral squamous cell carcinoma using targeted next-generation sequencing. Oral diseases. 2015;21(7):872-8. Epub 2015/07/15. doi: 10.1111/odi.12357. PubMed PMID: 26173098.

124. Chen SJ, Liu H, Liao CT, Huang PJ, Huang Y, Hsu A, Tang P, Chang YS, Chen HC, Yen TC. Ultra-deep targeted sequencing of advanced oral squamous cell carcinoma identifies a mutation-based prognostic gene signature. Oncotarget. 2015;6(20):18066-80. Epub 2015/05/20. doi: 10.18632/oncotarget.3768. PubMed PMID: 25980437; PMCID: Pmc4621868.

125. Comprehensive genomic characterization of head and neck squamous cell carcinomas. Nature. 2015;517(7536):576-82. Epub 2015/01/30. doi: 10.1038/nature14129. PubMed PMID: 25631445; PMCID: Pmc4311405.

126. Cortelazzi B, Verderio P, Ciniselli CM, Pizzamiglio S, Bossi P, Gloghini A, Gualeni AV, Volpi CC, Locati L, Pierotti MA, Licitra L, Pilotti S, Perrone F. Receptor tyrosine kinase profiles and human papillomavirus status in oropharyngeal squamous cell carcinoma. Journal of oral pathology & medicine : official publication of the International Association of Oral Pathologists and the American Academy of Oral Pathology. 2015;44(9):734-45. Epub 2014/12/17. doi: 10.1111/jop.12301. PubMed PMID: 25495427.

127. Cha JD, Kim HJ, Cha IH. Genetic alterations in oral squamous cell carcinoma progression detected by combining array-based comparative genomic hybridization and multiplex ligation-dependent probe amplification. Oral surgery, oral medicine, oral pathology, oral radiology, and endodontics. 2011;111(5):594-607. Epub 2011/02/22. doi: 10.1016/j.tripleo.2010.11.020. PubMed PMID: 21334929.

128. Tu HF, Chang KW, Chiang WF, Liu CJ, Yu EH, Liu ST, Lin SC. The frequent co-expression of the oncogenes PIK3CA and PAK1 in oral carcinomas. Oral oncology. 2011;47(3):211-6. Epub 2011/02/12. doi: 10.1016/j.oraloncology.2011.01.003. PubMed PMID: 21310649.

# Chapter 2 : Differential Compensation Mechanisms Define Resistance to PI3K Inhibitors in *PIK3CA* Amplified HNSCC [2]


## Abstract

**Objective**: Recent sequencing studies of head and neck squamous cell carcinomas (HNSCCs) have identified the phosphatidylinositol 3-kinase (PI3K) pathway as the most frequently mutated, oncogenic pathway in this cancer type. Despite the frequency of activating PIK3CA genomic alterations (the gene encoding the catalytic subunit of PI3K), targeted inhibitors of PI3K have not shown clinical efficacy as monotherapies. We hypothesized that co-dependent pathways, including the Ras-MEK-ERK pathway, may still be functional in the presence of PI3K inhibitors and might serve as mediators of this resistance.

**Methods:** We assessed the hypothesis using cell viability assays via resazurin and trypan blue exclusion assays and Western blot to characterize Ras-MEK-ERK pathway activity.

**Study Design**: We evaluated this hypothesis in six PIK3CA-amplified, PI3K inhibitor-resistant HNSCC cell lines following treatment with pan and alpha-isoform selective PI3K inhibitors (BKM120 and HS-173 respectively). We also tested the effect of combination treatment with PI3K inhibitor HS-173 and MEK inhibitor trametinib or EGFR inhibitor gefitinib.

**Results**: Our results displayed maintenance of Ras-MEK-ERK pathway activity in 4 of 6 HNSCC cell lines after PI3K inhibitor treatment. We also found that UM-SCC-69 and UM-SCC-


[2] This chapter was published in *Otorhinolaryngology-head and neck surgery* and completed in collaboration with the following authors: Elizabeth Leonard, Aditi Kulkarni, and J. Chad Brenner.

108 cells display synergistic responses to dual therapy with HS-173 and either trametinib or gefitinib.

**Conclusion**: This study suggests that inhibition of the PI3K and Ras-MEK-ERK pathways might be effective in some HNSCC patients; however, it also prompts the study of additional resistance mechanisms to identify synergistic combination therapies for tumors resistant to these di-therapies.

## Introduction

Head and neck squamous cell carcinoma (HNSCC) is the sixth most common form of cancer by incidence worldwide and represents ~3% of cancer cases in the United States. Common modalities used to treat HNSCC patients include surgery, radiation, and cytotoxic chemotherapy. Despite the use of these regimens, however, patient prognosis is poor and recurrence and metastasis are very common. Five year survival rates for HNSCC are only 40-50% and have remained unchanged for many years (Massano et al. 2006).

An increased understanding of the genetic alterations in HNSCC may guide the use of targeted therapies and improve patient survival (Ludwig et al. 2016). Recent sequencing studies have identified mutations and copy number changes in genes within a number of cellular pathways in HNSCCs. These genetic changes may contribute to cancer development or progression, and learning more about them will guide personalized medicine protocols for this cancer type, which seek to match patients with an effective treatment option given the specific genetic signature of their disease (Birkeland and Brenner 2015; Birkeland et al. 2015a; Birkeland et al. 2015b; Tillman BN 2015). Among the most comprehensive genetic analyses of HNSCCs is the The Cancer Genome Atlas (TCGA) dataset, which profiles somatic mutations and copy number alterations in 279 HNSCC patients. This study and others have identified the phosphatidylinositol 3-kinase (PI3K) pathway as the most frequently mutated, oncogenic targetable pathway in this cancer type (Comprehensive genomic characterization of head and neck squamous cell carcinomas 2015; Lui et al. 2013). Of the genes in the PI3K pathway, *PIK3CA*, which encodes the catalytic subunit and alpha isoform of PI3K, is the most frequently altered. Activating mutation and/or amplification of this gene were observed in 36.9% of the TCGA HNSCC cohort (Comprehensive genomic characterization of head and neck squamous cell carcinomas 2015). These aberrations lead to

increased cell growth and viability, may drive tumor progression, and are more commonly observed in advanced stage disease (Isaacsson Velho et al. 2015; Osaki et al. 2004).

Inhibitors of PI3K have been developed and tested in clinical trials for HNSCC as well as other cancer types. Despite frequent activation of the PI3K pathway and its importance in HNSCC; however, these therapies have shown limited efficacy in unmatched clinical trials to date. In one recent trial, for example, HNSCC patients were given docetaxel alone or in combination with PX-866, an oral pan-PI3K inhibitor. The addition of PX-866 did not improve progression free survival in this cohort (Jimeno et al. 2015).

Resistance to treatment with PI3K inhibitors is poorly understood, although some data has suggested that these compounds are more effective in patients with alterations in *PIK3CA* or loss of *PTEN*. (*PTEN* is a tumor suppressor gene that acts as a "brake" on PI3K function and is inactivated in 10% of HNSCC patients according to TCGA data.) While an analysis of early clinical trials for PI3K inhibitors showed that PI3K altered patients were more responsive to PI3K inhibitors than patients without *PIK3CA* mutation or *PTEN* loss, this study also indicated only an 18% overall response rate within the PI3K altered molecular subgroup (Janku et al. 2014). These findings suggest that important resistance mechanisms to PI3K inhibitors are frequently present, even in PI3K altered HNSCCs.

PI3K inhibitor resistance may be due to activation of a compensatory pathway, which cells utilize to grow and divide even in the absence of PI3K signaling. The Ras-MEK-ERK pathway, as an important contributor to cell proliferation and growth, is a likely candidate for codependence in cases of PI3K inhibitor resistance. Previous studies have demonstrated that PI3K and MEK inhibitors are synergistic in some HNSCCs (Mazumdar et al. 2014; Mohan et al. 2015; Wirtz et al. 2015), as well as in a variety of other cancer types (Ayub et al. 2015; Inaba et al. 2016; Sunayama

et al. 2010; Xing and Hogge 2013). In addition, based on preclinical evidence and frequent genetic alterations in HNSCC, trials for pan PI3K inhibitor BKM120 and alpha-isoform specific PI3K inhibitor BYL719 are ongoing (examples include: NCT02537223, NCT02051751 and NCT01602315). These agents are being tested in patients not only as monotherapies but also in combination with anti-EGFR antibody cetuximab. Inhibiting a receptor tyrosine kinase such as EGFR blocks Ras-MEK-ERK signaling and has shown efficacy in other cancer models (Serra et al. 2011). However, the specific patients that are responsive to mono- and combination therapies cannot currently be identified—each patient's tumor has a unique genetic signature and there is currently a lack of useful biomarkers to stratify patients and predict responses to treatment with PI3K inhibitor combination therapies.

In this study, we explore the sensitivity of several models with *PIK3CA* genetic alterations to combination therapies being considered for HNSCC personalized medicine trials. We sought to identify the relationships between drug sensitivity and resistance mechanisms in these models in order to begin to understand what percentages of patients would respond to each proposed combination therapy. We examined activation of the Ras-MEK-ERK pathway as a mechanism for resistance to PI3K inhibitors in PI3K altered HNSCC. To do this, we tested six HNSCC cell lines, each of which displayed both amplification of *PIK3CA* and resistance to PI3K inhibitor monotherapy treatment, for compensation through this pathway in the presence of PI3K inhibitors.

## Materials and Methods

### *Cell Culture*

UM-SCC cells (University of Michigan) are derived from human head and neck squamous cell carcinoma patient tumor samples and were cultured in a humidified incubator at 37 °C with 5%

(vol/vol) $CO_2$ as previously described (Brenner et al. 2010). Cells were cultured in DMEM with 10% FBS, 1X Pen/Strep, 1X NEAA. Details of DNA copy number analysis are being submitted as a separate manuscript. All cell lines were confirmed to contain wild type *PIK3CA* as previously reported from Nimblegen V2 exome capture based experiments (Liu et al. 2013).

*Chemicals*

BKM120, HS-173, trametinib, and gefitinib were purchased from Selleck Chemicals. All compounds were initially dissolved in 100% DMSO to 10 mM and then diluted to the indicated concentrations for studies *in vitro*.

*Western Blotting*

Cells at 70-80% confluency were treated with DMSO or inhibitor(s) for six hours prior to harvesting and lysing in radioimmunoprecipitation assay buffer. Ten micrograms of each cell harvest was used, and standard Western blot protocols were followed as previously described (Birkeland et al. 2016). Primary antibodies against pERK1/2 (Thr202/Tyr204) (1:1000, catalog No. 4370; Cell Signaling Technology), ERK (1:1000, catalog No. 4695; Cell Signaling Technology), pAKT (Ser473) (1:1000, catalog No. 4060; Cell Signaling Technology), AKT (1:1000, catalog No. 4685; Cell Signaling Technology), and HSP90 (1:2000, catalog No. 4877; Cell Signaling Technology) were incubated overnight at 4°C or for 1 hour at room temperature, followed by a goat anti-rabbit horseradish peroxidase (catalog No. 111-035-045; Jackson ImmunoResearch) secondary antibody at room temperature for 1 hour. The blots were then visualized with chemiluminescence and imaged. 300dpi or greater images were retained from all Westerns and representative blots are shown.

*Trypan Blue Assay*

To test for cell membrane integrity and access cell viability, 32,000 cells per well were seeded into 24-well cell culture plates. After 24 hours, cells were exposed to DMSO or inhibitor in a multipoint dose-response. After 72 hour exposure, cells were disaggregated in 50 uL of medium. 10 uL of the suspension was mixed with 10 uL of trypan blue (0.4% Invitorgen) and viability and total cell count were measured using Countess Automated Cell Counter (Invitrogen).

*Resazurin Assay*

To study relative cell viability, 2,000 cells per well were seeded in 384-well microplates using a Multiflo liquid handling dispensing system. After 24 hours, cells were treated with inhibitor or DMSO in a 10-point two-fold dilution series in quadruplicate. 96-well plates were prepared with inhibitors in 200X concentration and then diluted to 10X concentration in media in a second 96-well plate using the Agilent Bravo Automated Liquid Handling Platform and VWorks Automation Control Software. These inhibitors were then used to treat the cells with the desired compound concentration, again using liquid handling robotics. Cells were stained with resazurin (Sigma) in PBS for 12-24 hours before fluorescent signal intensity was quantified. Quantification occured 72 hours after treatment using the Cytation3 fluorescence plate reader at excitation and emission wavelengths of 540 and 612 nM, respectively.

*Statistical Analysis*

Statistical analyses were performed using GraphPad Prism 6 software. Unpaired, two-tailed Student's t-tests were conducted to compare total cell counts following DMSO and 1 μM trametinib treatment from trypan blue exclusion assays with $p<0.05$ considered statistically significant. For resazurin assays, $IC_{50}$ values were determined from the mean and standard deviation of at least quadruplicate measurements for each treatment and cell line.

## Results

*PIK3CA Alteration in HNSCC Cell Lines*

We first identified a panel of cell lines that displayed amplification of *PIK3CA* to comprise our HNSCC panel. Copy number amplification for the six cell lines ranged from 2.67 to 6, with UM-SCC-69 and -108 exhibiting the highest level of amplification with 6 and 4 copies of *PIK3CA*, respectively. UM-SCC-47 and -14A had lower levels of *PIK3CA* amplification, each with 2.67 copies of the gene as shown in Figure 2-1A. None of the six cell lines displayed mutations in *PIK3CA* (Liu et al. 2013).

*PIK3CA Amplified HNSCC Sensitivity to PI3K Inhibitors*

To then determine the sensitivity of the *PIK3CA* amplified HNSCC cell lines in our panel to PI3K inhibition, we used a resazurin cell viability assay to determine the $IC_{50}$ value for each cell line in response to alpha-isoform specific PI3K inhibitor HS-173 and the pan PI3K inhibitor BKM120. We identified similar sensitivity to these agents, consistent with common alterations in *PIK3CA* and the important role of the alpha isoform in HNSCC. UM-SCC-1 cells were the most sensitive, with $IC_{50}$ less than 1 μM for both inhibitors. UM-SCC-108 displayed the greatest resistance to a PI3K inhibitor, with an $IC_{50}$ close to 25 μM for HS-173 (Figure 2-1**,** Figure 2-2). Despite the moderate responses to these treatments, $IC_{50}$ values of these magnitudes are indicative of at least partial PI3K inhibitor resistance, suggesting the opportunity to assess combination therapies that are being advanced for clinical trials in these models.

*PI3K inhibitor resistant HNSCC cell lines display differential activation of the Ras-MEK-ERK pathway*

Thus, to learn more about the mechanisms of resistance of PI3K inhibitors in HNSCC, we first examined the activation of downstream PI3K and Ras-MEK-ERK pathway members after PI3K inhibitor treatment in each of the cell lines in our panel. We hypothesized that Ras-MEK-ERK pathway activity would be maintained if the pathway represents an important compensatory mechanism. We treated each cell line with 5 μM HS-173 or BKM120 and used Western blotting to assess phosphorylated and total levels of Akt and ERK (Figure 2-1B-G). In each cell line, Akt phosphorylation was reduced after treatment with HS-173 or BKM120, consistent with the effect of these drugs on downstream members of the PI3K pathway. In the UM-SCC-1 and UM-SCC-47 cells, phosphorylation of ERK was also reduced by 5 μM PI3K inhibitor treatment (Figure 2-1B, C). In the other four cell lines, ERK phosphorylation was maintained (Figure 2-1D-G). This maintenance of Ras-MEK-ERK pathway activity suggests that this pathway may be a co-dependent with the PI3K pathway in the UM-SCC-14A, 69, 92, and 108 cells.

*Potential Synergy of PI3K and MEK Inhibitors in HNSCC*

To explore the hypothesis that MEK signaling maintains viability in the presence of PIK3CA inhibition in some models, we then tested the combination of PI3K inhibitor HS-173 and MEK inhibitor trametinib in the panel of HNSCC cells. If Ras-MEK-ERK pathway activation is a mechanism of resistance to PI3K inhibitor treatment, adding trametinib as a second inhibitor might sensitize the cells to the inhibitors and result in a synergistic reduction in cell viability. Using a resazurin cell viability assay, we observed at least additive effects of these two agents in UM-SCC-69 and UM-SCC-108 cells (Figure 2-3). Lack of benefit from the combination with MEK inhibitor in other HNSCC cell lines was not due to the inability of trametinib to block

downstream Ras-MEK-ERK pathway activity, as 5 μM treatment resulted in complete inhibition of ERK phosphorylation via Western blotting (Figure 2-3, insets). We also performed trypan blue exclusion assays to examine the effect of this drug concentration on absolute cell viability in the two cell lines in which PI3K and MEK inhibitors displayed at least additive effects (Figure 2-4). Trypan blue dye assays demonstrated that while trametinib monotherapy inhibited cell proliferation, it did not reduce cell viability ($p<0.05$). Combining PI3K and MEK inhibitors led to further reductions in cell viability.

*Potential Synergy of PI3K and EGFR Inhibitors in HNSCC*

Ras-MEK-ERK pathway activity can also be inhibited more broadly using an agent targeted against a receptor tyrosine kinase such as the epidermal growth factor receptor (EGFR). EGFR is frequently amplified in HNSCC and cetuximab, a monoclonal EGFR antibody is the only FDA-approved targeted therapy for this cancer type and several trials are exploring this combination clinically. We hypothesized that blocking EGFR and the downstream Ras-MEK-ERK pathway in combination with PI3K might be a more effective treatment than using a PI3K and MEK inhibitor combination in some models. To explore this possibility, we treated the cell lines displaying Ras-MEK-ERK pathway activity after PI3K inhibitor treatment (UM-SCC-14A, 69, 92, and 108) with HS-173 in combination with gefitinib, a small molecule inhibitor of EGFR. Results of a resazurin cell viability assay for HS-173 in combination with gefitinib again indicated potential synergy in UM-SCC-69 and UM-SCC-108, but not UM-SCC-14A and UM-SCC-92 (Figure 2-5). We also treated these four cell lines with vehicle, 1 μM gefitnib, 1 μM HS-173, or a combination of the inhibitors at 1 μM each. Western blot analysis of each cell line indicated that ERK phosphorylation was reduced by gefitinib treatment and Akt phosphorylation was reduced by HS-173 treatment. These results are consistent with the effects of these inhibitors on

downstream members of the Ras-MEK-ERK and PI3K pathways, respectively. Treatment with both drugs led to decreased phosphorylation of both ERK and Akt, indicating that this combination caused the inhibition of expected targets (Figure 2-6).

## Discussion

In summary, our *PIK3CA* amplified HNSCC cell lines show intermediate to strong resistance to PI3K inhibitors suggesting that matched PI3K targeted therapies may not be effective as monotherapies in this cancer type. While some of the more sensitive UM-SCC cell lines in our panel display similar sensitivity to PI3K inhibitors as compared to *PIK3CA* mutant or *PTEN* deleted cancer cell lines with $IC_{50}$ of approximately 1 μM (Koul et al. 2012; Mueller et al. 2012), other resistant models (particularly UM-SCC-92) have $IC_{50}$ values closer those of fibroblast cells. This data is consistent with a phase 1/2 study of PX-866 and docetaxel in patients with solid tumors (NCT01204099), in which only a few HNSCC patients with *PIK3CA* amplification responded to the monotherapy despite pharmacodynamics experiments showing on target effect of the drug (Jimeno et al. 2015). As many groups have postulated that compensation occurs through either EGFR signaling or directly though alternative pathways activating Ras-MEK-ERK signaling, we also assessed response to dual inhibitor therapies targeting *PIK3CA* and EGFR or MEK/ERK signaling. These experiments showed 2/6 (33%) of the cell lines displayed additive to synergistic effects of alpha-isoform specific PI3K inhibitor HS-173 and MEK inhibitor trametinib or EGFR inhibitor gefitinib; there was no benefit of the addition of the Ras-MEK-ERK inhibitor in the other models. This data is promising and supports the preclinical data for combination trials simultaneously inhibiting both of these pathways (Mazumdar et al. 2014; Mohan et al. 2015; Wirtz et al. 2015). Our data predict that these treatments will lead to

response in a subset of tumors, but also suggests that additional unknown compensatory mechanisms are driving *PIK3CA* inhibitor resistance in other HNSCCs.

Thus, the data presented here suggest that multiple different pathways drive PI3K inhibitor resistance and additional work is needed to understand the frequencies with which each pathway is utilized and the biomarkers predicting which combination therapy would most benefit individual patients. While we didn't fully assess all combinations that have been suggested in the literature, our data provides the foundation for future studies in HNSCC that leverage unbiased approaches. Further testing of additional HNSCC cell lines, might identify other *PIK3CA* amplified models with more significant responses to PI3K monotherapy or to combinations that are advancing in clinical trials. Likewise, systematic discovery based approaches to identify novel combinations that inhibit the growth of models resistant to both the Ras-MEK-ERK + PI3K and EGFR + PI3K therapies are needed to understand the additional pathways driving resistance. These studies might also improve cell kill in an even more complex therapeutic setting (e.g. tri-therapy or cycled di-therapies). For example, exploring other *PIK3CA* amplified or mutated HNSCC models might allow us to stratify responses based on additional genetic alterations in the PI3K, Ras-MEK-ERK, and other cellular pathways. We could then assess genetics biomarkers (personalized medicine) to predict which patients might be most and least sensitive to a specific PI3K-based combination regimen. Indeed, focusing on developing therapies for the most highly recurrent compensatory pathways may be one approach to improving therapy.

We have entered an exciting time in the HNSCC field. Several institutions have initiated personalized medicine protocols, such as the MiOTOseq trial, which aim to characterize the molecular genetics of every consenting HNSCC patient that enters the clinic. These studies are likely to lead to the development of complex genetic databases and, hopefully, increase the

enrollment of HNSCC patients on appropriate interventional trials. As noted above, personalized trials have increased the overall survival of patients with HNSCC (Chau et al. 2016; Tsimberidou et al. 2014), but the overall rates of improvement have been underwhelming. As the field moves forward, we need to begin to understand how HNSCCs respond to matched targeted therapies in order to take the next step towards improving overall response. Here, we focused on understanding the combinations of resistance pathways to inhibitors of the most recurrently altered oncogenic pathway in HNSCC. Our data indicates a complex and differential response to matched therapy; it also suggests the value of future work utilizing unbiased approaches to nominate co-dependent pathways driving this resistance. Developing an improved understanding of resistance to matched therapies in HNSCC as well as the frequencies with which each resistance mechanism is observed represents one key step to improving the overall survival of patients enrolling in personalized medicine trials.

## Figures

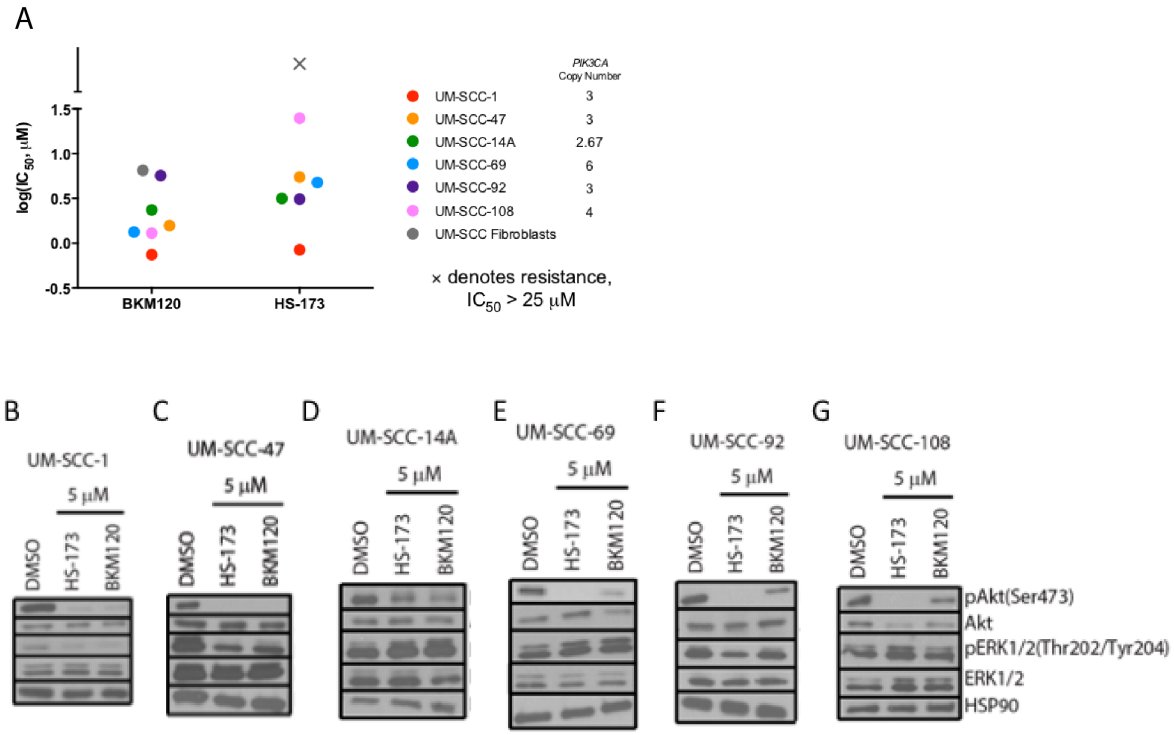


**Figure 2-1. Cell viability and Ras-MEK-ERK activity in response to PI3K inhibition.**

$IC_{50}$ via resazurin assay (A) and Western blot analysis of PI3K and Ras-MEK-ERK pathway activation in UM-SCC-1 (B), 47 (C), 14A (D), 69 (E), 92 (F), and 108 (G) following treatment with HS-173 and/or BKM120.

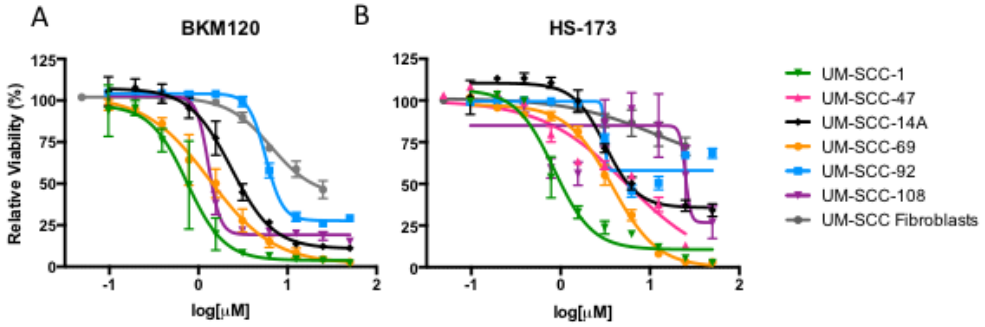


**Figure 2-2. Concentration response curves after PI3K inhibitor treatments in HNSCC cell lines and fibroblasts.**

Cell viability for UM-SCC-1, 47, 14A, 69, 92, 108 and fibroblasts after 72 hour treatment with increasing concentrations of PI3K inhibitors BKM120 (A) and HS-173 (B), as measured using a resazurin assay.

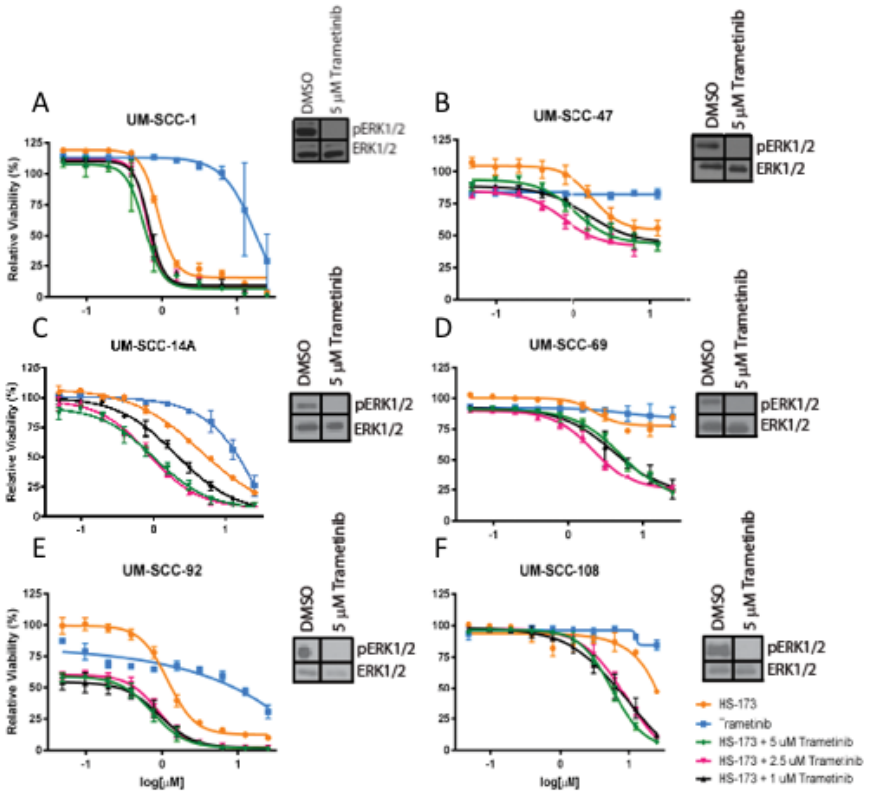


**Figure 2-3. Cell viability responses to co-treatment with HS-173 and trametinib via resaurin assays.**

Cell viability via resazurin assay and Ras-MEK-ERK pathway activation via Western blot analysis (insets) for UM-SCC-1 (A), 47 (B), 14A (C), 69 (D), 92 (E), and 108 (F) after treatment with trametinib and/or HS-173.

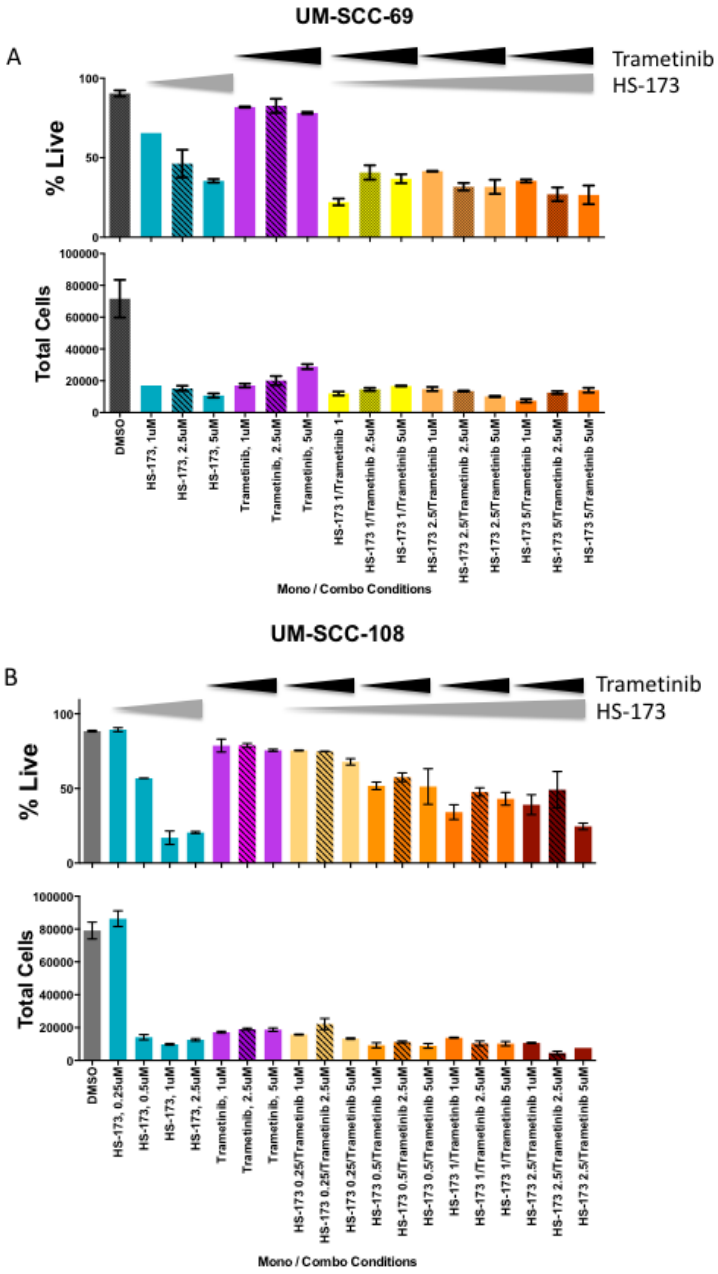


**Figure 2-4. Cell viability responses to co-treatment with HS-173 and trametinib via trypan blue exclusion assays.**

Live and total UM-SCC-69 (A) and UM-SCC-108 (B) cells after 72 hour treatment with increasing concentrations of trametinib and/or HS-173, as measured using a trypan blue exclusion assay.

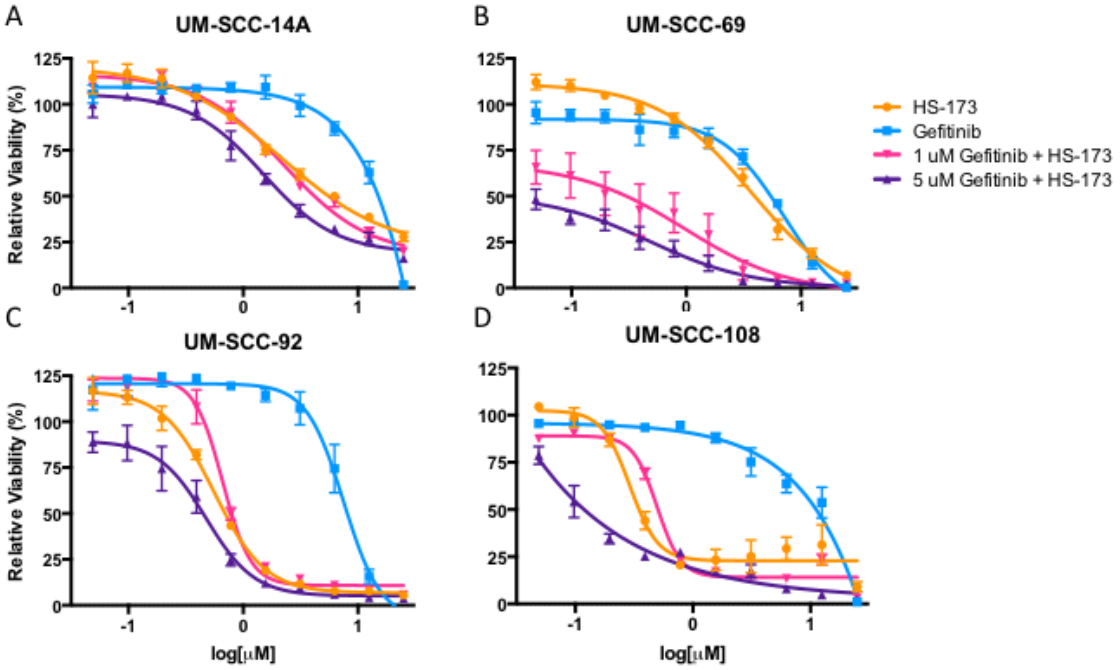


**Figure 2-5. Cell viability responses to co-treatment with HS-173 and gefitinib via resaurin assays.**

Cell viability for UM-SCC-14A (A), -69 (B), -92 (C), and -108 (D) after 72 hour treatment with increasing concentrations of gefitinib and/or HS-173, as measured using a resazurin assay.

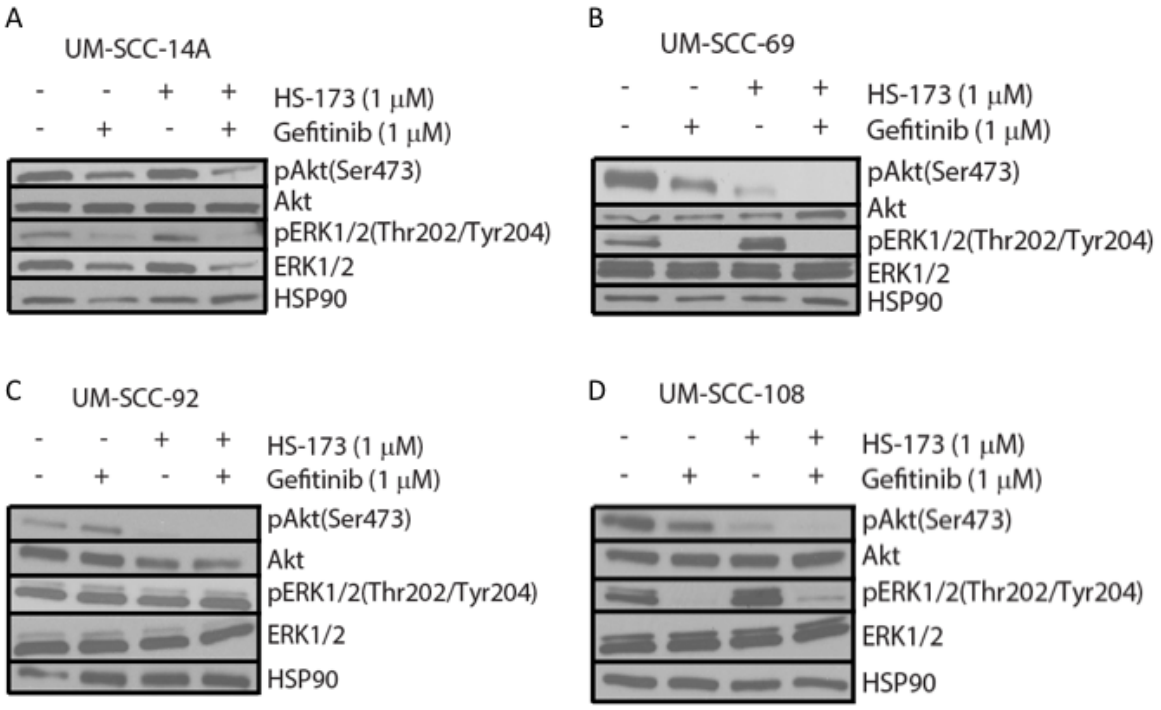


**Figure 2-6. Western blot analysis following co-treatment with HS-173 and gefitinib.**

Western blot analysis of downstream PI3K and RAS-MEK-ERK pathway activation in UM-SCC-14A (A), -69 (B), -92 (C), and -108 (D) following 6 hour treatment with 1 μM gefitinib and/or 1 μM HS-173.

## References


1. Massano J, Regateiro FS, Januario G, Ferreira A. Oral squamous cell carcinoma: review of prognostic and predictive factors. Oral surgery, oral medicine, oral pathology, oral radiology, and endodontics. 2006;102(1):67-76. Epub 2006/07/13. doi: 10.1016/j.tripleo.2005.07.038. PubMed PMID: 16831675.

2. Ludwig ML, Birkeland AC, Hoesli R, Swiecicki P, Spector ME, Brenner JC. Changing the paradigm: the potential for targeted therapy in laryngeal squamous cell carcinoma. Cancer Biol Med. 2016;13(1):87-100. Epub 2016/05/05. doi: 10.28092/j.issn.2095-3941.2016.0010. PubMed PMID: 27144065; PMCID: Pmc4850131.

3. Birkeland AC, Ludwig ML, Meraj TS, Brenner JC, Prince ME. The Tip of the Iceberg: Clinical Implications of Genomic Sequencing Projects in Head and Neck Cancer. Cancers. 2015;7(4):2094-109. Epub 2015/10/28. doi: 10.3390/cancers7040879. PubMed PMID: 26506389.

4. Birkeland AC, Uhlmann WR, Brenner JC, Shuman AG. Getting personal: Head and neck cancer management in the era of genomic medicine. Head & neck. 2015. Epub 2015/05/23. doi: 10.1002/hed.24132. PubMed PMID: 25995036; PMCID: Pmc4654712.

5. Birkeland AC, Brenner JC. Personalizing medicine in head and neck squamous cell carcinoma: The rationale for combination therapies. . Med Res Arch. 2015;3.

6. Tillman BN YM, Birkeland AC, Liu C, Hovelson DH, Cani AK, Palanisamy N, Carskadon S, Carey TE, Bradford CR, Tomlins S, McHugh JB, Spector ME, Brenner JC. . Targeted sequencing of an epidemiologically low risk patient defines Fibroblast Growth Factor Receptor family aberrations as a putative driver of head and neck squamous cell carcinoma. . Head Neck (in press). 2015.

7. Comprehensive genomic characterization of head and neck squamous cell carcinomas. Nature. 2015;517(7536):576-82. Epub 2015/01/30. doi: 10.1038/nature14129. PubMed PMID: 25631445; PMCID: Pmc4311405.

8. Lui VW, Hedberg ML, Li H, Vangara BS, Pendleton K, Zeng Y, Lu Y, Zhang Q, Du Y, Gilbert BR, Freilino M, Sauerwein S, Peyser ND, Xiao D, Diergaarde B, Wang L, Chiosea S, Seethala R, Johnson JT, Kim S, Duvvuri U, Ferris RL, Romkes M, Nukui T, Kwok-Shing Ng P, Garraway LA, Hammerman PS, Mills GB, Grandis JR. Frequent mutation of the PI3K pathway in head and neck cancer defines predictive biomarkers. Cancer discovery. 2013;3(7):761-9. Epub 2013/04/27. doi: 10.1158/2159-8290.cd-13-0103. PubMed PMID: 23619167; PMCID: Pmc3710532.

9. Osaki M, Oshimura M, Ito H. PI3K-Akt pathway: its functions and alterations in human cancer. Apoptosis. 2004;9(6):667-76. Epub 2004/10/27. doi: 10.1023/B:APPT.0000045801.15585.dd. PubMed PMID: 15505410.

10. Isaacsson Velho PH, Castro G, Jr., Chung CH. Targeting the PI3K Pathway in Head and Neck Squamous Cell Carcinoma. Am Soc Clin Oncol Educ Book. 2015:123-8. Epub 2015/05/21. doi: 10.14694/EdBook_AM.2015.35.123. PubMed PMID: 25993150.

11. Jimeno A, Bauman JE, Weissman C, Adkins D, Schnadig I, Beauregard P, Bowles DW, Spira A, Levy B, Seetharamu N, Hausman D, Walker L, Rudin CM, Shirai K. A randomized, phase 2 trial of docetaxel with or without PX-866, an irreversible oral phosphatidylinositol 3-kinase inhibitor, in patients with relapsed or metastatic head and neck squamous cell cancer. Oral oncology. 2015;51(4):383-8. Epub 2015/01/17. doi: 10.1016/j.oraloncology.2014.12.013. PubMed PMID: 25593016.

12. Janku F, Hong DS, Fu S, Piha-Paul SA, Naing A, Falchook GS, Tsimberidou AM, Stepanek VM, Moulder SL, Lee JJ, Luthra R, Zinner RG, Broaddus RR, Wheler JJ, Kurzrock R. Assessing PIK3CA and PTEN in early-phase trials with PI3K/AKT/mTOR inhibitors. Cell Rep. 2014;6(2):377-87. Epub 2014/01/21. doi: 10.1016/j.celrep.2013.12.035. PubMed PMID: 24440717; PMCID: Pmc4409143.

13. Wirtz ED, Hoshino D, Maldonado AT, Tyson DR, Weaver AM. Response of head and neck squamous cell carcinoma cells carrying PIK3CA mutations to selected targeted therapies. JAMA Otolaryngol Head Neck Surg. 2015;141(6):543-9. Epub 2015/04/10. doi: 10.1001/jamaoto.2015.0471. PubMed PMID: 25855885; PMCID: Pmc4474763.

14. Mohan S, Vander Broek R, Shah S, Eytan DF, Pierce ML, Carlson SG, Coupar JF, Zhang J, Cheng H, Chen Z, Van Waes C. MEK Inhibitor PD-0325901 Overcomes Resistance to PI3K/mTOR Inhibitor PF-5212384 and Potentiates Antitumor Effects in Human Head and Neck Squamous Cell Carcinoma. Clinical cancer research : an official journal of the American Association for Cancer Research. 2015;21(17):3946-56. Epub 2015/05/16. doi: 10.1158/1078-0432.ccr-14-3377. PubMed PMID: 25977343; PMCID: Pmc4558307.

15. Mazumdar T, Byers LA, Ng PK, Mills GB, Peng S, Diao L, Fan YH, Stemke-Hale K, Heymach JV, Myers JN, Glisson BS, Johnson FM. A comprehensive evaluation of biomarkers predictive of response to PI3K inhibitors and of resistance mechanisms in head and neck squamous cell carcinoma. Mol Cancer Ther. 2014;13(11):2738-50. Epub 2014/09/07. doi: 10.1158/1535-7163.mct-13-1090. PubMed PMID: 25193510; PMCID: Pmc4221385.

16. Inaba K, Oda K, Aoki K, Sone K, Ikeda Y, Miyasaka A, Kashiyama T, Fukuda T, Makii C, Arimoto T, Wada-Hiraike O, Kawana K, Yano T, Osuga Y, Fujii T. Synergistic antitumor effects of combination PI3K/mTOR and MEK inhibition (SAR245409 and pimasertib) in mucinous ovarian carcinoma cells by fluorescence resonance energy transfer imaging.

Oncotarget. 2016. Epub 2016/04/23. doi: 10.18632/oncotarget.8807. PubMed PMID: 27102436.

17. Sunayama J, Matsuda K, Sato A, Tachibana K, Suzuki K, Narita Y, Shibui S, Sakurada K, Kayama T, Tomiyama A, Kitanaka C. Crosstalk between the PI3K/mTOR and MEK/ERK pathways involved in the maintenance of self-renewal and tumorigenicity of glioblastoma stem-like cells. Stem Cells. 2010;28(11):1930-9. Epub 2010/09/22. doi: 10.1002/stem.521. PubMed PMID: 20857497.

18. Xing Y, Hogge DE. Combined inhibition of the phosphoinosityl-3-kinase (PI3Kinase) P110delta subunit and mitogen-extracellular activated protein kinase (MEKinase) shows synergistic cytotoxicity against human acute myeloid leukemia progenitors. Leuk Res. 2013;37(6):697-704. Epub 2013/03/26. doi: 10.1016/j.leukres.2013.03.003. PubMed PMID: 23522913.

19. Ayub A, Yip WK, Seow HF. Dual treatments targeting IGF-1R, PI3K, mTORC or MEK synergize to inhibit cell growth, induce apoptosis, and arrest cell cycle at G1 phase in MDA-MB-231 cell line. Biomed Pharmacother. 2015;75:40-50. Epub 2015/10/16. doi: 10.1016/j.biopha.2015.08.031. PubMed PMID: 26463630.

20. Serra V, Scaltriti M, Prudkin L, Eichhorn PJ, Ibrahim YH, Chandarlapaty S, Markman B, Rodriguez O, Guzman M, Rodriguez S, Gili M, Russillo M, Parra JL, Singh S, Arribas J, Rosen N, Baselga J. PI3K inhibition results in enhanced HER signaling and acquired ERK dependency in HER2-overexpressing breast cancer. Oncogene. 2011;30(22):2547-57. Epub 2011/02/01. doi: 10.1038/onc.2010.626. PubMed PMID: 21278786; PMCID: Pmc3107390.

21. Brenner JC, Graham MP, Kumar B, Saunders LM, Kupfer R, Lyons RH, Bradford CR, Carey TE. Genotyping of 73 UM-SCC head and neck squamous cell carcinoma cell lines. Head & neck. 2010;32(4):417-26. Epub 2009/09/18. doi: 10.1002/hed.21198. PubMed PMID: 19760794; PMCID: PMC3292176.

22. Liu J, Pan S, Hsieh MH, Ng N, Sun F, Wang T, Kasibhatla S, Schuller AG, Li AG, Cheng D, Li J, Tompkins C, Pferdekamper A, Steffy A, Cheng J, Kowal C, Phung V, Guo G, Wang Y, Graham MP, Flynn S, Brenner JC, Li C, Villarroel MC, Schultz PG, Wu X, McNamara P, Sellers WR, Petruzzelli L, Boral AL, Seidel HM, McLaughlin ME, Che J, Carey TE, Vanasse G, Harris JL. Targeting Wnt-driven cancer through the inhibition of Porcupine by LGK974. Proceedings of the National Academy of Sciences of the United States of America. 2013;110(50):20224-9. Epub 2013/11/28. doi: 10.1073/pnas.1314239110. PubMed PMID: 24277854; PMCID: Pmc3864356.

23. Birkeland AC, Yanik M, Tillman BN, Scott MV, Foltin SK, Mann JE, Michmerhuizen NL, Ludwig ML, Sandelski MM, Komarck CM, Carey TE, Prince ME, Bradford CR, McHugh JB, Spector ME, Brenner JC. Identification of Targetable ERBB2 Aberrations in Head and Neck Squamous Cell Carcinoma. JAMA otolaryngology-- head & neck surgery. 2016. Epub 2016/04/15. doi: 10.1001/jamaoto.2016.0335. PubMed PMID: 27077364.

24. Mueller A, Bachmann E, Linnig M, Khillimberger K, Schimanski CC, Galle PR, Moehler M. Selective PI3K inhibition by BKM120 and BEZ235 alone or in combination with chemotherapy in wild-type and mutated human gastrointestinal cancer cell lines. Cancer Chemother Pharmacol. 2012;69(6):1601-15. Epub 2012/05/01. doi: 10.1007/s00280-012-1869-z. PubMed PMID: 22543857.

25. Koul D, Fu J, Shen R, LaFortune TA, Wang S, Tiao N, Kim YW, Liu JL, Ramnarian D, Yuan Y, Garcia-Echevrria C, Maira SM, Yung WK. Antitumor activity of NVP-BKM120--a

selective pan class I PI3 kinase inhibitor showed differential forms of cell death based on p53 status of glioma cells. Clinical cancer research : an official journal of the American Association for Cancer Research. 2012;18(1):184-95. doi: 10.1158/1078-0432.CCR-11-1558. PubMed PMID: 22065080; PMCID: 3785365.

26. Tsimberidou AM, Wen S, Hong DS, Wheler JJ, Falchook GS, Fu S, Piha-Paul S, Naing A, Janku F, Aldape K, Ye Y, Kurzrock R, Berry D. Personalized medicine for patients with advanced cancer in the phase I program at MD Anderson: validation and landmark analyses. Clin Cancer Res. 2014;20(18):4827-36. Epub 2014/07/06. doi: 10.1158/1078-0432.ccr-14-0603. PubMed PMID: 24987059; PMCID: Pmc4518867.

27. Chau NG, Li YY, Jo VY, Rabinowits G, Lorch JH, Tishler RB, Margalit DN, Schoenfeld JD, Annino DJ, Goguen LA, Thomas T, Becker H, Haddad T, Krane JF, Lindeman NI, Shapiro GI, Haddad RI, Hammerman PS. Incorporation of Next-Generation Sequencing into Routine Clinical Care to Direct Treatment of Head and Neck Squamous Cell Carcinoma. Clinical cancer research : an official journal of the American Association for Cancer Research. 2016. doi: 10.1158/1078-0432.CCR-15-2314. PubMed PMID: 26763254.

# Chapter 3 : Rationale for Using Irreversible EGFR Inhibitors in Combination with PI3K Inhibitors for Advanced Head and Neck Squamous Cell Carcinoma[3]


## Abstract

Head and neck squamous cell carcinoma (HNSCC) is a common and debilitating form of cancer characterized by poor patient outcomes and low survival rates. In HNSCC, genetic aberrations in PI3K and EGFR pathway genes are common, and small molecules targeting these pathways have shown modest effects as monotherapies in patients. While emerging preclinical data support the combined use of PI3K and EGFR inhibitors in HNSCC, in-human studies have displayed limited clinical success so far. Here, we examined the responses of a large panel of patient-derived HNSCC cell lines to various combinations of PI3K and EGFR inhibitors, including EGFR agents with varying specificity and mechanistic characteristics. We confirmed the efficacy of PI3K and EGFR combination therapies, observing synergy with alpha isoform selective PI3K inhibitor HS-173 and irreversible EGFR/ERBB2 dual inhibitor afatinib in the majority of models tested. Surprisingly, however, our results demonstrated only modest improvement in response to HS-173 with reversible EGFR inhibitor gefitinib. This difference in efficacy was not explained by differences in ERBB target selectivity between afatinib and gefitinib; despite effectively disrupting ERBB2 phosphorylation, the addition of ERBB2 inhibitor CP-724714 failed to


[3] This chapter was published in *Molecular Pharmacology* and completed in collaboration with the following authors: Elizabeth Leonard, Chloe Matovina, Micah Harris, Gabrielle Herbst, Aditi Kulkarni, Jingyi Zhai, Hui Jiang, Thomas E. Carey, and J. Chad Brenner.

enhance the effect of HS-173 gefitinib dual-therapy. Accordingly, while irreversible ERBB inhibitors showed strong synergistic activity with HS-173 in our models, we observed that none of the reversible ERBB inhibitors were synergistic. Therefore, our results suggest that the ERBB inhibitor mechanism of action may be critical for enhanced synergy with PI3K inhibitors in HNSCC patients and motivate further preclinical studies for ERBB and PI3K combination therapies.

## Introduction

Head and neck squamous cell carcinoma (HNSCC) represents the sixth most common form of cancer by incidence worldwide and is often associated with either high alcohol and tobacco use or infection with high-risk human papilloma virus (HPV) (1, 2). The disease has 5-year survival rates of less than 50% for HPV negative tumors and around 80% for HPV positive tumors, and we believe that overall survival for patients will be improved by advancing novel therapeutic approaches that target aberrations common to different subsets of HNSCC tumors (3, 4). Furthermore, the development of effective rational combination therapies may be critical for overcoming common resistance mechanisms that emerge following targeted monotherapy. We believe this approach may have utility for both adapting clinical paradigms with adjuvant/neoadjuvant agents as well as advancing personalized medicine approaches through the development of rational combination therapies for the most prominent molecular alterations in HNSCC.

Of the potential targetable molecular alterations common to HNSCC, the phosphoinositide-3 kinase (PI3K) pathway is disrupted through genomic amplifications or activating point mutations in >30% of tumors (5-8) and the epidermal growth factor receptor (EGFR) is overexpressed in >90% of tumors (5, 6, 9). Inhibitors to each of these pathways have

already been advanced individually in HNSCC. For example, in a recent phase II trial, pan-PI3K inhibitor BKM120 (buparlisib) with paclitaxel improved survival as compared to paclitaxel and placebo in recurrent and metastatic HNSCC patients (10), and EGFR antibody cetuximab is currently in clinical use after demonstrating improved outcomes in combination with radiotherapy or cisplatin (11, 12). Thus, while PI3K and EGFR targeting therapies have been used with some clinical success, response rates are still relatively low and innate or acquired resistance mechanisms appear to be widespread (8, 10-14).

Preclinical data indicate that dual-therapies directed against both PI3K and EGFR pathways might improve responses in HNSCC (8, 15-20). Given these promising data, several clinical trials assessing the combination have been opened in HNSCC, most of which use the EGFR targeting antibody cetuximab in combination with various inhibitors of PI3K (e.g. NCT01816984, NCT2282371, NCT02822482). Unfortunately, however, one recently completed study showed no significant improvement in patient survival with the addition of pan-PI3K inhibitor PX-866 to cetuximab (21). These surprising data suggested that a deeper understanding of the molecular mechanisms of action that drive response to PI3K and EGFR therapies is necessary to fully interpret the results of these trials.

Here, due to the early reported disparity between *in vitro* and clinical trial results, we conducted further studies characterizing the responses to various classes of PI3K and EGFR dual therapies in HNSCC. We used a panel of genetically diverse HNSCC cell lines to examine responses to combinations of PI3K and EGFR inhibitors; in doing so, we sought to assess patterns of response that might translate to future clinical trial design and/or serve as a guide for future precision medicine protocols in HNSCC.

## Materials and Methods

*Cell Culture*

Cells were cultured in a humidified incubator at 37°C with 5% (vol/vol) $CO_2$. UM-SCC cells (University of Michigan) and Cal-33 cells (a kind gift from Dr. Anthony Nichols) were previously derived from HNSCC patient tumor samples and cultured in DMEM with 10% FBS, 1X Pen/Strep, 1X NEAA (22). HSC-2, HSC-4 (both from Japanese Collection of Research Bioresources through Sekisui XenoTech, Kansas City, KS) and Detroit 562 (American Type Culture Collection, Manassas, VA) cells were cultured in EMEM with 10% FBS, 1X Pen/Strep. All cell lines were genotyped to confirm authenticity and were mycoplasma negative.

Details of DNA copy number analysis are published elsewhere (23). All UM-SCC cell lines were confirmed to contain *PIK3CA* as previously reported from Nimblegen V2 exome capture based experiments (24). Cal-33, HSC-2 and HSC-4 copy number data were obtained from the publicly available canSAR database (25, 26). *EGFR* mutation status and/or copy number was similarly assessed using data from Nimblegen V2 exome capture based experiments (24) for UM-SCC cell lines, the canSAR database for HSC-2, HSC-4, and Cal-33 (25, 26), and previously published work for Detroit 562 (20).

*Genomic DNA Purification*

Cells from models with *PIK3CA* mutations (Cal-33, HSC-2, HSC-4, Detroit 562, UM-SCC-43, UM-SCC-19, UM-SCC-85) were harvested and washed in PBS, then frozen at -20°C. The thawed cell pellet was re-suspended in 700 μL of Nuclei Lysis Solution (Promega, Madison, WI) for one hour at 55°C. Then, 200 μL of Protein Precipitation Solution (Promega) was added to the sample, which was mixed and placed on ice for at least five minutes before being centrifuged at 13,000 RPM and 4°C for five minutes. The supernatant was transferred to a tube containing

600 μL of isopropanol and centrifuged at 13,000 RPM for one minute. After aspirating the resulting supernatant, the DNA pellet was washed in 200 μL of 70% ethanol, dried, and re-suspended in 30-50 μL of nuclease-free water.

*Sanger Sequencing*

Genomic DNA was amplified using PCR with Platinum *Taq* DNA Polymerase High Fidelity (Invitrogen, Carlsbad, CA), according to the manufacturer's instructions, and the primers with sequences listed in **Figure 3-1**. After being inserted into the pCR8 vector system or processed using the Qiagen QIAquick PCR purification kit, PCR products were submitted for Sanger sequencing at the University of Michigan DNA Sequencing Core on the 3730XL DNA Sequencer (Applied Biosystems, Foster City, CA) as described elsewhere (27). Sequences were aligned using the DNASTAR Lasergene software suite.

*Chemicals*

All compounds (BYL719, HS-173, BKM120, afatinib, gefitinib, erlotinib, BMS-599626, AEE788, TAK-285, CUDC-101, and dacomitinib) were purchased from Selleck Chemicals (Houston, TX). Each inhibitor was initially dissolved in 100% sterile dimethyl sulfoxide (DMSO) to 10 mM and then diluted in media to the indicated concentrations for studies *in vitro*. **Table 3-1** gives the chemical name for each inhibitor used here.

*Resazurin Cell Viability Assay*

Resazurin cell viability assays were performed as described previously (8, 28, 29). To study relative cell viability, 2,000 cells per well (for all cell lines except HSC-2, for which the cell density was reduced to 1,000 cells per well due to large cell size and rapid growth rate) were seeded (in 50 μL volume) in 384-well microplates using a Biotek (Winooski, VT) Multiflo liquid handling dispensing system. Cells were allowed to adhere overnight prior to treatment.

Inhibitors were prepared by hand from 10 mM stocks at 200X concentration in a 96 well plate, then diluted 10X concentration in media in a second 96-well plate using the Agilent (Santa Clara, CA) Bravo Automated Liquid Handling Platform and VWorks Automation Control Software. The intermediate plate with inhibitors in media was used to treat the cells with the desired compound concentration, again using liquid handling robotics, such that cells were treated with complete media containing 0.5% inhibitor or DMSO in a 10-point two-fold dilution series. Each treatment was administered in quadruplicate. Cells were stained with 10 μL of 440 μM resazurin (Sigma, St Louis, MO) dissolved in serum-free media for 12-24 hours before fluorescent signal intensity was quantified. Quantification occurred after 72 hour treatment using the Biotek Cytation3 fluorescence plate reader at excitation and emission wavelengths of 540 and 612 nm, respectively. Data were plotted using Prism 7 and fit with concentration response curves using the log(inhibitor) vs. response -- Variable slope model with four parameters ($IC_{50}$, top, bottom, and Hill slope) allowed to vary.

*Annexin V Apoptosis Assay*

To study Annexin V presentation, 115,000 Detroit 562 cells or 100,000 UM-SCC-59 cells per well were seeded in six-well plates. After 24 hours, media was aspirated and replaced with 3 mL of fresh, complete media. 1 mL of media containing DMSO or inhibitor(s) was added to each well. Cells were cultured for 72 hours, at which time, media was collected from each well. Each well was then washed in PBS, which was also collected. Finally, cells were trypsinized and added to the suspension. Samples were then centrifuged, washed once with PBS, and counted using the Countess Automated Cell Counter (Invitrogen). 100,000 cells per sample were stained with Annexin V FITC and PI using the Dead Cell Apoptosis Kit (ThermoFisher, Waltman, MA) according to manufacturer's instructions. 5 μL of Annexin V FITC and 5 μL of PI were added to

each sample. Samples were incubated at room temperature in the dark for 15 minutes and analyzed using the Bio-Rad ZE5 or MoFlo Astrios EQ Cell Sorter at the University of Michigan Flow Cytometry Core.

*Western Blotting*

Cells at 70-80% confluency were treated with DMSO or inhibitor prior to harvesting and lysing in radioimmunoprecipitation assay buffer (catalog No. 89900; ThermoFisher) containing 1% NP-40 and 0.1% SDS. 8-20 micrograms of each cell harvest were used, and standard Western blot protocols were followed as previously described (30). Primary antibodies (described in detail in **Table 3-2**) were incubated overnight at 4°C or for at least one hour at room temperature, followed by a goat anti-rabbit horseradish peroxidase (catalog No. 111-035-045; Jackson ImmunoResearch, West Grove, PA) secondary antibody at room temperature for one hour as described elsewhere (31). The blots were then visualized with chemiluminescence and imaged. 300dpi or greater images were digitally retained from all Westerns and representative blots are shown. ImageJ software was used to quantify protein expression and compare treatment responses.

*Synergy Analysis*

The effects of combination treatments were analyzed with Combenefit software (32) using the highest single agent (HSA) model (33-37). For each cell line and pair of inhibitors, the number of concentration combinations with scores greater than 20 were counted. These counts were averaged across at least two (and as many as five) independent replicates for each experiment. Experiments having more than eight concentration combinations with scores greater than 20 were considered additive or synergistic. We compared the number of concentration combinations with scores above 20 for HS-173 and afatinib (afatinib combination score) as well

as HS-173 and gefitinib (gefitinib combination score). Cell lines were considered more responsive to the afatinib combination if the afatinib combination score exceeded the gefitinib combination score by eight or more.

*Statistical Analysis*

To determine if statistically significant differences occurred with combination treatments, a two-way ANOVA was performed in R to compare the natural logarithm of the percentage of living cells following vehicle, HS-173, gefitinib or afatinib, or combination treatment. Specifically, this test was performed using type III analysis with the "Anova" function from the "car" package. The interaction between HS-173 and gefitinib or afatinib treatment indication was tested by F-test for the synergy effect of drug combination. In total, four separate tests on drug combination (HS-173 combined with gefitinib or afatinib for UM-SCC-59 and Detroit 562 cell lines) were performed simultaneously, so Bonferroni correction was used to adjust p-values.

## Results

*Subsets of HNSCCs Respond to PI3K + EGFR Inhibitor Combination Therapies*

To first probe the co-dependence of HNSCC cell lines to PI3K and EGFR pathway inhibitors, we compared the response of a small panel of models to the PI3Kα inhibitor HS-173 (38, 39) and irreversible pan-EGFR/ERBB2 inhibitor afatinib (40) as monotherapies and in combination. We selected HS-173 as the PI3K inhibitor as it was the most effective and isoform selective small molecule in our panel of cell lines. Afatinib was used as the ERBB inhibitor; this drug was approved by the FDA in 2016 as a first-line treatment for patients with non-small cell lung cancer whose tumors harbored mutations in EGFR. It has also displayed efficacy in HNSCC (NCT00514943) and is being evaluated in ongoing studies using various paradigms

(NCT01824823, NCT01415674, NCT01427478, NCT02979977). PI3K and ERBB inhibitor combination experiments were performed in four models with *PIK3CA* mutations (HSC-2, HSC-4, Detroit 562 and Cal-33, **Figure 3-1**) and one with high-level *PIK3CA* amplification (UM-SCC-59, 5 wild type copies) using a resazurin cell viability assay after 72 hour drug treatment and then validated by annexin V apoptosis assay (below). Our studies showed variable responses by cell line.

HSC-2, HSC-4 and Detroit 562 display a hotspot *PIK3CA* mutation (indicating activation of and likely dependence on the PI3K signaling pathway) but have limited responses to HS-173 and other PI3K inhibitors as monotherapies with $IC_{50}$ close to or exceeding 1 μM. In these three cell lines, we observed that the addition of afatinib to HS-173 resulted in dose-dependent improvements in the efficacy of PI3K inhibition (**Figure 3-2A-C**). These results represented drug synergy using the HSA model. This effect was also observed when pan-PI3K inhibitor BKM120 and another PI3Kα inhibitor, BYL719, were titrated with afatinib (**Figure 3-3A-B**), but not when p110β inhibitor TGX-221 was tested in combination (**Figure 3-3C**) suggesting that the synergistic dose combination response specifically requires inhibition of PI3Kα. Similarly, titrating afatinib into constant concentrations of HS-173 or BKM120 resulted in synergistic responses in combination-responsive *PIK3CA* mutant cell lines HSC-4 and Detroit 562 (**Figure 3-4**). In contrast, the data also demonstrated that one of the *PIK3CA* mutant HNSCC cell lines, Cal-33, as well as the *PIK3CA* amplified cell line, UM-SCC-59, showed little combination benefit (**Figure 3-2D-E**), suggesting that these models depend on alternative survival pathways.

After establishing that subsets of HNSCCs responded synergistically to HS-173 and afatinib, we examined the downstream signals in the PI3K and EGFR pathways in order to identify potential differences in signaling transduction pathways between two combination

responsive models (HSC-2 and Detroit 562) and one combination non-responsive model (Cal-33). Thus, following a 6-hour treatment with vehicle (DMSO), HS-173 monotherapy, afatinib monotherapy, or HS-173 and afatinib combination therapy, we evaluated EGFR and ERBB2 phosphorylation as well as effector signaling through AKT, MEK and ERK (**Figure 3-5**). As expected, afatinib monotherapy was sufficient to inhibit EGFR and ERBB2 phosphorylation. While the degree to which afatinib reduced ERBB2 phosphorylation in lysates from treated Detroit 562 cells was fairly minimal here, more robust effects on ERBB2 phosphorylation are visible after shorter treatment times (likely due to transient effects on receptor phosphorylation, see **Figure 3-8C** below). Downstream of these effects on EGFR and ERBB2 signaling, ERK and MEK phosphorylation are similarly decreased in non-responsive Cal-33 and responsive HSC-2 cell lines. Detroit 562 cells display minimal changes in MEK phosphorylation following treatment at this dose and time point, yet ERK phosphorylation is reduced somewhat. AKT phosphorylation, used as a readout of primarily PI3K but also EGFR pathway activity, was reduced in HS-173 monotherapy treated samples in each cell line. In the responsive HSC-2 cell line, a further reduction in AKT phosphorylation was evidenced with the addition of afatinib to HS-173. Thus, in both non-responsive and responsive models, inhibition of PI3K's downstream signaling through AKT and inhibition of ERBB signaling both at the receptor level and downstream through MEK and ERK was achieved (**Figure 3-5**). This indicates that the combination effect was not limited to models with reductions in effector signaling.

*Responses to PI3K + EGFR Inhibition Vary Based on Inhibitor Type*

We further investigated the role of ERBB inhibition in HS-173 and afatinib combination response by testing PI3Kα inhibitor HS-173 in combination with reversible EGFR inhibitor gefitinib in the responsive PI3K mutant HNSCC models Detroit 562 and HSC-2. Resazurin cell

viability experiments performed as above displayed a much less marked effect with HS-173 and gefitinib as compared to co-treatment with HS-173 and afatinib (**Figure 3-6A-B**). These effects were confirmed using an orthogonal annexin V apoptosis assay. For example, in the Detroit 562 cell line (synergistically responsive to HS-173 and afatinib), we observed higher levels of FITC positive (apoptotic) cells following di-therapy compared to what would be expected from additive effects of HS-173 and afatinib monotherapies (adjusted p-value = 0.009, two-way ANOVA). Importantly, no significant change in cell death was seen in the non-synergistically responsive UM-SCC-59 model (adjusted p-value = 1, two-way ANOVA), and HS-173 combinations with gefitinib were ineffective in both cell lines (adjusted p-values = 1, two-way ANOVA) (**Figure 3-7**). These data suggested a significant difference in the ability of gefitinib and afatinib to induce synergistic cell kill in our models.

Given this surprising observation, we expanded our original analyses on 5 cell lines to a larger panel of HNSCC models. Here, we selected an additional nine models with genetic characteristics of tumors most likely to receive PI3K or EGFR inhibitors in a precision medicine setting, including those with either *PIK3CA* mutations or high-level gene amplifications (greater than four copies). As evidence of this, additivity between HS-173 and gefitinib was only observed in 4/14 (29%) of models.

Importantly, much more significant "further benefit," which we define as including multiple synergistic dose combinations, was observed with HS-173 and afatinib combination therapy in 8/14 (57%) of models (**Figure 3-8A**). Of the four models that demonstrated additivity with gefitinib, three received further benefit with afatinib. The *in vitro* models that failed to display robust improvements in response to HS-173 with the addition of afatinib included Cal-33 (**Figure 3-2D**), UM-SCC-59 (**Figure 3-2E**), UM-SCC-19, UM-SCC-43, and UM-SCC-85

(**Figure 3-8A**). Interestingly, Cal-33, UM-SCC-19, UM-SCC-43, and UM-SCC-85, like some of the combination-responsive models discussed above, display activating mutations in *PIK3CA* (**Figure 3-1**). Cal-33 and UM-SCC-85 cells were among the most sensitive to PI3K inhibitor monotherapies, while UM-SCC-59 (with high-level amplification of wild-type *PIK3CA*) is one of the most resistant. Thus, neither *PIK3CA* mutation nor responsiveness to PI3K inhibitor monotherapy is a good predictor of responsiveness to HS-173 and afatinib co-treatment. Likewise, at least when considered as single variables, *PIK3CA* copy number (**Figure 3-8A**), *EGFR* copy number (**Figure 3-8A**), and ERBB protein expression (**Figure 3-8B**) are also poor indicators of combination response. Although mutations in *EGFR* have been shown to be closely linked to responses to EGFR inhibitors (41-46), the cell lines used here did not display such variants. Thus, neither sensitivity nor resistance to EGFR inhibitor monotherapies or combination therapies can be explained by the presence of L858R or T790M/C797S mutations, respectively. After our resazurin assay determined that the HS-173 and gefitinib combination was largely ineffective as compared to HS-173 and afatinib, we tested the combination of HS-173 and afatinib in UM-SCC-110 and patient-matched fibroblasts and demonstrated the inability of combination therapy to drive cell death in normal fibroblasts (**Figure 3-9**).

Together, these data strongly suggest important differences between afatinib- and gefitinib-based combinations in our model system. Given the differences between the inhibitors, we hypothesized that the greater effectiveness with afatinib over gefitinib may be due to 1) a broader spectrum of ERBB family member inhibition, and/or 2) irreversible as opposed to reversible inhibition of EGFR. To begin testing this hypothesis using combination responsive Detroit 562 cells, we performed a resazurin cell viability assay in which we compared the effects of HS-173 and gefitinib with or without ERBB2 specific inhibitor CP-724714 (**Figure 3-6B**).

This demonstrated that CP-724714 was unable to add to HS-173 and gefitinib in this assay and the total effect of this tri-therapy combination remained much less substantial than the effect of HS-173 and afatinib. This result suggested the possibility that ERBB2 inhibition did not account for the differences between inhibitors or that CP-724714 could not sufficiently inhibit ERBB2 signaling in our system.

Consequently, to validate that the doses of CP-724714 used here could sufficiently inhibit ERBB2 signaling, we performed Western blot analysis on lysates harvested from Detroit 562 cells following CP-724714 or afatinib treatment. At doses equivalent to or less than those used in resazurin cell viability assays, we observed that both CP-724714 and afatinib treatment resulted in robust inhibition of ERBB2 phosphorylation after 15 or 60 minutes (**Figure 3-6B**). We also examined lysates from HSC-2 cells following 2 hour treatment with each mono- or di-therapy (**Figure 3-6C**). This demonstrated decreased EGFR phosphorylation in gefitinib and afatinib treated samples, with a slightly greater loss of EGFR phosphorylation with afatinib than gefitinib. Phosphorylation of ERK, GAB1, and MEK, downstream of EGFR, were similar for gefitinib and afatinib treatments; in addition, co-treatment with HS-173 and gefitinib or afatinib did not reduce downstream ERBB signals beyond those levels seen with gefitinib and afatinib monotherapy treatments. Phosphorylation of PI3K pathway effector AKT was appropriately inhibited upon HS-173 treatment, but PDK1 and GSK3β phosphorylation remained unchanged. Together, these data suggest that ERBB2 inhibition alone may not be sufficient to explain differences between the gefitinib and afatinib combinations and therefore warrant further evaluation of differences between reversible and irreversible ERBB inhibitor combinations.

Thus, using a resazurin cell viability assay, we tested HS-173 in combination with three reversible ERBB inhibitors (erlotinib, BMS-599626, and CP-724714) and three irreversible

ERBB targeting agents (TAK285, CUDC-101, and dacomitinib) in HSC-2 and Detroit 562 cells. While we observed that 0/4 (0%) reversible ERBB inhibitors displayed synergistic dose combinations in either cell line, 3/4 (75%) and 4/4 (100%) irreversible ERBB targeting drugs had synergistic dose combinations with HS-173 in Detroit 562 and HSC-2 cells, respectively (**Table 3-3**, **Figure 3-10**). These data add support to the hypothesis that irreversible inhibition of EGFR and/or its ERBB family members may be important for achieving the most significant growth inhibition with PI3K and ERBB inhibitor combinations.

## Discussion

Our data are consistent with previous studies showing the benefit of PI3K and EGFR inhibitor combination therapies (8, 15-20) and also extend that work by discovering that PI3K inhibitors are much more effective in combination with irreversible than reversible EGFR inhibitors in HNSCC. In prior work comparing classes of EGFR targeting monotherapies in this cancer type, preclinical data demonstrated that irreversible EGFR inhibitors are superior to other EGFR targeting agents, including cetuximab (16, 47) and reversible inhibitor gefitinib (48). Similarly, previous work has shown that the addition of ERBB2 targeting antibodies pertuzumab (49) or trastuzumab (50) to gefitinib enhances its efficacy in HNSCC cell lines; however, our findings demonstrated that the broader specificity of irreversible inhibitors alone cannot explain these differences in sensitivity, as administering ERBB2 inhibitor CP-724714 with gefitinib and HS-173 did not enhance drug effects (**Figure 3-6**). Collectively, our data may suggest why greater improvements in patient survival following PI3K and EGFR combination therapies have not yet been observed in HNSCC and other cancers clinically and support the need for additional detailed studies of PI3K and EGFR combination therapies using irreversible ERBB inhibitors.

Of the published HNSCC studies evaluating PI3K and EGFR di-therapies, most have been performed with either cetuximab (15, 18, 19) or the reversible EGFR inhibitors (e.g. gefitinib, erlotinib) (17, 20). One exception is a recent report from Silva-Oliveira *et al.* that examined responses to PI3K pathway inhibitors (including AKT inhibitor MK-2206) with two different irreversible EGFR inhibitors (16). In this study, pharmacologic inhibition or siRNA knockdown of AKT resulted in improved sensitivity to afatinib and allitinib (a second irreversible EGFR inhibitor) in HN13 cells (16). The need to suppress AKT phosphorylation in responses to PI3K + EGFR drug combinations is supported by studies of both EGFR targeting antibodies (18, 51) and reversible inhibitors (16, 18, 20, 51). Importantly, in lung cancer models, irreversible EGFR inhibitors have sustained reductions in EGFR phosphorylation and an improved ability to decrease effector AKT phosphorylation as compared to reversible inhibitors (52). The inability of reversible EGFR inhibitors to sustain suppression of EGFR and AKT phosphorylation has been linked to altered receptor trafficking (53), a mechanism that does not affect the activity of irreversible inhibitors. In contrast, we did not observe greater reductions in AKT phosphorylation with HS-173 and afatinib than with gefitinib dual-therapy (**Figure 3-6C**). These data suggest that factors other than or in addition to the level of suppression of downstream EGFR effector signaling may be responsible for mediating combination benefit and/or that specific inhibitor combinations may be required to achieve synergistic cell death responses.

Of the emerging novel classes of PI3K and EGFR inhibitors that we evaluated here, several are already in advanced clinical development for HNSCC and other cancers as mono- and combination therapies. For example, BKM120 improved survival when administered with paclitaxel (versus paclitaxel and placebo) in a phase II HNSCC trial (10), and BYL719 monotherapy recently demonstrated safety in patients with solid tumors (54). Of the irreversible EGFR inhibitors that we evaluated, dacomitinib has shown efficacy beyond that of cetuximab in preclinical models (47) and is undergoing evaluation in phase II studies in recurrent and metastatic HNSCC patients (NCT00768664, NCT01449201). Afatinib, although still only

indicated for use in lung cancer patients, has also demonstrated similar efficacy to cetuximab (55) in HNSCC patients; this result is very promising given that cetuximab was approved for use in HNSCC with radiation or cytotoxic chemotherapy after successful phase 3 trials (11, 12). Afatinib is currently undergoing evaluation in a variety of treatment paradigms in HNSCC (including NCT01824823, NCT01427478, NCT02979977 and NCT01783587) and has also been tested in other solid tumor types as part of a combination therapy with inhibitors targeting PLK (NCT01206816), Src (NCT01999985), insulin-like growth factor receptor (IGFR) (NCT02191891), MEK (NCT02450656), or multiple receptor tyrosine kinases (NCT00998296), but not yet with PI3K inhibitors.

Many irreversible EGFR inhibitors have activity against both wildtype and mutated forms of EGFR (including those with T790M and/or C797S resistance mutations), which may contribute to their improved clinical efficacy over reversible drugs like gefitinib and erlotinib. Thus, the use of irreversible EGFR inhibitors with PI3K inhibitors in HNSCC may lead to more durable responses than reversible EGFR inhibitor combinations by eliminating not only EGFR mutations but also activation of compensatory signaling through PI3K as critical resistance mechanisms. Nevertheless, these combinations are still limited by other forms of resistance, including novel resistance mutations and co-dependent pathways, which will likely develop after prolonged exposure to even irreversible EGFR and PI3K inhibitor co-treatments.

Collectively, our work motivates the translation of specific PI3K and irreversible EGFR dual-therapies into xenograft mouse models and other more clinically relevant systems. If such studies confirm our *in vitro* findings, clinical trials evaluating these drug combinations will be warranted. More broadly, our data also motivate a need to develop additional biomarkers that can be used to determine not only if a drug inhibits its target, but also if the drug inhibits pivotal downstream effector pathways capable of rescuing cell survival. Indeed, our findings suggest that responses may be mediated by complex downstream signaling networks or other yet-unidentified factors. Developing the next generation of adaptive biomarkers and rationally designed matched combination therapies may therefore be one key to improved survival for HNSCC patients.

## Figures

| | | Primer (5'-3') | Chromatogram |
|---|---|---|---|
| UM-SCC-43 c.1633G>A E545K | F | CATCTGTGAATCCAGAGGGGA | TCACTGAGCAGG Reference |
| | R | AACATGCTGAGATCAGCCAAA | TCACTAAGCAGG Cell Line |
| HSC-4 c.1633G>A E545K | F | CATCTGTGAATCCAGAGGGGA | TCACTGAGCAGG Reference |
| | R | AACATGCTGAGATCAGCCAAA | TCACTAAGCAGG Cell Line |
| Cal-33 c.3014A>G H1047R | F | GCTCCAAACTGACCAAACTGT | TGCACATCATGGT Reference |
| | R | AATCGGTCTTTGCCTGCTGA | TGCACGTCATGGT Cell Line |
| HSC-2 c.3014A>G H1047R | F | GCTCCAAACTGACCAAACTGT | TGCACATCATGGT Reference |
| | R | AATCGGTCTTTGCCTGCTGA | TGCACGTCATGGT Cell Line |
| Detroit 562 c.3014A>G H1047R | F | GCTCCAAACTGACCAAACTGT | TGCACATCATGGT Reference |
| | R | AATCGGTCTTTGCCTGCTGA | TGCACGTCATGGT Cell Line |
| UM-SCC-85 c.3014A>G H1047R | F | GCTCCAAACTGACCAAACTGT | TGCACATCATGGT Reference |
| | R | AATCGGTCTTTGCCTGCTGA | TGCACGTCATGGT Cell Line |
| UM-SCC-19 c.3014A>G H1047R | F | GCTCCAAACTGACCAAACTGT | TGCACATCATGGT Reference |
| | R | AATCGGTCTTTGCCTGCTGA | TGCACGTCATGGT Cell Line |

**Figure 3-1. Sanger sequencing confirms *PIK3CA* mutations.**

Sanger sequencing confirmed E545K *PIK3CA* mutation in UM-SCC-43 and HSC-4 cells and H1047R *PIK3CA* mutation in Cal-33, HSC-2, Detroit 562, UM-SCC-19 and UM-SCC-85 cells.

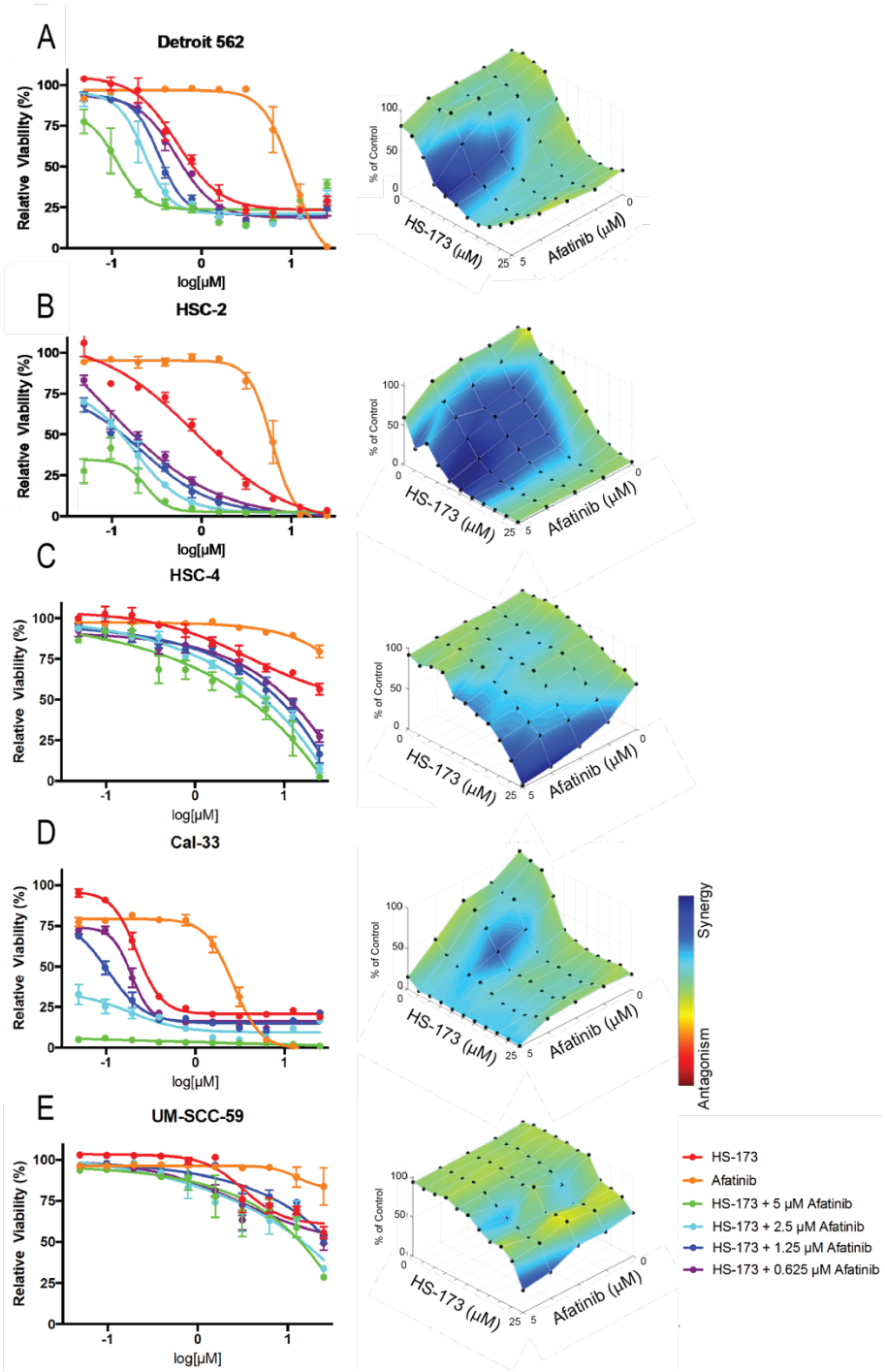


**Figure 3-2. Responses to HS-173 + afatinib treatment in HNSCC cell lines.**

(A) HSC-2, (B) HSC-4, (C) Detroit 562, (D) Cal-33, and (E) UM-SCC-59 were treated with increasing concentrations of PI3Kα inhibitor HS-173 and/or EGFR/ErbB2 inhibitor afatinib for 72 hours. Cell viability was measured using a resazurin cell viability assay. Each point is the mean and s.d. of quadruplicate determinations from a single experiment. Each experiment was

repeated independently at least three times with similar combination effects; representative data is shown along with analysis using Combenefit software (32).

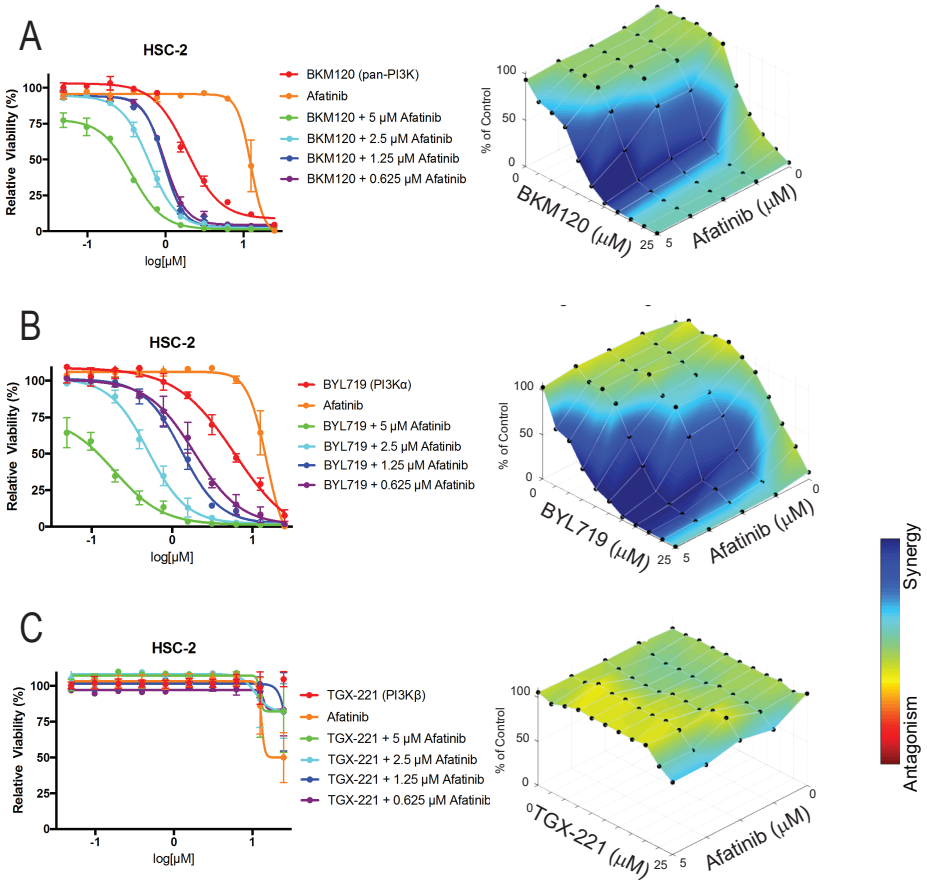


**Figure 3-3. Responses to treatment with afatinib and PI3K inhibitors with varying selectivity.**

HSC-2 cells were treated with increasing concentrations of pan-PI3K inhibitor BKM120 (A), PI3Kα inhibitor BYL719 (B), or PI3Kβ inhibitor TGX-221 (C) and/or EGFR/ERBB2 inhibitor afatinib for 72 hours. Cell viability was measured using a resazurin cell viability assay. Each point is the mean and s.d. of quadruplicate determinations from a single experiment. Each experiment was repeated independently at least two times with similar combination effects; representative data is shown along with analysis using Combenefit software (32).

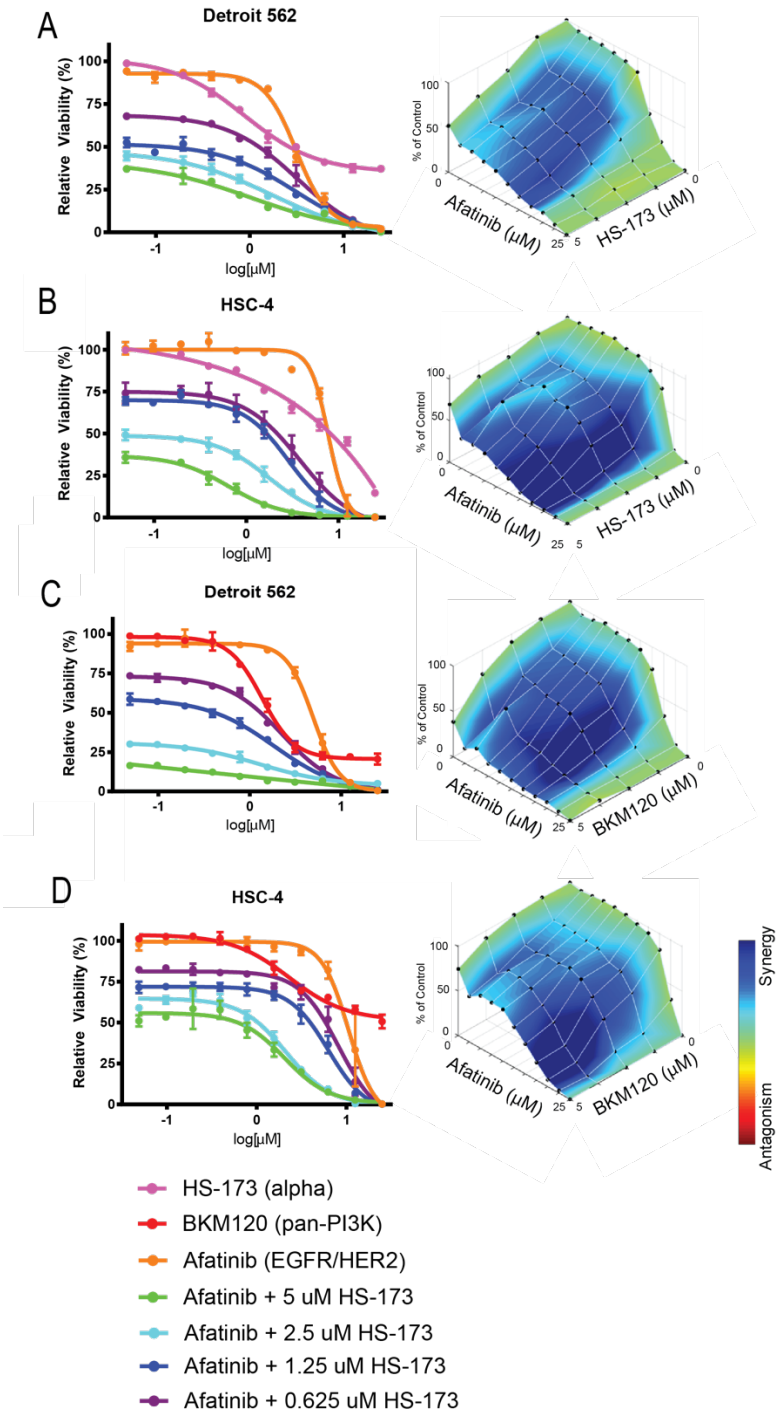


**Figure 3-4. Responses to reverse titration of afatinib and PI3K inhibitors.**

Detroit 562 (A, C) and HSC-4 (B, D) cells were treated with increasing concentrations of EGFR/ERBB2 inhibitor afatinib and/or pan-PI3K inhibitor BKM120 (A, B) or PI3Kα inhibitor HS-173 (C, D) for 72 hours. Cell viability was measured using a resazurin cell viability assay. Each point is the mean and s.d. of quadruplicate determinations from a single experiment. Each experiment was repeated independently two times with similar combination effects; representative data is shown along with analysis using Combenefit software (32).

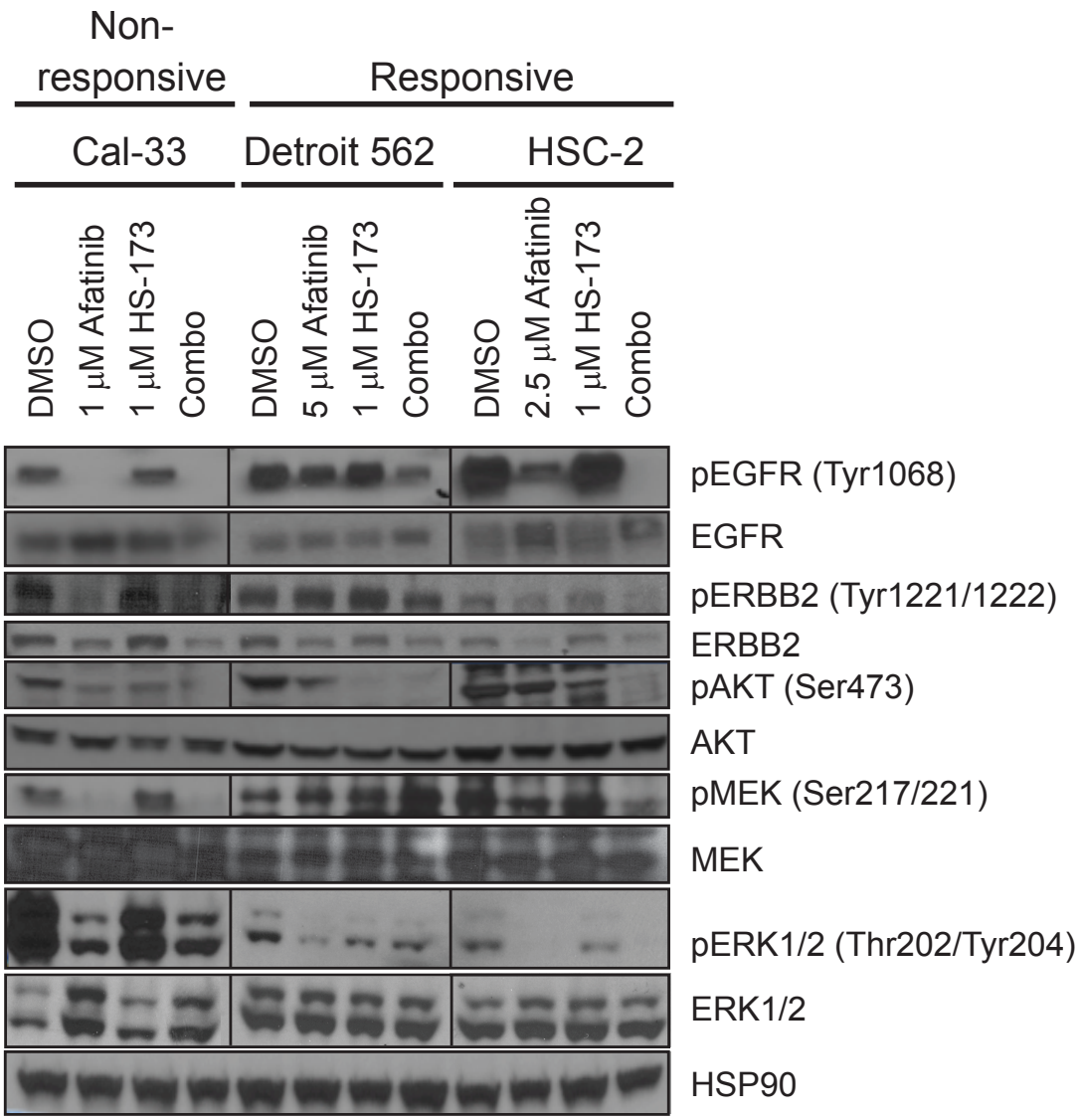


**Figure 3-5. Signaling responses to HS-173 + afatinib in combination responsive and non-responsive HNSCC cell lines.**

Western blot analysis of downstream PI3K and RAS-MEK-ERK pathway activation following six hour treatment with vehicle (DMSO), EGFR/ERBB2 inhibitor afatinib, PI3Kα inhibitor HS-173, and combination in Cal-33, Detroit 562 and HSC-2 cell lines. HSP90 was used as a loading control. Representative images are shown.

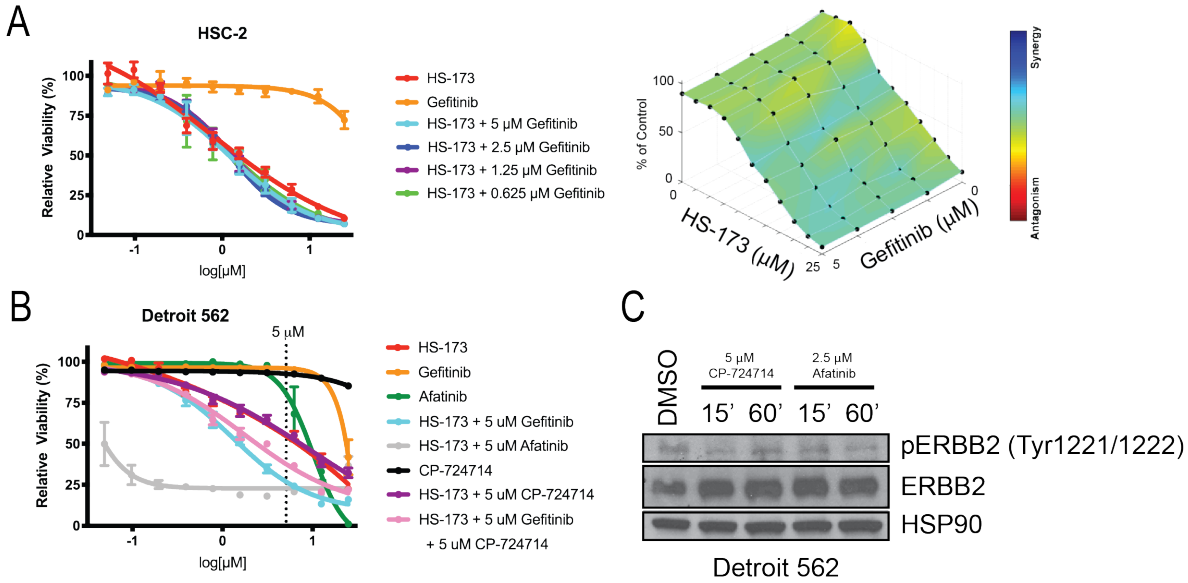


**Figure 3-6. Responses to HS-173 + ERBB inhibitor treatment in *PIK3CA* mutant HNSCC cells.**

(A) HSC-2 cells were treated with increasing concentrations of PI3Kα inhibitor HS-173 and/or EGFR inhibitor gefitinib for 72 hours. Cell viability was measured using a resazurin cell viability assay. Each point is the mean and s.d. of quadruplicate determinations from a single experiment. Each experiment was repeated independently at least three times with similar combination effects; representative data is shown along with analysis using Combenefit software (32). (B) Detroit 562 cells were treated with increasing concentrations of PI3Kα inhibitor HS-173 and/or EGFR gefitinib, ERBB2 inhibitor CP-724714, and/or EGFR/ERBB2 inhibitor afatinib for 72 hours. Cell viability was measured using a resazurin cell viability assay. Each point is the mean and s.d. of quadruplicate determinations from a single experiment. This experiment was repeated independently three times with similar combination effects; representative data is shown. (C) Western blot analysis of phosphorylated and total ERBB2 expression following treatment with vehicle (DMSO) or 15 or 60 minute treatment with either ERBB2 specific inhibitor CP-724714 or EGFR/ERBB2 inhibitor afatinib in Detroit 562 cells. HSP90 was used as a loading control.

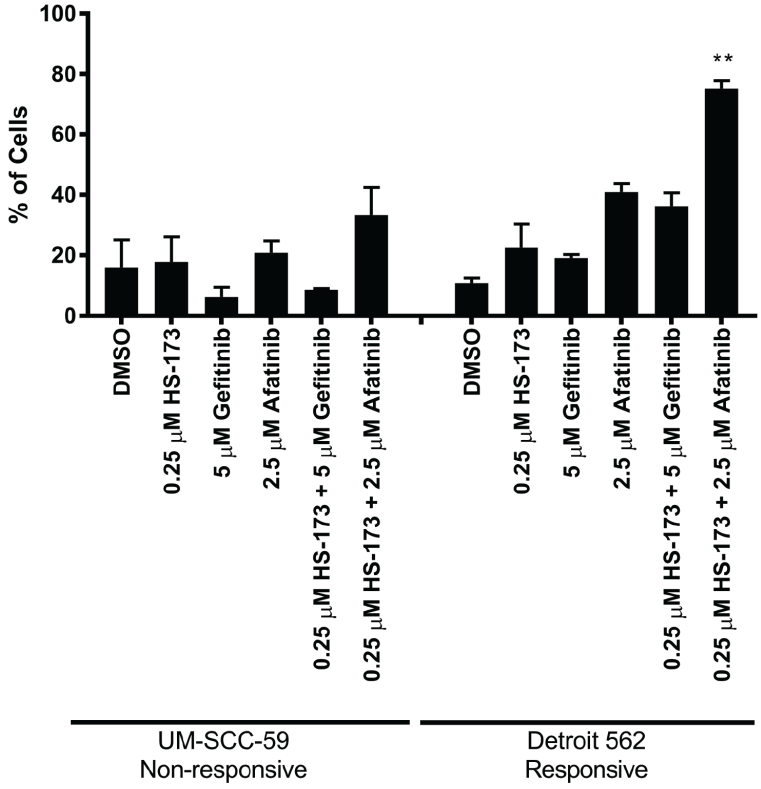


**Figure 3-7. Cell death responses to HS-173 + afatinib treatment in combination responsive and non-responsive HNSCC cell lines.**

Combination non-responsive model UM-SCC-59 and combination responsive model Detroit 562 were treated with vehicle (DMSO), PI3Kα inhibitor HS-173, reversible EGFR inhibitor gefitinib, and/or EGFR/ERBB2 irreversible inhibitor afatinib for 72 hours. Cell viability was measured using an annexin V apoptosis assay after cells were stained with FITC and PI. Data shown represents the mean and s.d. from 2-3 independent experiments. ** indicates significance with $p < 0.01$ using two-way ANOVA to compare vehicle, HS-173, afatinib, and combination, as described above in Materials and Methods. Comparisons for HS-173 and gefitinib combinations in each cell line and for HS-173 and afatinib combination in UM-SCC-59 were performed, but are not shown given the lack of significant interaction term.

A

| Cell Line | *PIK3CA* Mutation | *PIK3CA* Copy Number | *EGFR* Copy Number | Response: HS-173 + Gefitinib | Response: HS-173 + Afatinib |
|---|---|---|---|---|---|
| **Cal-33** | H1047R | 3 | 4 | | |
| **Detroit 562** | H1047R | Unknown | 3 | | |
| **HSC-2** | H1047R | 4 | 12 | | |
| **HSC-4** | E545K | 3 | 6 | | |
| **UM-SCC-19** | H1047R | 4 | 1 | | |
| **UM-SCC-43** | E545K | 3 | 3 | | |
| **UM-SCC-85** | H1047R | 2 | 4 | | |
| **UM-SCC-29** | WT | 4 | 4 | | |
| **UM-SCC-49** | WT | 5 | 5 | | |
| **UM-SCC-59** | WT | 5 | 23 | | |
| **UM-SCC-69** | WT | 6 | 15.67 | | |
| **UM-SCC-92** | WT | 3 | 2.33 | | |
| **UM-SCC-108** | WT | 4 | 3 | | |
| **UM-SCC-110** | WT | 3 | 4 | | |

| | |
|---|---|
| | Not Synergistic |
| | Additive |
| | Further Benefit vs HS-173 + Gefitinib |

B

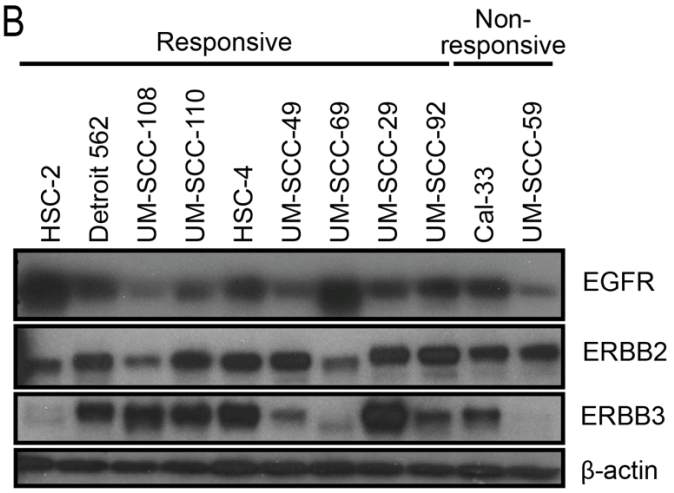


C

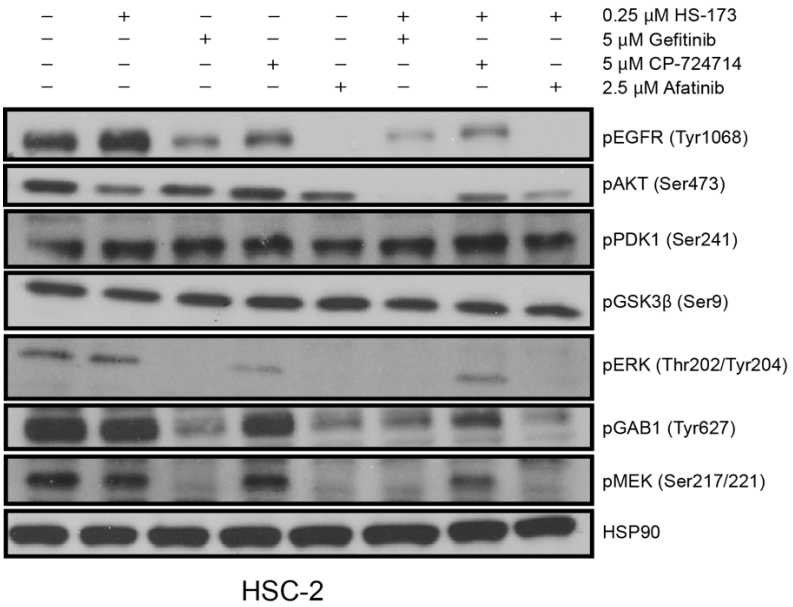


**Figure 3-8. Sensitivity of HNSCC Cell Lines to HS-173 and gefitinib or afatinib combination treatment.**

(A) Table shows mutation and copy number data for cell lines tested for sensitivity to HS-173 and gefitinib or afatinib. *PIK3CA* mutations were confirmed via Sanger sequencing. No cell lines displayed mutations in *EGFR*. *PIK3CA* and *EGFR* copy number were determined using the publicly available canSAR database (Bulusu et al., 2014; Halling-Brown et al., 2012) for Cal-33, HSC-2 and HSC-4 cells and using Oncomine for UM-SCC cells. Detroit 562 *EGFR* copy number was reported as previously published (Young et al., 2013). Combinatorial effects of HS-173 and gefitinib or afatinib were determined using resazurin cell viability assays after 72 hour drug treatment. Experiments with quadruplicate replicates were performed 2-5 times and combination benefit was assessed using Combenefit software (Di Veroli et al., 2016) as described above. 4/14 (29%) cell lines displayed additive effects following HS-173 and gefitinib co-treatment; 8/14 (57%) of models responded more favorably to combination treatment with HS-173 and afatinib. (B) Protein isolated from each cell line in the panel was used to perform

Western blot analysis for EGFR, ERBB2, and ERBB3. β-actin was used as a loading control. (C) Western blot analysis of downstream PI3K and RAS-MEK-ERK pathway activation following 2 hour treatment with vehicle (DMSO), PI3Kα inhibitor HS-173, reversible EGFR inhibitor gefitinib, reversible ERBB2 inhibitor CP-724714, EGFR/ERBB2 inhibitor afatinib, or combinations in HSC-2 cells. HSP90 was used as a loading control. Representative images are shown.

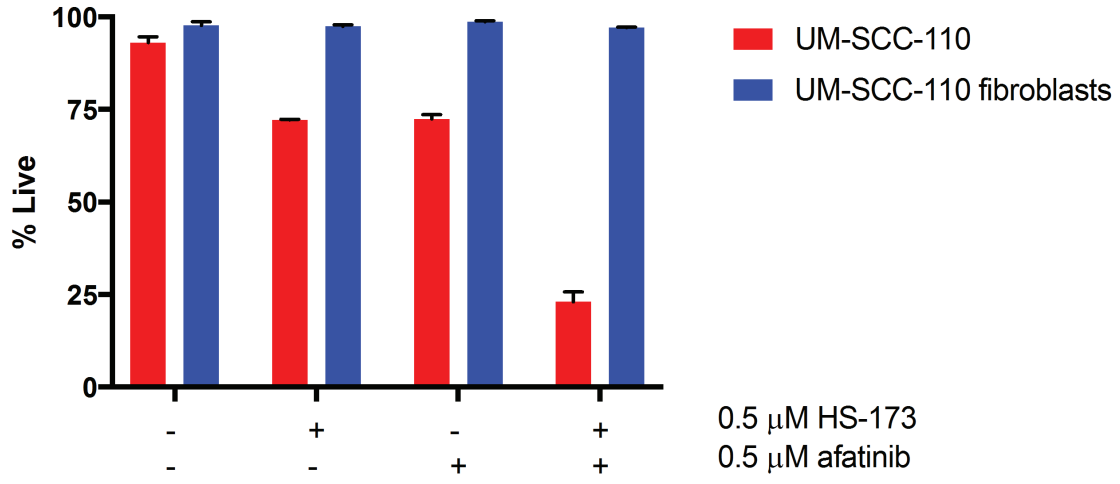


**Figure 3-9. SCC cells, but not matched fibroblasts, respond to HS-173 and afatinib co-treatment.**

UM-SCC-110 and matched fibroblasts from the same patient (UM-SCC-110 fibroblasts) were treated with vehicle (DMSO), PI3Kα inhibitor HS-173 and/or EGFR/ERBB2 inhibitor afatinib for 72 hours. Cell viability was measured using a resazurin cell viability assay. Data shown is the mean and s.d. of duplicate determinations.

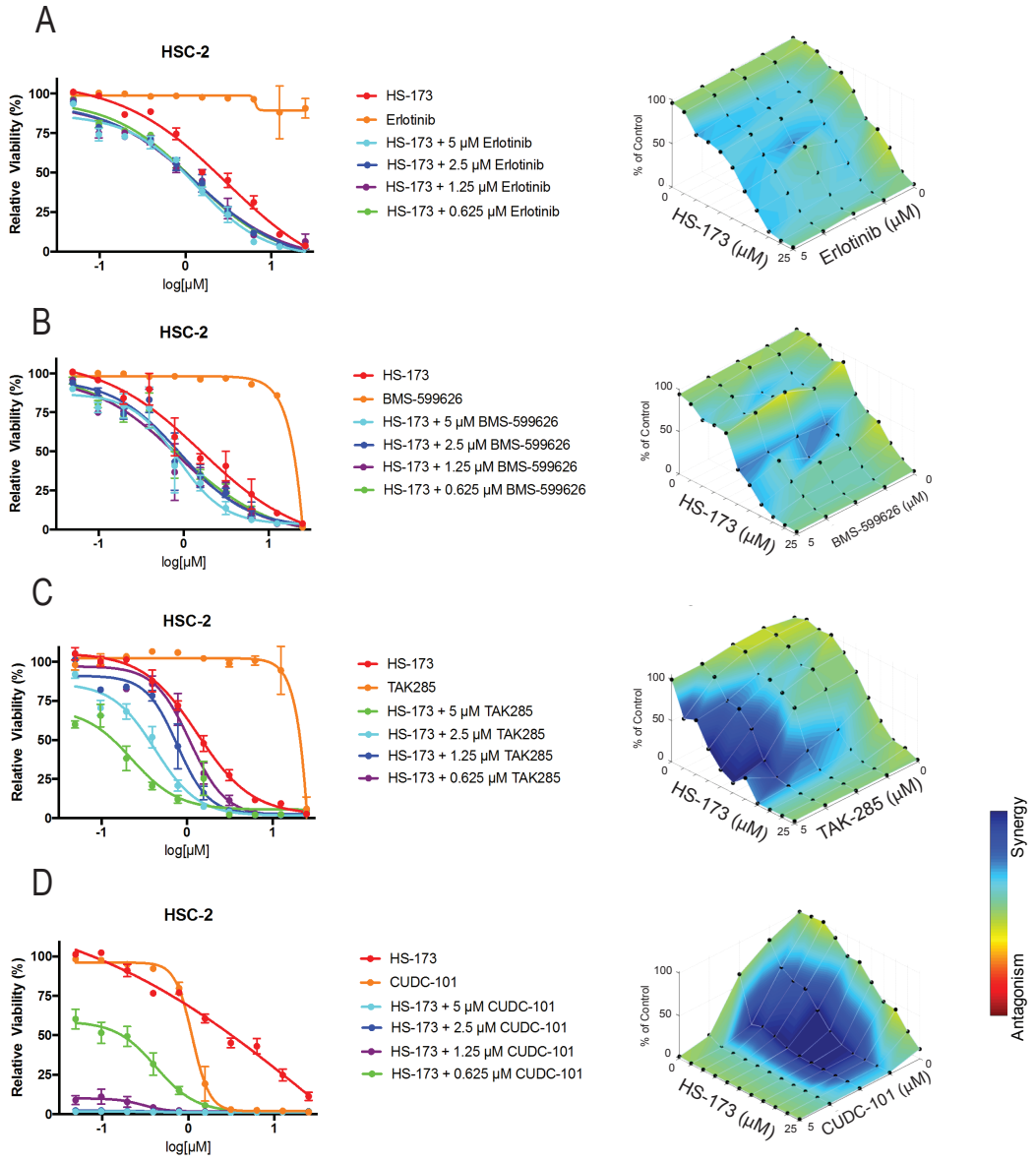


**Figure 3-10. Responses to PI3K and reversible or irreversible EGFR inhibitor combinations.**

HSC-2 cells were treated with increasing concentrations of PI3Kα inhibitor HS-173 and/or reversible EGFR inhibitor erlotinib (A), reversible EGFR/ERBB2 inhibitor BMS-599626, irreversible EGFR/ERBB2 inhibitor TAK285, or irreversible EGFR/ERBB2 inhibitor CUDC-101 (D) for 72 hours. Cell viability was measured using a resazurin cell viability assay. Each point is the mean and s.d. of quadruplicate determinations from a single experiment. Each experiment was repeated independently at least two times with similar combination effects; representative data is shown along with analysis using Combenefit software (32).

## Tables

**Table 3-1. Chemical Names for Inhibitors Used**

| Inhibitor | Chemical Name |
|---|---|
| HS-173 | 6-[5-[(phenylsulfonyl)amino]-3-pyridinyl]-imidazo[1,2-a]pyridine-3-carboxylic acid, ethyl ester |
| BKM120 | 5-(2,6-di-4-morpholinyl-4-pyrimidinyl)-4-(trifluoromethyl)-2-pyridinamine |
| BYL719 | (2S)-$N^1$-[4-methyl-5-[2-(2,2,2-trifluoro-1,1-dimethylethyl)-4-pyridinyl]-2-thiazolyl]-1,2-pyrrolidinedicarboxamide |
| TGX-221 | 7-methyl-2-(4-morpholinyl)-9-[1-(phenylamino)ethyl]-4H-pyrido[1,2-a]pyrimidin-4-one |
| Afatinib | N-[4-[(3-chloro-4-fluorophenyl)amino]-7-[[(3S)-tetrahydro-3-furanyl]oxy]-6-quinazolinyl]-4-(dimethylamino)-2-butenamide |
| Gefitinib | N-(3-chloro-4-fluorophenyl)-7-methoxy-6-[3-(4-morpholinyl)propoxy]-4-quinazolinamine |
| CP-724714 | 2-methoxy-N-[(2E)-3-[4-[[3-methyl-4-[(6-methyl-3-pyridinyl)oxy]phenyl]amino]-6-quinazolinyl]-2-propen-1-yl]-acetamide |
| Erlotinib | N-(3-ethynylphenyl)-6,7-*bis*(2-methoxyethoxy)-4-quinazolinamine |
| BMS-599626 | [4-[[1-[(3-Fluorophenyl)methyl]-1H-indazol-5-yl]amino]-5-methylpyrrolo[2,1-f][1,2,4]triazin-6-yl]carbamic acid (3S)-3-morpholinylmethyl ester |
| AEE788 | 6-[4-[(4-ethyl-1-piperazinyl)methyl]phenyl]-N-[(1R)-1-phenylethyl]-7H-pyrrolo[2,3-d]pyrimidin-4-amine |
| TAK-285 | N-(2-(4-(3-chloro-4-(3-(trifluoromethyl)phenoxy)phenylamino)-5H-pyrrolo[3,2-D]pyrimidin-5-yl)ethyl)-3-hydroxy-3-methylbutanamide |
| CUDC-101 | 7-[[4-[(3-ethynylphenyl)amino]-7-methoxy-6-quinazolinyl]oxy]-N-hydroxy-heptanamide |
| Dacomitinib | N-[4-[(3-chloro-4-fluorophenyl)amino]-7-methoxy-6-quinazolinyl]-4-(1-piperidinyl)-(2E)-butenamide |

**Table 3-2. Primary Antibody Conditions**

| Target | Supplier | Cat. No. | Dilution |
|---|---|---|---|
| pEGFR(Tyr1068) | Cell Signaling Technology | 3777 | 1:1000 |
| EGFR | Origene | TA312545 | 1:2000 |
| pERBB2(Tyr1221/1222) | Cell Signaling Technology | 2249 | 1:500 |
| HER2 | Cell Signaling Technology | 2165 | 1:1000 |
| pMEK(Ser217/221) | Cell Signaling Technology | 9121 | 1:1000 |
| MEK1/2 | Cell Signaling Technology | 8727 | 1:1000 |
| pERK1/2(Thr202/Tyr204) | Cell Signaling Technology | 4370 | 1:1000 |
| ERK1/2 | Cell Signaling Technology | 4695 | 1:1000 |
| pAKT(Ser473) | Cell Signaling Technology | 4060 | 1:1000 |
| AKT | Cell Signaling Technology | 4685 | 1:1000 |
| HSP90 | Cell Signaling Technology | 4877 | 1:2000 |
| β-actin | Cell Signaling Technology | 4970 | 1:2000 |

**Table 3-3. Combinatorial Effects of PI3K + ERBB Inhibitors in HNSCC Cell Lines.**

Combinatorial effects of PI3Kα inhibitor HS-173 and reversible or irreversible ERBB targeting agents in HSC-2 and Detroit 562 HNSCC cell lines. Synergy was assessed using Combenefit software (32). Synergy was not observed for PI3Kα inhibitor HS-173 with any reversible inhibitor in either cell line. 4/4 and 3/4 irreversible EGFR inhibitors were synergistic with HS-173 in HSC-2 and Detroit 562 cells, respectively.

| Inhibitor | Target | Reversible/ Irreversible | HSC-2 Synergy | Detroit 562 Synergy |
|---|---|---|---|---|
| Gefitinib | EGFR | Reversible | No | No |
| Erlotinib | EGFR | Reversible | No | No |
| BMS-566924 | EGFR/ERBB2 | Reversible | No | No |
| CP-724714 | ERBB2 | Reversible | No | No |
| Afatinib | EGFR/ERBB2 | Irreversible | Yes | Yes |
| TAK-285 | EGFR/ERBB2 | Irreversible | Yes | No |
| CUDC-101 | EGFR/ERBB2/HDAC | Irreversible | Yes | Yes |
| Dacomitinib | EGFR/ERBB2/ERBB4 | Irreversible | Yes | Yes |

## References


1. Kamangar F, Dores GM, Anderson WF. Patterns of cancer incidence, mortality, and prevalence across five continents: defining priorities to reduce cancer disparities in different geographic regions of the world. Journal of clinical oncology : official journal of the American Society of Clinical Oncology. 2006;24(14):2137-50. Epub 2006/05/10. doi: 10.1200/jco.2005.05.2308. PubMed PMID: 16682732.

2. Howlader N NA, Krapcho M, Miller D, Bishop K, Altekruse SF, Kosary CL, Yu M, Ruhl J, Tatalovich Z, Mariotto A, Lewis DR, Chen HS, Feuer EJ, Cronin KA. SEER Cancer Statistics Review, 1975-2013. SEER web site: National Cancer Institute; April 2016.

3. Giefing M, Wierzbicka M, Szyfter K, Brenner JC, Braakhuis BJ, Brakenhoff RH, Bradford CR, Sorensen JA, Rinaldo A, Rodrigo JP, Takes RP, Ferlito A. Moving towards personalised therapy in head and neck squamous cell carcinoma through analysis of next generation sequencing data. European journal of cancer. 2016;55:147-57. doi: 10.1016/j.ejca.2015.10.070. PubMed PMID: 26851381; PMCID: 4761501.

4. Ludwig ML, Birkeland AC, Hoesli R, Swiecicki P, Spector ME, Brenner JC. Changing the paradigm: the potential for targeted therapy in laryngeal squamous cell carcinoma. Cancer biology & medicine. 2016;13(1):87-100. doi: 10.28092/j.issn.2095-3941.2016.0010. PubMed PMID: 27144065; PMCID: 4850131.

5. Gillison ML, Chaturvedi AK, Anderson WF, Fakhry C. Epidemiology of Human Papillomavirus-Positive Head and Neck Squamous Cell Carcinoma. J Clin Oncol. 2015;33(29):3235-42. Epub 2015/09/10. doi: 10.1200/jco.2015.61.6995. PubMed PMID: 26351338.

6. Lui VW, Hedberg ML, Li H, Vangara BS, Pendleton K, Zeng Y, Lu Y, Zhang Q, Du Y, Gilbert BR, Freilino M, Sauerwein S, Peyser ND, Xiao D, Diergaarde B, Wang L, Chiosea S, Seethala R, Johnson JT, Kim S, Duvvuri U, Ferris RL, Romkes M, Nukui T, Kwok-Shing Ng P, Garraway LA, Hammerman PS, Mills GB, Grandis JR. Frequent mutation of the PI3K pathway in head and neck cancer defines predictive biomarkers. Cancer discovery. 2013;3(7):761-9. Epub 2013/04/27. doi: 10.1158/2159-8290.cd-13-0103. PubMed PMID: 23619167; PMCID: Pmc3710532.

7. Murugan AK, Munirajan AK, Tsuchida N. Genetic deregulation of the PIK3CA oncogene in oral cancer. Cancer Lett. 2013;338(2):193-203. Epub 2013/04/20. doi: 10.1016/j.canlet.2013.04.005. PubMed PMID: 23597702.

8. Michmerhuizen NL, Leonard E, Kulkarni A, Brenner JC. Differential compensation mechanisms define resistance to PI3K inhibitors in PIK3CA amplified HNSCC. Otorhinolaryngology-head and neck surgery. 2016;1(2):44-50. Epub 2016/12/23. PubMed PMID: 28004037; PMCID: PMC5167357.

9. Ozanne B, Richards CS, Hendler F, Burns D, Gusterson B. Over-expression of the EGF receptor is a hallmark of squamous cell carcinomas. The Journal of pathology. 1986;149(1):9-14. Epub 1986/05/01. doi: 10.1002/path.1711490104. PubMed PMID: 2425067.

10. Soulieres D, Faivre S, Mesia R, Remenar E, Li SH, Karpenko A, Dechaphunkul A, Ochsenreither S, Kiss LA, Lin JC, Nagarkar R, Tamas L, Kim SB, Erfan J, Alyasova A, Kasper S, Barone C, Turri S, Chakravartty A, Chol M, Aimone P, Hirawat S, Licitra L. Buparlisib and paclitaxel in patients with platinum-pretreated recurrent or metastatic squamous cell carcinoma of the head and neck (BERIL-1): a randomised, double-blind, placebo-controlled phase 2 trial. Lancet Oncol. 2017. Epub 2017/01/31. doi: 10.1016/s1470-2045(17)30064-5. PubMed PMID: 28131786.

11. Bonner JA, Harari PM, Giralt J, Azarnia N, Shin DM, Cohen RB, Jones CU, Sur R, Raben D, Jassem J, Ove R, Kies MS, Baselga J, Youssoufian H, Amellal N, Rowinsky EK, Ang KK. Radiotherapy plus cetuximab for squamous-cell carcinoma of the head and neck. The New England journal of medicine. 2006;354(6):567-78. Epub 2006/02/10. doi: 10.1056/NEJMoa053422. PubMed PMID: 16467544.

12. Vermorken JB, Mesia R, Rivera F, Remenar E, Kawecki A, Rottey S, Erfan J, Zabolotnyy D, Kienzer HR, Cupissol D, Peyrade F, Benasso M, Vynnychenko I, De Raucourt D, Bokemeyer C, Schueler A, Amellal N, Hitt R. Platinum-based chemotherapy plus cetuximab in head and neck cancer. The New England journal of medicine. 2008;359(11):1116-27. Epub 2008/09/12. doi: 10.1056/NEJMoa0802656. PubMed PMID: 18784101.

13. Rodon J, Brana I, Siu LL, De Jonge MJ, Homji N, Mills D, Di Tomaso E, Sarr C, Trandafir L, Massacesi C, Eskens F, Bendell JC. Phase I dose-escalation and -expansion study of buparlisib (BKM120), an oral pan-Class I PI3K inhibitor, in patients with advanced solid tumors. Invest New Drugs. 2014;32(4):670-81. Epub 2014/03/22. doi: 10.1007/s10637-014-0082-9. PubMed PMID: 24652201.

14. Boeckx C, Baay M, Wouters A, Specenier P, Vermorken JB, Peeters M, Lardon F. Anti-epidermal growth factor receptor therapy in head and neck squamous cell carcinoma: focus on potential molecular mechanisms of drug resistance. Oncologist. 2013;18(7):850-64. Epub 2013/07/04. doi: 10.1634/theoncologist.2013-0013. PubMed PMID: 23821327; PMCID: Pmc3720640.

15. D'Amato V, Rosa R, D'Amato C, Formisano L, Marciano R, Nappi L, Raimondo L, Di Mauro C, Servetto A, Fusciello C, Veneziani BM, De Placido S, Bianco R. The dual PI3K/mTOR inhibitor PKI-587 enhances sensitivity to cetuximab in EGFR-resistant human head and neck cancer models. Br J Cancer. 2014;110(12):2887-95. Epub 2014/05/16. doi: 10.1038/bjc.2014.241. PubMed PMID: 24823695; PMCID: Pmc4056056.

16. Silva-Oliveira RJ, Melendez M, Martinho O, Zanon MF, de Souza Viana L, Carvalho AL, Reis RM. AKT can modulate the in vitro response of HNSCC cells to irreversible EGFR inhibitors. Oncotarget. 2017;8(32):53288-301. Epub 2017/09/09. doi: 10.18632/oncotarget.18395. PubMed PMID: 28881811; PMCID: PMC5581110.

17. Anisuzzaman AS, Haque A, Wang D, Rahman MA, Zhang C, Chen Z, Chen ZG, Shin DM, Amin AR. In vitro and in vivo synergistic antitumor activity of the combination of BKM120 and erlotinib in head and neck cancer: Mechanism of apoptosis and resistance. Mol Cancer Ther. 2017. Epub 2017/01/26. doi: 10.1158/1535-7163.mct-16-0683. PubMed PMID: 28119490.

18. Rebucci M, Peixoto P, Dewitte A, Wattez N, De Nuncques MA, Rezvoy N, Vautravers-Dewas C, Buisine MP, Guerin E, Peyrat JP, Lartigau E, Lansiaux A. Mechanisms underlying resistance to cetuximab in the HNSCC cell line: role of AKT inhibition in bypassing this resistance. International journal of oncology. 2011;38(1):189-200. Epub 2010/11/27. PubMed PMID: 21109940.

19. Lattanzio L, Tonissi F, Monteverde M, Vivenza D, Russi E, Milano G, Merlano M, Lo Nigro C. Treatment effect of buparlisib, cetuximab and irradiation in wild-type or PI3KCA-mutated head and neck cancer cell lines. Invest New Drugs. 2015;33(2):310-20. Epub 2015/01/22. doi: 10.1007/s10637-015-0210-1. PubMed PMID: 25603975.

20. Young NR, Liu J, Pierce C, Wei TF, Grushko T, Olopade OI, Liu W, Shen C, Seiwert TY, Cohen EE. Molecular phenotype predicts sensitivity of squamous cell carcinoma of the head and neck to epidermal growth factor receptor inhibition. Molecular oncology. 2013;7(3):359-68. Epub 2012/12/04. doi: 10.1016/j.molonc.2012.11.001. PubMed PMID: 23200321; PMCID: Pmc3661759.

21. Jimeno A, Shirai K, Choi M, Laskin J, Kochenderfer M, Spira A, Cline-Burkhardt V, Winquist E, Hausman D, Walker L, Cohen RB. A randomized, phase II trial of cetuximab with or without PX-866, an irreversible oral phosphatidylinositol 3-kinase inhibitor, in patients with relapsed or metastatic head and neck squamous cell cancer. Annals of oncology : official journal of the European Society for Medical Oncology. 2015;26(3):556-61. Epub 2014/12/20. doi: 10.1093/annonc/mdu574. PubMed PMID: 25524478.

22. Brenner JC, Graham MP, Kumar B, Saunders LM, Kupfer R, Lyons RH, Bradford CR, Carey TE. Genotyping of 73 UM-SCC head and neck squamous cell carcinoma cell lines. Head & neck. 2010;32(4):417-26. Epub 2009/09/18. doi: 10.1002/hed.21198. PubMed PMID: 19760794; PMCID: PMC3292176.

23. Ludwig ML, Kulkarni A, Birkeland AC, Michmerhuizen NL, Foltin SK, Mann JE, Hoesli RC, Devenport SN, Jewell BM, Shuman AG, Spector ME, Carey TE, Jiang H, Brenner JC. The genomic landscape of UM-SCC oral cavity squamous cell carcinoma cell lines. Oral oncology. 2018;87:144-51. Epub 2018/12/12. doi: 10.1016/j.oraloncology.2018.10.031. PubMed PMID: 30527230; PMCID: PMC6349383.

24. Liu J, Pan S, Hsieh MH, Ng N, Sun F, Wang T, Kasibhatla S, Schuller AG, Li AG, Cheng D, Li J, Tompkins C, Pferdekamper A, Steffy A, Cheng J, Kowal C, Phung V, Guo G, Wang Y, Graham MP, Flynn S, Brenner JC, Li C, Villarroel MC, Schultz PG, Wu X, McNamara P, Sellers WR, Petruzzelli L, Boral AL, Seidel HM, McLaughlin ME, Che J, Carey TE, Vanasse

G, Harris JL. Targeting Wnt-driven cancer through the inhibition of Porcupine by LGK974. Proceedings of the National Academy of Sciences of the United States of America. 2013;110(50):20224-9. Epub 2013/11/28. doi: 10.1073/pnas.1314239110. PubMed PMID: 24277854; PMCID: Pmc3864356.

25. Halling-Brown MD, Bulusu KC, Patel M, Tym JE, Al-Lazikani B. canSAR: an integrated cancer public translational research and drug discovery resource. Nucleic Acids Res. 2012;40(Database issue):D947-56. Epub 2011/10/21. doi: 10.1093/nar/gkr881. PubMed PMID: 22013161; PMCID: Pmc3245005.

26. Bulusu KC, Tym JE, Coker EA, Schierz AC, Al-Lazikani B. canSAR: updated cancer research and drug discovery knowledgebase. Nucleic Acids Res. 2014;42(Database issue):D1040-7. Epub 2013/12/07. doi: 10.1093/nar/gkt1182. PubMed PMID: 24304894; PMCID: Pmc3964944.

27. Birkeland AC, Foltin SK, Michmerhuizen NL, Hoesli RC, Rosko AJ, Byrd S, Yanik M, Nor JE, Bradford CR, Prince ME, Carey TE, McHugh JB, Spector ME, Brenner JC. Correlation of Crtc1/3-Maml2 fusion status, grade and survival in mucoepidermoid carcinoma. Oral Oncol. 2017;68:5-8. Epub 2017/04/26. doi: 10.1016/j.oraloncology.2017.02.025. PubMed PMID: 28438292; PMCID: Pmc5433350.

28. Birkeland AC, Yanik M, Tillman BN, Scott MV, Foltin SK, Mann JE, Michmerhuizen NL, Ludwig ML, Sandelski MM, Komarck CM, Carey TE, Prince ME, Bradford CR, McHugh JB, Spector ME, Brenner JC. Identification of Targetable ERBB2 Aberrations in Head and Neck Squamous Cell Carcinoma. JAMA otolaryngology-- head & neck surgery. 2016;142(6):559-67. Epub 2016/04/15. doi: 10.1001/jamaoto.2016.0335. PubMed PMID: 27077364; PMCID: Pmc4911238.

29. Shum D, Radu C, Kim E, Cajuste M, Shao Y, Seshan VE, Djaballah H. A high density assay format for the detection of novel cytotoxic agents in large chemical libraries. Journal of enzyme inhibition and medicinal chemistry. 2008;23(6):931-45. Epub 2008/07/09. doi: 10.1080/14756360701810082. PubMed PMID: 18608772; PMCID: PMC3710589.

30. Birkeland AC, Yanik M, Tillman BN, Scott MV, Foltin SK, Mann JE, Michmerhuizen NL, Ludwig ML, Sandelski MM, Komarck CM, Carey TE, Prince ME, Bradford CR, McHugh JB, Spector ME, Brenner JC. Identification of Targetable ERBB2 Aberrations in Head and Neck Squamous Cell Carcinoma. JAMA otolaryngology-- head & neck surgery. 2016. Epub 2016/04/15. doi: 10.1001/jamaoto.2016.0335. PubMed PMID: 27077364.

31. Tillman BN, Yanik M, Birkeland AC, Liu CJ, Hovelson DH, Cani AK, Palanisamy N, Carskadon S, Carey TE, Bradford CR, Tomlins SA, McHugh JB, Spector ME, Chad Brenner J. Fibroblast growth factor family aberrations as a putative driver of head and neck squamous cell carcinoma in an epidemiologically low-risk patient as defined by targeted sequencing. Head Neck. 2016;38 Suppl 1:E1646-52. Epub 2016/02/06. doi: 10.1002/hed.24292. PubMed PMID: 26849095; PMCID: Pmc4844767.

32. Di Veroli GY, Fornari C, Wang D, Mollard S, Bramhall JL, Richards FM, Jodrell DI. Combenefit: an interactive platform for the analysis and visualization of drug combinations. Bioinformatics (Oxford, England). 2016;32(18):2866-8. Epub 2016/05/07. doi: 10.1093/bioinformatics/btw230. PubMed PMID: 27153664; PMCID: PMC5018366.

33. Greco WR, Bravo G, Parsons JC. The search for synergy: a critical review from a response surface perspective. Pharmacological reviews. 1995;47(2):331-85. Epub 1995/06/01. PubMed PMID: 7568331.

34. Bliss CI. The Toxicity of Poisons Applied Jointly. Annals of Applied Biology. 1939;26(3):585-615. doi: 10.1111/j.1744-7348.1939.tb06990.x.

35. Berenbaum MC. Criteria for analyzing interactions between biologically active agents. Advances in cancer research. 1981;35:269-335. Epub 1981/01/01. PubMed PMID: 7041539.

36. Mathews Griner LA, Guha R, Shinn P, Young RM, Keller JM, Liu D, Goldlust IS, Yasgar A, McKnight C, Boxer MB, Duveau DY, Jiang JK, Michael S, Mierzwa T, Huang W, Walsh MJ, Mott BT, Patel P, Leister W, Maloney DJ, Leclair CA, Rai G, Jadhav A, Peyser BD, Austin CP, Martin SE, Simeonov A, Ferrer M, Staudt LM, Thomas CJ. High-throughput combinatorial screening identifies drugs that cooperate with ibrutinib to kill activated B-cell-like diffuse large B-cell lymphoma cells. Proceedings of the National Academy of Sciences of the United States of America. 2014;111(6):2349-54. Epub 2014/01/29. doi: 10.1073/pnas.1311846111. PubMed PMID: 24469833; PMCID: Pmc3926026.

37. Borisy AA, Elliott PJ, Hurst NW, Lee MS, Lehar J, Price ER, Serbedzija G, Zimmermann GR, Foley MA, Stockwell BR, Keith CT. Systematic discovery of multicomponent therapeutics. Proceedings of the National Academy of Sciences of the United States of America. 2003;100(13):7977-82. Epub 2003/06/12. doi: 10.1073/pnas.1337088100. PubMed PMID: 12799470; PMCID: Pmc164698.

38. Lee H, Jung KH, Jeong Y, Hong S, Hong SS. HS-173, a novel phosphatidylinositol 3-kinase (PI3K) inhibitor, has anti-tumor activity through promoting apoptosis and inhibiting angiogenesis. Cancer letters. 2013;328(1):152-9. Epub 2012/08/30. doi: 10.1016/j.canlet.2012.08.020. PubMed PMID: 22929971.

39. Rumman M, Jung KH, Fang Z, Yan HH, Son MK, Kim SJ, Kim J, Park JH, Lim JH, Hong S, Hong SS. HS-173, a novel PI3K inhibitor suppresses EMT and metastasis in pancreatic cancer. Oncotarget. 2016;7(47):78029-47. Epub 2016/10/30. doi: 10.18632/oncotarget.12871. PubMed PMID: 27793006; PMCID: PMC5363641.

40. Li D, Ambrogio L, Shimamura T, Kubo S, Takahashi M, Chirieac LR, Padera RF, Shapiro GI, Baum A, Himmelsbach F, Rettig WJ, Meyerson M, Solca F, Greulich H, Wong KK. BIBW2992, an irreversible EGFR/HER2 inhibitor highly effective in preclinical lung cancer models. Oncogene. 2008;27(34):4702-11. Epub 2008/04/15. doi: 10.1038/onc.2008.109. PubMed PMID: 18408761; PMCID: Pmc2748240.

41. Paez JG, Janne PA, Lee JC, Tracy S, Greulich H, Gabriel S, Herman P, Kaye FJ, Lindeman N, Boggon TJ, Naoki K, Sasaki H, Fujii Y, Eck MJ, Sellers WR, Johnson BE, Meyerson M. EGFR mutations in lung cancer: correlation with clinical response to gefitinib therapy. Science (New York, NY). 2004;304(5676):1497-500. Epub 2004/05/01. doi: 10.1126/science.1099314. PubMed PMID: 15118125.

42. Lynch TJ, Bell DW, Sordella R, Gurubhagavatula S, Okimoto RA, Brannigan BW, Harris PL, Haserlat SM, Supko JG, Haluska FG, Louis DN, Christiani DC, Settleman J, Haber DA. Activating mutations in the epidermal growth factor receptor underlying responsiveness of non-small-cell lung cancer to gefitinib. The New England journal of medicine. 2004;350(21):2129-39. Epub 2004/05/01. doi: 10.1056/NEJMoa040938. PubMed PMID: 15118073.

43. Yu HA, Arcila ME, Rekhtman N, Sima CS, Zakowski MF, Pao W, Kris MG, Miller VA, Ladanyi M, Riely GJ. Analysis of tumor specimens at the time of acquired resistance to EGFR-TKI therapy in 155 patients with EGFR-mutant lung cancers. Clinical cancer research : an official journal of the American Association for Cancer Research. 2013;19(8):2240-7. Epub 2013/03/09. doi: 10.1158/1078-0432.Ccr-12-2246. PubMed PMID: 23470965; PMCID: PMC3630270.

44. Yu HA, Tian SK, Drilon AE, Borsu L, Riely GJ, Arcila ME, Ladanyi M. Acquired Resistance of EGFR-Mutant Lung Cancer to a T790M-Specific EGFR Inhibitor: Emergence of a Third Mutation (C797S) in the EGFR Tyrosine Kinase Domain. JAMA oncology. 2015;1(7):982-4. Epub 2015/07/17. doi: 10.1001/jamaoncol.2015.1066. PubMed PMID: 26181354; PMCID: PMC4665629.

45. Wu SG, Liu YN, Tsai MF, Chang YL, Yu CJ, Yang PC, Yang JC, Wen YF, Shih JY. The mechanism of acquired resistance to irreversible EGFR tyrosine kinase inhibitor-afatinib in lung adenocarcinoma patients. Oncotarget. 2016;7(11):12404-13. Epub 2016/02/11. doi: 10.18632/oncotarget.7189. PubMed PMID: 26862733; PMCID: PMC4914294.

46. Thress KS, Paweletz CP, Felip E, Cho BC, Stetson D, Dougherty B, Lai Z, Markovets A, Vivancos A, Kuang Y, Ercan D, Matthews SE, Cantarini M, Barrett JC, Janne PA, Oxnard GR. Acquired EGFR C797S mutation mediates resistance to AZD9291 in non-small cell lung cancer harboring EGFR T790M. Nature medicine. 2015;21(6):560-2. Epub 2015/05/06. doi: 10.1038/nm.3854. PubMed PMID: 25939061; PMCID: PMC4771182.

47. Ather F, Hamidi H, Fejzo MS, Letrent S, Finn RS, Kabbinavar F, Head C, Wong SG. Dacomitinib, an irreversible Pan-ErbB inhibitor significantly abrogates growth in head and neck cancer models that exhibit low response to cetuximab. PloS one. 2013;8(2):e56112. Epub 2013/02/14. doi: 10.1371/journal.pone.0056112. PubMed PMID: 23405260; PMCID: Pmc3566064.

48. Young NR, Soneru C, Liu J, Grushko TA, Hardeman A, Olopade OI, Baum A, Solca F, Cohen EE. Afatinib efficacy against squamous cell carcinoma of the head and neck cell lines in

vitro and in vivo. Targeted oncology. 2015;10(4):501-8. Epub 2015/01/07. doi: 10.1007/s11523-014-0353-6. PubMed PMID: 25559287; PMCID: Pmc4492891.

49. Erjala K, Sundvall M, Junttila TT, Zhang N, Savisalo M, Mali P, Kulmala J, Pulkkinen J, Grenman R, Elenius K. Signaling via ErbB2 and ErbB3 associates with resistance and epidermal growth factor receptor (EGFR) amplification with sensitivity to EGFR inhibitor gefitinib in head and neck squamous cell carcinoma cells. Clinical cancer research : an official journal of the American Association for Cancer Research. 2006;12(13):4103-11. Epub 2006/07/05. doi: 10.1158/1078-0432.ccr-05-2404. PubMed PMID: 16818711.

50. Kondo N, Ishiguro Y, Kimura M, Sano D, Fujita K, Sakakibara A, Taguchi T, Toth G, Matsuda H, Tsukuda M. Antitumor effect of gefitinib on head and neck squamous cell carcinoma enhanced by trastuzumab. Oncology reports. 2008;20(2):373-8. Epub 2008/07/19. PubMed PMID: 18636200.

51. Benavente S, Huang S, Armstrong EA, Chi A, Hsu KT, Wheeler DL, Harari PM. Establishment and characterization of a model of acquired resistance to epidermal growth factor receptor targeting agents in human cancer cells. Clinical cancer research : an official journal of the American Association for Cancer Research. 2009;15(5):1585-92. Epub 2009/02/05. doi: 10.1158/1078-0432.ccr-08-2068. PubMed PMID: 19190133; PMCID: Pmc2903727.

52. Kwak EL, Sordella R, Bell DW, Godin-Heymann N, Okimoto RA, Brannigan BW, Harris PL, Driscoll DR, Fidias P, Lynch TJ, Rabindran SK, McGinnis JP, Wissner A, Sharma SV, Isselbacher KJ, Settleman J, Haber DA. Irreversible inhibitors of the EGF receptor may circumvent acquired resistance to gefitinib. Proceedings of the National Academy of Sciences of the United States of America. 2005;102(21):7665-70. Epub 2005/05/18. doi: 10.1073/pnas.0502860102. PubMed PMID: 15897464; PMCID: Pmc1129023.

53. Wiley HS. Trafficking of the ErbB receptors and its influence on signaling. Experimental cell research. 2003;284(1):78-88. Epub 2003/03/22. PubMed PMID: 12648467.

54. Juric D, Rodon J, Tabernero J, Janku F, Burris HA, Schellens JHM, Middleton MR, Berlin J, Schuler M, Gil-Martin M, Rugo HS, Seggewiss-Bernhardt R, Huang A, Bootle D, Demanse D, Blumenstein L, Coughlin C, Quadt C, Baselga J. Phosphatidylinositol 3-Kinase alpha-Selective Inhibition With Alpelisib (BYL719) in PIK3CA-Altered Solid Tumors: Results From the First-in-Human Study. Journal of clinical oncology : official journal of the American Society of Clinical Oncology. 2018:Jco2017727107. Epub 2018/02/06. doi: 10.1200/jco.2017.72.7107. PubMed PMID: 29401002.

55. Seiwert TY, Fayette J, Cupissol D, Del Campo JM, Clement PM, Hitt R, Degardin M, Zhang W, Blackman A, Ehrnrooth E, Cohen EE. A randomized, phase II study of afatinib versus cetuximab in metastatic or recurrent squamous cell carcinoma of the head and neck. Ann Oncol. 2014;25(9):1813-20. Epub 2014/06/15. doi: 10.1093/annonc/mdu216. PubMed PMID: 24928832; PMCID: Pmc4143093.

# Chapter 4 : *Pik3ca* Mutation and *Notch1* Loss Accelerate Tumor Formation in a Transgenic Model of Head and Neck Squamous Cell Carcinoma


## Abstract

Head and neck squamous cell carcinoma (HNSCC) is characterized by a heterogeneous set of genetic alterations; these aberrations translate into a host of functional changes, which contribute to the aggressive nature of this disease and make the prediction of effective treatment paradigms difficult. Two of the most commonly dysregulated pathways in this cancer type include the phosphatidylinositol 3-kinase (PI3K) and NOTCH pathways. Both activation of PI3K and loss of NOTCH signaling have been shown to play oncogenic roles in HNSCC and have been studied using an array of preclinical models. Here, we examined the interplay between PI3K and NOTCH signaling *in vitro* and *in vivo*. We generated HNSCC cell lines with knockout of *PIK3CA* or *NOTCH1* using CRISPR/Cas9 techniques. UM-SCC-47 cells with *PIK3CA* partial knockout exhibited altered expression of *DLL1*, *HES2*, as well as genes involved in epithelial to mesenchymal transition. We also developed a transgenic mouse model to study co-alteration of genes in the PI3K and NOTCH signaling pathways using a tamoxifen-inducible, *K14*-Cre system to overexpress H1047R mutant *Pik3ca* and/or knockout of *Notch1*. Following chronic exposure to carcinogen 4-nitroquinoline N-oxide, K14; *Notch1*$^{c/c}$; *Pik3ca*$^{H1047R}$ mice displayed shorter time to endpoint compared to control mice or those mice with alterations in either *Notch1* or *Pik3ca*. These findings demonstrate the non-overlapping and synergistic contributions of PI3K and NOTCH alterations in HNSCC and motivate further studies on the

cross-talk between these pathways; such work could uncover unique molecular features and therapeutic vulnerabilities in the complex genetic landscape of HNSCC.

## Introduction

Head and neck squamous cell carcinoma (HNSCC) is a common and deadly form of cancer, accounting worldwide for 830,000 new diagnoses and 430,000 deaths per year (1, 2). HNSCC tumors are most often found in the epithelial tissue of the oral cavity, larynx, oropharynx, and hypopharynx (1). Their development is commonly associated with a variety of environmental risk factors, including excessive consumption of alcohol and/or tobacco and the presence of high-risk forms of human papilloma virus (HPV). Prognosis varies widely with tumor subsite and stage at presentation as well as with HPV status; the overall 5-year survival rate for oral cavity HNSCC patients is approximately 65%, but rates are much lower in cases of disease progression (3). Treatments also differ in individual cases depending on the severity and progression of the disease: common first-line treatments for early stage cancers include surgery or radiation therapy, and more advanced cancers are often treated with postoperative concomitant chemo-radiation in combination with cisplatin (1).

With the ever-increasing ease of performing next-generation sequencing, more and more studies have focused on genetic alterations that may be responsible for tumor formation or severity. In HNSCC, two of the most commonly altered pathways include the PI3K and Notch signaling pathways (4-6). For example, based on The Cancer Genome Atlas (TCGA) HNSCC dataset, approximately two-thirds of HNSCC tumors display genetic aberrations in PI3K pathway genes. Of these alterations, the most frequent and perhaps most notable is *PIK3CA* amplification or mutation, each of which is observed in 15-20% of patients (7-9).

An array of other studies, including those performed in our laboratory, have also demonstrated the presence of alterations in *PIK3CA* and the potential role for PI3K in HNSCC development and progression (6, 10-12). Unfortunately, there is a paucity of validated HNSCC

mouse models for altered PI3K signaling, despite the high rate of aberrations documented in TCGA. Common *PIK3CA* aberrations include mutations in the helical (E542K, E545K) and kinase (H1047R) domains of the gene; these specific amino acid changes are known to activate PI3K signaling (6, 13-15). In transgenic mouse models of breast and lung cancer, conditional expression of the *Pik3ca*$^{H1047R}$ mutant drives spontaneous adenocarcinomas (16, 17), allowing for *in vivo* trials of targeted therapeutics in these tumor types. At present, Du *et al.* have described the sole *in vivo* model of *PIK3CA* activation in HNSCC, which utilizes the a RU486-inducible *K5* promoter to conditionally overexpress wildtype *Pik3ca* in the mouse oral cavity and tongue. *Pik3ca* overexpression alone is insufficient to initiate carcinogenesis in this model, though subsequent chronic administration of tobacco analogue 4-NQO in drinking water results in the formation of invasive, poorly-differentiated tumors within six months as well as lymph node and lung metastases in roughly 40% of animals (18).

Similarly, deletion of *Pten* (which opposes PI3K signaling and acts as a tumor suppressor) is insufficient to drive *in vivo* HNSCC formation (19), but 4-NQO treatment of *Pten*$^{flox/flox}$*; K14-Cre* transgenic mice triggers multiple dysplastic and neoplastic lesions of the tongue, analogous to field cancerization seen in humans (20). Alternatively, reports of a double knockout of transforming growth factor-β (*Tgfbr1*) and *Pten* driven by the *K14* promoter in a Cre recombinase system describe spontaneous formation of invasive SCC of oral epithelia with full penetrance (21). Using this *Tgfbr1-Pten* knockout strain, promising antitumor efficacy of targeted PI3K and mTOR inhibitors has been achieved (22, 23).

Notch dysfunction, resulting in disruption of signaling pathways involved in embryologic differentiation, cellular proliferation, and maintenance of metabolic homeostasis (24), has been identified in many cancer types, including HNSCC (4, 5, 7). However, the exact function of the

Notch signaling in cancer is incompletely understood, as evidence has suggested a bimodal role, depending on the nature of the alteration (25). Activating mutations in Notch receptors were first identified in lymphomas (26), but more recent research in HNSCC has indicated that N-terminal, inactivating mutations in *NOTCH1* are present in at least 10-15% of tumors and may be a playing a tumor suppressive role in this cancer type (4, 5, 7, 27, 28).

Many previous mouse models have revealed an important but complex role for Notch signaling in tumor formation. Demehri *et al.* demonstrated, using several genetically engineered mouse models (GEMMs) with varying degrees of Notch signaling on the Msx2-Cre background, that mouse lifespan and age at spontaneous tumor onset was correlated with alteration severity: animals lacking gamma secretase activity did not survive, while those with loss of *Notch1* lived almost as long as wildtype littermates but developed skin tumors after roughly 1.5 years (29). This study also demonstrated that different Notch pathway members could affect survival and tumor phenotypes differently; mice without Notch effector *Rpbj* KO lived tumor-free for 4 months, while animals with knockout of *Notch1-3* also lived for approximately 4 months but displayed skin tumors at about 3 months of age (29). In a separate manuscript, Demehri *et al.* also showed that inactivation of Notch signaling leads to increased susceptibility to chemical carcinogenesis (30). Similarly, Nyman *et al*. recently demonstrated that transgenic mice expressing the dominant negative form of *Maml1* (*DNMAML1*) under the control of a tamoxifen-inducible K14 Cre displayed increased frequency and multiplicity of oral cancers (27). This effect was enhanced by the co-expression of *DnMaml1* with gain-of-function mutant $p53^{R172H}$ and especially with HPV oncogenes *E6* and *E7*. However, in another HPV-driven mouse model of oral cavity SCC, both *Notch1* overexpression (*LSL-KRAS*$^{G12D}$*/LSL-NICD/iHPV-Luc; K14-CreER*$^{tam}$) and bi-allelic deletion of the same gene (*LSL-KRAS*$^{G12D}$*/Notch1*$^{flox/flox}$*/iHPV-Luc; K14-*

*CreER*$^{tam}$) enhanced tumor growth and invasiveness (31). Taken together, these studies indicate that Notch signaling plays a multifaceted role in tumor initiation and that the means by which inactivation of this pathway is achieved may critically affect survival and/or tumor burden. Additionally, the immune system is an important component of these effects. Di Piazza *et al*. showed the striking ability of pro-inflammatory cytokine thymic stromal lymphopoietin (TSLP) to act directly on T-cells and protect against cutaneous carcinomas or, when genetically ablated, to promote tumor formation via increased Wnt signaling in *K5*-driven models of loss of *Notch1* and *Notch2* (32).

While substantial research efforts have investigated individual genetic alterations and their related signaling networks (including PI3K and Notch signaling as described above), far fewer studies have examined how the presence of multiple mutations or copy number alterations in genes from two or more separate pathways might impact HNSCC tumorigenesis and treatment response. Previous work using GEMMs with deficiencies in multiple Notch pathway genes suggests that other transgenic models with alterations in additional signaling networks may display additive or even synergistic phenotypes as well. Excitingly, recent work by Sambandam *et al.* indicates that preclinical HNSCC models with inactivation of *NOTCH1* may be more sensitive to PI3K inhibition, making *NOTCH1* loss a potential biomarker for response to these targeted therapies (33). Here, based on these results as well as the frequency of loss-of-function *NOTCH1* and activating *PIK3CA* mutations in HNSCC, we developed *in vitro* models of *PIK3CA* and *NOTCH1* knockout and a transgenic mouse model of *Notch1* loss and *Pik3ca* mutant overexpression to further study the overlap between PI3K and Notch signaling.

## Methods

*Cell Culture*

UM-SCC cells were maintained in DMEM with 10% FBS, 1X Pen/Strep, 1X NEAA at 37°C and 5% $CO_2$ (vol/vol). All cell lines were genotyped to confirm authenticity and were mycoplasma negative as described previously (34).

*Generation of CRISPR Cell Lines*

500 μL of lentiviral construct (Sigma Aldrich) with gRNA targeting the first exon of *PIK3CA* (sequence: 5'-GTTCACCTGATGATGGTCG-3') was added to UM-SCC-47 cells in a six-well plate that contained 2.5 mL of complete media with 10 μg/mL polybrene (EMD Millipore, Cat No: TR-1003-G). An additional well was left without virus as a control. After 1-2 weeks, cells were exposed to puromycin selection until non-transduced cells died. As an additional selection measure, cells were expanded and sorted for GFP positivity versus non-transduced, wildtype cells at the University of Michigan Flow Cytometry Core using the MoFlo Astrios EQ Cell Sorter. Cells expressing GFP were expanded and seeded in 10 cm dishes with 500-1000 cells per dish to isolate single-cell colonies. When colonies formed on these dishes, colony rings were used to isolate, trypsanize, and expand each individual colony to its own well in a 24 well plate. When these 24 well plates became confluent, each well was expanded to two wells. One of these wells was lysed and harvested to test for *PIK3CA* or *Notch1* expression using Western blot (see below), while the other was maintained in culture.

*Genomic DNA Isolation*

Cells were harvested and washed in PBS, then frozen at -20ºC. The pellet was then thawed and transferred to 700 μL of Nuclei Lysis Solution (Promega, Madison, WI) for 1 hour at 55ºC. 200 μL of Protein Precipitation Solution (Promega) was added to the sample, which was then mixed

and centrifuged at 13,000 RPM for two minutes. The supernatant was then transferred to a tube containing 600 μL of isopropanol, incubated for 15 minutes, and centrifuged at the same speed for another minute. The DNA pellet was washed in 70% ethanol, dried, and re-suspended in 35-50 μL of nuclease-free water.

*PCR and Sanger Sequencing*

DNA was amplified using PCR with Platinum Taq DNA Polymerase High Fidelity (Invitrogen) according to manufacturer's protocols and with primers that targeted the region of the guide RNA for *PIK3CA* (primer sequences: FWD: 5'-CCTCCACGACCATCATCAGG-3' and REV: 5'-TCTTCCCTTTCTGCTTCTGT-3') or *Notch1* (FWD: 5'-CTGGCTTTGTGGTT-3', REV: 5'-GTCCAGGATGTGGCACAAG-3'). PCR products were inserted into the pCR8 vector system (ThermoFisher, Cat No: K250020) and transformed into Mach1 competent cells, again according to manufacturer's protocols. Bacteria cultures from individual colonies on LB + spectinomycin plates were grown overnight and DNA was isolated using the Qiagen mini-prep protocol (Cat No: 27106) according to manufacturer's protocols. The DNA product was analyzed via Sanger sequencing at the University of Michigan DNA Sequencing Core on the 3730XL DNA Sequencer (Applied Biosystems). Sequences were aligned using the DNASTAR Lasergene software suite.

*Western Blotting*

Cells were grown to 70-80% confluency and lysed in radioimmunoprecipitation assay buffer (ThermoFisher, Cat No: 89900) containing 1% NP-40 and 0.1% SDS. 10-50 micrograms of each cell harvest were used, and standard western blot protocols were followed as previously described (35). Primary antibodies (described in detail in

Table 4-2) were applied overnight at 4°C or for at least one hour at room temperature, followed by a goat anti-rabbit horseradish peroxidase (Cat No: 111-035-045; Jackson ImmunoResearch, West Grove, PA) secondary antibody at room temperature for one hour as described elsewhere (36). The blots were then visualized with chemiluminescence and imaged. Images were digitally retained at 300 or greater dpi from all westerns and representative blots are shown.

*RNA Isolation and qPCR*

Cells were harvested in Qiazol (Cat No: 79306; Qiagen) and stored at -80°C. RNA was isolated using the Qiagen RNeasy Mini Kit (Cat No: 74106) according to manufacturer's protocols, and then quantified using the Qubit fluorometer (ThermoFisher). cDNA was synthesized using the SuperScript Vilo cDNA Synthesis kit (ThermoFisher, Cat No: 11754250, also using manufacturer's protocols, in the GeneAmp® PCR System 9700 (Applied Biosystems). qPCR analysis for each cDNA sample was performed with Quantitech SYBR green (catalog No: 204143; Qiagen) on the QuantStudio 5 instrument (ThermoFisher). Primers were purchased from Intregrated DNA Technologies and sequences are listed in **Table 4-3**.

*Transcriptome and Gene Set Enrichment Analysis*

Transcriptome analysis was performed using Illumina stranded transcriptome library preparation kits with 75 nucleotide paired end sequencing to >100x depth on an Illumina HiSEQ4000 for UM-SCC-47 and UM-SCC-47 *PIK3CA* CRISPR cells. No quality issues were identified in the analysis. To calculate gene expression in fragments per kilobase million (FPKM), we aligned reads using STAR (v2.5.3a) according to the standard two-step alignment process and the processed the data with Cufflinks (v2.2.1). Using the FPKM read counts, we then defined gene signatures that were >2-log2 fold upregulated or downregulated in the knockout model relative

to the control and uploaded the gene sets into GSEA (MIT, Broad) to identify significant overlap with Hallmark, KEGG and GO biological process pathways with false discovery rate (FDR) q-value < 0.05 considered significant.

*Inhibitors*

All inhibitors were purchased from Selleck Chemicals and dissolved in 100% DMSO to 10 mM, then diluted to their appropriate concentrations for use *in vitro*.

*Resazurin Cell Viability Assay*

2000 cells per well were seeded (in 50 μL volume) in 384 well microplates (Grenier, Cat No: 781091) and allowed to adhere overnight. The following day, inhibitors were prepared at 200X in 96-well plates. Inhibitors were dissolved in DMSO in a ten-point, two-fold dilution series. These inhibitors were then diluted 1:20 into complete media using the Agilent BRAVO Liquid Handing system. Finally, again using this liquid handling equipment, media containing inhibitor was added to each well of the cell plate at 1:10. Treatments were performed for 72 hours. 12-24 hours prior to the end of the treatment time point, 10 μL of 440 μM resazurin (Sigma, Cat No: R-7017) was added to each well of the plate. Signal was measured and quantified using the Biotek Cytation3 fluorescence plate reader at excitation and emission wavelengths of 540 and 612 nm, respectively. Using Prism 7, data were plotted and fit with concentration response curves using the log(inhibitor) vs. response -- Variable slope model with four parameters ($IC_{50}$, top, bottom, and Hill slope) allowed to vary.

*Animal Care*

Animals were housed in a vivarium accredited by the Assessment and Accreditation of Laboratory Animal Care at the University of Michigan. Veterinary care was provided by the University of Michigan Unit for Laboratory Animal Medicine (ULAM), and all procedures were

performed according to Institution for Animal Care and Use Committee-approved protocol PRO00008316. Mice with *Notch1* loss and/or *Pik3ca* mutation were originally obtained from the laboratory of Dr. Sunny Wong. To generate mice for experiments, we paired one healthy male and one healthy female mouse (both mice between the ages of 6 and 30 weeks). Male and female littermates were weaned and separated into their respective cages at 3 weeks of age.

*Genotyping*

At 3-4 weeks, ear clips were taken to obtain DNA samples for genotyping. DNA was extracted from clips using the Hot Sodium Hydroxide and Tris (HotSHOT) program, in which 75 μL of Basic Reagent was added to each sample (1g NaOH, 0.074g EDTA-disodium, adjusted to a volume of 1L with $ddH_2O$ for a pH of 12). Samples were placed on a 95°C heat block for 20-30 minutes and on ice for 5 minutes to allow the solution to cool. Once samples were cooled, 75 μL of Neutralizing Reagent (6.304g Tris-HCl, adjusted to a volume of 1L with $ddH_2O$ for a pH of 5) was added to each tube. Samples were kept on ice for genotyping or stored at -20°C overnight. PCR was used to obtain the K14, Notch1, and Pik3ca genotypes, using 2x GoTAQ Green PCR Master Mix (catalog No: M7122; Promega). Each PCR well contained 3.5 μL $ddH_20$, 5 μL GoTAQ Green, 0.5 μL of 20 μM primer mix (for K14, Notch1 or Pik3ca), and 1 μL genomic DNA isolated from the ear clip of an individual mouse. PCR products were evaluated using 2% agarose gels. Primer sequences, PCR protocols, and expected PCR product sizes are shown in **Table 4-1**.

*Tamoxifen*

At 5 weeks of age, mice with expression of K14 promoter and desired genotypes for *Notch1* and *Pik3ca* were induced using tamoxifen (Cat No: T5648, Sigma). Tamoxifen was prepared from

powder at 12.5 mg/mL in sterile corn oil and vortexed for 2 hours at room temperature prior to use. Mice received three intraperitoneal (i.p.) injections of tamoxifen at 50 mg/kg, once daily for three days.

*4-Nitroquinoline N-Oxide*

At 6 weeks of age, mice received 5 μg/mL 4-Nitroquinoline-N-oxide (4-NQO) (Sigma, Cat No: N8141), a tobacco analogue, via their drinking water. 4-NQO was prepared as described previously (18). 4-NQO powder was dissolved at 5 mg/mL in sterile propylene glycol (Sigma, Cat No: 4347) and vortexed for at least 2 hours at room temperature. 4-NQO was then diluted 1:100 in sterile water and filtered using a 0.2 μm filter for a final concentration of 50 μg/L. Drinking water containing 4-NQO was administered chronically for 16 weeks, with water prepared fresh and changed each week.

*Tumor Monitoring*

Each week, all mice on treatment were weighed and monitored for tumor formation and general health. Some mice developed adverse phenotypes and were treated as described in **Table 4-5**. Mice reached their endpoint based primarily on the basis of 20% weight loss, which suggested the presence of oral tumors that made eating and/or drinking difficult. As mice tended to gain weight in the 8 weeks following the initiation of 4-NQO administrations, mice were sacrificed if they exhibited 20% weight loss compared to the highest recorded weight during this time period. After 8 weeks of tumor monitoring, weights were compared to the rolling average weight, with 20% weight loss again resulting in sacrifice. Additional mice that died or required euthanasia due to signs of poor health prior to the weight loss endpoint were included in the analysis if tumor was visible upon tissue harvest.

*Tissue Harvest*

After being exposed to 4-NQO and reaching their endpoint, mice were humanely euthanized and dissected to look for visible tumor on the cheek, lip, and tongue. Tumors were photographed, collected, and fixed using formalin for no more than 72 hours. Tissues were then processed into FFPE blocks by the University of Michigan Rogel Comprehensive Cancer Center Research Histology and Immunoperoxidase Laboratory Core.

*Immunohistochemistry*

Immunohistochemistry was performed using standard protocols. Briefly, slides were deparaffinized at 58°C for 30 minutes, then rehydrated with xylene and ethanol, followed by a wash with deionized water. Antigen unmasking was performed at temperatures > 90°C for 1 hour in citrate buffer. After two washes with PBST, endogenous peroxidase was quenched. Following two additional PBST washes, 5% goat serum was used for blocking, and primary antibody (see **Table 4-4**) was applied overnight at 4°C. Following three PBST washes, secondary antibody was applied for 30 minutes at RT, then washed away with PBST. The Vectastain Elite ABC kit was used to add the avidin-biotinylated HRP complex, after which slides were washed with PBST three times and water once. Next, slides were incubated with DAB for 2-10 minutes and washed with water again. Hematoxylin was used as a counterstain, followed by another water wash and tissue dehydration using ethanol. Two xylene washes were performed, and slides were mounted. Slides were scored by a pathologist and representative images are shown.

*Statistical Analysis*

We modeled the time to endpoint as a continuous outcome in a linear regression model. Group was considered as the predictor and no censoring was performed. Pairwise comparisons were

made with either K14 or K14; *Notch1*$^{c/c}$; *Pik3ca*$^{H1047R}$ as the reference group. Maximum likelihood paramer estimates were obtained with $p < 0.05$ considered statistically significant.

## Results

*Co-Alteration of PI3K and Notch Pathways in TCGA*

We queried the HNSCC TCGA dataset to explore the rate of NOTCH and PI3K pathway co-alteration in patients with this cancer type. This analysis identified a majority of patients with mutation or copy number changes in one or both pathways. Of the 505 patients with mutation and copy number information available in TCGA, 198 (39.2%) tumors in this dataset had an alteration in a NOTCH pathway gene (*NOTCH1*, *NOTCH2*, *NOTCH3*, *NOTCH4*, *MAML1*, *MAML2*, *MAML3*), and 319 (63.2%) tumors had an alteration in the PI3K pathway (*PIK3CA*, *PTEN*, *PIK3CB*, *PIK3CD*, *PIK3CG*, *PIK3R1*, *PIK3R2*, *PIK3R3*, *PIK3R4*, *PIK3R5*, *PIK3R6*, *PIK3AP1*, *PIK3C2A*, *PIK3C2B*, *PIK3C2G*, *PIK3C3*, *AKT1*, *AKT2*, *AKT3*, *AKT1S1*, *AKTIP*, *EIF4B*, *EIF4E*, *EIF4EBP1*, *EIF4G1*, *FKBP1A*, *MTOR*, *PDK1*, *PDK2*, *RHEB*, *RPS6KB1*) (7-9). More than one quarter of patients (142/505, 28.1%) displayed alterations in both the NOTCH and PI3K signaling networks, and 26 of these tumors (5.1%) exhibited inactivating Notch1 alterations (deletion or N-terminal mutation) as well as potentially activating *PIK3CA* alterations (amplification or mutation) (**Figure 4-1**, **Table 4-6**).

*Characterization of PIK3CA Knockout HNSCC Cell Line Demonstrates Interplay Between PI3K and NOTCH Signaling Pathways*

We set out, therefore, to explore whether the Notch and PI3K signaling networks interacted using *in vitro* genetic knockout models, hypothesizing that alteration of PI3K or Notch signaling might affect the second pathway or a common functional outcome. We were first

interested in identifying changes that might occur after long-term depletion of signaling through the PI3K p110 alpha isoform. As noted above, *PIK3CA*, the gene which encodes this PI3K isoform, is frequently altered in HNSCCs, suggesting that it may be a common oncogenic driver. To study the consequences of loss of p110α, we used CRISPR-Cas9 technology to knockout *PIK3CA* in patient-derived UM-SCC-47 cells, a widely used model of HPV positive oral squamous cell carcinoma. UM-SCC-47 cells were transduced with a lentiviral construct including the Cas9 endonuclease as well as a guide RNA targeting the first exon of *PIK3CA*. Following selection and single-cell cloning, this method generated a daughter cell line with at least two unique deletions in regions near the gRNA sequence. One of these deletions is a loss of seven nucleotides, and the second deletion is three nucleotides in length (**Figure 4-2**). Although (1) some wildtype *PIK3CA* DNA may still be present and (2) three nucleotide deletions may allow effective translation of downstream regions of the protein following a single missing amino acid, protein expression of p110α was markedly reduced in this model (**Figure 4-3**). A resazurin cell viability assay demonstrated that the UM-SCC-47 CRISPR model displayed decreased sensitivity to alpha-isoform selective PI3K inhibitor HS-173 and pan-PI3K inhibitor BKM120 (**Figure 4-5**), further indicating that this model is a functional model of *PIK3CA* knockout. Growth rates and levels of AKT phosphorylation were similar between wildtype and *PIK3CA* partial knockout cells (**Figure 4-4**), although pAKT was slightly decreased with loss of p110α (as might be expected due to decreased PI3K signaling) (**Figure 4-3**). We observed no significant signaling changes in the Ras-MEK-ERK pathway and no compensation through other p110 isoforms in this model (**Figure 4-3**).

To continue to explore potential differences between the wildtype UM-SCC-47 and *PIK3CA* partial knockout models, we performed RNA sequencing on each cell line. This led us

to identify 84 genes that were >2 log2-fold increased and 189 that were >2 log2-fold decreased in the *PIK3CA* partial knockout model relative to wild type cells. Although the upregulated gene set was relatively small, gene set enrichment analysis (GSEA) defined significant overlap with genes in the interferon and epithelial to mesenchymal transition and TNF alpha via NFKB response pathways, consistent with an upregulation of anti-immune survival pathways (**Table 4-7**). Interestingly, the *PIK3CA* partial knockout cell line also displayed a mesenchymal morphology compared to UM-SCC-47 wildtype cells (**Figure 4-6**). The 189-gene downregulated gene set, in contrast, had significant overlap with genes in the mTOR KEGG pathway (FDR $q < 0.05$), confirming that the knockout deregulated known downstream PI3K effector pathways. Surprisingly, Go-ontology enrichment analysis with GSEA software identified significant enrichments in pathways related to tissue development and epidermal differentiation, which contained a few genes in common between the gene sets (**Table 4-7**). These common genes driving the significance of the interaction included *DLL1* and two keratins (*K5* and *K14*), which are known to be regulated by NOTCH signaling in HNSCC (28, 37, 38). Further analysis of the downregulated gene set also identified another known NOTCH effector, *HES2*, as >2 log2-fold decreased between the knockout and wild type models. Decreased expression of *DLL1* and *HES2* was confirmed via qPCR (**Figure 4-7**). Taken together, then, the GSEA data confirmed that the *PIK3CA* partial knockout inactivated mTOR signaling, increased an anti-immune response, and inhibited NOTCH signaling pathways in this model. Thus, co-alterations in PI3K and Notch pathways could lead to deregulation of epidermal differentiation and may not only be frequent, but also consequential, in HNSCC.

*Transgenic Mouse Model of* Notch1 *Loss and H1047R* Pik3ca *Mutation Displays Accelerated Tumor Formation*

Having observed these effects *in vitro*, we decided to develop an *in vivo* model to study PI3K pathway activation and NOTCH deficiency in HNSCC. Few previous studies have examined the role of aberrant PI3K signaling in transgenic mouse models of HNSCC (18), particularly via activating mutation of *PIK3CA*, and we are unaware of any other models that can be used to evaluate simultaneous alteration of these two pathways. We selected the H1047R *PIK3CA* mutation, one of the "hotspot" alterations in this gene. This mutation is observed in many human cancers, including breast, colorectal, lung, and HNSCC tumors and has a known role in the activation of PI3K signaling (6, 7, 14, 15). *NOTCH1* has been identified as one of the most frequently altered genes in HNSCC tumors (4, 5, 7), and loss of Notch signaling has been shown to contribute to tumorigenesis in other transgenic mouse models of this cancer type (27). Therefore, our model uses two of the most common genetic alterations in the PI3K and NOTCH signaling pathways to mimic PI3K aberrant and/or Notch deficient HNSCCs.

To develop this model, we used the tamoxifen-inducible, Cre recombinase system to drive the expression of transgenes under the control of a K14 promoter. As K14 is expressed in epithelial cells, including those of the oral mucosa, this expression system was a suitable choice to study cancers originating in the oral cavity. Here, we modeled activation of PI3K signaling via the expression of H1047R mutant *Pik3ca* and/or loss of Notch signaling via knockout of the first exon of *Notch1* in K14 positive cells (**Figure 4-8**).

To induce the formation of head and neck tumors in our transgenic mouse model, we treated mice with a well-validated chemical carcinogen, 4-Nitroquinoline N-oxide (4-NQO). Exposure to 4-NQO, commonly achieved via chronic treatment in drinking water, leads to the

formation of reactive oxygen species that can cause double stranded breaks in DNA (39, 40). As a result, tumors observed following treatment with 4-NQO serve as a model of smoking-induced HNSCCs (39, 41-44). For this study, we administered 4-NQO to mice at 50 ug/mL via chronic exposure in drinking water. Treatments began at six weeks of age and continued for 16 weeks (18).

During 4-NQO treatment as well as afterward, weekly health checks were performed to assess the time to endpoint. When mice reached 20% loss of body weight, we humanely euthanized the animals and checked the lip, cheek, and tongue tissue for the presence of any visible lesions. We also included animals requiring euthanasia prior to the 20% loss of body weight endpoint if they displayed visible lesions upon sacrifice. In our current analysis (which may be updated with additional animals as further histologic data is generated and statistical tests are performed), cohorts of eight or nine animals comprised each of the four genetic backgrounds: K14 only, K14 with *Pik3ca* H1047R mutation (K14; *Pik3ca*$^{H1047R}$), K14 with *Notch1* knockout (K14; *Notch1*$^{c/c}$), and K14 with both *Pik3ca* mutation and *Notch1* knockout (K14; *Notch1*$^{c/c}$; *Pik3ca*$^{H1047R}$). All eight of the mice in the K14; *Notch1*$^{c/c}$; *Pik3ca*$^{H1047R}$ group had visible lesions, while 5/9 (55.6%) animals in K14; *Notch1*$^{c/c}$ group, 6/8 (75%) mice in the K14; *Pik3ca*$^{H1047R}$ group, and 8/9 (88.9%) mice in the K14 group had visible lesions (**Figure 4-9, Table 4-8**). Of these mice, each had visible lesions identified in at least one and as many as three anatomic subsites (**Figure 4-9, Table 4-8**). When lesions were present and subsite information was available, the average number per mouse was varied by genotype, ranging from an average of 1 lesion per mouse for the K14; *Notch1*$^{c/c}$ group to 2.16 lesions per mouse in the K14; *Pik3ca*$^{H1047R}$ group (**Figure 4-9**, **Table 4-8**). Consistent with expression driven by K14, dorsal skin tumors were observed in a small subset of mice (**Figure 4-9, Table 4-8**). The tongue was the most common site for lesions overall

and within all genotypes except K14; *Notch1*$^{c/c}$ (**Figure 4-9, Table 4-8**). Although mice of each genotype developed comparable lesions in this experiment, the time to endpoint was more disparate between groups. Each of the groups with genetic alteration in *Pik3ca* and/or *Notch1* displayed decreased time to endpoint as compared to *K14* only control mice, with the double alteration mice also reaching endpoint more quickly than either K14; *Notch1*$^{c/c}$ or K14; *Pik3ca*$^{H1047R}$ animals (**Figure 4-10**). This result indicates that *Notch1* loss and *Pik3ca* mutation act synergistically in this transgenic model and provides support for the hypothesis that alteration of both NOTCH and PI3K pathway genes could substantially affect HNSCC outcomes.

To more fully characterize the lesions in each of our four transgenic mouse strains (K14, K14; *Pik3ca*$^{H1047R}$, K14; *Notch1*$^{c/c}$, and K14; *Notch1*$^{c/c}$; *Pik3ca*$^{H1047R}$), we identified squamous cell carcinoma samples from each group and performed immunohistochemistry (**Table 4-9, Figure 4-11**). While our initial analysis only included one sample per genotype, we identified several patterns of interest. First, p110α was high in all samples, including those without the *Pik3ca*$^{H1047R}$ transgene (**Figure 4-11**). Similarly, pPDK1(Ser241) and p63 staining was high in all samples (**Figure 4-11**). While previous western blot analysis of lysates from tumor and normal samples from K14; *Pik3ca*$^{H1047R}$ mice indicated confirmed AKT phosphorylation in SCC samples (**Figure 4-12**), pAKT staining by IHC was disparate between groups (**Figure 4-11**). Higher levels of AKT phosphorylation were seen in K14 and K14; *Notch1*$^{c/c}$ SCCs, perhaps driven by high expression of p110α. Interestingly, CD8 infiltration reciprocated survival data, with the greatest infiltration the K14; *Notch1*$^{c/c}$; *Pik3ca*$^{H1047R}$ sample, intermediate infiltration in K14; *Pik3ca*$^{H1047R}$ and K14; *Notch1*$^{c/c}$ tumors, and low infiltration in the case of K14 alone (**Figure 4-13**). PD-L1 scores were moderate in the K14; *Notch1*$^{c/c}$ tumor and lower in the K14;

*Notch1*$^{c/c}$; *Pik3ca*$^{H1047R}$ and K14; *Pik3ca*$^{H1047R}$ sample; all three of these, however, displayed higher PD-L1 intensity than the tumor from the K14 mouse.

## Discussion

Our results show that both overexpression of H1047R mutant *PIK3CA* and loss of *NOTCH1* are pivotal events for HNSCC pathogenesis derived from *K14* positive cells. The overlapping ability of aberrations in these two pathways to drive HNSCC development and/or progression is suggested by the aberration rates in PI3K and NOTCH signaling in HNSCC TCGA patient tumors (7) and the altered expression of *DLL1, HES2*, EMT- and differentiation-related genes in our cell line model of partial *PIK3CA* knockout. Furthermore, we also show in a transgenic mouse model that the combining H1047R mutant *Pik3ca* and *Notch1* loss drives a more aggressive cancer phenotype, displaying earlier onset of endpoint than disruption of either gene individually. This data suggests that although the pathways are clearly linked, mutant *PIK3CA* and *NOTCH1*-driven pathways are not completely overlapping as disruption of both pathways has an additive functional effect on disease pathogenesis.

The significance of our study is supported by recent work from Sambandam *et al.*, which shows that *NOTCH1*-mutant HNSCC cell lines are highly sensitive to PI3K/mTOR inhibitors (33). The discovery of the relationship between these two pathways in cell line and xenograft models was reinforced further by their data showing that a PDK1-dependent mechanism drove resistance to PI3K inhibitors in *NOTCH1* wild type models, but not in *NOTCH1* mutant models. Interestingly, a previous study in which mice with *K5*-driven overexpression of wildtype *PIK3CA* were treated with 4-NQO for 16 weeks demonstrated a strong correlation of aggressive tumor behavior with PDK1 signaling, as poorly differentiated or metastatic tumors had

significantly higher p110α and PDK1 protein expression (18). Although NOTCH status was not specifically tested in the 4-NQO-treated *K5-PIK3CA* mice, we might hypothesize, based on the data on Samdandam *et al.* (33), that NOTCH alterations were not present. Our model, however, does not recapitulate this evidence for PDK1's role in PI3K signaling: immunohistochemistry data, although limited to a small number of animals with validated SCC, suggests that there is no difference in PDK1 expression in tumors from K14 only, K14; Notch1$^{c/c}$, and K14; *Notch1*$^{c/c}$; Pik3ca$^{H1047R}$ mice. Rather, all stains from 4-NQO-induced SCC tumors displayed strong staining covering most of the tumor area. Less intense staining was observed in normal tissues, epithelial dysplasias, and spontaneous SCCs (no 4-NQO treatment). These results suggest that another mechanism, outside of high PDK1 expression, mediates the effects of PI3K signaling in this model. Additional immunohistochemical data suggests that this effect is not mediated by activation of canonical downstream PI3K effector AKT or by expression of p63. Alternatively, CD8 infiltration was highest in the K14; *Notch1*$^{c/c}$; Pik3ca$^{H1047R}$ SCC sample, which may indicate an important role for the immune system in this model. In light of this, it is interesting to note that PDL1 staining was most intense in mice with alterations in *Pik3ca* and/or *Notch1*. While the results require validation in additional tumor specimens, these data suggest that T-cell exhaustion may be observed in animals with more significant tumor burden and earlier tumor onset. Further studies are needed to assess the presence of other markers of T-cell exhaustion, such as CTLA-4 and Tim-3. If validated, the state of these T-cells could contribute to accelerated tumor formation in K14; *Notch1*$^{c/c}$; Pik3ca$^{H1047R}$ mice as the immune system fails to efficiently recognize and eliminate foreign tumor cells. A role for PI3K signaling in immune responses has been previously reported (45), and is further exhibited by the differential

expression of interferon alpha and gamma signaling pathways in GSEA analysis of our *PIK3CA* partial knockout cell model (**Table 4-7**).

Alternatively, the presence of the H1047R *Pik3ca* mutation in our transgenic mouse model presents a second possible factor that could contribute to the lack of PDK1-dependence. The differential mechanisms downstream of mutant and wildtype *PIK3CA* are not well-understood; it is possible that activation of this oncogene via mutation, amplification, or overexpression promotes signaling through differential or other currently unidentified pathways. These differences are difficult to compare *in vitro* as many cell lines exhibit additional copies of the 3q chromosome (10), which may be a side-effect of the changes necessary for tumor cells to survive outside of the host environment (46) and it is unclear how many copies of this gene are necessary for functional alterations in PI3K signaling. Previous studies assessing *PIK3CA* amplification and overexpression have indicated that either may predict poor prognosis for HNSCC patients, while mutation status does not stratify outcomes (47). Similar studies have also proposed mechanisms including inactivation of YAP, a member of the Hippo signaling pathway, as an additional downstream PI3K target responsible for changes in tumor progression (48).

Despite the potential for alternative effector signaling in our *PIK3CA* mutant model and the one with wildtype *PIK3CA* overexpression developed by Du *et al.* (18), the time to tumor formation appears similar. While this evidence may suggest that *PIK3CA* mutation does not further induce tumor formation as compared to *PIK3CA* overexpression alone, these results are difficult to compare due to confounding factors including the specific genetic driver of *PIK3CA* overexpression (*K14* vs *K5*) and the specificity of each endpoint protocol. It would be informative to explore the characteristics of a model in which our mutant *Pik3ca* transgene was

replaced by wildtype *Pik3ca* to more definitively compare the effects of PI3K activation via mutation rather than overexpression alone.

In summary, our results here provide evidence for differential but coordinating effects of signaling through the PI3K and NOTCH pathways. We demonstrate that these alterations are clinically relevant through our analysis of genetic data from patients in the HNSCC TCGA cohort and explore their mechanistic function using cell line knockout models lacking *PIK3CA* or *NOTCH1*. Our *in vitro* studies reveal alterations in gene expression related to epithelial to mesenchymal transition and keratinocyte differentiation. Finally, we used a Cre-inducible, *K14*-driven transgenic mouse model displaying two of the most common alterations in these signaling pathways, *Pik3ca* mutation and *Notch1* loss, in order to assess the tumorigenic potential of changes in one or both of these genes. We showed that the co-alteration of PI3K and Notch signaling accelerated tumor formation, displaying at least additive effects when compared to changes in just one of these pathways. Together, these findings suggest that PI3K-altered, NOTCH-deficient tumors may represent a unique and targetable subset of HNSCCs. While restoring the loss of NOTCH signaling will be difficult to achieve clinically and come with other toxicities due to the bimodal role of this pathway, PI3K inhibitors may have greater efficacy in individuals with inactivating mutations or deletion of *NOTCH1*, especially when observed with activation of *PIK3CA*. Studies to evaluate this hypothesis are ongoing; we eager await the results of a clinical trial to determine the efficacy of PI3K/mTOR inhibitor bimeralisib in *NOTCH1*-altered HNSCCs (NCT03740100).

**Acknowledgements**

Thank you especially to C. Heenan as well as to E. Leonard, S. Devenport, and B. Marinelli for their work with the transgenic mice. For help with immunoblotting, qPCR, and generation and characterization of *PIK3CA* partial knockout model, particular thanks to E. Leonard and J. Wang, as well as to V. Nair, C. Matovina, M. Harris, G. Herbst, A. Bachand, and D. Kim. Thank you to T. Moghbeli and Y.L. Lei for immunohistochemistry. Thank you to E. Bellile, J. Zhai, and H. Jiang for statistical analysis. Thank you to J.C. Brenner for GSEA analysis as well as oversight and guidance in experimental design and interpretation.

## Figures

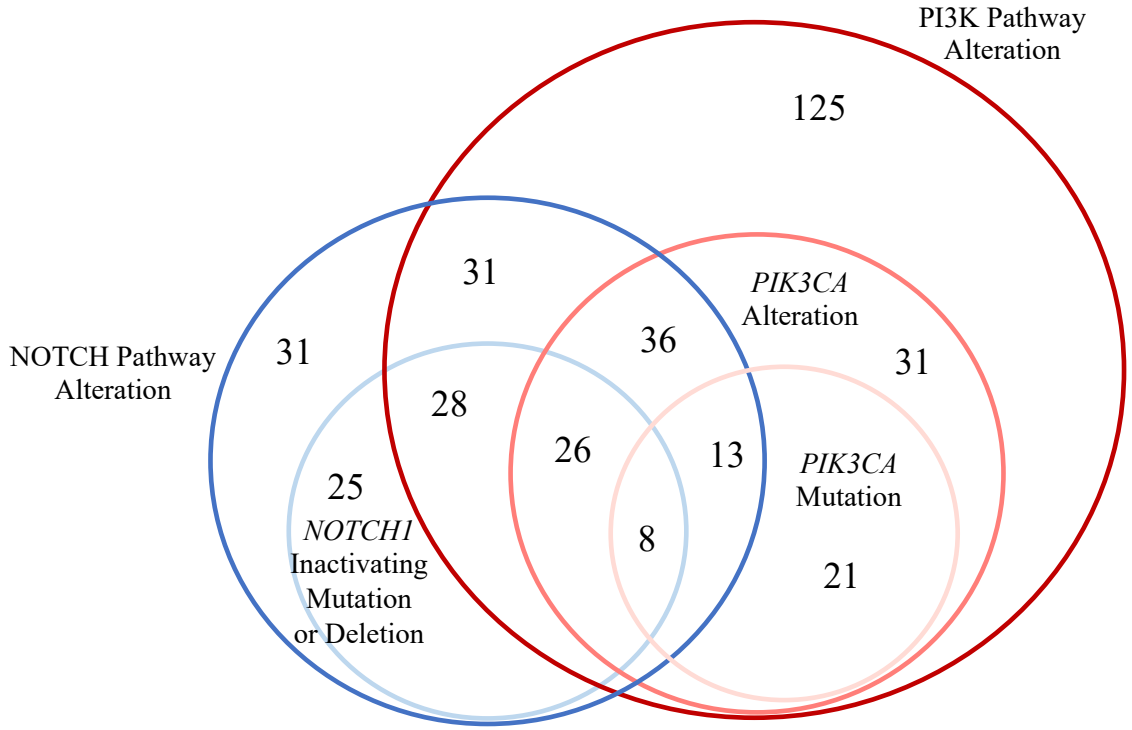


**Figure 4-1. Venn diagram for co-alteration of PI3K and NOTCH genes in TCGA HNSCC cohort.**

TCGA HNSCC patients with available mutation copy number data (n = 505) data were evaluated for the presence of indicated genetic changes. Pathway or gene alterations included all mutations and gene deletion or amplification (two additional copies). *NOTCH1* inactivating mutations occurred before amino acid 1440. *PIK3CA* mutations included any nonsynonymous mutations (excluding missense, frameshift, splice site, and deletion mutations).

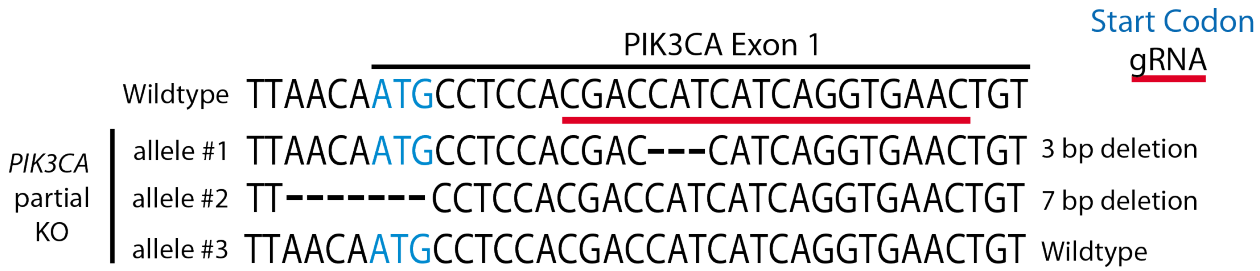


**Figure 4-2. Sanger sequencing for UM-SCC-47 wildtype and *PIK3CA* partial knockout cells.**

Schematic of sanger sequencing results from UM-SCC-47 *PIK3CA* partial knockout, showing 3 bp deletion and 7 bp deletion in *PIK3CA*. Low levels of wildtype *PIK3CA* DNA may remain. The gRNA (red) was in exon 1 of *PIK3CA*.

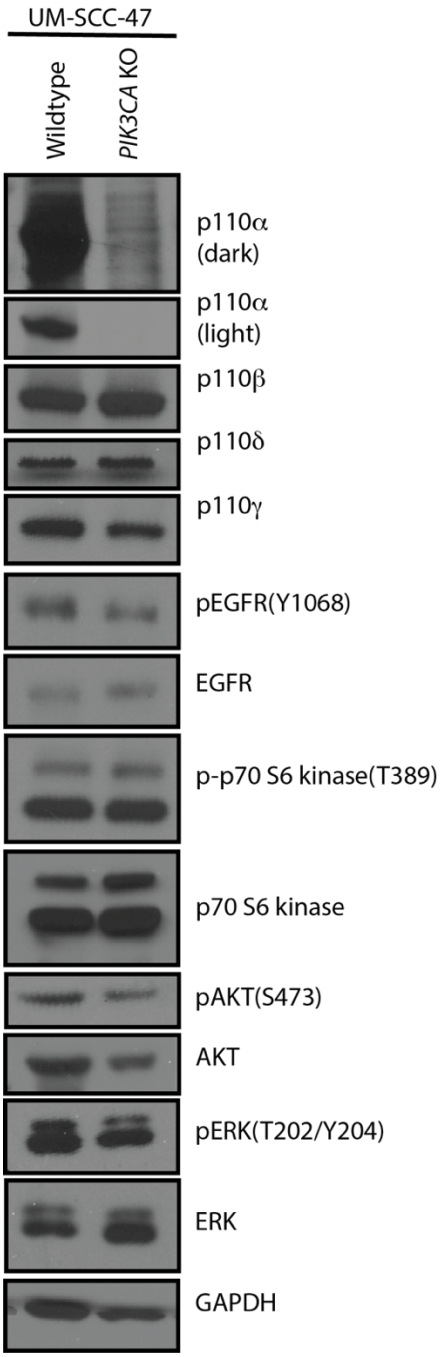


**Figure 4-3. Western blot analysis of UM-SCC-47 wildtype and *PIK3CA* partial knockout cells.**

Protein expression of pAKT(Ser473), AKT, and pEGFR(Y1068) was reduced in UM-SCC-47 *PIK3CA* partial knockout compared to wildtype cells, while other PI3K isoforms and effectors were expressed at similar levels in both cell lines.

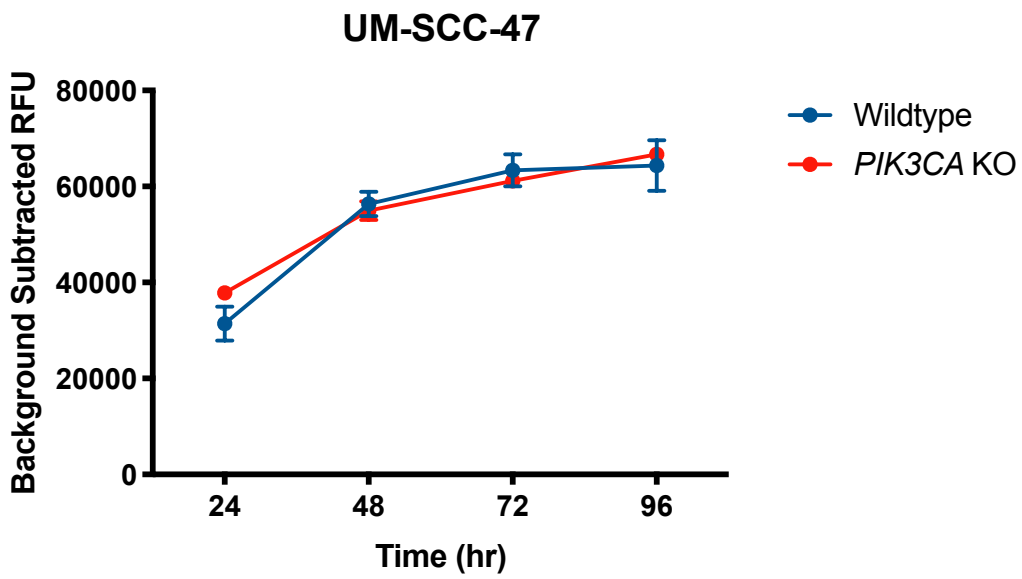


**Figure 4-4. Growth rates for UM-SCC-47 wildtype and *PIK3CA* partial knockout cells.**

Cells were cultured for the indicated periods of time and stained with resazurin for 24 hours. Wildtype and *PIK3CA* partial knockout cells displayed similar rates of proliferation.

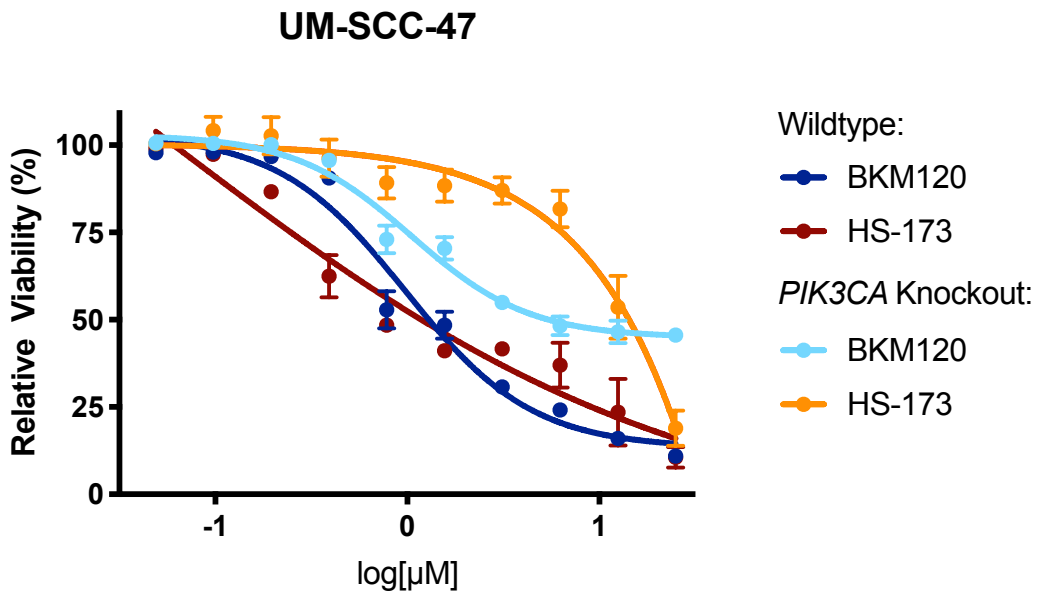


**Figure 4-5. UM-SCC-47 *PIK3CA* partial knockout cells display reduced sensitivity to PI3K inhibition as compared to wildtype UM-SCC-47 control cells.**

Cells were treated with increasing concentrations of pan-PI3K inhibitor BKM120 and alpha-isoform selective PI3K inhibitor HS-173 in quadruplicate for 72 hours. Representative data is shown.

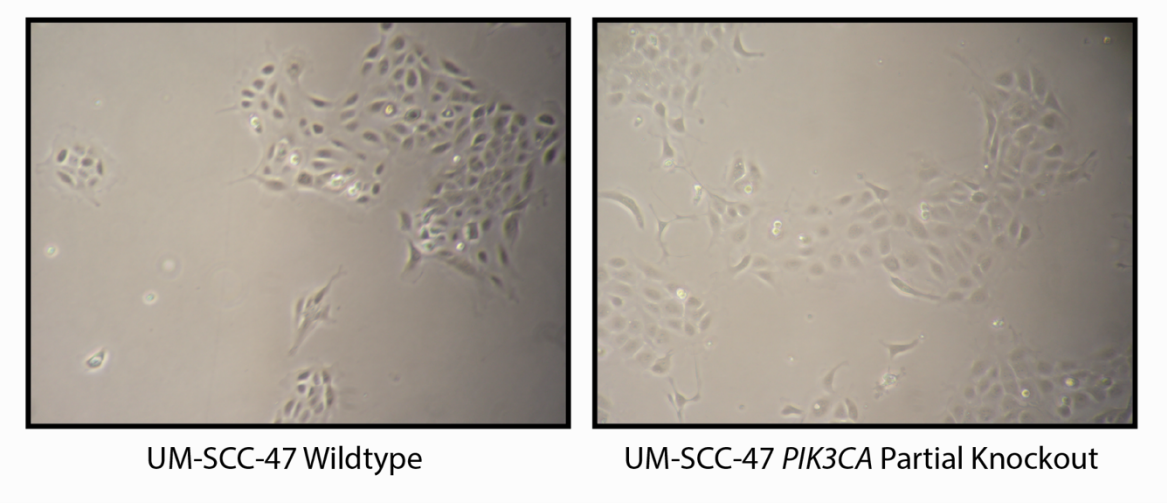


**Figure 4-6. Images of UM-SCC-47 wildtype and PIK3CA partial knockout cells.**

UM-SCC-47 *PIK3CA* partial knockout cells displayed a more mesenchymal morphology than UM-SCC-47 wildtype cells.

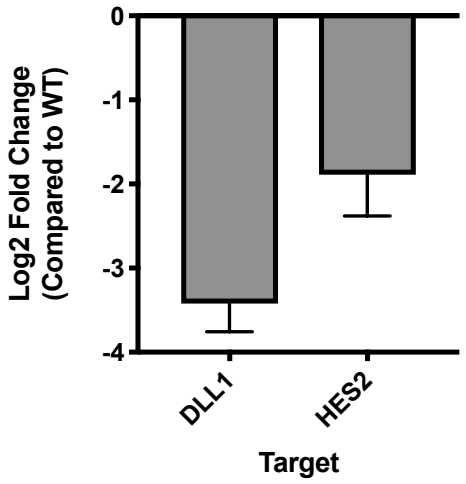


**Figure 4-7. qPCR validation of differential *DLL1* and *HES2* Gene Expression in UM-SCC-47 *PIK3CA partial* knockout cells.**

Log2 fold change in mRNA expression of DLL1 and HES2 in UM-SCC-47 *PIK3CA* partial knockout cells as calculated using the ΔΔCt method compared to UM-SCC-47 wildtype control cells.

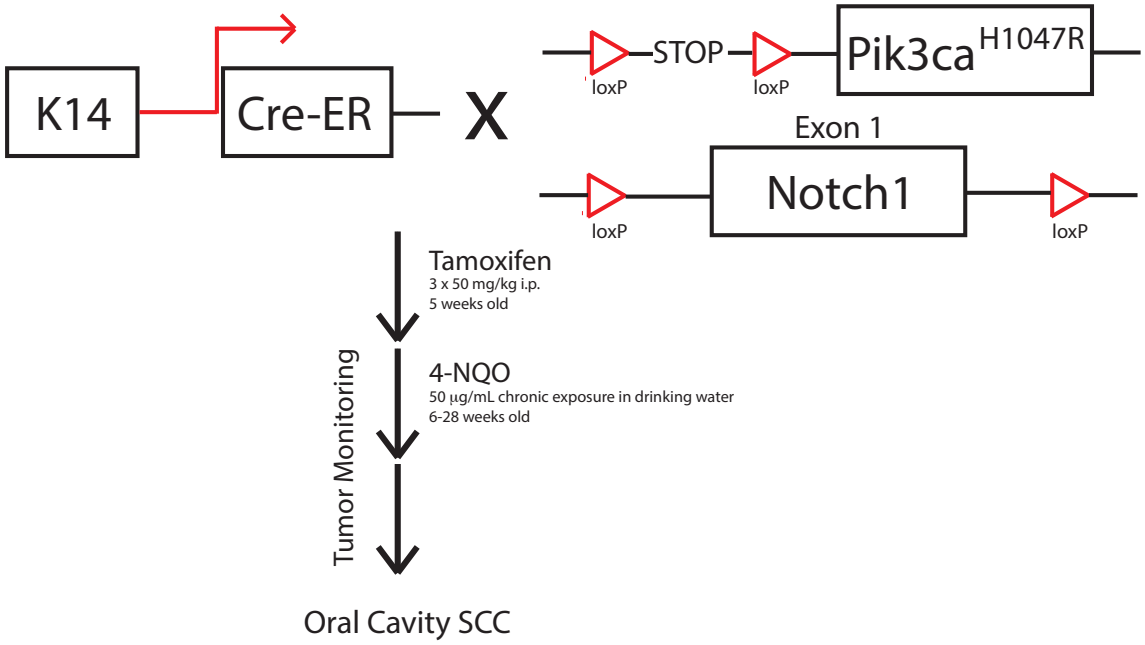


**Figure 4-8. Schema for K14; *Pik3ca; Notch1* mouse model.**

Mutant *Pik3ca* and loss of Notch1 were expressed under the control of a K14-driven Cre recombinase. Mice were administered tamoxifen to induce transgene expression and chronically treated with 4-NQO in their drinking water for 16 weeks. We monitored tumor formation and weight loss endpoints during and after 4-NQO treatment.

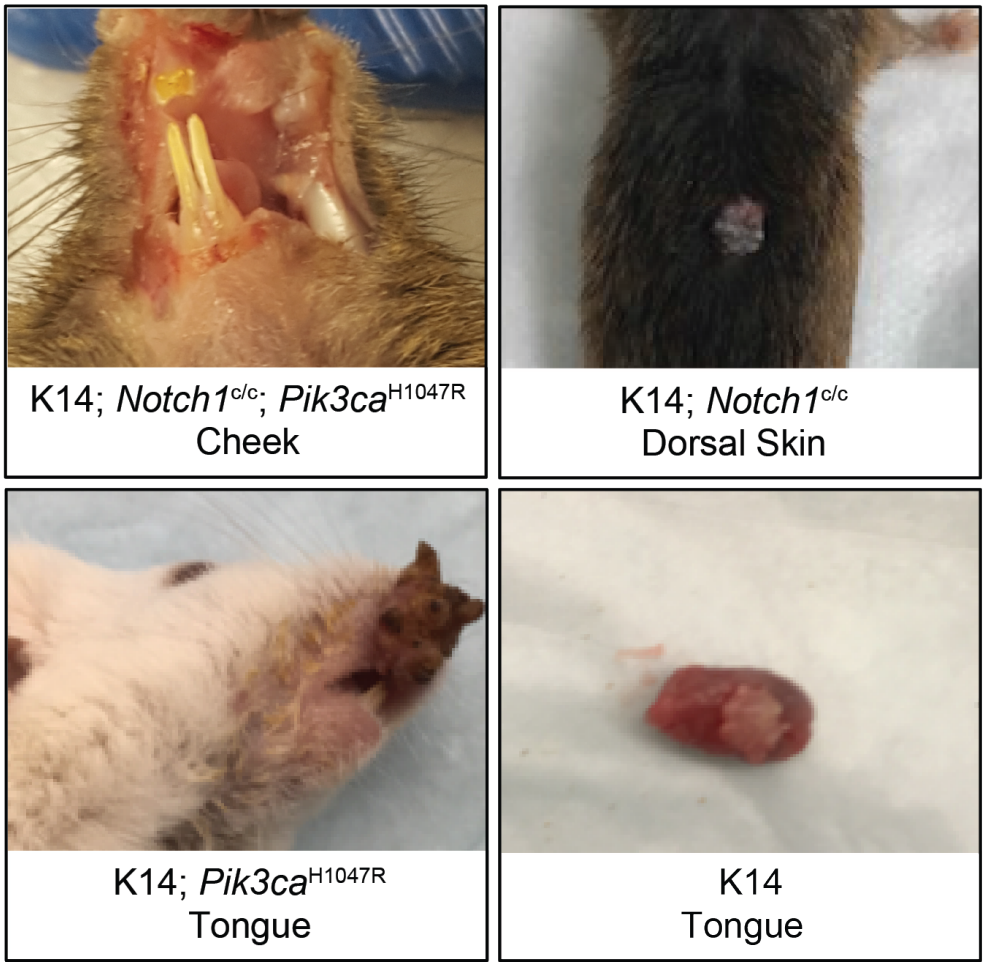


**Figure 4-9. Representative images of tumors observed in transgenic mice following 4-NQO exposure.**

Tumor images at time of euthanasia in K14; *Notch1*$^{c/c}$; *Pik3ca*$^{H1047R}$, K14, *Notch1*$^{c/c}$, K14; *Pik3ca*$^{H1047R}$, and K14 and mice.

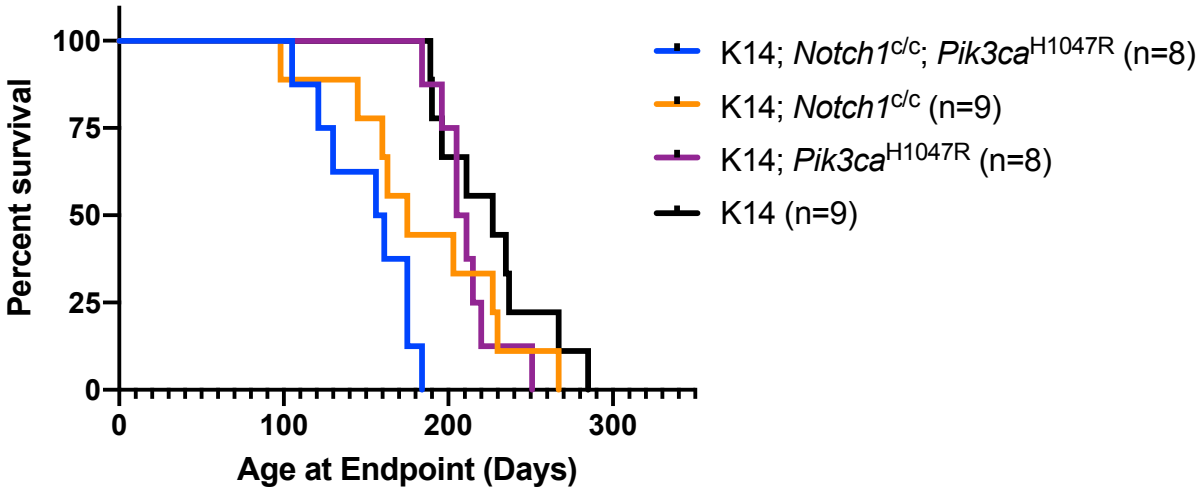


**Figure 4-10. Time to endpoint in transgenic mice with loss of *Notch1* or overexpression of mutant *Pik3ca*.**

Time to endpoint (20% loss of body weight and/or visible lesion upon euthanasia) for mice with K14 (n=9), K14; *Pik3ca*$^{H1047R}$ (n=8), K14; *Notch1*$^{c/c}$ (n=9), and K14; *Notch1*$^{c/c}$; *Pik3ca*$^{H1047R}$ (n=8) genotypes.

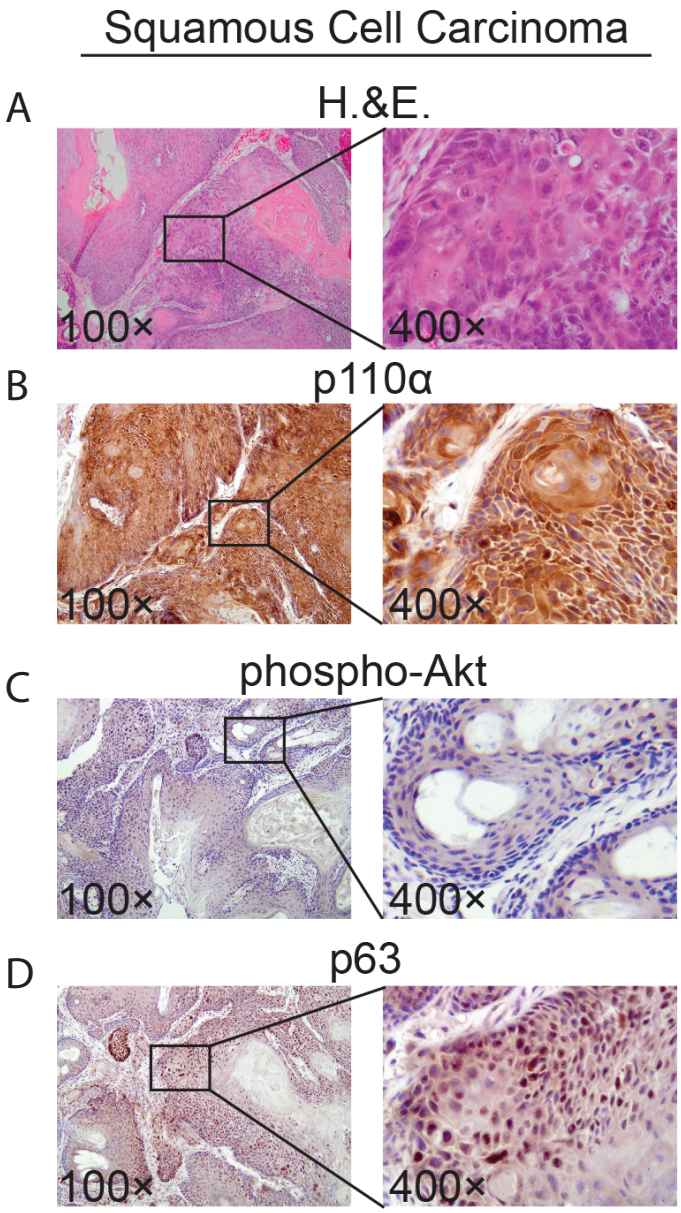


**Figure 4-11. Representative staining for transgenic mice.**

Images of slides from K14; *Pik3ca*$^{H1047R}$ squamous cell carcinoma samples stained with (A) hematoxylin and eosin (H.&E.), (B) p110α, (C) pAKT(Ser473), and (D) p63.

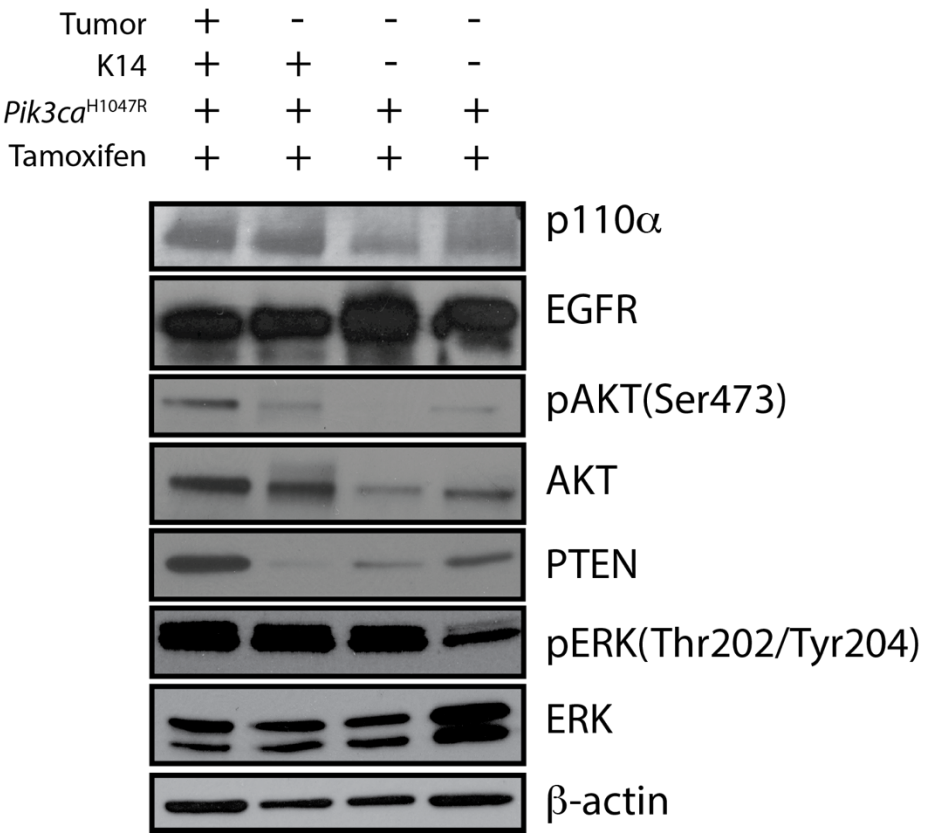


**Figure 4-12. Western blot analysis of PI3K, EGFR, and downstream effectors in *Pik3ca$^{H1047R}$* mouse tissue.**

p110α is overexpressed in K14; Pik3ca$^{H1047R}$ mouse tissues, and pAKT(Ser473) and PTEN are increased in tumor tissue. There is little change in protein expression for EGFR or downstream pathway (phosphorylated and total ERK) members. β-actin was used as a loading control.

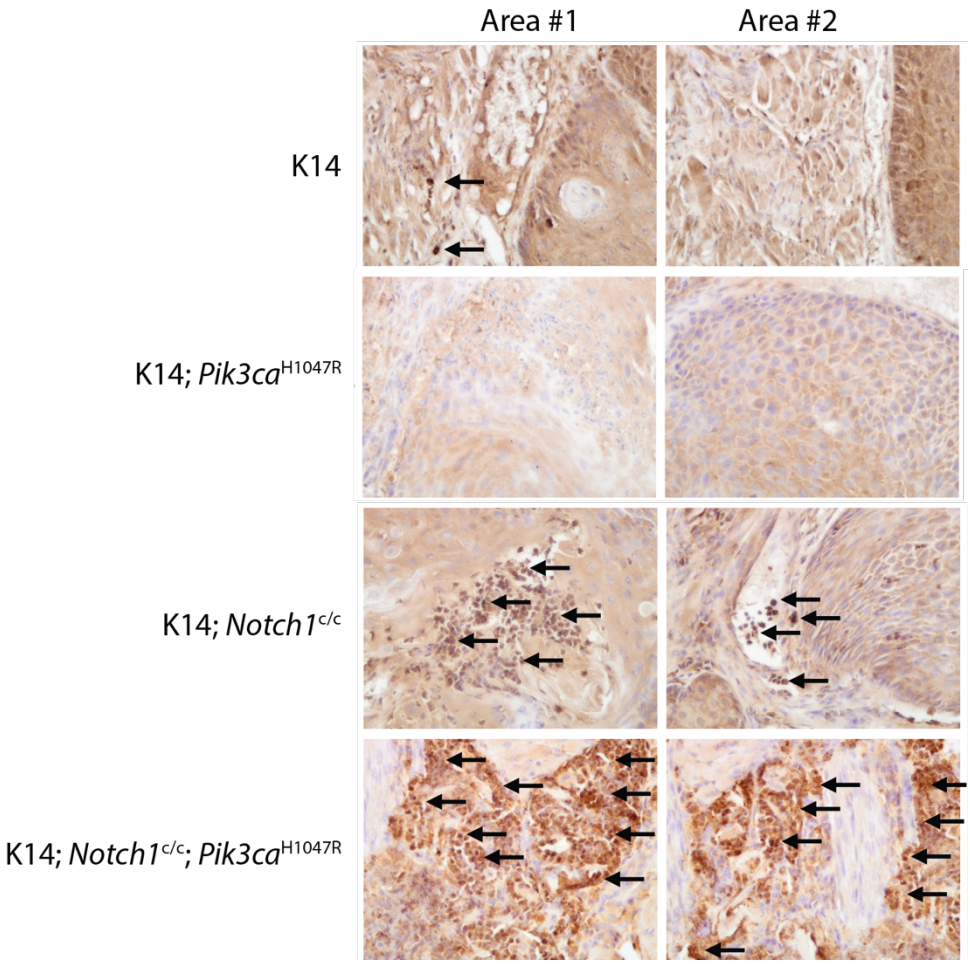


**Figure 4-13. CD8 IHC in transgenic mouse SCC tumors.**

Representative images of CD8 staining in transgenic mouse SCC tumors. Dense intralesional infiltration was observed in K14; *Pik3ca*$^{H1047R}$; *Notch1*$^{c/c}$ tissues, moderate intralesional infiltration in K14; *Notch1*$^{c/c}$ tissues, and low intralesional infiltration in K14; *Pik3ca*$^{H1047R}$ and K14 tissues.

## Tables

**Table 4-1. PCR primers, protocols, and product sizes for genotyping.**

| Target | Rosa26Pik3ca | Notch1 | Generic Cre |
|---|---|---|---|
| Primers<br>(5' to 3' sequences) | Mutant: GCG AAG AGT TTG TCC TCA ACC<br>Common: AAA GTC GCT CTG AGT TGT TAT<br>Reverse: GGA GCG GGA GAA ATG GAT ATG | Forward: CCA ACT GCA CTC TTC CAG TAA TCG AAG<br>Reverse: TGC CTC AGT TCA AAC ACA AGA TAC GAG GGG | Forward: CAT GCT TCA TCG TCG GTC C<br>Reverse: GAT CAT CAG CTA CAC CAG AG |
| PCR Program | 94°C for 4 min<br>40 cycles:<br>94°C for 30 sec<br>58°C for 30 sec<br>72°C for 1 min<br>72°C for 10 min | 94°C for 4 min<br>35 cycles:<br>94°C for 30 sec<br>56°C for 30 sec<br>72°C for 1 min<br>72°C for 10 min | 94°C for 4 min<br>35 cycles:<br>94°C for 30 sec<br>56°C for 30 sec<br>72°C for 1 min<br>72°C for 10 min |
| Product Size | Wild type allele: 650 bp<br>Mutant allele: 340 bp | Wild type allele: 478 bp<br>Mutant allele: 550 bp | 374 bp |

**Table 4-2. Primary antibody conditions for western blot analysis.**

| Target | Supplier | Cat. No. | Dilution |
|---|---|---|---|
| p110α | Cell Signaling Technology | 4249 | 1:1000 |
| pEGFR(Tyr1068) | Cell Signaling Technology | 3777 | 1:1000 |
| EGFR | Origene | TA312545 | 1:2000 |
| p-p70 S6 kinase (Thr389) | Cell Signaling Technology | 9234 | 1:500 |
| p70 S6 kinase | Cell Signaling Technology | 2708 | 1:1000 |
| pMEK(Ser217/221) | Cell Signaling Technology | 9121 | 1:1000 |
| MEK1/2 | Cell Signaling Technology | 8727 | 1:1000 |
| pERK1/2(Thr202/Tyr204) | Cell Signaling Technology | 4370 | 1:1000 |
| ERK1/2 | Cell Signaling Technology | 4695 | 1:1000 |
| pAKT(Ser473) | Cell Signaling Technology | 4060 | 1:1000 |
| AKT | Cell Signaling Technology | 4685 | 1:1000 |
| HSP90 | Cell Signaling Technology | 4877 | 1:2000 |
| GAPDH | Cell Signaling Technology | 5174 | 1:2000 |

**Table 4-3. qPCR primer sequences.**

| Primer | Sequence (5’ to 3’) |
|---|---|
| HES2 | F: CATCAACCAGAGCCTGAG<br>R: CACGGTCATTTCCAGGAC |
| DLL1 | F: ACTATAACCTCGTGCAGGACC,<br>R: TCAGATGCTTCTCCACCCCTG |
| β-actin | F: 5’-AAGTGTGACGTGGACATCCG-3’<br>R:5’-GATGTGACAGCTCCCCACAC-3’ |
| HPRT | F: 5’-AGATGGTCAAGGTCGCAAGC-3’<br>R: 5’-ATGACACAAACATGATTCAAATCCC-3’ |
| RPL19 | F: 5’-CCGCTTACCTATGCCCATGT-3’<br>R: 5’-AAATCGCCAATGCCAACTCC-3’ |

**Table 4-4. Primary antibody conditions for IHC.**

| Target | Supplier | Cat. No. | Dilution |
|---|---|---|---|
| pAKT(Ser473) | Cell Signaling Technologies | 4060 | 1:50 |
| pPDK1(Ser241) | Abcam | ab52893 | 1:100 |
| CD8 | Abcam | ab203035 | 1:200 |
| PDL1 | Cell Signaling Technologies | 64988 | 1:200 |
| p110α | Cell Signaling Technologies | 4249 | 1:50 |
| p63 | Proteintech | 12143-1-AP1 | 1:200 |

**Table 4-5. Adverse phenotypes noted in transgenic mice with *Notch1* and/or *Pik3ca* alterations and corresponding treatments.**

| **Phenotype** | **Genotype Affected** | **Treatment** |
|---|---|---|
| Eye Lesions | K14; *Notch1*$^{c/c}$ and K14; *Notch1*$^{c/c}$; *Pik3ca*$^{H1047R}$ | Ophthalmic ointment, applied daily |
| Long Nails | K14; *Notch1*$^{c/c}$ and K14; *Notch1*$^{c/c}$; *Pik3ca*$^{H1047R}$ | Trimming |
| Swollen Lymph Nodes | K14; *Notch1*$^{c/+}$; *Pik3ca*$^{H1047R}$ | Close monitoring by veterinary staff |
| Swollen Feet | K14; *Notch1*$^{c/+}$; *Pik3ca*$^{H1047R}$ | None |

**Table 4-6. Co-alteration of PI3K and NOTCH genes in TCGA HNSCC cohort.**

Number (and percent) of patients (n = 505) with the presence (1) or absence (0) of the indicated PI3K and NOTCH pathway alteration in TCGA HNSCC cohort (7-9).

| | | PI3K Pathway Alteration | | *PIK3CA* Alteration | | *PIK3CA* Mutation | | All Tumors |
|---|---|---|---|---|---|---|---|---|
| | | 0 | 1 | 0 | 1 | 0 | 1 | |
| Notch Pathway Alteration | 0 | 182 (36.0%) | 125 (24.8%) | 255 (50.5%) | 52 (10.3%) | 286 (56.6%) | 21 (4.2%) | 307 (60.8%) |
| | 1 | 56 (11.1%) | 142 (28.1%) | 115 (22.8%) | 83 (16.4%) | 177 (35.0%) | 21 (4.2%) | 198 (39.2%) |
| Notch1 Inactivation | 0 | 161 (31.9%) | 257 (50.1%) | 317 (62.8%) | 101 (20.0%) | 385 (76.2%) | 34 (6.7%) | 419 (82.9%) |
| | 1 | 25 (5.0%) | 62 (12.3%) | 53 (12.3%) | 34 (6.7%) | 78 (15.4%) | 8 (1.6%) | 86 (17.0%) |
| All Tumors | | 186 (36.8%) | 319 (63.2%) | 370 (73.3%) | 135 (26.7%) | 463 (91.6%) | 42 (8.3%) | 505 (100%) |

**Table 4-7. GSEA in UM-SCC-47 wildtype and *PIK3CA* partial knockout cells.**

Gene set enrichment analysis was performed with genes differentially expressed between UM-SCC-47 wildtype and *PIK3CA* partial knockout cells to identify significant overlap with Hallmark, KEGG and GO biological process pathways. Differentially expressed genes were defined as those >2-log2 fold upregulated or downregulated in the knockout model relative to the wildtype control. Gene Set Name is the pathway enriched, # of Genes in Gene Set is the number of genes in the GSEA pathway being tested, and # Genes in Overlap is the number of differentially expressed genes in the indicated gene set.

| Gene Set Name | # Genes in Gene Set (K) | # Genes in Overlap (k) | k/K | p-value | FDR q-value |
|---|---|---|---|---|---|
| Hallmark_Interferon_ Alpha_Response | 97 | 5 | 0.0515 | 9.06E-07 | 4.19E-05 |
| Hallmark_Interferon_ Gamma_Response | 200 | 6 | 0.03 | 1.68E-06 | 4.19E-05 |
| Hallmark_Epithelial_ Mesenchymal_Transition | 200 | 5 | 0.025 | 3.09E-05 | 3.86E-04 |
| Hallmark_TNFA Signaling_Via_NFKB | 200 | 5 | 0.025 | 3.09E-05 | 3.86E-04 |

**Table 4-8. Lesion subsite information for transgenic mice.**

For each genotype, the total number of mice as well as the number of mice with lesions is shown. In cases where lesion subsite information was known, the number of mice with lip, tongue, cheek, and skin lesions is listed along with the total number of lesions per group and the average number of lesions per animal. Total lesions and lesions per mouse are calculated based on the animals having lesions with known subsites.

| | K14; Notch1$^{c/c}$; Pik3ca $^{H1047R}$ | K14; Notch1$^{c/c}$ | K14; Pik3ca$^{H1047R}$ | K14 |
|---|---|---|---|---|
| Mice in Group | 8 | 9 | 8 | 9 |
| Mice with Lesion | 8 | 5 | 7 | 8 |
| Mice with Lesion Subsite Known | 7 | 3 | 6 | 8 |
| Mice with Lip Lesion | 3 | 0 | 4 | 0 |
| Mice with Tongue Lesion | 2 | 3 | 6 | 8 |
| Mice with Cheek Lesion | 3 | 0 | 3 | 3 |
| Mice with Skin Lesion | 2 | 1 | 0 | 0 |
| Total Lesions | 10 | 4 | 13 | 11 |
| Lesions/Mouse | 1.43 | 1.33 | 2.17 | 1.38 |

**Table 4-9. IHC scoring summary for transgenic mouse squamous cell carcinoma samples.**

Scores for SCC samples from transgenic mice. For intensity, 1 indicates weak staining, 2 indicates moderate staining, and 3 indicates strong staining. For area, 1 indicates 0-25% of stained cells, 2 indicates 25-50% of stained cells, 3 indicates 50-75% of stained cells, and 4 indicates 75-100% of stained cells. For CD8, 1 indicates poor intralesional infiltration, 2 indicates moderate intralesional infiltration, and 3 indicates dense intralesional infiltration.

| | | p110α | | | pPDK1(Ser241) | | | pAKT(Ser473) | | | p63 | | | CD8 | PD-L1 | | |
|---|---|---|---|---|---|---|---|---|---|---|---|---|---|---|---|---|---|
| Genotype | Subsite | Area | Intensity | Score | Area | Intensity | Score | Area | Intensity | Score | Area | Intensity | Score | | Area | Intensity | Score |
| K14; Notch1$^{c/c}$; Pik3ca$^{H1047R}$ | Cheek | 4 | 3 | 12 | 4 | 3 | 12 | 1 | 1 | 1 | 3 | 3 | 9 | 3 | 1 | 3 | 3 |
| K14; Notch1$^{c/c}$ | Lip | 4 | 3 | 12 | 4 | 3 | 12 | 3 | 3 | 9 | 4 | 3 | 12 | 2 | 2 | 3 | 6 |
| K14; Pik3ca$^{H1047R}$ | Cheek | 4 | 3 | 12 | N/A | N/A | N/A | 3 | 1 | 3 | 4 | 3 | 12 | 1 | 1 | 2 | 2 |
| K14 | Tongue | 4 | 3 | 12 | 4 | 3 | 12 | 4 | 3 | 12 | 4 | 3 | 12 | 1 | 1 | 1 | 1 |

**References**

1. Cramer JD, Burtness B, Le QT, Ferris RL. The changing therapeutic landscape of head and neck cancer. Nature reviews Clinical oncology. 2019. Epub 2019/06/14. doi: 10.1038/s41571-019-0227-z. PubMed PMID: 31189965.

2. Bray F, Ferlay J, Soerjomataram I, Siegel RL, Torre LA, Jemal A. Global cancer statistics 2018: GLOBOCAN estimates of incidence and mortality worldwide for 36 cancers in 185 countries. CA: a cancer journal for clinicians. 2018;68(6):394-424. Epub 2018/09/13. doi: 10.3322/caac.21492. PubMed PMID: 30207593.

3. Howlader N NA, Krapcho M, Miller D, Bishop K, Altekruse SF, Kosary CL, Yu M, Ruhl J, Tatalovich Z, Mariotto A, Lewis DR, Chen HS, Feuer EJ, Cronin KA. SEER Cancer Statistics Review, 1975-2016. SEER web site: National Cancer Institute; April 2019.

4. Agrawal N, Frederick MJ, Pickering CR, Bettegowda C, Chang K, Li RJ, Fakhry C, Xie TX, Zhang J, Wang J, Zhang N, El-Naggar AK, Jasser SA, Weinstein JN, Trevino L, Drummond JA, Muzny DM, Wu Y, Wood LD, Hruban RH, Westra WH, Koch WM, Califano JA, Gibbs RA, Sidransky D, Vogelstein B, Velculescu VE, Papadopoulos N, Wheeler DA, Kinzler KW, Myers JN. Exome sequencing of head and neck squamous cell carcinoma reveals inactivating mutations in NOTCH1. Science (New York, NY). 2011;333(6046):1154-7. Epub 2011/07/30. doi: 10.1126/science.1206923. PubMed PMID: 21798897; PMCID: Pmc3162986.

5. Stransky N, Egloff AM, Tward AD, Kostic AD, Cibulskis K, Sivachenko A, Kryukov GV, Lawrence MS, Sougnez C, McKenna A, Shefler E, Ramos AH, Stojanov P, Carter SL, Voet D, Cortes ML, Auclair D, Berger MF, Saksena G, Guiducci C, Onofrio RC, Parkin M, Romkes M, Weissfeld JL, Seethala RR, Wang L, Rangel-Escareno C, Fernandez-Lopez JC, Hidalgo-Miranda A, Melendez-Zajgla J, Winckler W, Ardlie K, Gabriel SB, Meyerson M, Lander ES, Getz G, Golub TR, Garraway LA, Grandis JR. The mutational landscape of head and neck squamous cell carcinoma. Science (New York, NY). 2011;333(6046):1157-60. Epub 2011/07/30. doi: 10.1126/science.1208130. PubMed PMID: 21798893; PMCID: Pmc3415217.

6. Lui VW, Hedberg ML, Li H, Vangara BS, Pendleton K, Zeng Y, Lu Y, Zhang Q, Du Y, Gilbert BR, Freilino M, Sauerwein S, Peyser ND, Xiao D, Diergaarde B, Wang L, Chiosea S, Seethala R, Johnson JT, Kim S, Duvvuri U, Ferris RL, Romkes M, Nukui T, Kwok-Shing Ng P, Garraway LA, Hammerman PS, Mills GB, Grandis JR. Frequent mutation of the PI3K pathway in head and neck cancer defines predictive biomarkers. Cancer discovery. 2013;3(7):761-9. Epub 2013/04/27. doi: 10.1158/2159-8290.cd-13-0103. PubMed PMID: 23619167; PMCID: Pmc3710532.

7. Comprehensive genomic characterization of head and neck squamous cell carcinomas. Nature. 2015;517(7536):576-82. Epub 2015/01/30. doi: 10.1038/nature14129. PubMed PMID: 25631445; PMCID: Pmc4311405.

8. Cerami E, Gao J, Dogrusoz U, Gross BE, Sumer SO, Aksoy BA, Jacobsen A, Byrne CJ, Heuer ML, Larsson E, Antipin Y, Reva B, Goldberg AP, Sander C, Schultz N. The cBio cancer genomics portal: an open platform for exploring multidimensional cancer genomics data. Cancer

discovery. 2012;2(5):401-4. Epub 2012/05/17. doi: 10.1158/2159-8290.cd-12-0095. PubMed PMID: 22588877; PMCID: Pmc3956037.

9. Gao J, Aksoy BA, Dogrusoz U, Dresdner G, Gross B, Sumer SO, Sun Y, Jacobsen A, Sinha R, Larsson E, Cerami E, Sander C, Schultz N. Integrative analysis of complex cancer genomics and clinical profiles using the cBioPortal. Science signaling. 2013;6(269):pl1. Epub 2013/04/04. doi: 10.1126/scisignal.2004088. PubMed PMID: 23550210; PMCID: Pmc4160307.

10. Ludwig ML, Kulkarni A, Birkeland AC, Michmerhuizen NL, Foltin SK, Mann JE, Hoesli RC, Devenport SN, Jewell BM, Shuman AG, Spector ME, Carey TE, Jiang H, Brenner JC. The genomic landscape of UM-SCC oral cavity squamous cell carcinoma cell lines. Oral oncology. 2018;87:144-51. Epub 2018/12/12. doi: 10.1016/j.oraloncology.2018.10.031. PubMed PMID: 30527230; PMCID: PMC6349383.

11. Michmerhuizen NL, Leonard E, Kulkarni A, Brenner JC. Differential compensation mechanisms define resistance to PI3K inhibitors in PIK3CA amplified HNSCC. Otorhinolaryngology-head and neck surgery. 2016;1(2):44-50. Epub 2016/12/23. PubMed PMID: 28004037; PMCID: PMC5167357.

12. Michmerhuizen NL, Leonard E, Matovina C, Harris M, Herbst G, Kulkarni A, Zhai J, Jiang H, Carey TE, Brenner JC. Rationale for Using Irreversible Epidermal Growth Factor Receptor Inhibitors in Combination with Phosphatidylinositol 3-Kinase Inhibitors for Advanced Head and Neck Squamous Cell Carcinoma. Molecular pharmacology. 2019;95(5):528-36. Epub 2019/03/13. doi: 10.1124/mol.118.115162. PubMed PMID: 30858165.

13. Qiu W, Schonleben F, Li X, Ho DJ, Close LG, Manolidis S, Bennett BP, Su GH. PIK3CA mutations in head and neck squamous cell carcinoma. Clinical cancer research : an official journal of the American Association for Cancer Research. 2006;12(5):1441-6. Epub 2006/03/15. doi: 10.1158/1078-0432.ccr-05-2173. PubMed PMID: 16533766; PMCID: Pmc1780023.

14. Samuels Y, Diaz LA, Jr., Schmidt-Kittler O, Cummins JM, Delong L, Cheong I, Rago C, Huso DL, Lengauer C, Kinzler KW, Vogelstein B, Velculescu VE. Mutant PIK3CA promotes cell growth and invasion of human cancer cells. Cancer cell. 2005;7(6):561-73. Epub 2005/06/14. doi: 10.1016/j.ccr.2005.05.014. PubMed PMID: 15950905.

15. Samuels Y, Wang Z, Bardelli A, Silliman N, Ptak J, Szabo S, Yan H, Gazdar A, Powell SM, Riggins GJ, Willson JK, Markowitz S, Kinzler KW, Vogelstein B, Velculescu VE. High frequency of mutations of the PIK3CA gene in human cancers. Science (New York, NY). 2004;304(5670):554. Epub 2004/03/16. doi: 10.1126/science.1096502. PubMed PMID: 15016963.

16. Liu P CH, Santiago S, et al. Oncogenic PIK3CA-driven mammary tumors frequently recur via PI3K pathway-dependent and PI3K pathway-independent mechanisms. . Nat Med. 2011;17:1116-20.

17. Engelman JA, Chen L, Tan X, Crosby K, Guimaraes AR, Upadhyay R, Maira M, McNamara K, Perera SA, Song Y, Chirieac LR, Kaur R, Lightbown A, Simendinger J, Li T, Padera RF, Garcia-Echeverria C, Weissleder R, Mahmood U, Cantley LC, Wong KK. Effective use of PI3K and MEK inhibitors to treat mutant Kras G12D and PIK3CA H1047R murine lung cancers. Nature medicine. 2008;14(12):1351-6. Epub 2008/11/26. doi: 10.1038/nm.1890. PubMed PMID: 19029981; PMCID: PMC2683415.

18. Du L, Chen X, Cao Y, Lu L, Zhang F, Bornstein S, Li Y, Owens P, Malkoski S, Said S, Jin F, Kulesz-Martin M, Gross N, Wang XJ, Lu SL. Overexpression of PIK3CA in murine head and neck epithelium drives tumor invasion and metastasis through PDK1 and enhanced TGFbeta signaling. Oncogene. 2016;35(35):4641-52. Epub 2016/02/16. doi: 10.1038/onc.2016.1. PubMed PMID: 26876212; PMCID: PMC4985507.

19. Bian Y HB, Sun ZJ, et al. Loss of TGF-Beta signaling and PTEN promotes head and neck squamous cell carcinoma through cellular senescence evasion and cancer-related inflammation. . Oncogene. 2012;31:3322-32.

20. Squarize CH CR, Abrahao AC, Molinolo A, Lingen MW, Gutkind JS. PTEN deficiency contributes to the development and progression of head and neck cancer. . Neoplasia. 2013;15(5):461-71.

21. Bian Y, Hall B, Sun ZJ, Molinolo A, Chen W, Gutkind JS, Waes CV, Kulkarni AB. Loss of TGF-beta signaling and PTEN promotes head and neck squamous cell carcinoma through cellular senescence evasion and cancer-related inflammation. Oncogene. 2012;31(28):3322-32. Epub 2011/11/01. doi: 10.1038/onc.2011.494. PubMed PMID: 22037217; PMCID: PMC3270146.

22. Herzog A BY, Vander Broek R, et al. PI3K/mTOR inhibitor PF-04691502 antitumor activity is enhanced with induction of wild-type TP53 in human xenograft and murine knockout models of head and neck cancer. . Clin Cancer Res. 2013;19(14):3808-19.

23. Sun ZJ ZL, Hall B, Bian Y, Gutkind JS, Kulkarni AB. Chemopreventive and chemotherapeutic actions of mTOR inhibitor in genetically defined head and neck squamous cell carcinoma mouse model. . Clin Cancer Res. 2012;18(19):5304-13.

24. Kopan R IM. The canonical Notch signaling pathway: unfolding the activation mechanism. . Cell. 2009;137(2):216-33.

25. Porcheri C, Meisel CT, Mitsiadis T. Multifactorial Contribution of Notch Signaling in Head and Neck Squamous Cell Carcinoma. International journal of molecular sciences. 2019;20(6). Epub 2019/03/29. doi: 10.3390/ijms20061520. PubMed PMID: 30917608; PMCID: PMC6471940.

26. Ellisen LW, Bird J, West DC, Soreng AL, Reynolds TC, Smith SD, Sklar J. TAN-1, the human homolog of the Drosophila notch gene, is broken by chromosomal translocations in T

lymphoblastic neoplasms. Cell. 1991;66(4):649-61. Epub 1991/08/23. doi: 10.1016/0092-8674(91)90111-b. PubMed PMID: 1831692.

27. Nyman PE, Buehler D, Lambert PF. Loss of Function of Canonical Notch Signaling Drives Head and Neck Carcinogenesis. Clinical cancer research : an official journal of the American Association for Cancer Research. 2018;24(24):6308-18. Epub 2018/08/09. doi: 10.1158/1078-0432.Ccr-17-3535. PubMed PMID: 30087145; PMCID: PMC6295262.

28. Fukusumi T, Califano JA. The NOTCH Pathway in Head and Neck Squamous Cell Carcinoma. Journal of dental research. 2018;97(6):645-53. Epub 2018/03/01. doi: 10.1177/0022034518760297. PubMed PMID: 29489439; PMCID: PMC5960881.

29. Demehri S, Turkoz A, Manivasagam S, Yockey LJ, Turkoz M, Kopan R. Elevated epidermal thymic stromal lymphopoietin levels establish an antitumor environment in the skin. Cancer cell. 2012;22(4):494-505. Epub 2012/10/20. doi: 10.1016/j.ccr.2012.08.017. PubMed PMID: 23079659; PMCID: PMC3480666.

30. Demehri S, Turkoz A, Kopan R. Epidermal Notch1 loss promotes skin tumorigenesis by impacting the stromal microenvironment. Cancer cell. 2009;16(1):55-66. Epub 2009/07/04. doi: 10.1016/j.ccr.2009.05.016. PubMed PMID: 19573812; PMCID: PMC2705757.

31. Zhong R BR, Faber PW, et al. Notch1 activation or loss promotes HPV-induced oral tumorigenesis. . Cancer Res. 2015;75(18):3958-69.

32. Di Piazza M, Nowell CS, Koch U, Durham AD, Radtke F. Loss of cutaneous TSLP-dependent immune responses skews the balance of inflammation from tumor protective to tumor promoting. Cancer cell. 2012;22(4):479-93. Epub 2012/10/20. doi: 10.1016/j.ccr.2012.08.016. PubMed PMID: 23079658.

33. Sambandam V, Frederick MJ, Shen L, Tong P, Rao X, Peng S, Singh R, Mazumdar T, Huang C, Li Q, Pickering CR, Myers JN, Wang J, Johnson FM. PDK1 mediates NOTCH1-mutated head and neck squamous carcinoma vulnerability to therapeutic PI3K/mTOR inhibition. Clinical cancer research : an official journal of the American Association for Cancer Research. 2019. Epub 2019/02/17. doi: 10.1158/1078-0432.Ccr-18-3276. PubMed PMID: 30770351.

34. Brenner JC, Graham MP, Kumar B, Saunders LM, Kupfer R, Lyons RH, Bradford CR, Carey TE. Genotyping of 73 UM-SCC head and neck squamous cell carcinoma cell lines. Head & neck. 2010;32(4):417-26. Epub 2009/09/18. doi: 10.1002/hed.21198. PubMed PMID: 19760794; PMCID: PMC3292176.

35. Birkeland AC, Yanik M, Tillman BN, Scott MV, Foltin SK, Mann JE, Michmerhuizen NL, Ludwig ML, Sandelski MM, Komarck CM, Carey TE, Prince ME, Bradford CR, McHugh JB, Spector ME, Brenner JC. Identification of Targetable ERBB2 Aberrations in Head and Neck Squamous Cell Carcinoma. JAMA otolaryngology-- head & neck surgery. 2016. Epub 2016/04/15. doi: 10.1001/jamaoto.2016.0335. PubMed PMID: 27077364.

36. Tillman BN, Yanik M, Birkeland AC, Liu CJ, Hovelson DH, Cani AK, Palanisamy N, Carskadon S, Carey TE, Bradford CR, Tomlins SA, McHugh JB, Spector ME, Chad Brenner J. Fibroblast growth factor family aberrations as a putative driver of head and neck squamous cell carcinoma in an epidemiologically low-risk patient as defined by targeted sequencing. Head Neck. 2016;38 Suppl 1:E1646-52. Epub 2016/02/06. doi: 10.1002/hed.24292. PubMed PMID: 26849095; PMCID: Pmc4844767.

37. Arumugam A, Weng Z, Chaudhary SC, Afaq F, Elmets CA, Athar M. Keratin-6 driven ODC expression to hair follicle keratinocytes enhances stemness and tumorigenesis by negatively regulating Notch. Biochemical and biophysical research communications. 2014;451(3):394-401. Epub 2014/08/06. doi: 10.1016/j.bbrc.2014.07.129. PubMed PMID: 25094045; PMCID: PMC4165545.

38. Snijders AM, Schmidt BL, Fridlyand J, Dekker N, Pinkel D, Jordan RC, Albertson DG. Rare amplicons implicate frequent deregulation of cell fate specification pathways in oral squamous cell carcinoma. Oncogene. 2005;24(26):4232-42. Epub 2005/04/13. doi: 10.1038/sj.onc.1208601. PubMed PMID: 15824737.

39. Tang XH, Knudsen B, Bemis D, Tickoo S, Gudas LJ. Oral cavity and esophageal carcinogenesis modeled in carcinogen-treated mice. Clin Cancer Res. 2004;10(1 Pt 1):301-13. Epub 2004/01/22. PubMed PMID: 14734483.

40. Ramotar D, Belanger E, Brodeur I, Masson JY, Drobetsky EA. A yeast homologue of the human phosphotyrosyl phosphatase activator PTPA is implicated in protection against oxidative DNA damage induced by the model carcinogen 4-nitroquinoline 1-oxide. J Biol Chem. 1998;273(34):21489-96. Epub 1998/08/15. PubMed PMID: 9705277.

41. Ikenaga M, Ichikawa-Ryo H, Kondo S. The major cause of inactivation and mutation by 4-nitroquinoline 1-oixde in Escherichia coli: excisable 4NQO-purine adducts. J Mol Biol. 1975;92(2):341-56. Epub 1975/02/25. PubMed PMID: 806692.

42. Venkat JA, Shami S, Davis K, Nayak M, Plimmer JR, Pfeil R, Nair PP. Relative genotoxic activities of pesticides evaluated by a modified SOS microplate assay. Environ Mol Mutagen. 1995;25(1):67-76. Epub 1995/01/01. PubMed PMID: 7875128.

43. Panigrahi GB, Walker IG. The N2-guanine adduct but not the C8-guanine or N6-adenine adducts formed by 4-nitroquinoline 1-oxide blocks the 3'-5' exonuclease action of T4 DNA polymerase. Biochemistry. 1990;29(8):2122-6. Epub 1990/02/27. PubMed PMID: 2109634.

44. Thomas DC, Husain I, Chaney SG, Panigrahi GB, Walker IG. Sequence effect on incision by (A)BC excinuclease of 4NQO adducts and UV photoproducts. Nucleic Acids Res. 1991;19(2):365-70. Epub 1991/01/25. PubMed PMID: 1901645; PMCID: Pmc333603.

45. Shayan G, Srivastava R, Li J, Schmitt N, Kane LP, Ferris RL. Adaptive resistance to anti-PD1 therapy by Tim-3 upregulation is mediated by the PI3K-Akt pathway in head and neck

cancer. Oncoimmunology. 2017;6(1):e1261779. Epub 2017/02/16. doi: 10.1080/2162402x.2016.1261779. PubMed PMID: 28197389; PMCID: PMC5283618.

46. Li H, Wawrose JS, Gooding WE, Garraway LA, Lui VW, Peyser ND, Grandis JR. Genomic analysis of head and neck squamous cell carcinoma cell lines and human tumors: a rational approach to preclinical model selection. Molecular cancer research : MCR. 2014;12(4):571-82. Epub 2014/01/16. doi: 10.1158/1541-7786.Mcr-13-0396. PubMed PMID: 24425785; PMCID: PMC3989421.

47. Chau NG, Li YY, Jo VY, Rabinowits G, Lorch JH, Tishler RB, Margalit DN, Schoenfeld JD, Annino DJ, Goguen LA, Thomas T, Becker H, Haddad T, Krane JF, Lindeman NI, Shapiro GI, Haddad RI, Hammerman PS. Incorporation of Next-Generation Sequencing into Routine Clinical Care to Direct Treatment of Head and Neck Squamous Cell Carcinoma. Clinical cancer research : an official journal of the American Association for Cancer Research. 2016;22(12):2939-49. Epub 2016/01/15. doi: 10.1158/1078-0432.Ccr-15-2314. PubMed PMID: 26763254.

48. Garcia-Escudero R, Segrelles C, Duenas M, Pombo M, Ballestin C, Alonso-Riano M, Nenclares P, Alvarez-Rodriguez R, Sanchez-Aniceto G, Ruiz-Alonso A, Lopez-Cedrun JL, Paramio JM, Lorz C. Overexpression of PIK3CA in head and neck squamous cell carcinoma is associated with poor outcome and activation of the YAP pathway. Oral oncology. 2018;79:55-63. Epub 2018/03/31. doi: 10.1016/j.oraloncology.2018.02.014. PubMed PMID: 29598951.

# Chapter 5 : Small Molecule Profiling Identifies Novel PI3K inhibitor Resistance Mechanisms in Head and Neck Squamous Cell Carcinoma

## Abstract

High-throughput, small molecule profiling studies have provided important advances in drug development, including in the identification and optimization of targeted therapies for various cancer types. Given the limitations of these treatments, which often display inadequate efficacy as monotherapies due to both intrinsic and acquired resistance, novel approaches are needed to improve clinical responses. Here, we sought to improve the effects of targeted phosphatidylinositol 3-kinase (PI3K) inhibitors in head and neck squamous cell carcinoma (HNSCC) by using these agents in combination with other small molecules inhibiting pathways that might be responsible for drug resistance. To do so, we developed and optimized a combinatorial screening approach that utilized a resazurin cell viability assay. This assay was used to test a library of >1400 clinically-relevant small molecule inhibitors alone and in combination with two PI3K inhibitors in ten patient-derived HNSCC cell lines, generating >150K data points characterizing the landscape of combinatorial PI3K inhibitor responses in HNSCC and potentially other PI3K-driven cancer types. Our results demonstrated that dual treatment with inhibitors of PI3K and several upstream RTKs resulted in synergistic responses, but that combinations targeting downstream PI3K effectors were less effective. We more fully characterized the phenotypic effects of one of our most effective drug pairs, PI3K and ALK/IGF-1R inhibitor di-therapy, by assessing its effects on cell viability, apoptosis, and cell

cycle in a diverse panel of cell lines. We also further investigated the role of *ALK* and *IGF-1R* in PI3K inhibitor responses using CRISPR/Cas9 approaches and demonstrated using a kinase knockout library that genetic knockout of *ALK* or *IGF-1R* can result in sensitivity to PI3K inhibitor treatment. Finally, PI3K inhibitor pictilisib and ALK/IGF-1R inhibitor brigatinib were tested in a xenograft model, and combination treatment resulted in a synergistic reduction in tumor volume. Based on the efficacy of PI3K and ALK/IGF-1R inhibitor co-treatments, our findings motivate further pre-clinical evaluation of these therapies and offer a dataset that might provide improved treatment options and better prognoses for patients with HNSCC and other cancer types.

## Introduction

In recent years, targeted therapies have shown promise as effective treatment options for cancer patients; however, significant challenges in target identification and patient selection remain and limit the optimal uses of these cancer therapeutics. Previously, unbiased small molecule profiling studies have provided an efficient means by which to prioritize leads for further validation and in doing so have successfully delivered solutions for many shortcomings of targeted therapy treatments. The generation of large screening datasets has effectively aided the optimization of compounds with activity against established targets, the design of additional molecules to alter previously understudied drug targets, and the identification of biomarkers to guide personalized medicine protocols (1-7). In spite of these advances, both innate and acquired mechanisms of resistance to these targeted inhibitors impede the durability of patient responses and present a major, ongoing concern. One potential means of overcoming resistance is using two or more targeted agents simultaneously; such combination treatments may inhibit signaling pathways that are upregulated in the presence of a single agent and thereby re-sensitize

tumor cells and deliver improved responses. Here, we sought to address the problem of resistance to targeted therapy using high throughput screening techniques. Using a specific drug class and tumor type, our study seeks to demonstrate the validity of this approach. Specifically, we generated >150,000 data points using small molecule combinations to identify and target factors driving resistance to phosphatidylinositol 3-kinase (PI3K) inhibitors in head and neck squamous cell carcinoma (HNSCC).

HNSCC has long been characterized by poor responses to treatment, and survival statistics remain dire today. This form of cancer is the sixth most common by incidence worldwide (8) and affects 830,000 new patients each year (9, 10). HNSCCs occur in various sites of the upper aerodigestive tract, including the oral cavity, larynx, oropharynx and hypopharynx. Many HNSCC cases can be attributed to the excessive use of tobacco and/or alcohol or to infection with high-risk strains of human papilloma virus (HPV). While surgery, radiation, and cytotoxic chemotherapy are the most frequently used treatments for HNSCC patients, recurrence and metastasis remain widespread. Furthermore, despite the FDA approval of epidermal growth factor receptor (EGFR) antibody cetuximab and immunotherapy (programmed death (PD)-1 checkpoint blockade via pembrolizumab and nivolumab) (11-15), response rates remain low and patient selection is an ongoing challenge. The identification of additional drug targets and biomarkers for response is therefore an area of unmet and urgent need in this cancer type.

Sequencing studies have provided insight into other targeted therapies that may prove effective in HNSCC. Of these, inhibitors of PI3K are one promising option, given that genes in the PI3K pathway are altered via mutation or copy number alteration in as many as 2/3 of HNSCCs (16-18). Disappointingly, early clinical studies using PI3K pathway inhibitors have

shown underwhelming efficacy and/or limiting toxicity for these agents in head and neck cancer patients (19, 20). One of the most promising of these studies, a recent phase 2 trial of buparlisib (BKM120) in recurrent and metastatic HNSCC, demonstrated that this PI3K inhibitor provided benefit beyond that achieved with standard-of-care paclitaxel in a subset of recurrent/metastatic head and neck cancer patients; nevertheless, the majority of PI3K inhibitor-treated patients were non-responsive (20). In light of these findings, we proposed that the addition of other inhibitors to PI3K pathway targeting drugs might improve responses. Some PI3K inhibitor combination trials are ongoing in HNSCC, but these have to date not improved progression-free, overall response rate, or overall survival (21), and the trials have been limited to agents targeting PI3K and EGFR (eg: NCT01816984, NCT2282371, NCT02822482) or PI3K and CDK4/6 (NCT03065062).

In order to better define the landscape of resistance to PI3K inhibitors in HNSCC and prioritize additional combination inhibitors for evaluation in future clinical studies, we tested a library of small molecule inhibitors in a diverse panel of PI3K aberrant HNSCC cell lines as single agents and combinations with PI3K inhibitors. In doing so, we sought to uncover both expected and unexpected synergistic drug pairs, which could be validated and advanced in additional HNSCC models. As a whole, we present here a wealth of data regarding responses to mono- and dual-therapy treatments and provide as a resource that might inform future clinical studies and precision medicine protocols in HNSCC and other cancer types.

## Methods

*Cell Culture*

Cells were cultured in a humidified incubator at 37°C with 5% (vol/vol) $CO_2$. UM-SCC cells (University of Michigan) and Cal-33 cells (a kind gift from Dr. Anthony Nichols) were previously derived from HNSCC patient tumor samples and cultured in DMEM with 10% FBS, 1X Pen/Strep, 1X NEAA (22). HSC-2, HSC-4 (both from Japanese Collection of Research Bioresources) and Detroit 562 (from American Type Culture Collection) cells were cultured in EMEM with 10% FBS, 1X Pen/Strep. All cell lines were genotyped to confirm authenticity, as described previously (22), and were tested to confirm lack of mycoplasma contamination.

For small molecule profiling studies (both in experiments using the Selleckchem inhibitor library and in the secondary validation screen), low-passage cell lines were frozen in large aliquots (5-10 million cells each). After aliquots were thawed, in order to minimize genetic drift over extended periods of time in culture, cells were passaged five or fewer times before fresh stocks were obtained and used. A single lot of FBS was used for all small molecule profiling and reverse-format validation experiments.

Details of DNA copy number analysis for UM-SCC cell lines are published elsewhere (23). All UM-SCC cell lines were confirmed to contain *PIK3CA* as previously reported (24). Cal-33, HSC-2, and HSC-4 copy number data were obtained from the publicly available canSAR database (25, 26). *PIK3CA* alterations were previously confirmed via Sanger sequencing (27).

*Chemicals*

All compounds, including inhibitor libraries using in small molecule profiling, were purchased from Selleck Chemicals. For small molecule profiling, the Selleckchem inhibitor library (**Appendix 1**) was purchased and aliquoted into daughter plates, each of which was subjected to

five or fewer freeze-thaw cycles before being retired from use. All other compounds were initially dissolved in 100% sterile DMSO to 10 mM and then diluted in media to the indicated concentrations for studies *in vitro*.

*Resazurin Cell Viability Assay*

To study relative cell viability, 2,000 cells per well (for all cell lines except HSC-2, for which the cell density was reduced to 1,000 cells per well due to large cell size and rapid growth rate) were seeded (in 50 μL volume) in 384-well microplates using a Multiflo liquid handling dispensing system. The following day, cells were treated with complete media containing inhibitor or DMSO using the Agilent Bravo Automated Liquid Handling Platform and VWorks Automation Control Software. For small molecule profiling studies, the Selleckchem inhibitor library (**Appendix 1**) was diluted 20X into complete media (3 μL inhibitor into 60 μL media) and mixed well, for a final concentration of 500 μM. A second intermediate plate was generated by transferring 14 μL of 500 μM inhibitor in media to into the first quadrant of a 384 deep well plate (Axygen, Cat No: 14-222-227), which contained 90 μL of complete media in quadrants 1 and 3 and 70 μL of complete media in quadrants 2 and 4. 30 μL from the first quadrant was transferred, and 10 μL from the first quadrant was transferred to the third quadrant . For the final dilution, 30 μL of inhibitor in media from the third quadrant was added to the fourth quadrant. Following each transfer, ten pipetting cycles were performed to ensure complete and thorough mixing of the inhibitor with the media. This intermediate plate was then diluted 10X onto cells to achieve final drug concentrations of approximately 5, 1.5, 0.5, and 0.15 μM. Each well of cells was also treated with media containing DMSO (positive control wells and monotherapy plates) or PI3K inhibitor (combination plates) using the Multiflo liquid handling dispensing system. PI3K inhibitor concentrations were determined based on pilot experiments evaluating

AKT phosphorylation and cell viability after treatment (data not shown) and are listed in **Table 5-1**. For all other resazurin experiments (including secondary validation screens), cells were treated with 0.5% inhibitor or DMSO in a 10-point two-fold dilution series in quadruplicate. To accomplish this, 96-well plates were prepared with inhibitors in 200X concentration and then diluted to 10X concentration in media in a second 96-well plate. These inhibitors were then used to treat the cells with the desired compound concentration, again using liquid handling robotics. In all cases, cells were stained with 10 μL of 440 μM resazurin (Sigma) dissolved in serum-free media for 12-24 hours before fluorescent signal intensity was quantified. Quantification occurred after 72 hour treatment using the Cytation3 fluorescence plate reader at excitation and emission wavelengths of 540 and 612 nm, respectively. To generate concentration response curves, data were plotted in Prism 8 using the log(inhibitor) vs. response -- Variable slope model with four parameters ($IC_{50}$, top, bottom, and Hill slope) allowed to vary.

*Trypan Blue Dye Exclusion Assay*

To test for cell membrane integrity and access cell viability, 24,000 cells per well were seeded into 24-well cell culture plates. The following day, cells were exposed to DMSO or inhibitor in a multipoint dose-response. After 72 hour exposure, cells were trypsinized, pelleted, and resuspended in in 50 μL of medium. 10 μL of the suspension was mixed with 10 μL of trypan blue dye (0.4% Invitrogen) and viability was measured using Countess Automated Cell Counter (Invitrogen). Both total cell number and percent viability were recorded for the assay.

*Annexin V Apoptosis Assay*

To study Annexin V presentation, 100,000 cells per well (for all cell lines except Detroit 562, for which the cell density was increased to 115,000 cells per well as used in previous studies (27)) were seeded in six-well plates. After 24 hours, media was aspirated and replaced with 3 mL of

complete media and 1 mL of media containing DMSO or inhibitor(s). Cells were cultured for 72 hours. At this time point, media was collected from each well. Each well was then washed in PBS, which was also collected. Finally, cells were trypsinized and added to the suspension. Samples were then centrifuged, washed once with PBS, and counted using the Countess Automated Cell Counter (Invitrogen). 50,000 cells per sample were stained with Annexin V FITC and PI using the Dead Cell Apoptosis Kit (Cat No: V13241; ThermoFisher) according to manufacturer's instructions. 2.5 μL of Annexin V FITC and 2.5 μL of PI were added to each sample. Samples were incubated at room temperature in the dark for 15 minutes and analyzed using the Bio-Rad ZE5 Cell Sorter at the University of Michigan Flow Cytometry Core.

*Cell Cycle Analysis*

To perform cell cycle analysis, 300,000 Detroit 562 cells per well or 350,000 HSC-4 cells per well were seeded in six-well plates. After 24 hours, media was aspirated and replaced with 2 mL of complete media containing DMSO or inhibitor(s). Cells were cultured for 24 hours, and 10 μM EdU was added to each well during the final hour of treatment. At the 24 hour time point, media was aspirated from each well. Each well was then washed in PBS. Finally, cells were trypsinized and collected. Samples were then centrifuged and washed once with 1% BSA in PBS (Invitrogen). Each sample was fixed, permeabilized, and stained using the Click-it EdU Flow Cytometry Assay kit (Cat No: C10425, ThermoFisher) according to manufacturer's instructions. Cells were resuspended in 500 μL of FxCycle PI/Rnase Staining Solution (Cat No: F10797; Invitrogen) and analyzed using the Bio-Rad ZE5 Cell Sorter at the University of Michigan Flow Cytometry Core.

*Western Blotting*

Cells at 70-80% confluency were treated with DMSO or inhibitor prior to harvesting and lysing in radioimmunoprecipitation assay buffer (Cat No. 89900; ThermoFisher) containing 1% NP-40 and 0.1% SDS. 8-50 micrograms of each cell harvest was used, and standard western blot protocols were followed as previously described (28). Primary antibodies (described in detail in **Table 5-2**) were incubated overnight at 4°C or for at least 1 hour at room temperature, followed by a goat anti-rabbit horseradish peroxidase (Cat No. 111-035-045; Jackson ImmunoResearch) secondary antibody at room temperature for 1 hour as described (29). The blots were then visualized with chemiluminescence and imaged. 300dpi or greater images were digitally retained from all westerns and representative blots are shown.

*Combination Inhibitor Response Analysis*

To compare effects of inhibitors from our small molecule library as monotherapies and in combination with PI3K inhibitors, we developed a scoring scheme to rank the inhibitors based on their effects in each cell line. This score (S) was calculated from the difference in relative viability between the monotherapy and combination therapy treatment at each concentration of library inhibitor using the formula:

$$S = \sqrt{\max\left(0, sign(s_1)s_1^2 + sign(s_2)s_2^2 + sign(s_3)s_3^2 + sign(s_4)s_4^2\right)}$$

where $s_1$, $s_2$, $s_3$, and $s_4$ are the scores (i.e. absolute difference) of the four doses and sign($s_i$) is the sign (+1 for positive numbers and -1 for negative numbers) of $s_i$.

In order to eliminate effects of non-biological responses, we added two additional qualifications: (1) for monotherapies, if treatment with a higher concentration of library inhibitor resulted in an unexpected higher viability, the viability was set as that of the adjacent lower

concentration, and (2) for combinations, if a lower concentration of library inhibitor resulted in an unexpected lower viability, the viability will be set as that with the adjacent higher concentration. These qualifications minimize the effect of any non-biological responses on the score and/or rank of an inhibitor. Any score less than zero (indicating that combination treatment increased cell viability as compared to monotherapy) was set as zero. Separate scores were generated to assess the effect of PI3K inhibitor combination with each PI3K targeting agent (HS-173 or BKM120). These scores were combined to generate a score evaluating effects conserved with both inhibitors using the formula:

$$S = \left(\frac{\sqrt{s_H} + \sqrt{s_B}}{2}\right)^2$$

where $s_H$ and $s_B$ represent the scores for HS-173 (H) and BKM120 (B) in the individual cell lines.

To prioritize inhibitors tested in secondary validation screening, compounds from the validation set were categorized into three groups based on their effect in combination with HS-173. The first group of inhibitors did not decrease cell viability as monotherapy over the concentration range tested and did not improve the efficacy of HS-173, thus representing false positives from the profiling experiment and/or combinations with effects specific to cell lines that were not tested in validation screens. The second group of inhibitors had some efficacy as monotherapies and improved the response to HS-173. However, the combination effects were additive and/or not dose-dependent. The final group of inhibitors represented compounds that appeared synergistic with HS-173, improving the effect of PI3K inhibitor monotherapy in a manner that could not be explained by monotherapy effects alone.

Synergy scores across multiple cell lines were combined as a weighted average to evaluate the recurrence of potentially synergistic combination effects across various HNSCC models. To calculate this recurrence score, PI3K inhibitor synergy scores from individual cell lines were used in the following equation, analogous to the one above for evaluating the effects of combinations with BKM120 and HS-173:

$$S = \left(\frac{\sqrt{s_{1H}} + \sqrt{s_{1B}} + \sqrt{s_{2H}} + \sqrt{s_{2B}} + \cdots + \sqrt{s_{10H}} + \sqrt{s_{10B}}}{20}\right)^2$$

where $s_{1H}$, $s_{1B}$, $s_{2H}$, $s_{2B}$, …, $s_{10H}$, and $s_{10B}$ represent the combined scores for erlotinib (H) and gefitinib (B) in the individual cell lines.

The relative combination effects of HS-173 and the top inhibitors from the validation screen (AZD3463, entrectinib, TAE226 and PCI-24781) were compared using the scores generated by Chalice Bioinformatics software (Horizon Discovery Group) using the Loewe model of synergy (30-32). Chalice software was also used to evaluate the effect of various PI3K and RTK inhibitors in **Figure 5-5**, **Figure 5-6**, **Figure 5-7**, and **Figure 5-8**. Combenefit software (33) was used to generate synergy plots, also using the Loewe model of synergy. For **Figure 5-14**, an R script was written (modeled after the Chalice software and Loewe synergy model) to assess the combination effect of any dual-therapy. This program will be made available at a later date as further optimization is currently being performed.

*Heatmaps*

Unsupervised hierarchical clustering was performed using Multiple Experiment Viewer (MEV) to order responses by cell line-PI3K inhibitor combinations in **Figure 5-5**. Heatmaps were generated using GraphPad Prism 8 software.

*Kinase Library Preparation*

UM-SCC-108 cells were transduced with the Human Kinase Lentiviral CRISPR Pool (Sigma Aldrich HKCRISPR). Conditions for transduction were established for a multiplicity of infection (MOI) of 30%. After 7 days of puromycin selection, the cells were expanded and seeded per treatment. To preserve at least 300x coverage, 3 million cells per treatment were needed. Triplicate pools of cells were treated with DMSO, 0.25 μM HS-173 or 0.25 μM BKM120. Inhibitors were applied for three days, then cells were cultured in media without drug for three days. This treatment was applied for two cycles and at the end of the second cycle, DNA was extracted from the remaining cells using Gentra Puregene Cell Kit (Qiagen).

To preserve coverage of the Kinase Library, 12 μg of DNA was used to PCR amplify the gRNA sequence using the Herculase ii Fusion DNA Polymerase (Agilent, Cat No: 600675). 2 reactions with 6 μg input DNA was amplified with the following primers:

PCR #1 Forward : AATGGACTATCATATGCTTACCGTAACTTGAAAGTATTTCG

PCR #2 Reverse: CTCGATTAATTAAGGTTGCTCACTTGTCGACTAATGC

The two reactions were then combined, and 5 μL were used to set up the second round of PCR reactions, using the following primers:

PCR #2 Forward:

AATGATACGGCGACCACCGAGATCTACACTCTTTCCCTACACGACGCTCTTCCGATC

T(1-9bp stagger)<u>AAGTAGAG</u>tcttgtggaaaggacgaaacaccg

PCR #2 Reverse:

CAAGCAGAAGACGGCATACGAGATTCGCCTTAGTGACTGGAGTTCAGACGTGTGCT

CTTCCGATCTataacggactagccttattttaac

Uppercase sequence represents Illumina adapters. The forward primer has the TruSeq Universal Adapter, and the reverse primer consists of Illumina P7, 8bp index, and multiplexing PCR primer 2.0. The underlined sequence represents an 8bp barcode. Lowercase letters are the priming sites for the lentiviral construct.

The PCR products were gel extracted and purified using Gel Extraction PCR Purification Kit (Qiagen). Samples were then submitted to the University of Michigan DNA Sequencing Core for sequencing with Illumina MiSeq V3 Kit.

*Analysis of Kinase CRISPR Library*

Reads were demultiplexed by barcode and then mapped to the corresponding reference library using an in-house python script. gRNA counts were input into Model-based Analysis of Genome-wide CRISPR/Cas9 knockouts (MAGeCK, v0.5.2) (34). MAGeCK algorithms calculated significant gRNAs and genes, and genes with an α-RRA score of ≤ 0.05 were considered significantly depleted.

*RNA Isolation and qPCR*

Cells were harvested in Qiazol (Cat No: 79306; Qiagen) and stored at -80°C. RNA was isolated using the Qiagen RNeasy Mini Kit (Cat No: 74106) according to manufacturer's protocols, and then quantified using the Qubit fluorometer (ThermoFisher). cDNA was synthesized using the SuperScript Vilo cDNA Synthesis kit (Cat No: 11754250; ThermoFisher), also using manufacturer's protocols, in the GeneAmp® PCR System 9700 (Applied Biosystems). qPCR analysis for each cDNA sample was performed with Quantitech SYBR green (Cat No: 204143; Qiagen) on the QuantStudio instrument (ThermoFisher). Primers were purchased from Intregrated DNA Technologies and sequences are listed in

Table 5-3. Analysis was performed using QuantStudio Design &Analysis Software v1.3.1 software (ThermoFisher) and Microsoft Excel. Changes in cycle times were compared to the geomean of three housekeeping genes (β-actin, HPRT, and RPL19). Triplicate determinations for each sample were compared to controls.

*Generation of CRISPR Knockout Cell Lines*

HSC-4 cells were seeded in six-well plates and transfected with TrueCut Cas9 Protein v2 and gRNA using Lipofectamine™ CRISPRMAX™ Transfection Reagent (Invitrogen) using manufacturer's protocols. For ALK and IGF-1R, respectively, the following crRNA sequences were obtained from ThermoFisher and used: 5'-GCTCCGAGGAGGAT-3' and 5'-TCACGGTCATTACC-3'. Cells were expanded and isolated as clones using single-cell dilution.

*Genomic DNA Isolation*

Cells were harvested and washed in PBS, then frozen at -20ºC. The pellet was then thawed and transferred to 700 µL of Nuclei Lysis Solution (Promega) for 1 hour at 55ºC. 200 µL of Protein Precipitation Solution (Promega) was added to the sample, which was then mixed and centrifuged at 13,000 RPM for two minutes. The supernatant was then transferred to a tube containing 600 µL of isopropanol, incubated for 15 minutes, and centrifuged at the same speed for another minute. The DNA pellet was washed in 70% ethanol, dried, and re-suspended in 35-50 µL of nuclease-free water.

*PCR and Sanger Sequencing*

DNA from HSC-4 knockout cells was amplified using PCR with Platinum Taq DNA Polymerase High Fidelity (Invitrogen) according to manufacturer's protocols and with primers that targeted the region of the guide RNA for ALK (primer sequences: FWD: 5'-

CGACGCAACCCTCCAAGAT-3' and REV: 5'-AGGAGGCCGTTTACTACT-3') or IGF-1R (primer sequences: FWD: 5'-CGACATCCGCAACGACTATC-3' and REV: 5'-GAGGTTGGGGAAGAGGTCTC -3'). PCR products were inserted into the pCR8 vector system (Cat No: K250020, ThermoFisher) and transformed into Mach1 competent cells, again according to manufacturer's protocols. Bacteria cultures from individual colonies on LB + spectinomycin plates were grown overnight and DNA was isolated using the Qiagen mini-prep protocol (Cat No: 27106) according to manufacturer's protocols. The DNA product was analyzed via Sanger sequencing at the University of Michigan DNA Sequencing Core on the 3730XL DNA Sequencer (Applied Biosystems). Sequences were aligned using the DNASTAR Lasergene software suite.

*Xenografts*

Animals were housed in a vivarium accredited by the Assessment and Accreditation of Laboratory Animal Care at the University of Michigan. Veterinary care was provided by the University of Michigan Unit for Laboratory Animal Medicine (ULAM), and all procedures were performed according to Institution for Animal Care and Use Committee-approved protocol PRO00008065. Athymic nude mice (both male and female, 1-3 months old) were subcutaneously injected with 2 million UM-SCC-108 cells per flank. After allowing tumors to become palpable (~1 week following injection), treatment with vehicle (10% NMP, 90% PEG300), pictilisib (100 mg/kg), brigatinib (50 mg/kg), or combination was administered via oral gavage in 200 μL per 20 g mouse three times per week for three weeks. Inhibitors were prepared fresh or used after storage at 4°C for no more than 1 week. To improve inhibitor solubility in vehicle, sonication was used for at least 5 cycles of 20 sec at 50% amplitude and 10-20 sec off using the Branson Digital Sonifier. Weights and tumor volumes (measured using

calipers and calculated using the formula width x length 2 x pi/6) were recorded 2-3 times per week. General health was monitored with euthanasia required upon loss of 20% body weight (as compared to highest weight recorded), the presence of ulceration exceeding half the surface area of the tumor, tumor length greater than 20 mm, or tumor volume greater than 3000 $mm^3$.

*Statistical Analysis*

To determine if statistically significant differences occurred with combination treatments in trypan blue dye exclusion and annexin V apoptosis assays, a two-way ANOVA was performed in R to compare the natural logarithm of the percentage of living cells following vehicle, PI3K inhibitor monotherapy, RTK monotherapy, or combination treatment. Specifically, this test was performed using type III analysis with the "Anova" function from the "car" package. Bonferroni correction was used to adjust p-values.

For comparisons of tumor volumes in xenograft studies, an unpaired, t-test was used to compare the average tumor volume for mice from each group using Prism 8 software.

## Results

To identify potential mechanisms of resistance to PI3K inhibitor monotherapies in HNSCC, we tested a library of small molecule inhibitors in combination with vehicle (DMSO) or low concentrations of two PI3K inhibitors in a diverse panel of patient-derived HNSCC cell lines (**Appendix 1**). To select PI3K inhibitors for these studies, we performed preliminary experiments, which demonstrated that pan and p110α selective pharmacologic agents were more effective than those directed against p110β, γ, and δ (**Figure 5-1**), consistent with the fact that activating aberrations in *PIK3CA* are more frequent than alterations in other PI3K pathway gene in HNSCC (16-18, 35). Based on recent clinical trials demonstrating the ability of BKM120 (36,

37) to extend progression free and overall survival in recurrent and metastatic HNSCC (20, 38), we chose this inhibitor for use in combination studies. HS-173 was the most effective selective p110α inhibitor in our preliminary data, and as such was chosen as the second combinatory PI3K inhibitor (39, 40). Concentrations for these inhibitors were selected such that they inhibited viability (relative to vehicle-treated controls) by no more than 25% yet demonstrated reduced downstream signaling (assessed based on decreased AKT phosphorylation at the Ser473 residue following drug treatment, data not shown) (**Table 5-1**).

The ten cell lines used in this study were chosen to represent clinical HNSCC cases that would be nominated for biomarker-driven trials of PI3K inhibitor combinations. Each cell line model displayed genetic alteration in *PIK3CA:* four harbored *PIK3CA* mutations (HSC-2, HSC-4, Detroit 562, and UM-SCC-43), while the others had amplification of wild type *PIK3CA* with an average copy number anywhere between 2.67 (UM-SCC-55) to 6 (UM-SCC-69) copies of this gene (23, 27). As HPV negative and oral cavity HNSCCs represent those patients with the poorest clinical prognosis (41), most of the selected cell lines also displayed lack of high risk HPV strains and were derived from oral cavity subsites. UM-SCC-104, which is HPV positive, and Detroit 562, which was derived from a metastatic pharynx cancer, are the only exceptions.

The small molecule library used for these profiling experiments included 1406 inhibitors, most of which are FDA-approved or in clinical development for cancer or other diseases. Inhibitors were classified into 23 pathways based on their molecular targets (**Appendix 1**, **Figure 5-2**) and were used to treat cells for 72 hours before viability was measured using a resazurin cell viability assay. The initial phase of our small molecule profiling studies generated more than 150,000 data points characterizing nearly 15,000 drug-cell line pairs. Each of these drug-cell line pairs represents a library inhibitor tested at four concentrations, ranging from

approximately 0.15 to 5 μM. Each inhibitor was used as a single agent and in combination with the two PI3K inhibitors, and results were quantified using a synergy score for each PI3K inhibitor combination (HS-173 score, BKM120 score) or the collective effect of both PI3K inhibitor combinations (PI3K inhibitor score) (**Figure 5-5A**, also see Materials and Methods for further details on scoring schemes). Clustering of these scores by cell line (**Figure 5-5A**) revealed that HS-173 and BKM120 scores for 9/10 (90%) of models grouped together, as would be expected. Cell lines with mutations in *PIK3CA* clustered in two groups—Detroit 562, UM-SCC-43, and HSC-2 HS-173 scores aligned together, while HSC-4 and HSC-2 BKM120 scores clustered in a separate group. *PIK3CA* copy number and gene expression did not seem to affect clustering.

In order to nominate potentially synergistic PI3K inhibitor combinations from these profiling experiments, we selected 96 inhibitors from our 1406-member library (**Appendix 1**) and tested them in a validation screen. These agents were chosen based on two main factors: (1) magnitude of synergy score and (2) recurrence of potential synergistic effects across cell line models. To quantitatively compare these two factors for each inhibitor, we developed a "recurrent synergy score", which combined the HS-173 score and BKM120 score for each of the ten cell lines into a single metric of potential synergy with PI3K inhibitors. Based on this summary score, the second most effective PI3K inhibitor combination therapy in our screen was irreversible EGFR/ERBB2 inhibitor afatinib. This was strong initial validation for our approach, as previous work from our laboratory and other groups has demonstrated the important role of the epidermal growth factor receptor (EGFR) in PI3K inhibitor resistance in HNSCC (27, 42-48). Additional combinations with potential synergy include those inhibiting both PI3K and anaplastic lymphoma kinase (ALK), AKT, insulin-like growth factor receptor (IGF-1R), aurora

kinase, Bcl-2, histone deacetylase complex (HDAC), and focal adhesion kinase (FAK). Other inhibitors with high recurrent synergy scores were included in the validation set to increase the overall diversity of the combinations that we considered: together, these 96 inhibitors included drugs directed against more than 75 different target genes.

Each of the inhibitors in the validation set was tested using a reverse-format approach: instead of titrating library inhibitors against a single concentration of PI3K inhibitor as in the original screen, four-point concentration response curves were generated for p110α-selective inhibitor HS-173 as a monotherapy and with four concentrations of each inhibitor from the validation set (**Figure 5-3**). These experiments were performed in *PIK3CA* mutant models HSC-2, HSC-4, and Detroit 562 and validated using positive control combination HS-173 + afatinib and negative control combination HS-173 + AZD4547 (**Figure 5-4**) (27). Each inhibitor from the validation set, based on its effect with HS-173, was then manually placed in one of three groups (no combination effect, additive, or synergistic). Approximately 25% of the inhibitors in the validation set were confirmed as potentially synergistic in one or more of these three models using the reverse-format screen. Of the potentially synergistic inhibitors, five pathways were further prioritized with 1-3 inhibitors considered for each pathway: ALK (tested using ALK/IGF-1R inhibitor AZD3463 and ALK/Ros1/Trk inhibitor entrectinib), JAK (AZ960, AT9263, and TG-101348), IGF-1R (BMS-754807 and ADW541), FAK (PF-566271 and TAE226), and HDAC (PCI-24781). Of these ten compounds, AZD3463, entrectinib, TAE226, and PCI-24781 showed the greatest efficacy in combination with HS-173 in HSC-2, HSC-4, and Detroit 562 cells and as such were characterized in a large panel of HNSCC cell lines, including models with variation in genetic characteristics, gene expression profiles, and HPV status (**Figure 5-5C**, **Figure 5-6, Figure 5-7**). Responses were quantified using the Chalice score, which is based on

the Loewe synergy model (32). A subset of cell lines displayed synergistic responses to each PI3K inhibitor combination, while others responded additively or did not respond to mono- or dual-therapy. In general, these responses did not correlate with *PIK3CA* mutation status or expression level (**Figure 5-5C**, **Figure 5-7**); in this dataset, Chalice score was significantly higher for HS-173 and TAE226 combination treatment in cell lines with *PIK3CA* mutations (**Figure 5-5Ciii**), but this association was lost on further analysis with independent PI3K and FAK inhibitor combinations (**Figure 5-14**).

Using a *PIK3CA* amplified model with a CRISPR kinome library available in our lab, we then set out to complement our small molecule profiling approach by identifying genes that, when knocked out, conferred sensitivity to PI3K inhibitor monotherapy. UM-SCC-108 cells had been previously transduced with the Human Kinase CRISPR Knockout Library, which contains gRNAs targeting 684 kinases with approximately nine gRNAs per gene. We treated the UM-SCC-108 kinome knockout library cells with DMSO, 0.25 μM HS-173, or 0.5 μM BKM120 for 14 days and sequenced the remaining cells. We then used the MAGeCK algorithm to identify gRNAs and genes that were significantly depleted in HS-173 or BKM120-treated samples relative to controls. This analysis identified 118 gRNAs that were significantly depleted (p-value $\leq 0.05$) in the BKM120-treated population and 124 gRNAs that were significantly depleted in the HS-173-treated population. Of these, 21 gRNAs overlapped between the two PI3K inhibitor treatments. Consistent with other studies, knockout of *AXL* and *ERBB3* increased sensitivity to PI3K inhibition (31, 49, 50). In support of our small molecule profiling results, which demonstrated that UM-SCC-108 cells were synergistically responsive to PI3K and ALK/IGF-1R inhibitors, *ALK* knockout cells were significantly depleted after BKM120 treatment ($p = 0.014$) and *IGF-1R* knockout cells were significantly depleted after HS-173 treatment ($p = 0.0027$).

Given the efficacy of HS-173 in combination with AZD3463 or entrectinib in several HNSCC models and the results of the kinase knockout screen, we next performed further experiments to validate and characterize the potential role for ALK and/or IGF-1R signaling as a mechanism of resistance to PI3K inhibitor treatment. ALK fusions play an important oncogenic role in other cancer types, including lung cancer and neuroblastoma (51-55); to date, the clinical use of ALK inhibitors has been primarily limited to ALK-fusion positive patients of these cancer types. On the other hand, ALK fusions are rarely observed in HNSCC (~1%) (56), and ALK inhibitors have not been used effectively as monotherapies in cases lacking these fusions. Recent preclinical data suggests that co-targeting ALK and EGFR may be effective in some HNSCCs (57, 58), but the combined effect of PI3K and ALK inhibition has not been examined in cancers at this anatomic site. To investigate the co-dependence of PI3K and ALK in HNSCC, we first determined the responses of three HPV negative, *PIK3CA* mutant cell lines (HSC-2, HSC-4, and Detroit 562) to a panel of PI3K and ALK inhibitors in various combinations (**Figure 5-8**). We observed responses that were additive to synergistic with HS-173, BKM120 and pictilisib (59) in combination with inhibitors targeting ALK and/or IGF-1R (AZD3463, entrectinib, crizotinib, TAE684, BMS-754807, and brigatinib). Synergistic responses were not observed with p110β inhibitor TGX-221 , demonstrating the specific role of PI3K's alpha isoform in synergistic responses. Similarly, replacing ALK/IGF-1R inhibitors with Trk inhibitor PF-06273340 or FGFR inhibitor BGJ398 did not recapitulate synergistic responses in any of the models, suggesting a need to inhibit ALK/IGF-1R.

We then expanded our analysis to cell lines with amplification of wildtype *PIK3CA* or HPV positivity. Using trypan blue exclusion assays, we tested the effect of PI3K inhibitor monotherapy (pictilisib, BKM120, or TGX-221 as a negative control), ALK inhibitor

monotherapy (brigatinib), and each PI3K and ALK inhibitor combination. Pictilisib and brigatinib combinations caused a significant reduction in the percentage of living cells in all models, with BKM120 combinations trending toward statistical significance (**Figure 5-8B**, see **Table 5-5** for p-values by two-way ANOVA). Next, annexin V apoptosis assays were used to determine the percent of FITC positive cells in HSC-4, Detroit 562, UM-SCC-103 and UM-SCC-69 after vehicle, PI3K inhibitor monotherapy, ALK inhibitor monotherapy, or dual-therapy. For each cell line, pictilisib and brigatinib combination-treated cells displayed significantly higher levels of FITC positivity than monotherapies (**Figure 5-8C**). BKM120 and brigatinib combinations trended toward synergistic responses, while TGX-221 and brigatinib combinations, as expected, resulted in levels of apoptosis that were comparable to monotherapies (**Table 5-6**). Apoptotic responses were confirmed using western blot for caspase and PARP cleavage in the same four cell lines (**Figure 5-8D**, **Figure 5-9**). Similarly, cell death by apoptosis was observed with HS-173 and AZD3463 combinations (**Figure 5-10**). Synergistic drug combinations also affected the cell cycle in *PIK3CA* mutant HSC-4 cells, resulting in a reduction in the percentage of cells going through S-phase (as measured using EdU positivity) (**Figure 5-8E**).

Because brigatinib has been reported to inhibit not only ALK but also other targets (most notably IGF-1R (60), we took a genetic approach to determine whether ALK, IGF-1R, or both were contributing to combination responses in HSC-4 cells. We hypothesized that loss of the critical mediator of response would sensitize cells to treatment with PI3K inhibitor monotherapy. Using CRISPR/Cas9, we generated and characterized genetic knockouts of *ALK* and *IGF-1R* (**Figure 5-11A**, **Figure 5-12**). No dramatic differences were noted in sensitivity to PI3K inhibition in the *ALK* or *IGF-1R* knockout cell lines as compared to those seen in wildtype HSC-4. Notably, AKT inhibitor GDC-0068 was more effective in HSC-4 cells lacking *ALK* (**Figure**

**5-11B**). RNA sequencing is currently being performed to evaluate differences in gene expression between wildtype and knockout cell lines and identify additional mediators of PI3K inhibitor resistance. qPCR experiments for a small panel of genes did not demonstrate significant differences in mRNA levels for *AKT1*, *PDK1*, *IGF-1R*, or *PIK3CA* between HSC-4 wildtype and *ALK* knockout or HSC-4 wildtype and *IGF-1R* knockout cells (**Figure 5-13**). *ALK* gene expression was ~4-fold lower in *IGF-1R* knockout cells; however, this decrease does not suggest that ALK signaling is preventing PI3K inhibitor sensitivity in the *IGF-1R* knockout model.

We next sought to validate other potentially synergistic combinations and compare them to PI3K + ALK inhibitor dual-therapies. To do this, we first tested a subset of the molecular pathways that might mediate resistance to PI3K inhibitor treatment based on our small molecule profiling experiments. Again using resazurin cell viability experiments, we tested inhibitors of each proposed compensatory pathway in combination with pictilisib. In most cases, we used two inhibitors of each pathway to eliminate effects that might be specific to a single RTK inhibitor and not to a class of inhibitors with a common target. These combinations were evaluated in six HNSCC cell lines: two cell lines with *PIK3CA* mutations (HSC-4 and Detroit 562) and four with amplification of wildtype *PIK3CA* (HPV negative: UM-SCC-108 and UM-SCC-59, HPV positive: UM-SCC-47 and UM-SCC-104). Synergistic effects were again quantified based on the Loewe model of synergy (**Figure 5-14**) (32), which demonstrated that ALK, IGF-1R, AURKA, FAK, FGFR, and/or HDAC inhibition might also enhance cell death when combined with PI3K inhibitor treatment. For some RTK targets, including those involving FGFR and FAK inhibitors, one of two similar RTK-targeting agents was more synergistic in combination with pictilisib than the other. This effect may be due to polypharmacology, as has been reported for

ponatinib and TAE226 (61, 62), and was also observed using orthogonal western blot analyses. Ponatinib and pictilisib co-treatment led to PARP cleavage in HSC-4 cells, while more specific FGFR inhibitors BGJ398 and AZD4547 did not result in the same level of apoptosis when used in combination with pictilisib (**Figure 5-16**). Using this same approach to detect apoptotic responses, we confirmed the results of our resazurin cell viability assays by showing that combinations of pictilisib and ALK inhibitor brigatinib, IGF-1R inhibitor ADW742, FAK inhibitor TAE226, FGFR inhibitor ponatinib, and aurora kinase inhibitor ENMD-2076 lead to increased expression of cleaved PARP in HSC-4 and UM-SCC-108 following 24 hour treatment (**Figure 5-15**). Similar effects for RTK inhibitor combinations were seen in a larger panel of cell lines, including UM-SCC-116, which does not display aberration in *PIK3CA* via mutation or copy number amplification (**Figure 5-15**).

After evaluating this panel of primarily upstream RTK inhibitors in combination with pictilisib, we wanted to determine if the synergistic combinations effects that we observed were mediated by rescue of a downstream pathway. We hypothesized that if such a downstream effector (for example, AKT) was responsible for resistance to PI3K inhibition, then an inhibitor specifically targeting this effector would display synergy in combination with a PI3K inhibitor. To test this, we again used a panel of HNSCC cell lines including three with *PIK3CA* mutant cell lines (HSC-4, Detroit 562, and HSC-2) and three with amplification of wildtype *PIK3CA* (HPV negative: UM-SCC-103, HPV positive: UM-SCC-47 and UM-SCC-104) and treated each with PI3K inhibitor BKM120 in combination with an inhibitor of a pathway downstream of PI3K or other RTKs. These combinations included BKM120 and ALK/Ros1 inhibitor brigatinib (positive control for PI3K + RTK synergy), AKT inhibitor MK-2206, mTOR inhibitor rapamycin, PDK1 inhibitor GSK-2233470, or JAK inhibitor TG-101348. Similar to the effects

observed with pictilisib and AKT inhibitor combinations, BKM120 and MK-2206 combination did not display synergy when used together. Similar results were observed for mTOR, PDK1, and JAK inhibitors in HSC-4 cells (**Figure 5-17**). This was confirmed using western blot analysis, which showed that co-treatment with BKM120 and brigatinib, but not other inhibitors, induced PARP cleavage (**Figure 5-18**). Responses in other cell lines recapitulated these effects, with only JAK inhibition providing greater reduction in cell viability than monotherapies in a subset of cell lines (**Figure 5-19**). Given that JAK inhibitors ruxolitinib and tofacinib were not synergistic with pictilisib (**Figure 5-14)**, the effects of TG-101348 may be drug-specific and mediated by additional effects to inhibit FLT3 or bromodomains (61).

Finally, we assessed the efficacy of PI3K and ALK inhibitor combinations *in vivo* using a xenograft model of UM-SCC-108. Following the establishment of tumors, we treated mice with vehicle, monotherapy, or combination therapy. We performed pharmacodynamic experiments to assess drug-indcued changes on a molecular level. As expected, pictilisib reduced AKT phosphorylation after 1 hour treatment, both as a single agent and dual-therapy (**Figure 5-20**). Additionally, after 6 hour treatment, pictilisib alone or in combination with brigatinib induced the expression of apoptotic markers cleaved caspase 3 and cleaved PARP (**Figure 5-21**). We then administered vehicle, monotherapy, and dual-therapy three times per week for three weeks to assess the effects of pictilisib and brigatinib on tumor growth. We compared the average tumor volume for mice in each of the treatment arms, noting no significant difference in tumor volume between vehicle- and brigatinib-treated mice ($p = 0.11$, unpaired t-test). In contrast, pictilisib monotherapy slowed tumor growth as compared to vehicle ($p = 0.0013$, unpaired t-test), and the addition of brigatinib to pictilisib treatment resulted in a further significant reduction in tumor volume ($p = 0.024$ compared to pictilisib monotherapy, $p < 0.0001$ compared to vehicle,

unpaired t-tests) (**Figure 5-22**); this indicated a synergistic response. Minimal toxicity was observed, as all mice maintained their body weight over the course of the treatment period (**Figure 5-23**), which suggests that such combinations might also display limited side-effect profiles if administered in human patients. After three weeks of treatment, given the surprisingly strong anti-tumor effect of this combination, we continued to administer pictilisib or combination to a subset of the mice in these two experimental groups to assess differences in time to endpoint between these two groups. Although only five mice were included in each arm of this study, three of the five combination-treated mice lived two or more weeks beyond the date when all pictilisib animals reached their tumor endpoint (**Figure 5-24**). As a whole, these results confirm the synergy of pictilisib and brigatinib *in vivo* and suggest that this combination may provide significant tumor growth delay despite the development of acquired resistance.

## Discussion

Previous publications have demonstrated preclinical and clinical rationale for PI3K inhibitor treatment in HNSCC (20, 35, 63) and suggested combinatorial approaches to improve responses to such therapies (27, 31, 43, 49, 50). Here, by performing high throughput combinatorial studies of PI3K inhibitor responses, we provide rationale for dual-therapy approaches as well as nominate novel drug pairs for evaluation using *in vitro* and *in vivo* models of HNSCC. One of these combination treatments involves co-treatment with PI3K and ALK-targeting agents; together, these inhibitors, such as pictilisib and brigatinib, induce apoptosis in a diverse panel of HNSCC cell lines and delay tumor growth in a mouse model.

The mechanistic link between PI3K and ALK in HNSCC is incompletely understood. Previous work has demonstrated synergistic effects of EGFR and ALK inhibition in HNSCC

models, demonstrating that ALK signaling may play a critical role in this cancer type despite the lack of ALK gene fusions or amplifications observed in other types of tumors (57, 58). Our HSC-4 ALK knockout cell line is more responsive than wildtype HSC-4 cells to AKT inhibitor GDC-0068 (**Figure 5-11**). Interestingly, Gonzales *et al.* noted that EGFR + ALK inhibitor combination treatments provide further reductions in AKT phosphorylation compared to monotherapies (57). One possibility, then, is that further inhibiting AKT, which is downstream of both EGFR and PI3K, mediates response to ALK inhibitor treatment. However, our data indicates that pictilisib monotherapy, at concentrations that are insufficient to induce apoptosis, sufficiently blocks AKT phosphorylation at the serine 473 residue after six and 24 hour treatment periods (data not shown). While this suggests that other signals may also be critically important, we have not considered the maintenance of AKT inactivation, other AKT phosphorylation sites, or total AKT protein levels. Additionally, it remains to be determined if ALK + AKT inhibitor combinations have greater than additive effects.

In fact, the sensitivity of ALK knockout cells to AKT inhibition is somewhat surprising as our studies using a set of PI3K combinations that inhibit upstream RTK and downstream effectors demonstrated that the RTK inhibitor combinations (including those targeting IGF-1R, FAK, AURKA, and others) produced responses similar to PI3K + ALK inhibitor therapies. Such responses, however, were not observed with PI3K + AKT, mTOR, BCL-2, or PDK1 inhibitors. This could be due to the contributions of multiple RTKs to PI3K inhibitor resistance, with each RTK playing a partial, albeit critical, role. Furthermore, these RTK inhibitors are not perfectly selective and might have activity against more than one critical resistance mechanism. In these cases, synergistic responses may require tamping down multiple RTKs and their overlapping effectors. While the development of less selective inhibitors is often discouraged due to the

increased potential for toxicity, "off-target" effects may actually increase the efficacy of some of these agents in HNSCC and other cancer types and act as a means of suppressing pathways that would otherwise mediate tumor progression or recurrence. For example, ponatinib has been described as an inhibitor of BCR-ABL, FGFR, SRC, MEK, JUN, and other signaling pathways (64, 65), but has a striking effect with pictilisib in UM-SCC-59 cells, a model previously characterized as fairly non-responsive to PI3K inhibitor alone (27). Consistent with this, pictilisib and ponatinib co-treatment induced apoptosis in HSC-4 cells, while other FGFR inhibitor combinations were less effective (**Figure 5-16**). Similarly, brigatinib's effects may not be solely due to its inhibition of ALK signaling, but also due to inhibition of IGF-1R or even EGFR signaling (66). Such findings highlight the ongoing challenges of developing safer inhibitors that display broad-spectrum kinase activity.

An additional challenge not addressed in our study is the selection of patients most likely to respond to any specific PI3K inhibitor therapy. Our results indicate that pictilisib and brigatinib, as well as other PI3K inhibitor combinations, are capable of inducing apoptosis in cell lines with disparate *PIK3CA* mutation status, copy number, and expression levels (**Figure 5-7**, **Figure 5-15**). HPV status is also not a stratifying factor. These results, unfortunately, are in line with other studies that have demonstrated similar difficulty in predicting PI3K inhibitor responses (27, 67, 68) and suggest that other or multiple factors, including not only mutations and copy number changes, but also protein or mRNA transcript levels (69, 70), may be important mediators of response. One recent paper suggested that *NOTCH1* mutation status may predict responses to PI3K inhibitor monotherapy (63), but combinatorial responses, involving a larger host of factors (both drug-related and otherwise), will likely only make patient selection more difficult. In order to generate the statistical power needed to detect factors predictive of response

to PI3K inhibitor combinations, additional cell line and mouse models of HNSCC will need to be tested.

Taken as a whole, this work provides a rich dataset examining resistance to targeted PI3K inhibitors and demonstrates the successful use of drug pairs to inhibit PI3K and co-dependent signaling networks in HNSCC. For the first time, we report the synergy of PI3K and ALK inhibitors in cancers without ALK fusions, giving additional support to the role for ALK signaling in HNSCC specifically. Further studies of other novel combinations are warranted; similar experiments could also be performed with other agents or in additional cancer types. Using these approaches to better understand sensitivity and resistance to targeted therapy may be instrumental in improving outcomes for HNSCC and other cancer patients.

**Acknowledgements**

Thank you to J. Zhai and H. Jiang for statistical analysis and to M. Ludwig, E. Gensterblum-Miller, and A. Kulkarni for performing and analyzing the results of the kinome knockout screen. Thank you to S. Foltin for assistance with resazurin cell viability experiments and generation of the ALK and IGF-1R knockout models. Thank you especially to J. Wang as well as to E. Leonard, V. Nair, C. Matovina, M. Harris, G. Herbst, A. Bachand, and D. Kim for help with immunoblotting and characterization of *ALK* and *IGF-1R* knockout models. Thank you to B. Marinelli, M. Ludwig, and J. Wang for assistance with xenograft experiments. Thank you to J.C. Brenner for oversight and guidance in experimental design and interpretation.

## Figures

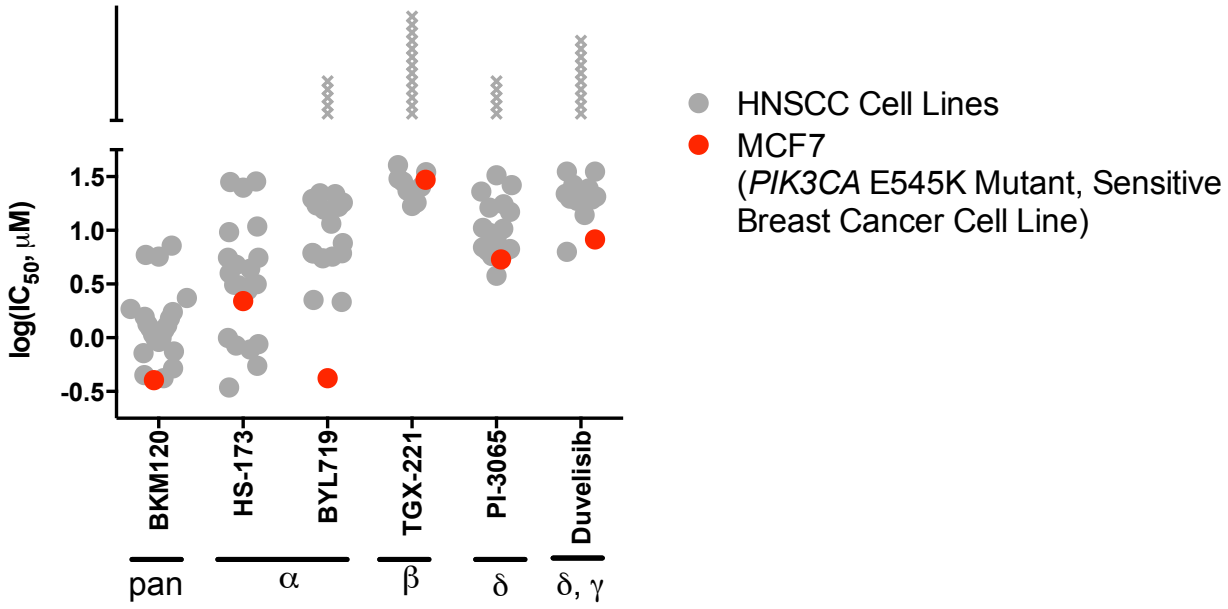


**Figure 5-1. Response of HNSCC and MCF-7 cell lines to PI3K inhibitor monotherapies.**

HNSCC and MCF-7 breast cancer cell lines were treated with increasing concentrations of PI3K inhibitors for 72 hours. MCF-7 was used as a model known to have high sensitivity to PI3K inhibitors (71). Cell viability was measured using a resazurin cell viability assay, and $IC_{50}$ values were determined as described in Materials and Methods. X denotes resistance with $IC_{50}$ value greater than 50 μM, the highest concentration tested in these experiments.

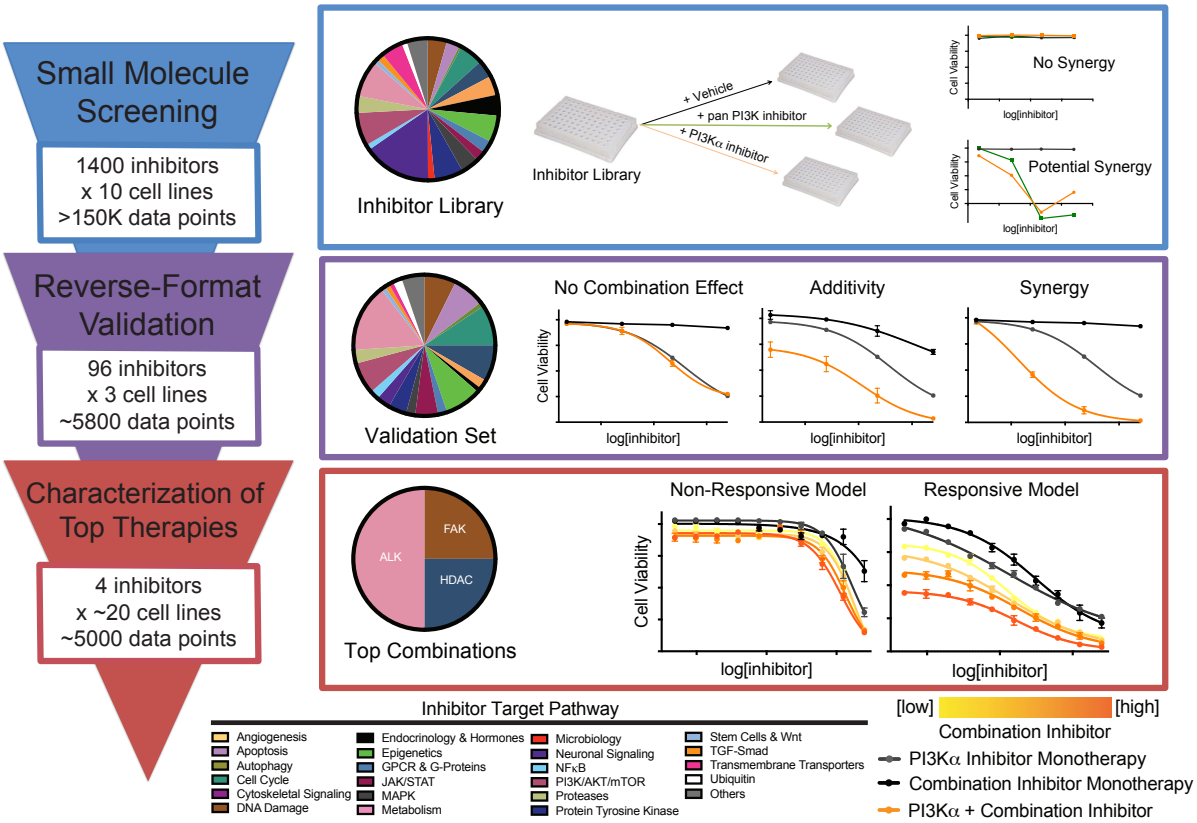


**Figure 5-2. Schematic for high throughput combinatorial screen.**

An inhibitor library with 1406 compounds targeting a diverse set of cellular pathways (see **Appendix 1**) was used to treat ten HNSCC cell lines. Inhibitors from the library were applied at four concentrations as monotherapies and in combination with low concentrations of PI3K inhibitors HS-173 and BKM120. Potentially synergistic compounds were tested using a validation assay where HS-173 was titrated into constant concentrations of 96 promising inhibitors from initial screening. Inhibitors with synergy upon repeat testing were tested in a diverse panel of HNSCC cell lines in high-density concentration response experiments.

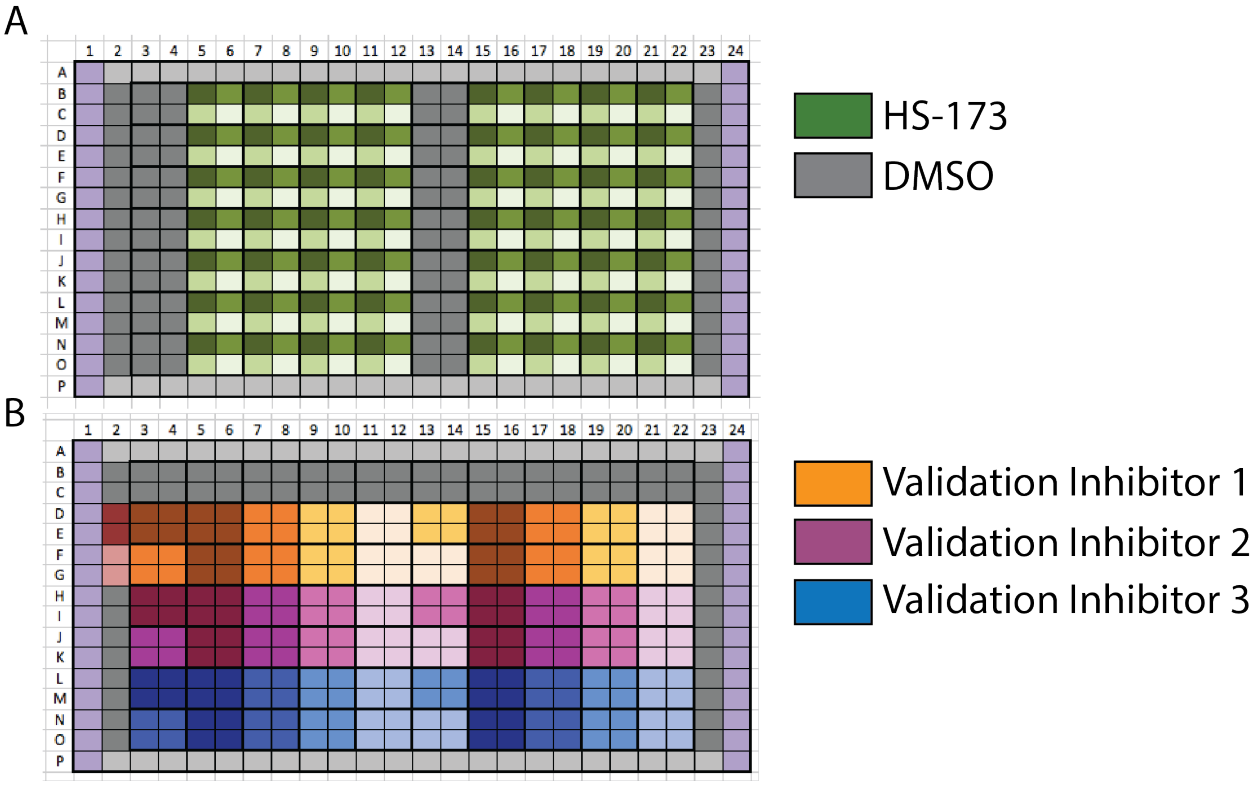


**Figure 5-3. Schematic for validation screening.**

(A) Cells were treated first with DMSO or titrations of HS-173 as shown. (B) Validation inhibitors were added such that each combination was tested in quadruplicate for four concentrations of HS-173 and four concentrations of each validation inhibitor. Resazurin cell viability experiments were performed to assess responses after 72 hours and prioritize inhibitors for further studies.

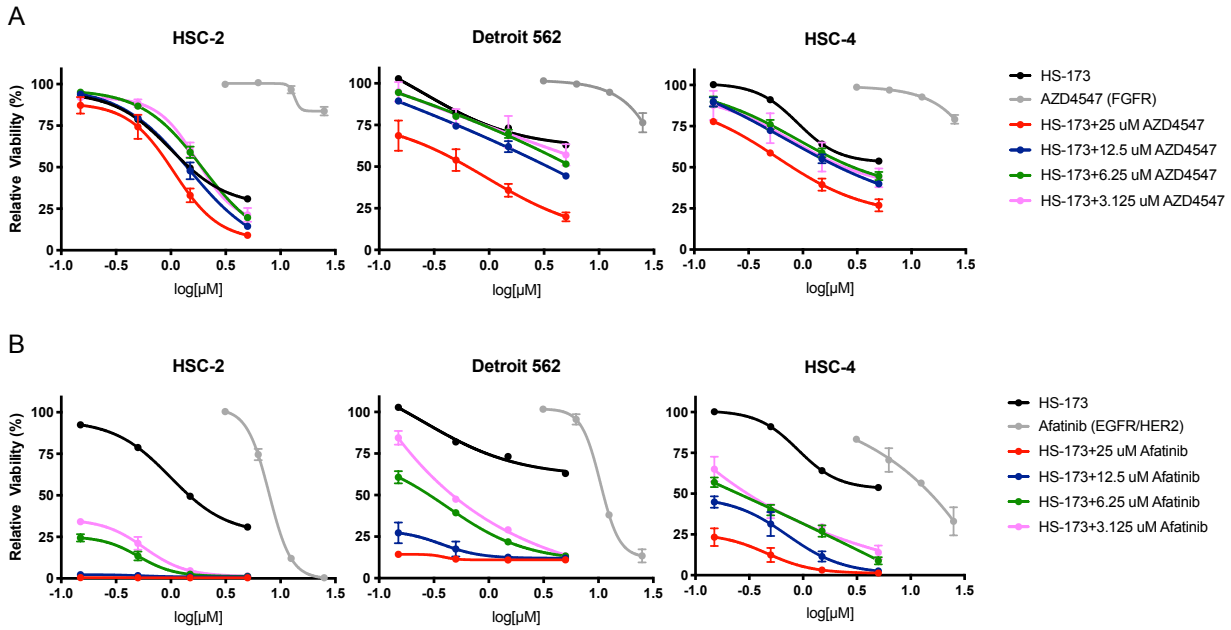


**Figure 5-4. Synergistic and non-synergistic PI3K inhibitor combinations for optimization of reverse-format validation screen.**

HSC-2, Detroit 562, and HSC-4 cells were treated with PI3K inhibitor HS-173 and/or (A) negative control FGFR inhibitor AZD4547 or (B) positive control EGFR/HER2 inhibitor afatinib for 72 hours. Cell viability was measured using a resazurin cell viability assay. Mean +/- SD for quadruplicate determinations from a single representative experiment are shown.

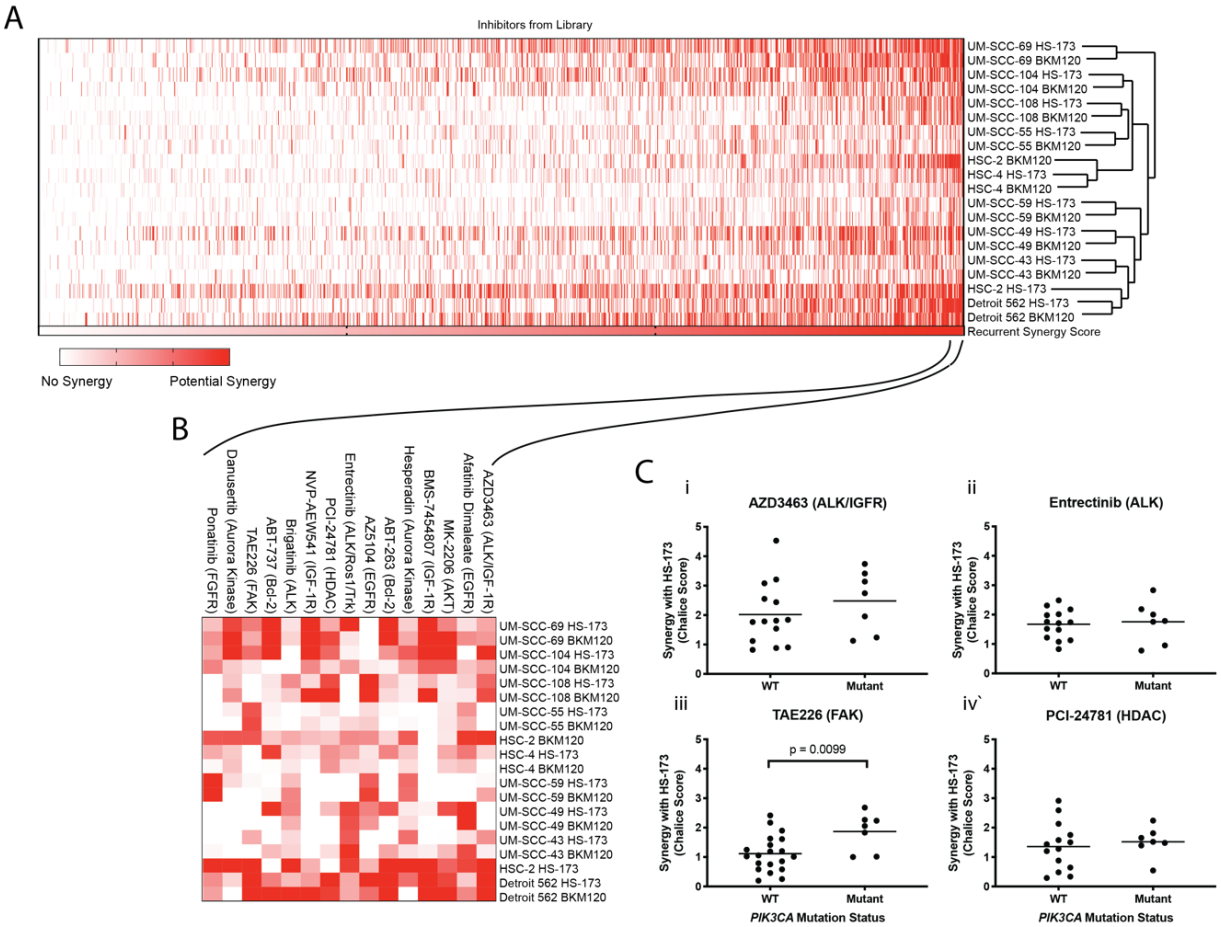


**Figure 5-5. Workflow for small molecule profiling and selection of promising inhibitor combinations.**

(A) HNSCC cell lines were treated with a small molecule inhibitor library (**Appendix 1**) as monotherapies and in combination with low concentrations of two PI3K inhibitors. A heat map was generated based on statistical scoring for each inhibitor and evaluation of the recurrence of effect across the HNSCC cell line panel as described in Materials and Methods above. Cell lines were arranged using unsupervised hierarchical clustering. (B) Magnification of top-scoring inhibitors from (A), which are potentially synergistic with PI3K inhibitors. (C) Validation of top-scoring, recurrent PI3K inhibitor combinations using resazurin cell viability assays in a diverse panel of HNSCC cell lines with quantification using Chalice score (Horizon Discovery). *PIK3CA* mutation status stratifies responses to HS-173 and TAE226 (iii) but not other combinations.

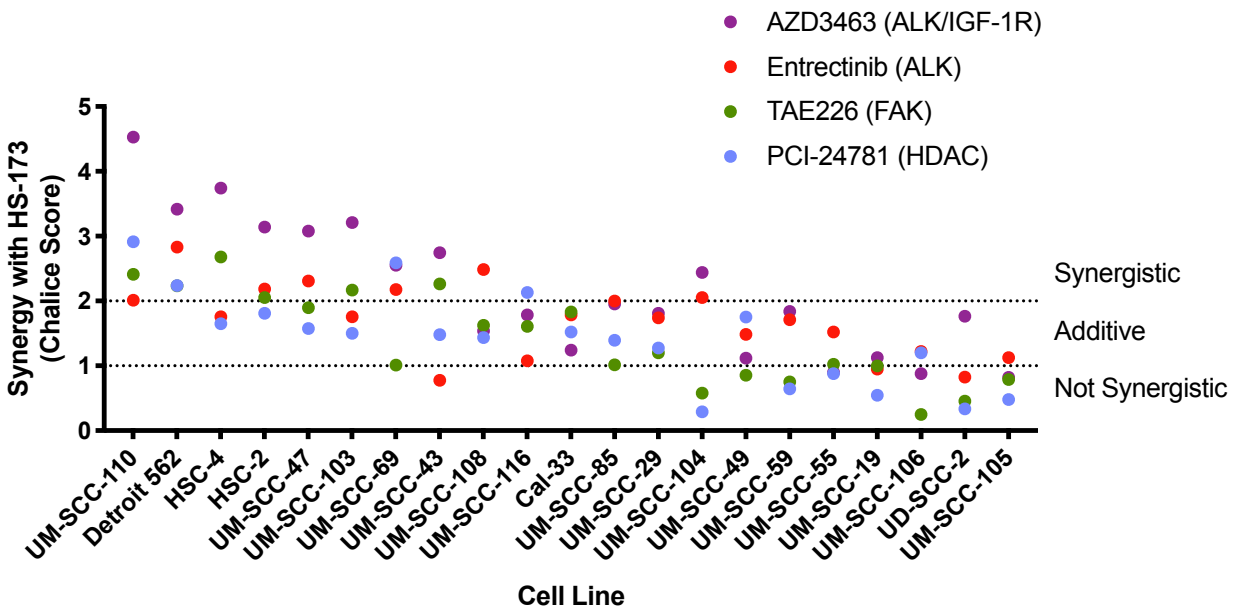


**Figure 5-6. Responses to validated PI3K inhibitor combinations in a diverse panel of HNSCC cell lines.**

HS-173 and AZD3463, entrectinib, TAE226, or PCI-24781 were administered to HNSCC cell lines with varying genetic status and HPV status (UM-SCC-47, UM-SCC-104, UD-SCC-2, and UM-SCC-105 are HPV positive) as monotherapies and in combination. Experimental conditions mimicked those shown below in **Figure 5-8A** with PI3K inhibitor titrated into four constant concentrations of combination inhibitor. UM-SCC-105 and UM-SCC-55 cells were treated with AZD3463 and PCI-24781 combinations at 10X lower concentrations than other cell lines due to incrased sensitivity to these agents when administered as monotherapies. Experiments were performed at least twice with quantification using Chalice score (Horizon Discovery). Average synergy scores are shown.

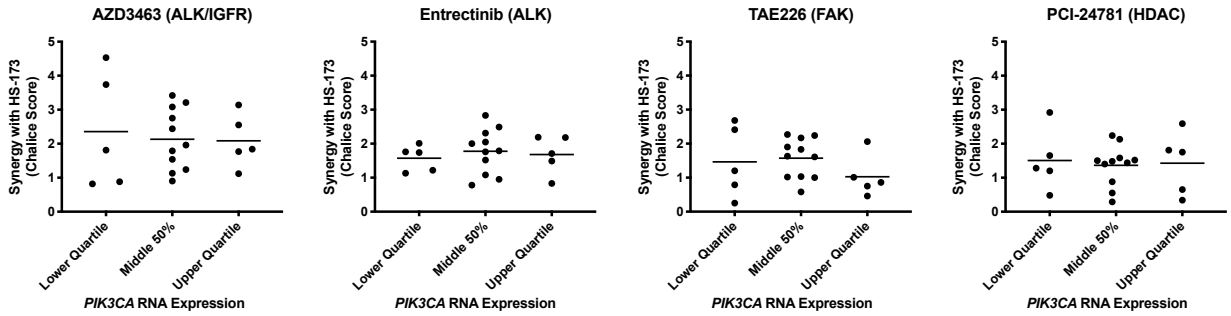


**Figure 5-7. *PIK3CA* gene expression level does not predict response to PI3K inhibitor treatment.**

HS-173 and AZD3463, entrectinib, TAE226, or PCI-24781 were administered to HNSCC cell lines and results were quantified using Chalice score (Horizon Discovery). RNA sequencing studies published elsewhere were used to separate cell lines into mRNA expression level subsets (23, 72).

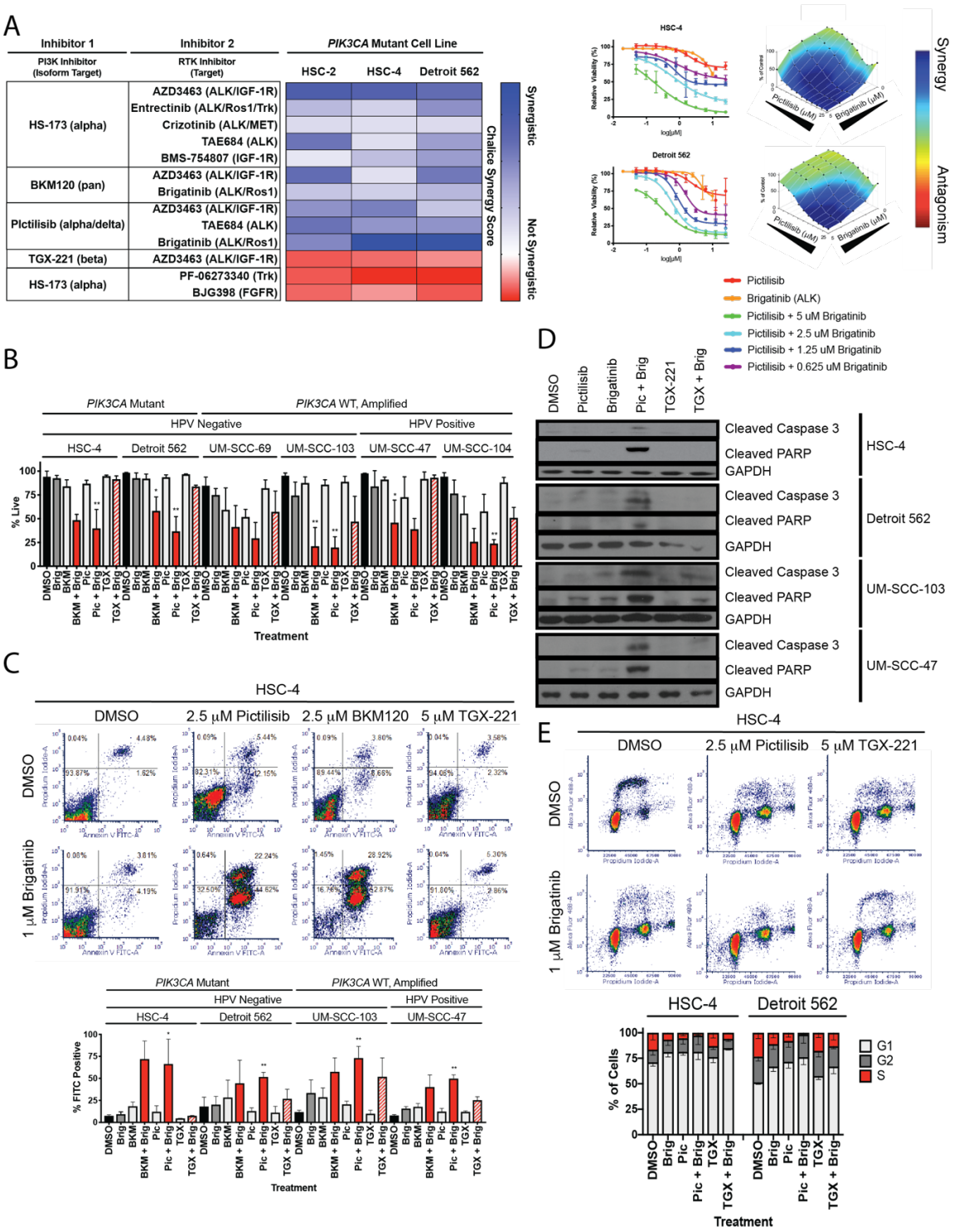


**Figure 5-8. Orthogonal assays confirm cell death, apoptosis, and cell cycle arrest following PI3K + ALK inhibitor dual-therapy.**

(A) HSC-2, HSC-4, and Detroit 562 cells were treated with increasing concentrations of PI3K inhibitors and/or RTK inhibitors as indicated in the table for 72 hours. Cell viability was measured using a resazurin cell viability assay as shown in representative images. Synergy of each combination was evaluated using Chalice score (Horizon Discovery). Each combination experiment was performed at least twice in all three cell lines, with average Chalice scores used to create a heat map. Representative concentration response curves for HSC-4 and Detroit 562 cells after treatment with PI3K inhibitor pictilisib and ALK inhibitor brigatinib are shown along with analysis using Combenefit software (33). (B) HNSCC cells were treated with vehicle (DMSO), PI3K alpha/delta-isoform inhibitor pictilisib (0.5 μM for UM-SCC-69 and UM-SCC-104, 1 μM for Detroit 562, UM-SCC-103, and UM-SCC-47, 2.5 μM for HSC-4), pan-PI3K inhibitor BKM120 (1 μM for Detroit 562, UM-SCC-69, UM-SCC-103, UM-SCC-47, and UM-SCC-104, 2.5 μM for HSC-4), PI3K beta-isoform inhibitor TGX-221 (5 μM), and/or ALK inhibitor brigatinib (0.25 μM for UM-SCC-69, 0.5 μM for UM-SCC-47 and UM-SCC-104, 0.75 μM for UM-SCC-103, 1 μM for HSC-4 and Detroit 562). Cell viability was measured using trypan blue dye exclusion assays after 72 hour treatment. Data shown are average +/- SD from at least three independent determinations. (C) FITC positivity was measured using annexin V apoptosis assays after 72 hour treatment with inhibitors at concentrations as above. Representative images for HSC-4 cells are shown along quantification (average +/- SD) from at least three independent determinations. (D) Cleaved caspase 3 and cleaved PARP were detected via western blot after 24 hour treatment with concentrations as above. GAPDH was used as a loading control. Experiments were performed at least twice, and representative images are shown. (E) *PIK3CA* mutant HNSCC cells were treated with inhibitor concentrations as above for 24 hours. EdU vs PI assays were used to assess cell cycle progression. Representative data for HSC-4 and quantification (average +/- SD) from at least three independent determinations are shown. For panels (B) and (C), statistics were performed using two-way ANOVA with Bonferroni correction to compare vehicle and monotherapy treatments to combination treatment. All p-values are reported in **Table 5-5** and **Table 5-6**, respectively. * indicates $p < 0.05$, and ** indicates $p < 0.01$.

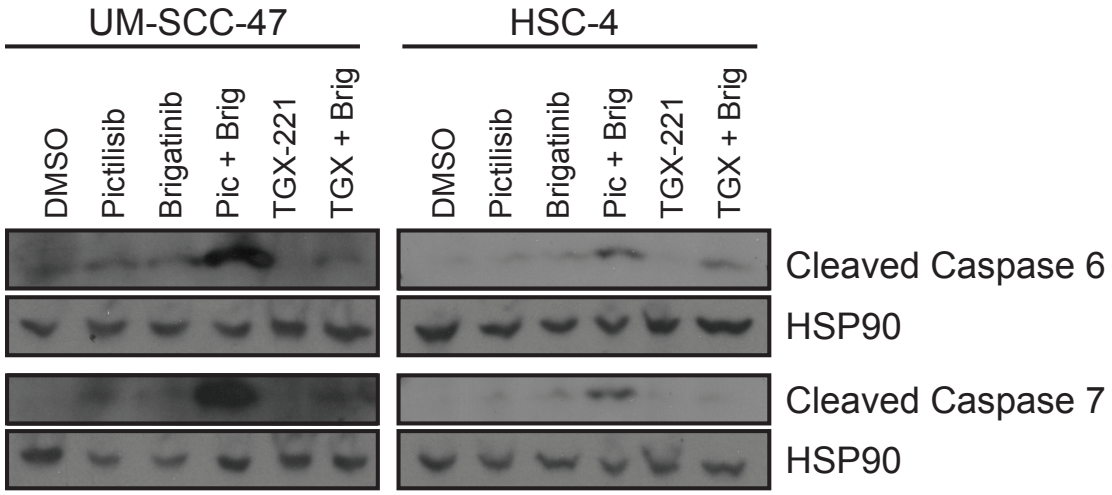


**Figure 5-9. Pictilisib and brigatinib co-treatment induce cleavage of Caspase 6 and Caspase 7 in UM-SCC-47 and HSC-4 cells.**

Cleaved caspase 6 and cleaved caspase 7 were detected via western blot after 24 hour treatment with vehicle (DMSO), PI3K alpha/delta-isoform inhibitor pictilisib (1 μM for UM-SCC-47, 2.5 μM for HSC-4), PI3K beta-isoform inhibitor TGX-221 (5 μM), and/or ALK inhibitor brigatinib (0.5 μM for UM-SCC-47, 1 μM for HSC-4). HSP90 was used as a loading control. Experiments were performed at least twice, and representative images are shown.

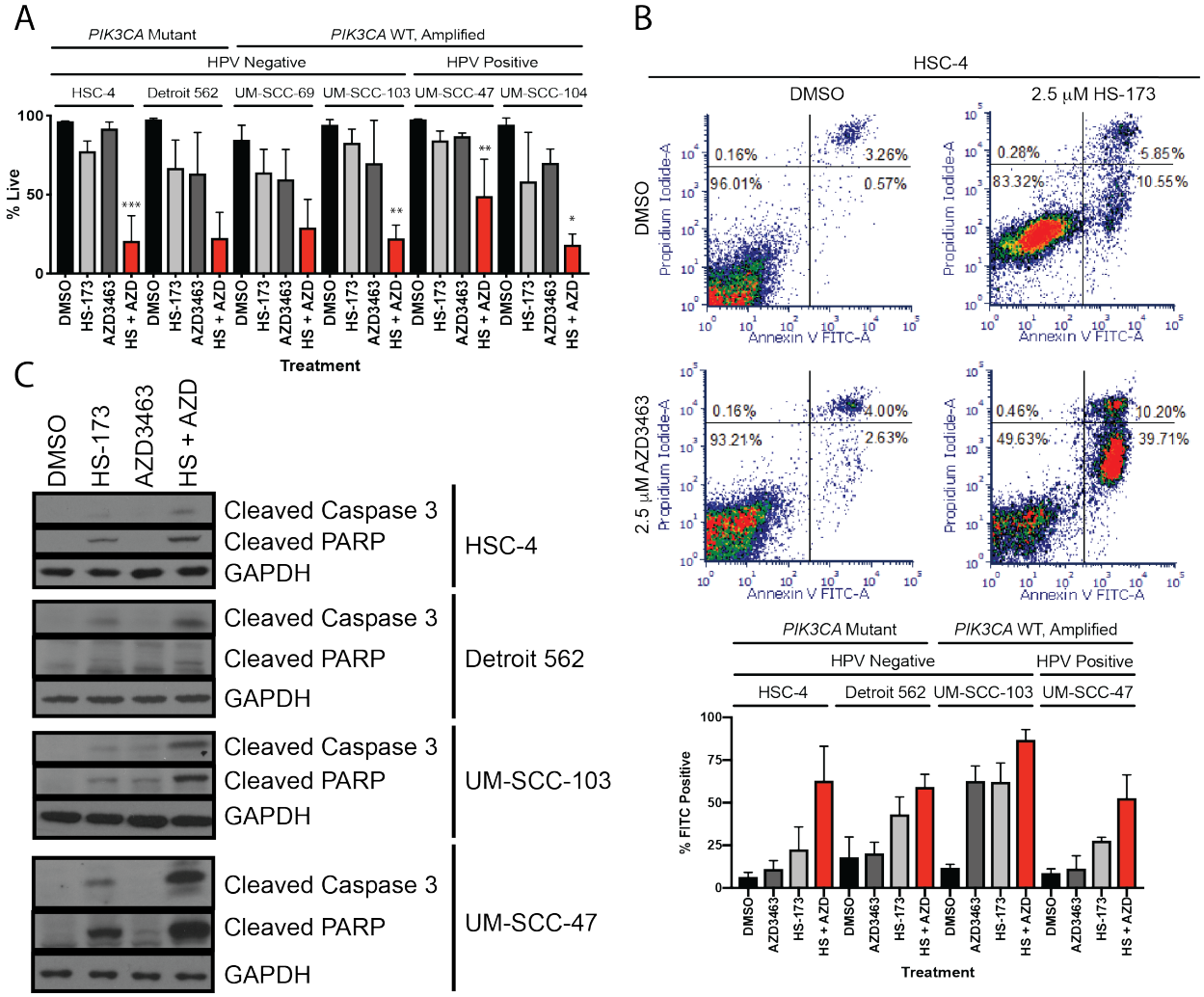


**Figure 5-10. PI3K inhibitor HS-173 and ALK/IGF-1R inhibitor AZD3463 recapitulate synergistic effects on cell death and apoptosis.**

(A) HNSCC cells were treated with vehicle (DMSO), PI3K alpha-isoform inhibitor HS-173 (0.5 μM for Detroit 562 and UM-SCC104, 1 μM for UM-SCC-69, UM-SCC-103, and UM-SCC-47, 2.5 μM for HSC-4), and/or ALK/IGF-1R inhibitor AZD3463 (0.5 μM for UM-SCC-69 and UM-SCC-47, 1 μM for UM-SCC-103 and UM-SCC-104, 2.5 μM for HSC-4 and Detroit 562). Cell viability was measured using trypan blue dye exclusion assays after 72 hour treatment. Data shown are average +/- SD from at least triplicate determinations as a result of no less than two independent experiments. (B) FITC positivity was measured using annexin V apoptosis assays after 72 hour treatment with inhibitors at concentrations as above. Representative images for HSC-4 cells are shown along quantification (average +/- SD) from at least three independent determinations. (C) Cleaved caspase 3 and cleaved PARP were detected via western blot after 24 hour treatment with concentrations as above. GAPDH was used as a loading control. Experiments were performed at least twice, and representative images are shown. For panels (A) and (B), statistics were performed using two-way ANOVA to compare vehicle and monotherapy treatments to combination treatment. * indicates $p < 0.05$, ** indicates $p < 0.01$, and *** indicates $p < 0.001$. All p-values are reported in **Table 5-7**.

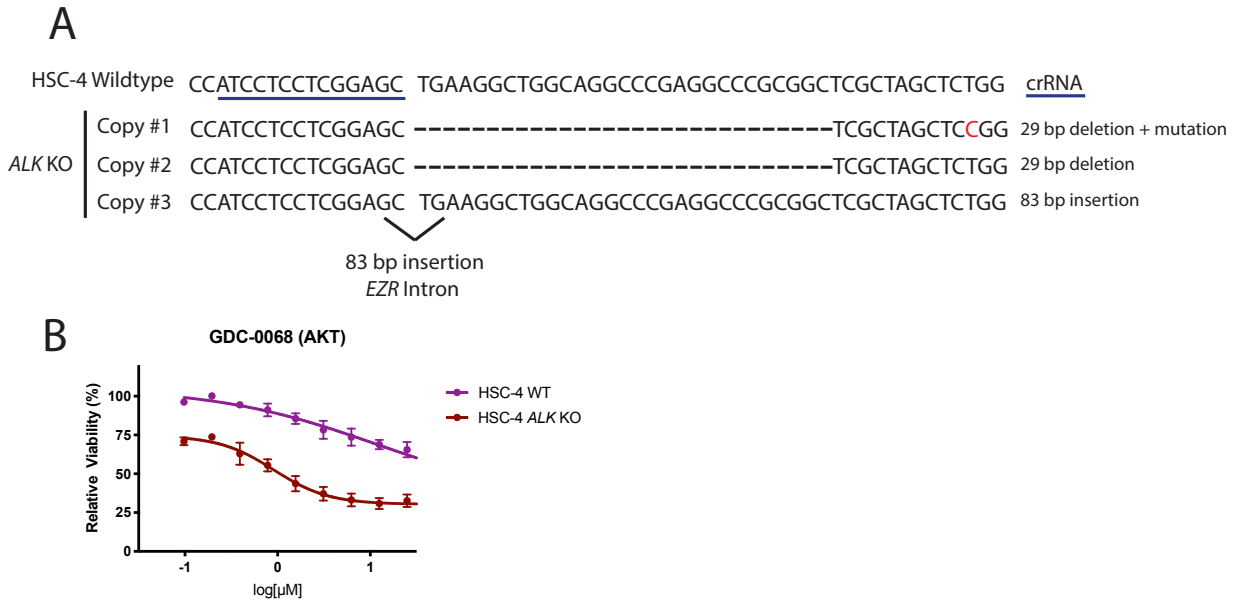


**Figure 5-11. HSC-4 *ALK* knockout cells are more responsive to AKT inhibitor GDC-0068 than HSC-4 wildtype cells.**

(A) Schematic of sanger sequencing results from HSC-4 *ALK* knockout cells, showing copies of *ALK* with 29 bp deletion with or without additional point mutation and a third copy with a 83 bp insertion of an intronic region of the *EZR* gene. (B) HSC-4 wildtype and *ALK* knockout cells were treated with increasing concentrations of GDC-0068 for 72 hours. Cell viability was measured using a resazurin cell viability assay. Experiments were repeated at least two times with similar results. Mean +/- SD for quadruplicate determinations from a single representative experiment are shown.

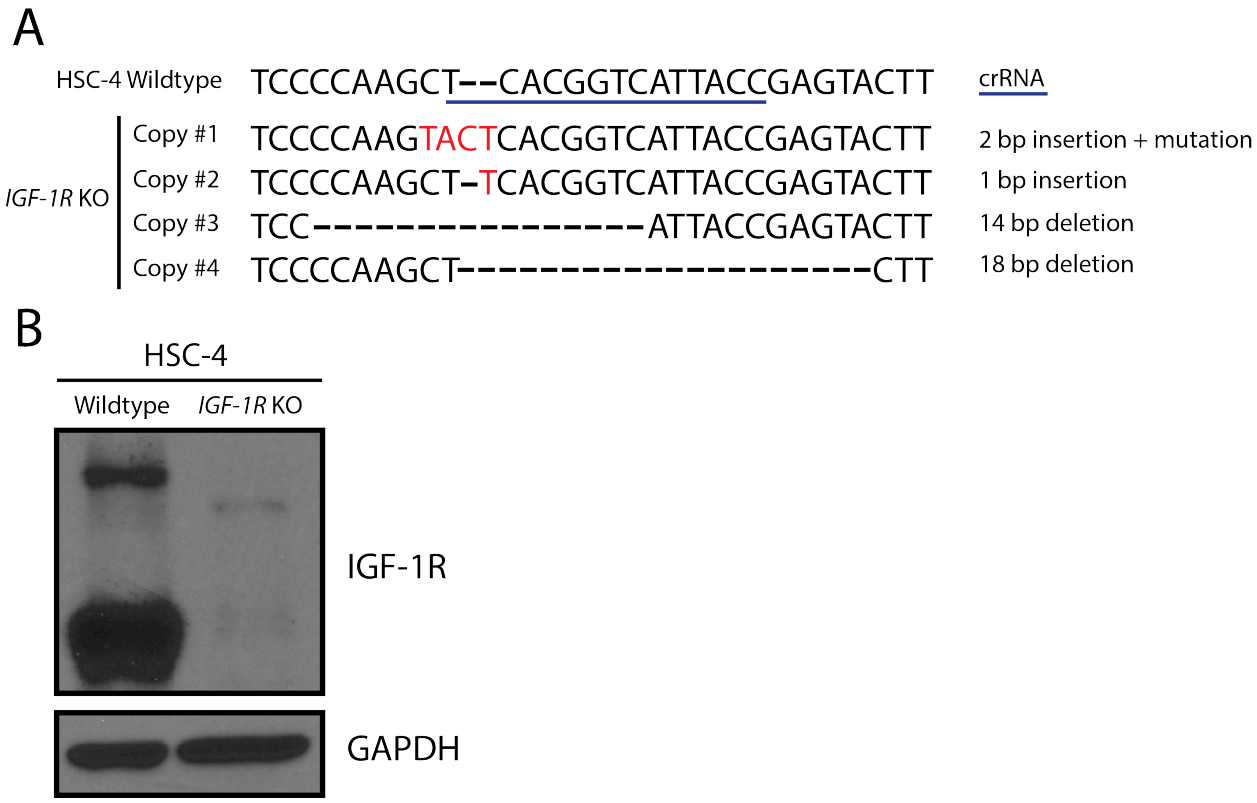


**Figure 5-12. Sanger sequencing and western blot analysis confirm *IGF-1R* knockout in HSC-4 cells.**

(A) Schematic of sanger sequencing results from HSC-4 *IGF-1R* knockout cells, showing one copy of *IGF-1R* with mutation and two bp deletion as well as three additional copies with unique deletions of 1, 14, and 18 bp. (B) Western blot analysis of HSC-4 wildtype and *IGF-1R* knockout cells shows lack of IGF-1R protein expression in *IGF-1R* knockout cells.

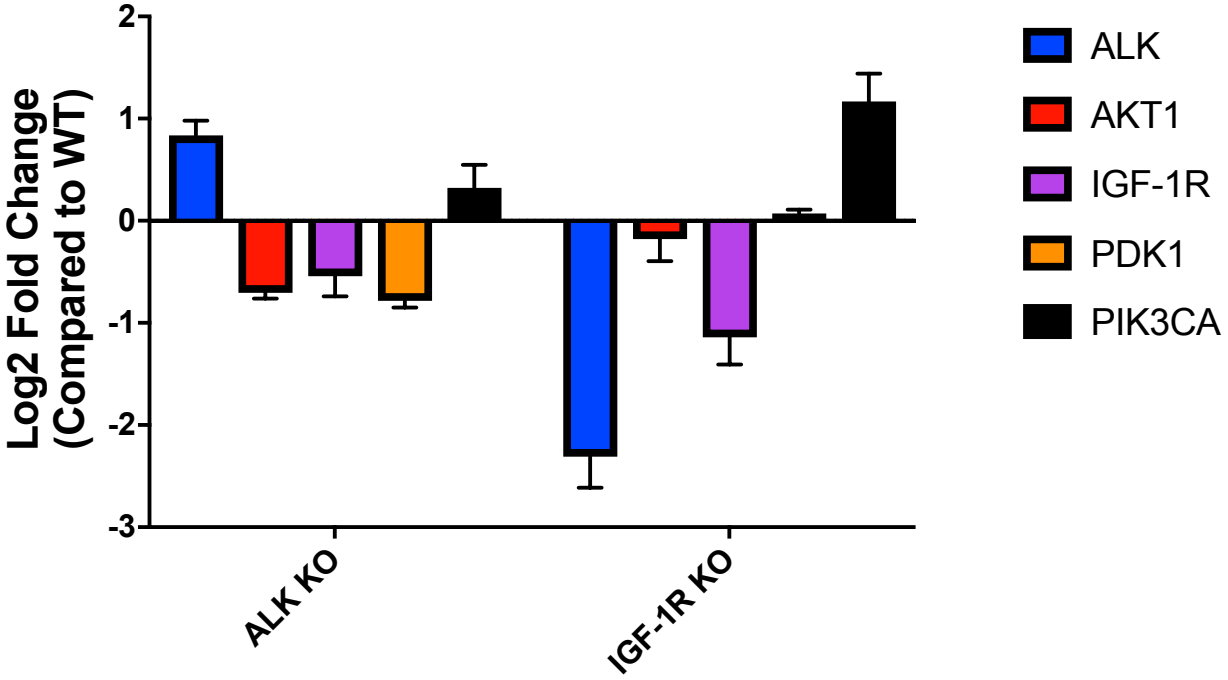


**Figure 5-13. Gene expression in HSC-4 wildtype and *ALK* or *IGF-1R* knockout cells.**

Log2 fold change in gene expression of *ALK*, *AKT1*, *IGF-1R*, *PDK1*, and *PIK3CA* in HSC-4 *ALK* or *IGF-1R* knockout cells as calculated using the ΔΔCt method compared to HSC-4 wildtype control cells.

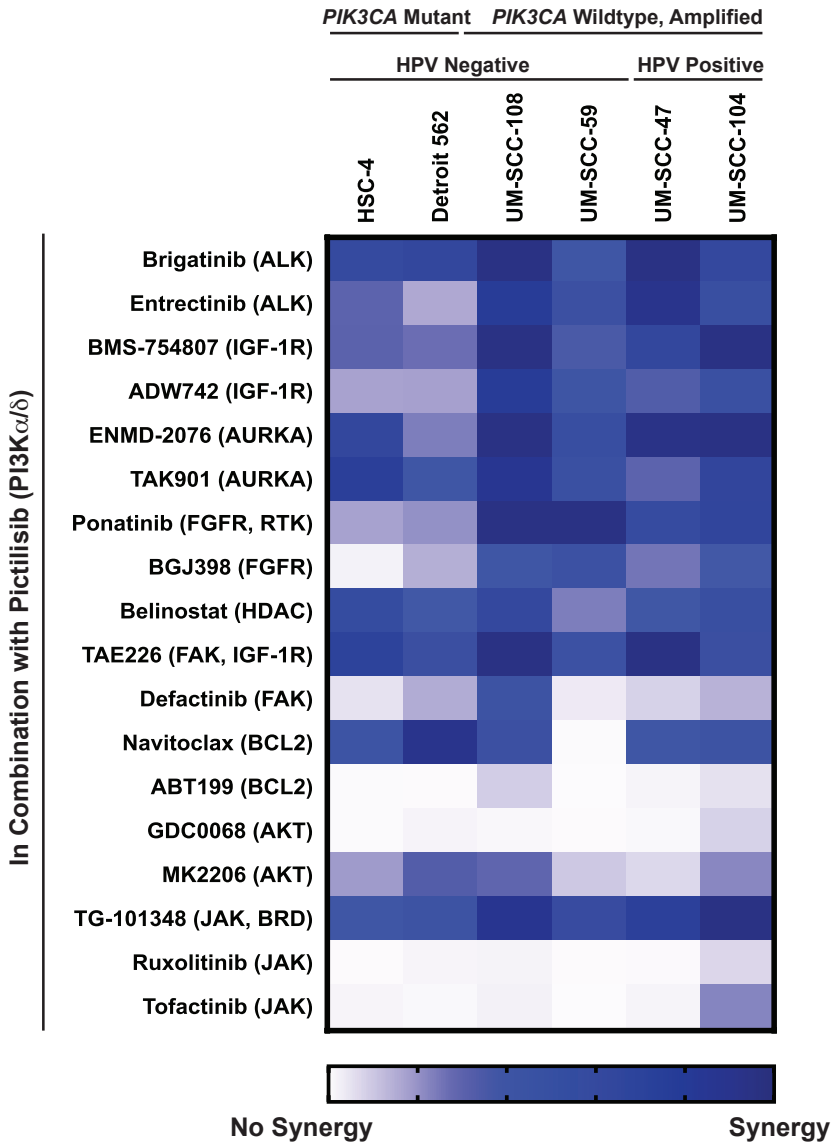


**Figure 5-14. HNSCC cell lines respond to PI3K inhibitor pictilisib in combination with inhibitors targeting ALK, IGF-1R, and other RTKs.**

HSC-4 cells were treated with increasing concentrations of PI3Kα/δ inhibitor pictilisib and/or indicated RTK inhibitors for 72 hours. Cell viability was measured using a resazurin cell viability assay. Responses were scored based on the Loewe synergy model.

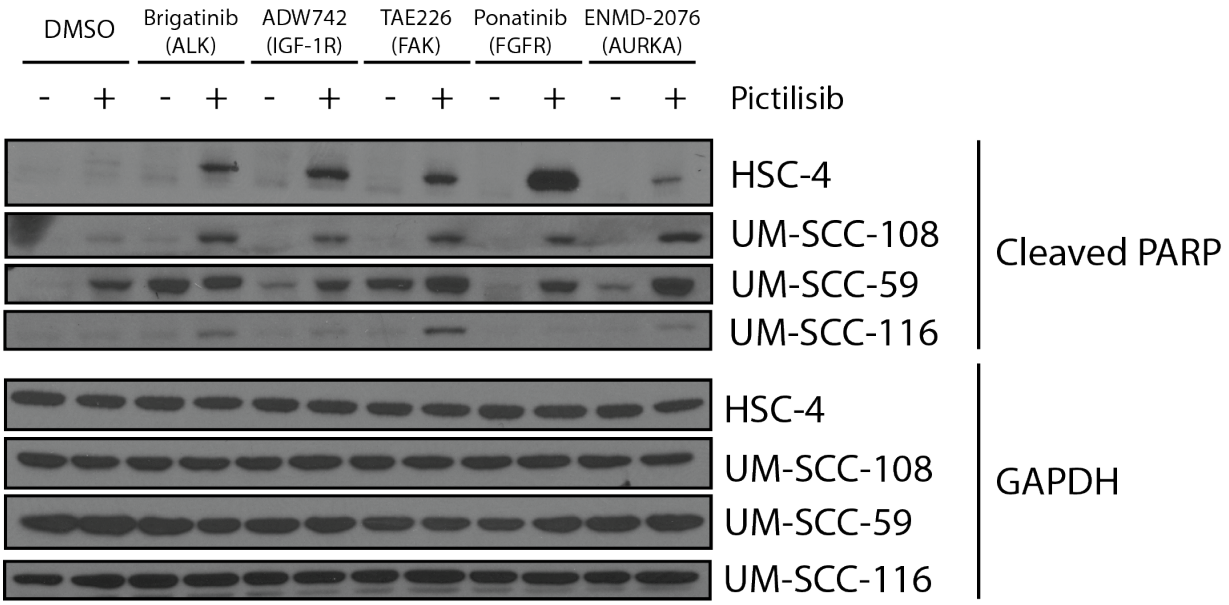


**Figure 5-15. RTK + PI3K inhibitor combinations induce PARP cleavage.**

HNSCC cells were treated for 24 hours with DMSO or PI3K inhibitor pictilisib (2.5 μM for HSC-4 and UM-SCC-59, 1 μM for all other cell lines) +/- brigatinib (0.5 μM for UM-SCC-108, 1 μM for all other cell lines), ADW742 (2.5 μM), TAE266 (1 μM for UM-SCC-108, 2.5 μM for all other cell lines), ponatinib (0.5 μM for UM-SCC-59, 1 μM for all other cell lines), or ENMD-2076 (1 μM for UM-SCC-59, 2.5 μM for all other cell lines). HSC-4 cells exhibit E545K *PIK3CA* mutation, while other cell lines (with the exception of UM-SCC-116 cells, which is *PIK3CA* wildtype and copy neutral) display at least one additional copy of wildtype *PIK3CA*. Experiments were performed at least twice for each cell line, and representative images are shown. GAPDH was used as a loading control.

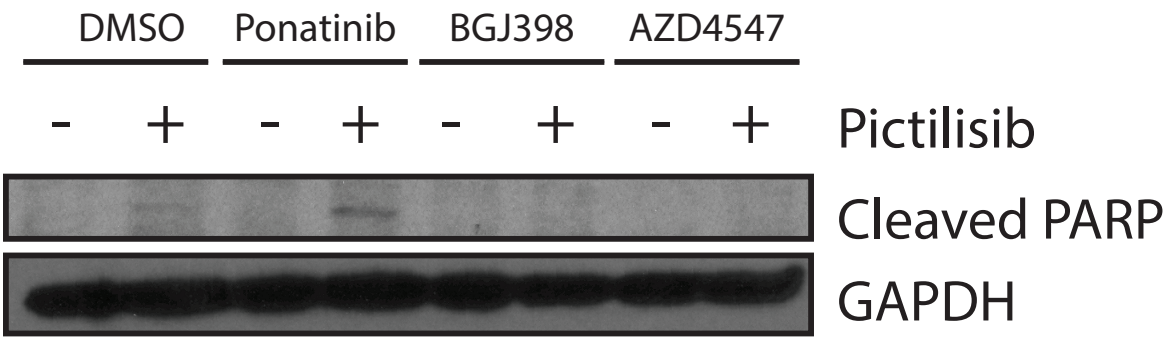


**Figure 5-16. PI3K inhibitor combination with ponatinib, but not other FGFR inhibitors, induces PARP Cleavage.**

HSC-4 cells were treated for 24 hours with DMSO or PI3K inhibitor pictilisib (2.5 μM) +/- ponatinib (1 μM), BGJ398 (5 μM), or AZD4547 (5 μM). GAPDH was used as a loading control.

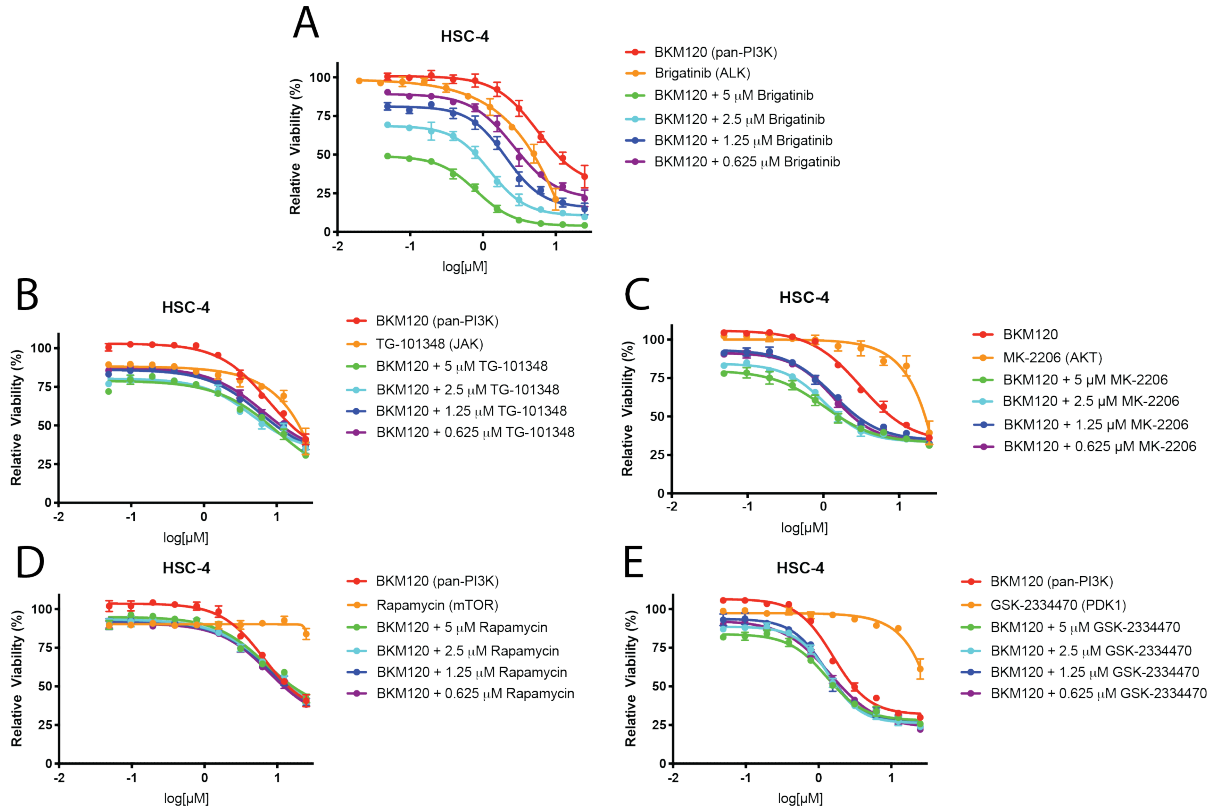


**Figure 5-17. Combinatory inhibition of PI3K and downstream effectors does not result in synergistic responses.**

HSC-4 cells were treated with increasing concentrations of pan-PI3K inhibitor BKM120 and/or ALK inhibitor brigatinib (A), JAK inhibitor TG-101348 (B), AKT inhibitor MK-2206 (C), mTOR inhibitor rapamycin (D), or PDK1 inhibitor GSK-22334470 (E) for 72 hours. Cell viability was measured using a resazurin cell viability assay. Each point is the mean and s.d. of quadruplicate determinations from a single experiment. Each experiment was repeated independently at least two times with similar combination effects; representative data is shown.

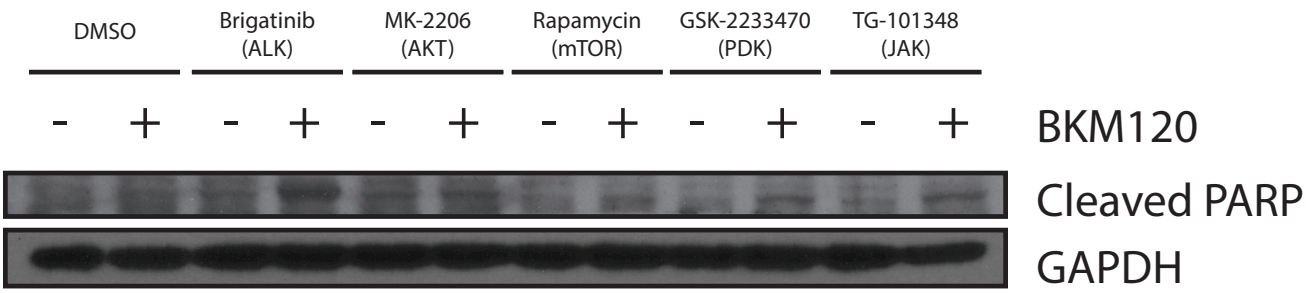


**Figure 5-18. PI3K inhibitor combinations targeting downstream effectors do not induce apoptosis.**

HSC-4 cells were treated for 24 hours with DMSO or PI3K inhibitor BKM120 (1 μM) +/- brigatinib (1 μM), MK-2206 (5 μM), rapamycin (5 μM), GSK-2233470 (5 μM), or TG-101348 (2.5 μM). GAPDH was used as a loading control.

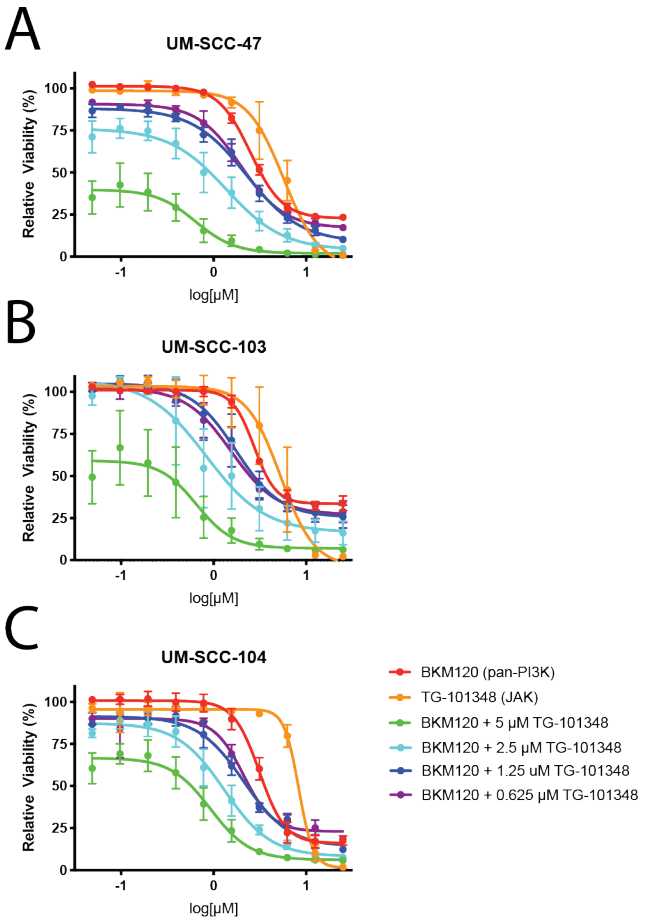


**Figure 5-19. PI3K inhibitor BKM120 and JAK inhibitor TG-101348 are synergistic in a subset of HNSCC cell lines.**

UM-SCC-47 (A), UM-SCC-103 (B), and UM-SCC-104 (C) cells were treated with increasing concentrations of pan-PI3K inhibitor BKM120 and/or JAK inhibitor TG-101348 for 72 hours. Cell viability was measured using a resazurin cell viability assay. Each point is the mean and s.d. of quadruplicate determinations from a single experiment. Each experiment was repeated independently at least two times with similar combination effects; representative data is shown.

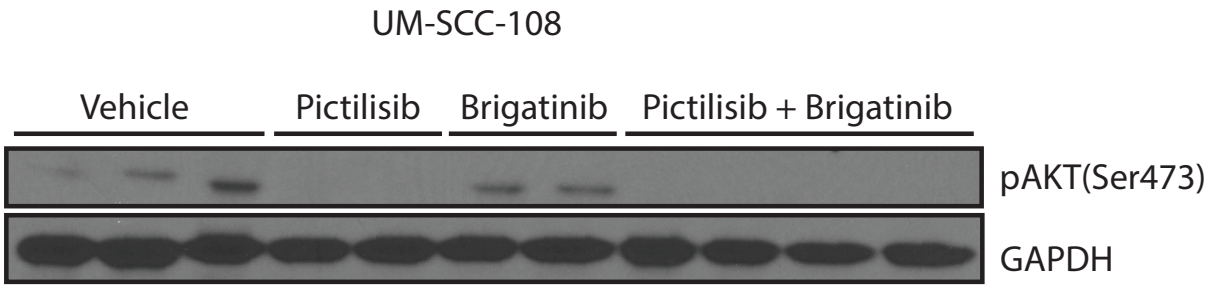


**Figure 5-20. Pictilisib treatment reduces AKT phosphorylation *in vivo*.**

Athymic nude mice bearing UM-SCC-108 xenografts were treated with vehicle, pictilisib (100 mg/kg), brigatinib (50 mg/kg), or combination for 1 hour, then euthanized. Tumors were harvested and lysed, followed by western blot analysis of indicated proteins. GAPDH was used as a loading control.

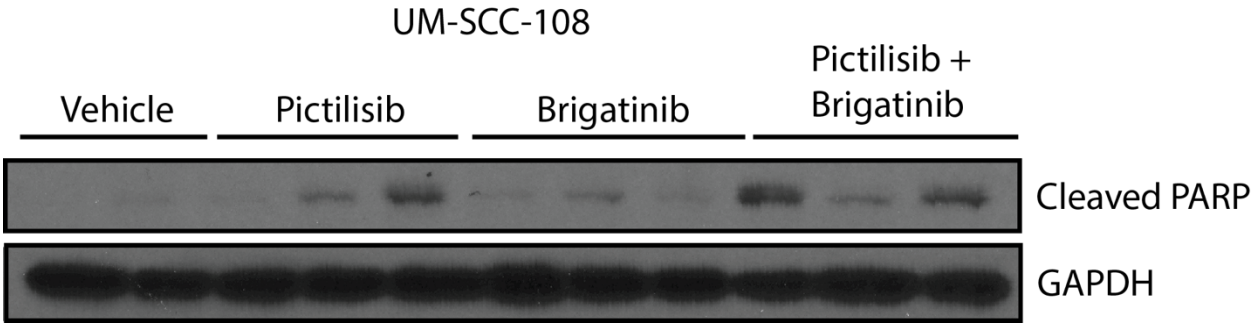


**Figure 5-21. Pictilisib induces apoptosis *in vivo*.**

Athymic nude mice bearing UM-SCC-108 xenografts were treated with vehicle, pictilisib (100 mg/kg), brigatinib (50 mg/kg), or a combination of pictilisib and brigatinib for 6 hours, then euthanized. Tumors were harvested and lysed, followed by western blot analysis of indicated proteins. GAPDH was used as a loading control.

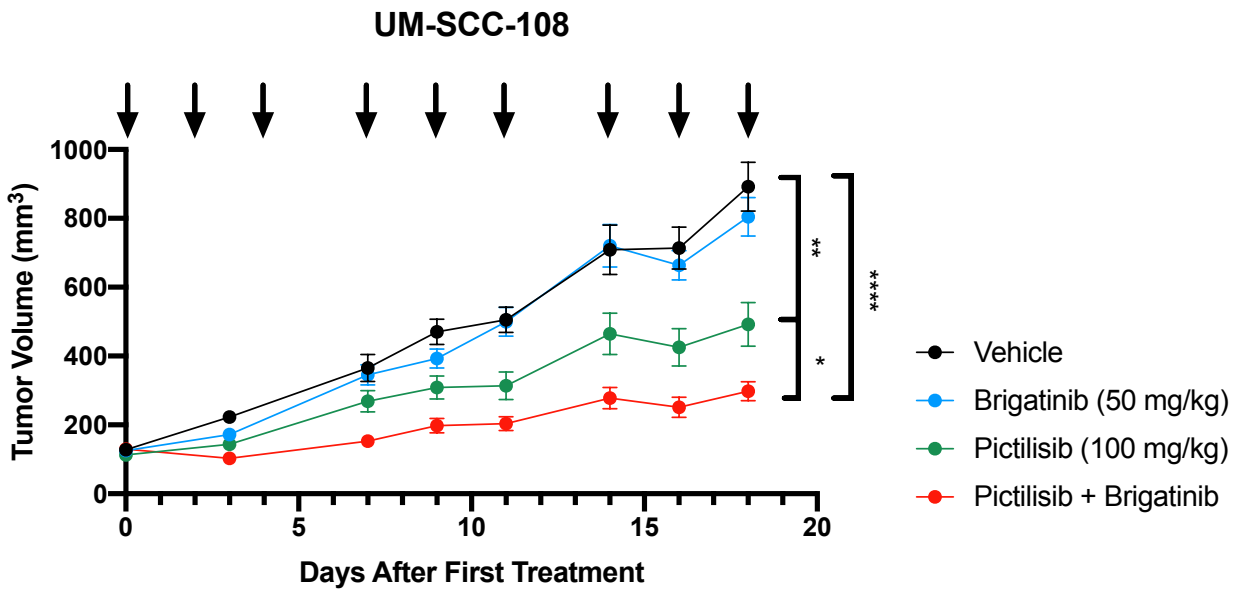


**Figure 5-22. UM-SCC-108 xenografts respond synergistically to combination treatment with pictilisib and brigatinib.**

UM-SCC-108 cells (2 million cells/tumor) were injected bilaterally into the flanks of athymic nude mice. One week later, mice began treatment with vehicle, pictilisib (100 mg/kg), brigatinib (50 mg/kg), or combination via oral gavage 3 times per week. Treatment continued for 3 weeks. The average and SEM for tumor volume (n=20-26 tumors per group) are shown. Statistics were performed using the average tumor volume for each mouse and unpaired t-tests. * indicates $p < 0.05$, ** inidicates $p < 0.01$, and *** indicates $p < 0.001$.

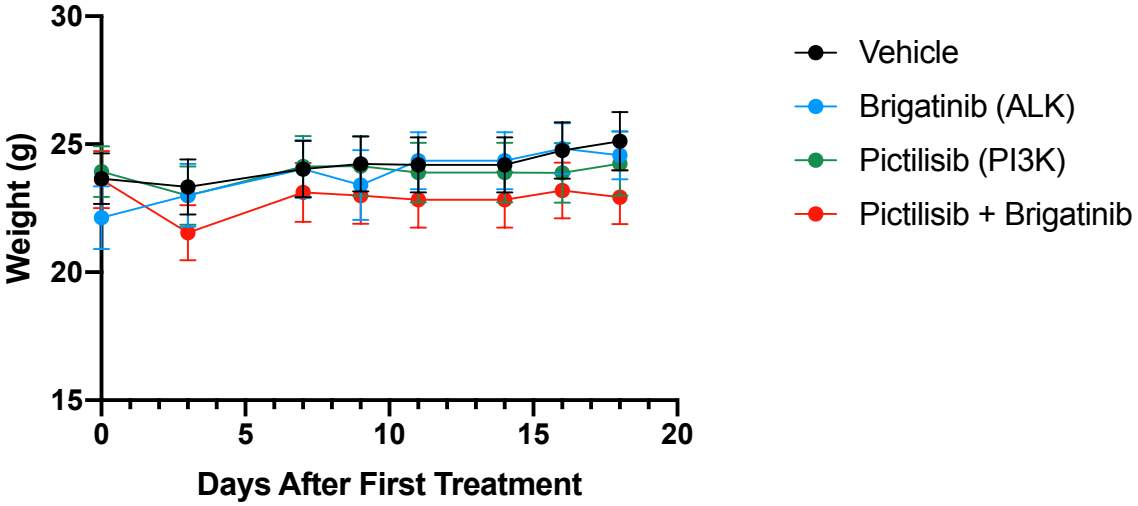


**Figure 5-23. Mice bearing UM-SCC-108 xenografts maintained weight during treatment.**

UM-SCC-108 cells (2 million cells/tumor) were injected bilaterally into the flanks of athymic nude mice. One week later, mice began treatment with vehicle, pictilisib (100 mg/kg), brigatinib (50 mg/kg), or combination via oral gavage 3 times per week. Treatment continued for 3 weeks. The average and SD of the weights for mice in each treatment group (n = 10-13) are shown.

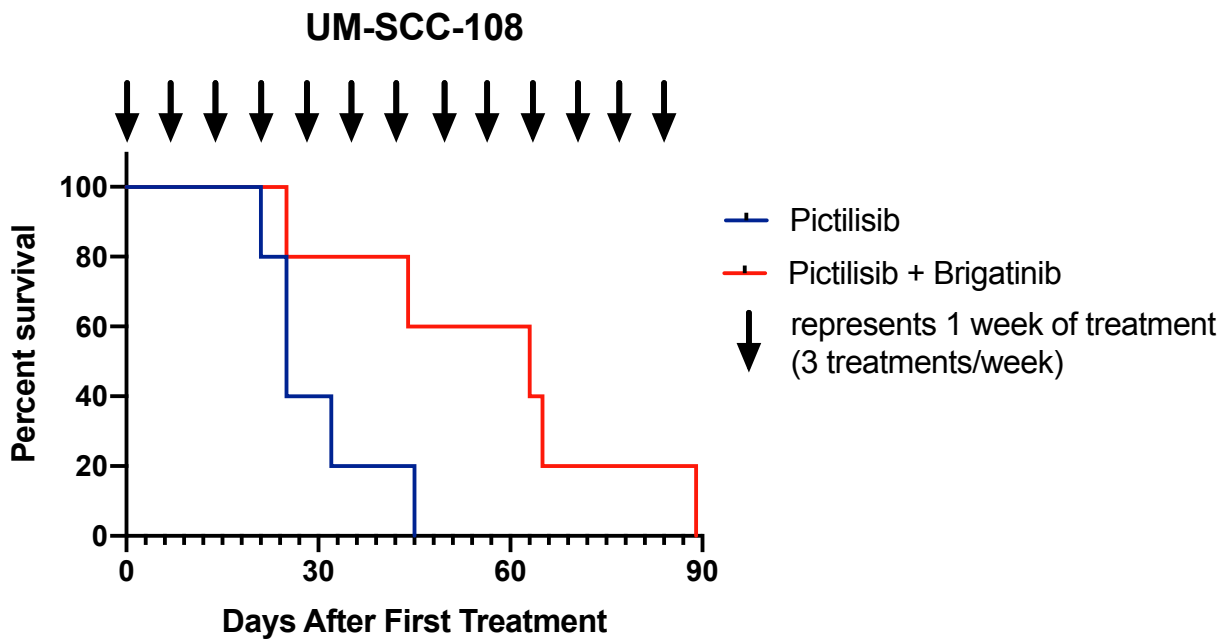


**Figure 5-24. Combination treatment with pictilisib and brigatinib extends time to tumor endpoint in UM-SCC-108 xenografts.**

UM-SCC-108 cells (2 million cells/tumor) were injected bilaterally into the flanks of athymic nude mice. One week later, mice began treatment with pictilisib (100 mg/kg) or pitilisib and brigatinib (50 mg/kg) via oral gavage 3 times per week. Treatment continued until mice reached their tumor endpoint (20% loss of body weight, tumor volume > 3000 $mm^3$, or ulceration greater than half the surface area of the tumor), after which point mice were humanely euthanized.

## Tables

**Table 5-1. PI3K inhibitor concentrations for small molecule profiling.**

| Cell Line | HS-173 Concentration (μM) | BKM120 Concentration (μM) |
|---|---|---|
| UM-SCC-49 | 0.25 | 0.25 |
| UM-SCC-108 | 0.25 | 0.25 |
| UM-SCC-55 | 0.25 | 0.25 |
| UM-SCC-59 | 0.25 | 0.25 |
| UM-SCC-43 | 0.25 | 0.25 |
| HSC-4 | 0.25 | 0.25 |
| Detroit 562 | 1 | 1.5 |
| HSC-2 | 0.5 | 0.5 |
| UM-SCC-104 | 0.25 | 0.25 |
| UM-SCC-69 | 0.25 | 0.25 |

**Table 5-2. Primary antibodies for western blot analysis.**

| Target | Supplier | Cat. No. | Dilution |
|---|---|---|---|
| IGF-1R | Cell Signaling Technology | 9750 | 1:1000 |
| pAKT (Ser473) | Cell Signaling Technology | 4060 | 1:1000 |
| Cleaved Caspase 3 | Cell Signaling Technology | 9664 | 1:500 |
| Cleaved Caspase 6 | Cell Signaling Technology | 9761 | 1:500 |
| Cleaved Caspase 7 | Cell Signaling Technology | 8438 | 1:500 |
| Cleaved PARP | Cell Signaling Technology | 5625 | 1:500 |
| GAPDH | Cell Signaling Technology | 5174 | 1:2000 |

**Table 5-3. qPCR primer sequences.**

| Primer | Sequence |
|---|---|
| AKT1 | F: 5'-TCACGTTGGTCCACATCCTG-3'<br>R: 5'-GCACAAACGAGGGGAGTACA-3' |
| PIK3CA | F: 5'-AGAGCCCCGAGCGTTTCTG-3'<br>R: 5'-CATCAAGTGGATGCCCAACA-3' |
| ALK | F:5'-GAATACTGCACCCAGGACCC-3'<br>R:5'-GCCTCACAGGCACTTTCTCT-3' |
| IGF-1R | F: 5'-GCCGACGAGTGGAGAAATCTG-3'<br>R: 5'-TGGAGGTAGCCCTCGATCAC-3' |
| PDK1 | F: 5'-CTGTGATACGGATCAGAAACCG-3'<br>R: 5'-TCCACCAAACAATAAAGAGTGCT-3' |
| β-actin | F: 5'-AAGTGTGACGTGGACATCCG-3'<br>R: 5'-GATGTGACAGCTCCCCACAC-3' |
| HPRT | F: 5'-AGATGGTCAAGGTCGCAAGC-3'<br>R: 5'-ATGACACAAACATGATTCAAATCCC-3' |
| RPL19 | F: 5'-CCGCTTACCTATGCCCATGT-3'<br>R: 5'-AAATCGCCAATGCCAACTCC-3' |

**Table 5-4. Kinase library knockout screen identifies genes significantly depleted after PI3K inhibitor treatment.**

UM-SCC-108 cells transduced with the Human Kinase CRISPR Knockout Library were treated with 0.25 mM HS-173 or 0.5 mM BKM120 for 14 days. DNA was harvested and sequencing was performed. The MAGeCK algorithm (34) was used to identify genes that were significantly depleted compared to vehicle-treated controls (p-value < 0.05), which are highlighted in yellow. Note that guide RNAs targeting *FAK* and *AURKA* were not included in the library.

| Gene | BKM120 p-value | HS-173 p-value |
|---|---|---|
| *IGF-1R* | 0.0027 | 0.1872 |
| *ALK* | 0.1834 | 0.0144 |
| *EGFR* | 0.0911 | 0.2276 |
| *ERBB2* | 0.6216 | 0.0158 |
| *ERBB3* | 0.9272 | 0.0020 |
| *ERBB4* | 0.5186 | 0.3459 |
| *AXL* | 0.1210 | 0.0170 |
| *AURKB* | 0.1267 | 0.4239 |
| *AURKC* | 0.1629 | 0.2633 |
| *AKT1* | 0.1264 | 0.0947 |
| *AKT2* | 0.3303 | 0.0033 |
| *AKT3* | 0.0255 | 0.3707 |
| *PDK1* | 0.0895 | 0.2056 |
| *MTOR* | 0.0338 | 0.0605 |
| *JAK1* | 0.1435 | 0.3878 |
| *JAK2* | 0.0243 | 0.9897 |
| *JAK3* | 0.0565 | 0.4200 |
| *FGFR1* | 0.9566 | 0.6241 |
| *FGFR2* | 0.1226 | 0.0135 |
| *FGFR3* | 0.9490 | 0.1247 |
| *CDK4* | 0.0868 | 0.1082 |
| *CDK6* | 0.1208 | 0.7335 |

**Table 5-5. Statistical analysis for trypan blue dye exclusion assays testing BKM120, pictilisib, and TGX-221 in combination with brigatinib.**

Two-way ANOVAs were performed in R to compare the natural logarithm of the percentage of living cells following vehicle, PI3K inhibitor monotherapy, brigatinib monotherapy, or combination treatment. Bonferroni correction was used to adjust p-values. Significant results (ANOVA adjusted p-value < 0.05) are highlighted in red.

| Cell Line | Drug combination | ANOVA p-value | ANOVA adjusted p-value |
|---|---|---|---|
| HSC-4 | BKM + Brig | 5.70E-06 | 1.71E-05 |
| HSC-4 | Pic + Brig | 5.60E-04 | 1.69E-03 |
| HSC-4 | TGX + Brig | 7.60E-01 | 1.00E+00 |
| Detroit 562 | BKM + Brig | 5.64E-03 | 1.69E-02 |
| Detroit 562 | Pic + Brig | 1.43E-03 | 4.28E-03 |
| Detroit 562 | TGX + Brig | 9.61E-02 | 2.88E-01 |
| UM-SCC-69 | BKM + Brig | 2.86E-01 | 8.57E-01 |
| UM-SCC-69 | Pic + Brig | 1.93E-02 | 5.81E-02 |
| UM-SCC-69 | TGX + Brig | 1.06E-01 | 3.19E-01 |
| UM-SCC-103 | BKM + Brig | 2.00E-04 | 6.00E-04 |
| UM-SCC-103 | Pic + Brig | 5.77E+00 | 1.73E-05 |
| UM-SCC-103 | TGX + Brig | 1.11E-01 | 3.32E-01 |
| UM-SCC-47 | BKM + Brig | 1.30E-02 | 3.92E-02 |
| UM-SCC-47 | Pic + Brig | 4.64E-02 | 1.39E-01 |
| UM-SCC-47 | TGX + Brig | 3.15E-01 | 9.44E-01 |
| UM-SCC-104 | BKM + Brig | 1.75E-02 | 8.26E-02 |
| UM-SCC-104 | Pic + Brig | 3.07E-03 | 9.21E-03 |
| UM-SCC-104 | TGX + Brig | 2.83E-02 | 8.50E-02 |

**Table 5-6. Statistical analysis for annexin V apoptosis assays testing BKM120, pictilisib, and TGX-221 in combination with brigatinib.**

Two-way ANOVAs were performed in R to compare the natural logarithm of the percentage of living cells following vehicle, PI3K inhibitor monotherapy, brigatinib monotherapy, or combination treatment. Bonferroni correction was used to adjust p-values. Significant results (ANOVA adjusted p-value < 0.05) are highlighted in red.

| Cell line | Drug combination | ANOVA p-value | ANOVA adjusted p-value |
|---|---|---|---|
| HSC-4 | BKM + Brig | 2.83E-02 | 8.49E-02 |
| HSC-4 | Pic + Brig | 1.59E-02 | 4.76E-02 |
| HSC-4 | TGX + Brig | 6.83E-01 | 1.00E+00 |
| Detroit 562 | BKM + Brig | 3.49E-01 | 1.00E+00 |
| Detroit 562 | Pic + Brig | 8.34E-04 | 2.50E-03 |
| Detroit 562 | TGX + Brig | 2.90E-01 | 8.70E-01 |
| UM-SCC-103 | BKM + Brig | 2.30E-01 | 6.89E-01 |
| UM-SCC-103 | Pic + Brig | 3.07E-03 | 9.21E-03 |
| UM-SCC-103 | TGX + Brig | 1.80E-01 | 5.40E-01 |
| UM-SCC-47 | BKM + Brig | 9.74E-02 | 2.92E-01 |
| UM-SCC-47 | Pic + Brig | 3.70E-05 | 1.11E-04 |
| UM-SCC-47 | TGX + Brig | 6.59E-02 | 1.98E-01 |

**Table 5-7. Statistical analysis for annexin V apoptosis and trypan blue dye exclusion assays testing HS-173 in combination with AZD3463.**

Two-way ANOVAs were performed in R to compare the natural logarithm of the percentage of living cells following vehicle, HS-173 monotherapy, AZD3463 monotherapy, or combination treatment. Bonferroni correction was used to adjust p-values. Significant results (ANOVA adjusted p-value < 0.05) are highlighted in red.

| Cell Line | Annexin V p-value | Trypan Blue p-value |
|---|---|---|
| HSC-4 | 8.91E-02 | 6.86E-04 |
| Detroit 562 | 1.29E-01 | 9.03E-02 |
| UM-SCC-69 | N/A | 5.17E-02 |
| UM-SCC-103 | 5.37E-01 | 1.52E-03 |
| UM-SCC-47 | 6.32E-02 | 2.74E-03 |
| UM-SCC-104 | N/A | 1.57E-02 |

## References

1. Garnett MJ, Edelman EJ, Heidorn SJ, Greenman CD, Dastur A, Lau KW, Greninger P, Thompson IR, Luo X, Soares J, Liu Q, Iorio F, Surdez D, Chen L, Milano RJ, Bignell GR, Tam AT, Davies H, Stevenson JA, Barthorpe S, Lutz SR, Kogera F, Lawrence K, McLaren-Douglas A, Mitropoulos X, Mironenko T, Thi H, Richardson L, Zhou W, Jewitt F, Zhang T, O'Brien P, Boisvert JL, Price S, Hur W, Yang W, Deng X, Butler A, Choi HG, Chang JW, Baselga J, Stamenkovic I, Engelman JA, Sharma SV, Delattre O, Saez-Rodriguez J, Gray NS, Settleman J, Futreal PA, Haber DA, Stratton MR, Ramaswamy S, McDermott U, Benes CH. Systematic identification of genomic markers of drug sensitivity in cancer cells. Nature. 2012;483(7391):570-5. Epub 2012/03/31. doi: 10.1038/nature11005. PubMed PMID: 22460902; PMCID: Pmc3349233.

2. Barretina J, Caponigro G, Stransky N, Venkatesan K, Margolin AA, Kim S, Wilson CJ, Lehar J, Kryukov GV, Sonkin D, Reddy A, Liu M, Murray L, Berger MF, Monahan JE, Morais P, Meltzer J, Korejwa A, Jane-Valbuena J, Mapa FA, Thibault J, Bric-Furlong E, Raman P, Shipway A, Engels IH, Cheng J, Yu GK, Yu J, Aspesi P, Jr., de Silva M, Jagtap K, Jones MD, Wang L, Hatton C, Palescandolo E, Gupta S, Mahan S, Sougnez C, Onofrio RC, Liefeld T, MacConaill L, Winckler W, Reich M, Li N, Mesirov JP, Gabriel SB, Getz G, Ardlie K, Chan V, Myer VE, Weber BL, Porter J, Warmuth M, Finan P, Harris JL, Meyerson M, Golub TR, Morrissey MP, Sellers WR, Schlegel R, Garraway LA. The Cancer Cell Line Encyclopedia enables predictive modelling of anticancer drug sensitivity. Nature. 2012;483(7391):603-7. Epub 2012/03/31. doi: 10.1038/nature11003. PubMed PMID: 22460905; PMCID: Pmc3320027.

3. Basu A, Bodycombe NE, Cheah JH, Price EV, Liu K, Schaefer GI, Ebright RY, Stewart ML, Ito D, Wang S, Bracha AL, Liefeld T, Wawer M, Gilbert JC, Wilson AJ, Stransky N, Kryukov GV, Dancik V, Barretina J, Garraway LA, Hon CS, Munoz B, Bittker JA, Stockwell BR, Khabele D, Stern AM, Clemons PA, Shamji AF, Schreiber SL. An interactive resource to identify cancer genetic and lineage dependencies targeted by small molecules. Cell. 2013;154(5):1151-61. Epub 2013/09/03. doi: 10.1016/j.cell.2013.08.003. PubMed PMID: 23993102; PMCID: PMC3954635.

4. Yang W, Soares J, Greninger P, Edelman EJ, Lightfoot H, Forbes S, Bindal N, Beare D, Smith JA, Thompson IR, Ramaswamy S, Futreal PA, Haber DA, Stratton MR, Benes C, McDermott U, Garnett MJ. Genomics of Drug Sensitivity in Cancer (GDSC): a resource for therapeutic biomarker discovery in cancer cells. Nucleic acids research. 2013;41(Database issue):D955-61. Epub 2012/11/28. doi: 10.1093/nar/gks1111. PubMed PMID: 23180760; PMCID: PMC3531057.

5. Seashore-Ludlow B, Rees MG, Cheah JH, Cokol M, Price EV, Coletti ME, Jones V, Bodycombe NE, Soule CK, Gould J, Alexander B, Li A, Montgomery P, Wawer MJ, Kuru N, Kotz JD, Hon CS, Munoz B, Liefeld T, Dancik V, Bittker JA, Palmer M, Bradner JE, Shamji AF, Clemons PA, Schreiber SL. Harnessing Connectivity in a Large-Scale Small-Molecule Sensitivity Dataset. Cancer discovery. 2015;5(11):1210-23. Epub 2015/10/21. doi: 10.1158/2159-8290.Cd-15-0235. PubMed PMID: 26482930; PMCID: PMC4631646.

6. Lindsley CW, Zhao Z, Leister WH, Robinson RG, Barnett SF, Defeo-Jones D, Jones RE, Hartman GD, Huff JR, Huber HE, Duggan ME. Allosteric Akt (PKB) inhibitors: discovery and SAR of isozyme selective inhibitors. Bioorganic & medicinal chemistry letters. 2005;15(3):761-4. Epub 2005/01/25. doi: 10.1016/j.bmcl.2004.11.011. PubMed PMID: 15664853.

7. Dudgeon DD, Shinde SN, Shun TY, Lazo JS, Strock CJ, Giuliano KA, Taylor DL, Johnston PA, Johnston PA. Characterization and optimization of a novel protein-protein interaction biosensor high-content screening assay to identify disruptors of the interactions between p53 and hDM2. Assay and drug development technologies. 2010;8(4):437-58. Epub 2010/07/29. doi: 10.1089/adt.2010.0281. PubMed PMID: 20662736; PMCID: PMC2929144.

8. Kamangar F, Dores GM, Anderson WF. Patterns of cancer incidence, mortality, and prevalence across five continents: defining priorities to reduce cancer disparities in different geographic regions of the world. Journal of clinical oncology : official journal of the American Society of Clinical Oncology. 2006;24(14):2137-50. Epub 2006/05/10. doi: 10.1200/jco.2005.05.2308. PubMed PMID: 16682732.

9. Cramer JD, Burtness B, Le QT, Ferris RL. The changing therapeutic landscape of head and neck cancer. Nature reviews Clinical oncology. 2019. Epub 2019/06/14. doi: 10.1038/s41571-019-0227-z. PubMed PMID: 31189965.

10. Bray F, Ferlay J, Soerjomataram I, Siegel RL, Torre LA, Jemal A. Global cancer statistics 2018: GLOBOCAN estimates of incidence and mortality worldwide for 36 cancers in 185 countries. CA: a cancer journal for clinicians. 2018;68(6):394-424. Epub 2018/09/13. doi: 10.3322/caac.21492. PubMed PMID: 30207593.

11. Bonner JA, Harari PM, Giralt J, Azarnia N, Shin DM, Cohen RB, Jones CU, Sur R, Raben D, Jassem J, Ove R, Kies MS, Baselga J, Youssoufian H, Amellal N, Rowinsky EK, Ang KK. Radiotherapy plus cetuximab for squamous-cell carcinoma of the head and neck. The New England journal of medicine. 2006;354(6):567-78. Epub 2006/02/10. doi: 10.1056/NEJMoa053422. PubMed PMID: 16467544.

12. Vermorken JB, Mesia R, Rivera F, Remenar E, Kawecki A, Rottey S, Erfan J, Zabolotnyy D, Kienzer HR, Cupissol D, Peyrade F, Benasso M, Vynnychenko I, De Raucourt D, Bokemeyer C, Schueler A, Amellal N, Hitt R. Platinum-based chemotherapy plus cetuximab in head and neck cancer. The New England journal of medicine. 2008;359(11):1116-27. Epub 2008/09/12. doi: 10.1056/NEJMoa0802656. PubMed PMID: 18784101.

13. Ferris RL, Blumenschein G, Jr., Fayette J, Guigay J, Colevas AD, Licitra L, Harrington K, Kasper S, Vokes EE, Even C, Worden F, Saba NF, Iglesias Docampo LC, Haddad R, Rordorf T, Kiyota N, Tahara M, Monga M, Lynch M, Geese WJ, Kopit J, Shaw JW, Gillison ML. Nivolumab for Recurrent Squamous-Cell Carcinoma of the Head and Neck. The New England journal of medicine. 2016;375(19):1856-67. Epub 2016/10/11. doi: 10.1056/NEJMoa1602252. PubMed PMID: 27718784; PMCID: PMC5564292.

14. Cohen EEW, Soulieres D, Le Tourneau C, Dinis J, Licitra L, Ahn MJ, Soria A, Machiels JP, Mach N, Mehra R, Burtness B, Zhang P, Cheng J, Swaby RF, Harrington KJ. Pembrolizumab versus methotrexate, docetaxel, or cetuximab for recurrent or metastatic head-and-neck squamous cell carcinoma (KEYNOTE-040): a randomised, open-label, phase 3 study. Lancet (London, England). 2019;393(10167):156-67. Epub 2018/12/05. doi: 10.1016/s0140-6736(18)31999-8. PubMed PMID: 30509740.

15. Mok TSK, Wu YL, Kudaba I, Kowalski DM, Cho BC, Turna HZ, Castro G, Jr., Srimuninnimit V, Laktionov KK, Bondarenko I, Kubota K, Lubiniecki GM, Zhang J, Kush D, Lopes G. Pembrolizumab versus chemotherapy for previously untreated, PD-L1-expressing, locally advanced or metastatic non-small-cell lung cancer (KEYNOTE-042): a randomised, open-label, controlled, phase 3 trial. Lancet (London, England). 2019;393(10183):1819-30. Epub 2019/04/09. doi: 10.1016/s0140-6736(18)32409-7. PubMed PMID: 30955977.

16. Comprehensive genomic characterization of head and neck squamous cell carcinomas. Nature. 2015;517(7536):576-82. Epub 2015/01/30. doi: 10.1038/nature14129. PubMed PMID: 25631445; PMCID: Pmc4311405.

17. Cerami E, Gao J, Dogrusoz U, Gross BE, Sumer SO, Aksoy BA, Jacobsen A, Byrne CJ, Heuer ML, Larsson E, Antipin Y, Reva B, Goldberg AP, Sander C, Schultz N. The cBio cancer genomics portal: an open platform for exploring multidimensional cancer genomics data. Cancer discovery. 2012;2(5):401-4. Epub 2012/05/17. doi: 10.1158/2159-8290.cd-12-0095. PubMed PMID: 22588877; PMCID: Pmc3956037.

18. Gao J, Aksoy BA, Dogrusoz U, Dresdner G, Gross B, Sumer SO, Sun Y, Jacobsen A, Sinha R, Larsson E, Cerami E, Sander C, Schultz N. Integrative analysis of complex cancer genomics and clinical profiles using the cBioPortal. Science signaling. 2013;6(269):pl1. Epub 2013/04/04. doi: 10.1126/scisignal.2004088. PubMed PMID: 23550210; PMCID: Pmc4160307.

19. Jimeno A, Bauman JE, Weissman C, Adkins D, Schnadig I, Beauregard P, Bowles DW, Spira A, Levy B, Seetharamu N, Hausman D, Walker L, Rudin CM, Shirai K. A randomized, phase 2 trial of docetaxel with or without PX-866, an irreversible oral phosphatidylinositol 3-kinase inhibitor, in patients with relapsed or metastatic head and neck squamous cell cancer. Oral oncology. 2015;51(4):383-8. Epub 2015/01/17. doi: 10.1016/j.oraloncology.2014.12.013. PubMed PMID: 25593016.

20. Soulieres D, Faivre S, Mesia R, Remenar E, Li SH, Karpenko A, Dechaphunkul A, Ochsenreither S, Kiss LA, Lin JC, Nagarkar R, Tamas L, Kim SB, Erfan J, Alyasova A, Kasper S, Barone C, Turri S, Chakravartty A, Chol M, Aimone P, Hirawat S, Licitra L. Buparlisib and paclitaxel in patients with platinum-pretreated recurrent or metastatic squamous cell carcinoma of the head and neck (BERIL-1): a randomised, double-blind, placebo-controlled phase 2 trial. The Lancet Oncology. 2017;18(3):323-35. Epub 2017/01/31. doi: 10.1016/s1470-2045(17)30064-5. PubMed PMID: 28131786.

21. Jimeno A, Shirai K, Choi M, Laskin J, Kochenderfer M, Spira A, Cline-Burkhardt V, Winquist E, Hausman D, Walker L, Cohen RB. A randomized, phase II trial of cetuximab with or without PX-866, an irreversible oral phosphatidylinositol 3-kinase inhibitor, in patients with

relapsed or metastatic head and neck squamous cell cancer. Annals of oncology : official journal of the European Society for Medical Oncology. 2015;26(3):556-61. Epub 2014/12/20. doi: 10.1093/annonc/mdu574. PubMed PMID: 25524478.

22. Brenner JC, Graham MP, Kumar B, Saunders LM, Kupfer R, Lyons RH, Bradford CR, Carey TE. Genotyping of 73 UM-SCC head and neck squamous cell carcinoma cell lines. Head & neck. 2010;32(4):417-26. Epub 2009/09/18. doi: 10.1002/hed.21198. PubMed PMID: 19760794; PMCID: PMC3292176.

23. Ludwig ML, Kulkarni A, Birkeland AC, Michmerhuizen NL, Foltin SK, Mann JE, Hoesli RC, Devenport SN, Jewell BM, Shuman AG, Spector ME, Carey TE, Jiang H, Brenner JC. The genomic landscape of UM-SCC oral cavity squamous cell carcinoma cell lines. Oral oncology. 2018;87:144-51. Epub 2018/12/12. doi: 10.1016/j.oraloncology.2018.10.031. PubMed PMID: 30527230; PMCID: PMC6349383.

24. Liu J, Pan S, Hsieh MH, Ng N, Sun F, Wang T, Kasibhatla S, Schuller AG, Li AG, Cheng D, Li J, Tompkins C, Pferdekamper A, Steffy A, Cheng J, Kowal C, Phung V, Guo G, Wang Y, Graham MP, Flynn S, Brenner JC, Li C, Villarroel MC, Schultz PG, Wu X, McNamara P, Sellers WR, Petruzzelli L, Boral AL, Seidel HM, McLaughlin ME, Che J, Carey TE, Vanasse G, Harris JL. Targeting Wnt-driven cancer through the inhibition of Porcupine by LGK974. Proceedings of the National Academy of Sciences of the United States of America. 2013;110(50):20224-9. Epub 2013/11/28. doi: 10.1073/pnas.1314239110. PubMed PMID: 24277854; PMCID: Pmc3864356.

25. Halling-Brown MD, Bulusu KC, Patel M, Tym JE, Al-Lazikani B. canSAR: an integrated cancer public translational research and drug discovery resource. Nucleic Acids Res. 2012;40(Database issue):D947-56. Epub 2011/10/21. doi: 10.1093/nar/gkr881. PubMed PMID: 22013161; PMCID: Pmc3245005.

26. Bulusu KC, Tym JE, Coker EA, Schierz AC, Al-Lazikani B. canSAR: updated cancer research and drug discovery knowledgebase. Nucleic Acids Res. 2014;42(Database issue):D1040-7. Epub 2013/12/07. doi: 10.1093/nar/gkt1182. PubMed PMID: 24304894; PMCID: Pmc3964944.

27. Michmerhuizen NL, Leonard E, Matovina C, Harris M, Herbst G, Kulkarni A, Zhai J, Jiang H, Carey TE, Brenner JC. Rationale for Using Irreversible Epidermal Growth Factor Receptor Inhibitors in Combination with Phosphatidylinositol 3-Kinase Inhibitors for Advanced Head and Neck Squamous Cell Carcinoma. Molecular pharmacology. 2019;95(5):528-36. Epub 2019/03/13. doi: 10.1124/mol.118.115162. PubMed PMID: 30858165.

28. Birkeland AC, Yanik M, Tillman BN, Scott MV, Foltin SK, Mann JE, Michmerhuizen NL, Ludwig ML, Sandelski MM, Komarck CM, Carey TE, Prince ME, Bradford CR, McHugh JB, Spector ME, Brenner JC. Identification of Targetable ERBB2 Aberrations in Head and Neck Squamous Cell Carcinoma. JAMA otolaryngology-- head & neck surgery. 2016. Epub 2016/04/15. doi: 10.1001/jamaoto.2016.0335. PubMed PMID: 27077364.

29. Tillman BN, Yanik M, Birkeland AC, Liu CJ, Hovelson DH, Cani AK, Palanisamy N, Carskadon S, Carey TE, Bradford CR, Tomlins SA, McHugh JB, Spector ME, Chad Brenner J. Fibroblast growth factor family aberrations as a putative driver of head and neck squamous cell carcinoma in an epidemiologically low-risk patient as defined by targeted sequencing. Head Neck. 2016;38 Suppl 1:E1646-52. Epub 2016/02/06. doi: 10.1002/hed.24292. PubMed PMID: 26849095; PMCID: Pmc4844767.

30. Maust JD, Frankowski-McGregor CL, Bankhead A, 3rd, Simeone DM, Sebolt-Leopold JS. Cyclooxygenase-2 Influences Response to Cotargeting of MEK and CDK4/6 in a Subpopulation of Pancreatic Cancers. Molecular cancer therapeutics. 2018;17(12):2495-506. Epub 2018/09/27. doi: 10.1158/1535-7163.Mct-18-0082. PubMed PMID: 30254182; PMCID: PMC6279520.

31. Badarni M, Prasad M, Balaban N, Zorea J, Yegodayev KM, Ben-Zion J, Dinur AB, Grenman R, Rotblat B, Cohen L, Elkabets M. Repression of AXL expression by AP-1/JNK blockage overcomes resistance to PI3Ka therapy. JCI insight. 2019;5. Epub 2019/03/13. doi: 10.1172/jci.insight.125341. PubMed PMID: 30860495.

32. Loewe S, Musichnek H. Effect of combinations: mathematical basis of the problem. Arch Exp Pathol Pharmakol. 1926;114:313-26.

33. Di Veroli GY, Fornari C, Wang D, Mollard S, Bramhall JL, Richards FM, Jodrell DI. Combenefit: an interactive platform for the analysis and visualization of drug combinations. Bioinformatics (Oxford, England). 2016;32(18):2866-8. Epub 2016/05/07. doi: 10.1093/bioinformatics/btw230. PubMed PMID: 27153664; PMCID: PMC5018366.

34. Li W, Xu H, Xiao T, Cong L, Love MI, Zhang F, Irizarry RA, Liu JS, Brown M, Liu XS. MAGeCK enables robust identification of essential genes from genome-scale CRISPR/Cas9 knockout screens. Genome Biol. 2014;15(12):554. Epub 2014/12/06. doi: 10.1186/s13059-014-0554-4. PubMed PMID: 25476604; PMCID: 4290824.

35. Lui VW, Hedberg ML, Li H, Vangara BS, Pendleton K, Zeng Y, Lu Y, Zhang Q, Du Y, Gilbert BR, Freilino M, Sauerwein S, Peyser ND, Xiao D, Diergaarde B, Wang L, Chiosea S, Seethala R, Johnson JT, Kim S, Duvvuri U, Ferris RL, Romkes M, Nukui T, Kwok-Shing Ng P, Garraway LA, Hammerman PS, Mills GB, Grandis JR. Frequent mutation of the PI3K pathway in head and neck cancer defines predictive biomarkers. Cancer discovery. 2013;3(7):761-9. Epub 2013/04/27. doi: 10.1158/2159-8290.cd-13-0103. PubMed PMID: 23619167; PMCID: Pmc3710532.

36. Burger MT, Pecchi S, Wagman A, Ni ZJ, Knapp M, Hendrickson T, Atallah G, Pfister K, Zhang Y, Bartulis S, Frazier K, Ng S, Smith A, Verhagen J, Haznedar J, Huh K, Iwanowicz E, Xin X, Menezes D, Merritt H, Lee I, Wiesmann M, Kaufman S, Crawford K, Chin M, Bussiere D, Shoemaker K, Zaror I, Maira SM, Voliva CF. Identification of NVP-BKM120 as a Potent, Selective, Orally Bioavailable Class I PI3 Kinase Inhibitor for Treating Cancer. ACS medicinal chemistry letters. 2011;2(10):774-9. Epub 2011/10/13. doi: 10.1021/ml200156t. PubMed PMID: 24900266; PMCID: PMC4017971.

37. Maira SM, Pecchi S, Huang A, Burger M, Knapp M, Sterker D, Schnell C, Guthy D, Nagel T, Wiesmann M, Brachmann S, Fritsch C, Dorsch M, Chene P, Shoemaker K, De Pover A, Menezes D, Martiny-Baron G, Fabbro D, Wilson CJ, Schlegel R, Hofmann F, Garcia-Echeverria C, Sellers WR, Voliva CF. Identification and characterization of NVP-BKM120, an orally available pan-class I PI3-kinase inhibitor. Molecular cancer therapeutics. 2012;11(2):317-28. Epub 2011/12/23. doi: 10.1158/1535-7163.mct-11-0474. PubMed PMID: 22188813.

38. Bendell JC, Rodon J, Burris HA, de Jonge M, Verweij J, Birle D, Demanse D, De Buck SS, Ru QC, Peters M, Goldbrunner M, Baselga J. Phase I, dose-escalation study of BKM120, an oral pan-Class I PI3K inhibitor, in patients with advanced solid tumors. Journal of clinical oncology : official journal of the American Society of Clinical Oncology. 2012;30(3):282-90. Epub 2011/12/14. doi: 10.1200/jco.2011.36.1360. PubMed PMID: 22162589.

39. Lee H, Jung KH, Jeong Y, Hong S, Hong SS. HS-173, a novel phosphatidylinositol 3-kinase (PI3K) inhibitor, has anti-tumor activity through promoting apoptosis and inhibiting angiogenesis. Cancer letters. 2013;328(1):152-9. Epub 2012/08/30. doi: 10.1016/j.canlet.2012.08.020. PubMed PMID: 22929971.

40. Rumman M, Jung KH, Fang Z, Yan HH, Son MK, Kim SJ, Kim J, Park JH, Lim JH, Hong S, Hong SS. HS-173, a novel PI3K inhibitor suppresses EMT and metastasis in pancreatic cancer. Oncotarget. 2016;7(47):78029-47. Epub 2016/10/30. doi: 10.18632/oncotarget.12871. PubMed PMID: 27793006; PMCID: PMC5363641.

41. Howlader N NA, Krapcho M, Miller D, Bishop K, Altekruse SF, Kosary CL, Yu M, Ruhl J, Tatalovich Z, Mariotto A, Lewis DR, Chen HS, Feuer EJ, Cronin KA. SEER Cancer Statistics Review, 1975-2016. SEER web site: National Cancer Institute; April 2019.

42. Rebucci M, Peixoto P, Dewitte A, Wattez N, De Nuncques MA, Rezvoy N, Vautravers-Dewas C, Buisine MP, Guerin E, Peyrat JP, Lartigau E, Lansiaux A. Mechanisms underlying resistance to cetuximab in the HNSCC cell line: role of AKT inhibition in bypassing this resistance. International journal of oncology. 2011;38(1):189-200. Epub 2010/11/27. PubMed PMID: 21109940.

43. Michmerhuizen NL, Leonard E, Kulkarni A, Brenner JC. Differential compensation mechanisms define resistance to PI3K inhibitors in PIK3CA amplified HNSCC. Otorhinolaryngology-head and neck surgery. 2016;1(2):44-50. Epub 2016/12/23. PubMed PMID: 28004037; PMCID: PMC5167357.

44. Young NR, Liu J, Pierce C, Wei TF, Grushko T, Olopade OI, Liu W, Shen C, Seiwert TY, Cohen EE. Molecular phenotype predicts sensitivity of squamous cell carcinoma of the head and neck to epidermal growth factor receptor inhibition. Molecular oncology. 2013;7(3):359-68. Epub 2012/12/04. doi: 10.1016/j.molonc.2012.11.001. PubMed PMID: 23200321; PMCID: Pmc3661759.

45. D'Amato V, Rosa R, D'Amato C, Formisano L, Marciano R, Nappi L, Raimondo L, Di Mauro C, Servetto A, Fusciello C, Veneziani BM, De Placido S, Bianco R. The dual PI3K/mTOR inhibitor PKI-587 enhances sensitivity to cetuximab in EGFR-resistant human head and neck cancer models. British journal of cancer. 2014;110(12):2887-95. Epub 2014/05/16. doi: 10.1038/bjc.2014.241. PubMed PMID: 24823695; PMCID: PMC4056056.

46. Lattanzio L, Tonissi F, Monteverde M, Vivenza D, Russi E, Milano G, Merlano M, Lo Nigro C. Treatment effect of buparlisib, cetuximab and irradiation in wild-type or PI3KCA-mutated head and neck cancer cell lines. Investigational new drugs. 2015;33(2):310-20. Epub 2015/01/22. doi: 10.1007/s10637-015-0210-1. PubMed PMID: 25603975.

47. Silva-Oliveira RJ, Melendez M, Martinho O, Zanon MF, de Souza Viana L, Carvalho AL, Reis RM. AKT can modulate the in vitro response of HNSCC cells to irreversible EGFR inhibitors. Oncotarget. 2017;8(32):53288-301. Epub 2017/09/09. doi: 10.18632/oncotarget.18395. PubMed PMID: 28881811; PMCID: PMC5581110.

48. Anisuzzaman AS, Haque A, Wang D, Rahman MA, Zhang C, Chen Z, Chen ZG, Shin DM, Amin AR. In Vitro and In Vivo Synergistic Antitumor Activity of the Combination of BKM120 and Erlotinib in Head and Neck Cancer: Mechanism of Apoptosis and Resistance. Molecular cancer therapeutics. 2017;16(4):729-38. Epub 2017/01/26. doi: 10.1158/1535-7163.Mct-16-0683. PubMed PMID: 28119490.

49. Brand TM, Hartmann S, Bhola NE, Li H, Zeng Y, O'Keefe RA, Ranall MV, Bandyopadhyay S, Soucheray M, Krogan NJ, Kemp C, Duvvuri U, LaVallee T, Johnson DE, Ozbun MA, Bauman JE, Grandis JR. Cross-talk Signaling between HER3 and HPV16 E6 and E7 Mediates Resistance to PI3K Inhibitors in Head and Neck Cancer. Cancer research. 2018;78(9):2383-95. Epub 2018/02/15. doi: 10.1158/0008-5472.Can-17-1672. PubMed PMID: 29440171.

50. Elkabets M, Pazarentzos E, Juric D, Sheng Q, Pelossof RA, Brook S, Benzaken AO, Rodon J, Morse N, Yan JJ, Liu M, Das R, Chen Y, Tam A, Wang H, Liang J, Gurski JM, Kerr DA, Rosell R, Teixido C, Huang A, Ghossein RA, Rosen N, Bivona TG, Scaltriti M, Baselga J. AXL mediates resistance to PI3Kalpha inhibition by activating the EGFR/PKC/mTOR axis in head and neck and esophageal squamous cell carcinomas. Cancer cell. 2015;27(4):533-46. Epub 2015/04/16. doi: 10.1016/j.ccell.2015.03.010. PubMed PMID: 25873175; PMCID: Pmc4398915.

51. Chen Y, Takita J, Choi YL, Kato M, Ohira M, Sanada M, Wang L, Soda M, Kikuchi A, Igarashi T, Nakagawara A, Hayashi Y, Mano H, Ogawa S. Oncogenic mutations of ALK kinase in neuroblastoma. Nature. 2008;455(7215):971-4. Epub 2008/10/17. doi: 10.1038/nature07399. PubMed PMID: 18923524.

52. Janoueix-Lerosey I, Lequin D, Brugieres L, Ribeiro A, de Pontual L, Combaret V, Raynal V, Puisieux A, Schleiermacher G, Pierron G, Valteau-Couanet D, Frebourg T, Michon J, Lyonnet S, Amiel J, Delattre O. Somatic and germline activating mutations of the ALK kinase receptor in neuroblastoma. Nature. 2008;455(7215):967-70. Epub 2008/10/17. doi: 10.1038/nature07398. PubMed PMID: 18923523.

53. George RE, Sanda T, Hanna M, Frohling S, Luther W, 2nd, Zhang J, Ahn Y, Zhou W, London WB, McGrady P, Xue L, Zozulya S, Gregor VE, Webb TR, Gray NS, Gilliland DG, Diller L, Greulich H, Morris SW, Meyerson M, Look AT. Activating mutations in ALK provide a therapeutic target in neuroblastoma. Nature. 2008;455(7215):975-8. Epub 2008/10/17. doi: 10.1038/nature07397. PubMed PMID: 18923525; PMCID: PMC2587486.

54. Morris SW, Kirstein MN, Valentine MB, Dittmer KG, Shapiro DN, Saltman DL, Look AT. Fusion of a kinase gene, ALK, to a nucleolar protein gene, NPM, in non-Hodgkin's lymphoma. Science (New York, NY). 1994;263(5151):1281-4. Epub 1994/03/04. doi: 10.1126/science.8122112. PubMed PMID: 8122112.

55. Soda M, Choi YL, Enomoto M, Takada S, Yamashita Y, Ishikawa S, Fujiwara S, Watanabe H, Kurashina K, Hatanaka H, Bando M, Ohno S, Ishikawa Y, Aburatani H, Niki T, Sohara Y, Sugiyama Y, Mano H. Identification of the transforming EML4-ALK fusion gene in non-small-cell lung cancer. Nature. 2007;448(7153):561-6. Epub 2007/07/13. doi: 10.1038/nature05945. PubMed PMID: 17625570.

56. Yoshihara K, Wang Q, Torres-Garcia W, Zheng S, Vegesna R, Kim H, Verhaak RG. The landscape and therapeutic relevance of cancer-associated transcript fusions. Oncogene. 2015;34(37):4845-54. Epub 2014/12/17. doi: 10.1038/onc.2014.406. PubMed PMID: 25500544; PMCID: PMC4468049.

57. Gonzales CB, De La Chapa JJ, Saikumar P, Singha PK, Dybdal-Hargreaves NF, Chavez J, Horning AM, Parra J, Kirma NB. Co-targeting ALK and EGFR parallel signaling in oral squamous cell carcinoma. Oral oncology. 2016;59:12-9. Epub 2016/07/18. doi: 10.1016/j.oraloncology.2016.05.007. PubMed PMID: 27424178; PMCID: PMC5460536.

58. Ouyang X, Barling A, Lesch A, Tyner JW, Choonoo G, Zheng C, Jeng S, West TM, Clayburgh D, Courtneidge SA, McWeeney SK, Kulesz-Martin M. Induction of anaplastic lymphoma kinase (ALK) as a novel mechanism of EGFR inhibitor resistance in head and neck squamous cell carcinoma patient-derived models. Cancer biology & therapy. 2018;19(10):921-33. Epub 2018/06/02. doi: 10.1080/15384047.2018.1451285. PubMed PMID: 29856687; PMCID: PMC6300392.

59. Folkes AJ, Ahmadi K, Alderton WK, Alix S, Baker SJ, Box G, Chuckowree IS, Clarke PA, Depledge P, Eccles SA, Friedman LS, Hayes A, Hancox TC, Kugendradas A, Lensun L, Moore P, Olivero AG, Pang J, Patel S, Pergl-Wilson GH, Raynaud FI, Robson A, Saghir N, Salphati L, Sohal S, Ultsch MH, Valenti M, Wallweber HJ, Wan NC, Wiesmann C, Workman P, Zhyvoloup A, Zvelebil MJ, Shuttleworth SJ. The identification of 2-(1H-indazol-4-yl)-6-(4-methanesulfonyl-piperazin-1-ylmethyl)-4-morpholin-4-yl-t hieno[3,2-d]pyrimidine (GDC-0941) as a potent, selective, orally bioavailable inhibitor of class I PI3 kinase for the treatment of cancer. Journal of medicinal chemistry. 2008;51(18):5522-32. Epub 2008/08/30. doi: 10.1021/jm800295d. PubMed PMID: 18754654.

60. Stanicka J, Rieger L, O'Shea S, Cox O, Coleman M, O'Flanagan C, Addario B, McCabe N, Kennedy R, O'Connor R. FES-related tyrosine kinase activates the insulin-like growth factor-1 receptor at sites of cell adhesion. Oncogene. 2018;37(23):3131-50. Epub 2018/03/16. doi: 10.1038/s41388-017-0113-z. PubMed PMID: 29540831.

61. Ciceri P, Muller S, O'Mahony A, Fedorov O, Filippakopoulos P, Hunt JP, Lasater EA, Pallares G, Picaud S, Wells C, Martin S, Wodicka LM, Shah NP, Treiber DK, Knapp S. Dual kinase-bromodomain inhibitors for rationally designed polypharmacology. Nature chemical biology. 2014;10(4):305-12. Epub 2014/03/04. doi: 10.1038/nchembio.1471. PubMed PMID: 24584101; PMCID: PMC3998711.

62. Liu TJ, LaFortune T, Honda T, Ohmori O, Hatakeyama S, Meyer T, Jackson D, de Groot J, Yung WK. Inhibition of both focal adhesion kinase and insulin-like growth factor-I receptor kinase suppresses glioma proliferation in vitro and in vivo. Molecular cancer therapeutics. 2007;6(4):1357-67. Epub 2007/04/14. doi: 10.1158/1535-7163.Mct-06-0476. PubMed PMID: 17431114.

63. Sambandam V, Frederick MJ, Shen L, Tong P, Rao X, Peng S, Singh R, Mazumdar T, Huang C, Li Q, Pickering CR, Myers JN, Wang J, Johnson FM. PDK1 mediates NOTCH1-mutated head and neck squamous carcinoma vulnerability to therapeutic PI3K/mTOR inhibition. Clinical cancer research : an official journal of the American Association for Cancer Research. 2019. Epub 2019/02/17. doi: 10.1158/1078-0432.Ccr-18-3276. PubMed PMID: 30770351.

64. Gozgit JM, Wong MJ, Moran L, Wardwell S, Mohemmad QK, Narasimhan NI, Shakespeare WC, Wang F, Clackson T, Rivera VM. Ponatinib (AP24534), a multitargeted pan-FGFR inhibitor with activity in multiple FGFR-amplified or mutated cancer models. Molecular cancer therapeutics. 2012;11(3):690-9. Epub 2012/01/13. doi: 10.1158/1535-7163.Mct-11-0450. PubMed PMID: 22238366.

65. Liu C, Mu X, Wang X, Zhang C, Zhang L, Yu B, Sun G. Ponatinib Inhibits Proliferation and Induces Apoptosis of Liver Cancer Cells, but Its Efficacy Is Compromised by Its Activation on PDK1/Akt/mTOR Signaling. Molecules (Basel, Switzerland). 2019;24(7). Epub 2019/04/10. doi: 10.3390/molecules24071363. PubMed PMID: 30959969.

66. Uchibori K, Inase N, Araki M, Kamada M, Sato S, Okuno Y, Fujita N, Katayama R. Brigatinib combined with anti-EGFR antibody overcomes osimertinib resistance in EGFR-mutated non-small-cell lung cancer. Nature communications. 2017;8:14768. Epub 2017/03/14. doi: 10.1038/ncomms14768. PubMed PMID: 28287083; PMCID: PMC5355811.

67. Soulieres D, Licitra L, Mesia R, Remenar E, Li SH, Karpenko A, Chol M, Wang YA, Solovieff N, Bourdeau L, Sellami D, Faivre S. Molecular Alterations and Buparlisib Efficacy in Patients with Squamous Cell Carcinoma of the Head and Neck: Biomarker Analysis from BERIL-1. Clinical cancer research : an official journal of the American Association for Cancer Research. 2018;24(11):2505-16. Epub 2018/03/02. doi: 10.1158/1078-0432.Ccr-17-2644. PubMed PMID: 29490986.

68. Cai Y, Dodhia S, Su GH. Dysregulations in the PI3K pathway and targeted therapies for head and neck squamous cell carcinoma. Oncotarget. 2017;8(13):22203-17. Epub 2017/01/22. doi: 10.18632/oncotarget.14729. PubMed PMID: 28108737; PMCID: PMC5400658.

69. Zhang Y, Kwok-Shing Ng P, Kucherlapati M, Chen F, Liu Y, Tsang YH, de Velasco G, Jeong KJ, Akbani R, Hadjipanayis A, Pantazi A, Bristow CA, Lee E, Mahadeshwar HS, Tang J, Zhang J, Yang L, Seth S, Lee S, Ren X, Song X, Sun H, Seidman J, Luquette LJ, Xi R, Chin L, Protopopov A, Westbrook TF, Shelley CS, Choueiri TK, Ittmann M, Van Waes C, Weinstein JN, Liang H, Henske EP, Godwin AK, Park PJ, Kucherlapati R, Scott KL, Mills GB, Kwiatkowski DJ, Creighton CJ. A Pan-Cancer Proteogenomic Atlas of PI3K/AKT/mTOR Pathway Alterations. Cancer cell. 2017;31(6):820-32.e3. Epub 2017/05/23. doi: 10.1016/j.ccell.2017.04.013. PubMed PMID: 28528867; PMCID: PMC5502825.

70. Singh A, Greninger P, Rhodes D, Koopman L, Violette S, Bardeesy N, Settleman J. A gene expression signature associated with "K-Ras addiction" reveals regulators of EMT and tumor cell survival. Cancer cell. 2009;15(6):489-500. Epub 2009/05/30. doi: 10.1016/j.ccr.2009.03.022. PubMed PMID: 19477428; PMCID: PMC2743093.

71. Serra V, Eichhorn PJ, Garcia-Garcia C, Ibrahim YH, Prudkin L, Sanchez G, Rodriguez O, Anton P, Parra JL, Marlow S, Scaltriti M, Perez-Garcia J, Prat A, Arribas J, Hahn WC, Kim SY, Baselga J. RSK3/4 mediate resistance to PI3K pathway inhibitors in breast cancer. The Journal of clinical investigation. 2013;123(6):2551-63. Epub 2013/05/03. doi: 10.1172/jci66343. PubMed PMID: 23635776; PMCID: Pmc3668839.

72. Mann JE, Kulkarni A, Birkeland AC, Kafelghazal J, Eisenberg J, Jewell BM, Ludwig ML, Spector ME, Jiang H, Carey TE, Brenner JC. The molecular landscape of the University of Michigan laryngeal squamous cell carcinoma cell line panel. Head & neck. 2019. Epub 2019/05/16. doi: 10.1002/hed.25803. PubMed PMID: 31090975.

# Chapter 6 : Summary and Perspectives

## Summary

In my thesis, I studied the role of the phosphatidylinositol 3-kinase (PI3K) pathway in head and neck squamous cell carcinoma (HNSCC); specifically, I evaluated the hypothesis that resistance to PI3K inhibitors is due to compensatory signaling and can be overcome using inhibitors of co-dependent pathways in combination with PI3K targeting agents. My work first evaluated the possibility that the inhibition of EGFR, which is overexpressed in the majority of HNSCC tumors, sensitizes HNSCC cells to PI3K inhibition. These studies were performed via various pharmacologic treatments in a diverse set of *in vitro* HNSCC models. Second, I examined the interplay between PI3K and Notch signaling, as inactivation of *NOTCH1* is a common event in HNSCC. My work demonstrated that loss of NOTCH and activation of PI3K signaling cooperate to decrease time to endpoint in a transgenic mouse model. Finally, I took an unbiased approach to nominate other signaling pathways that could compensate in the presence of PI3K inhibitors and thereby drive treatment resistance. Using a small molecule profiling screen, I nominated several synergistic drug pairs and validated these dual-therapies using additional experiments. I chose to focus on the combination of PI3K inhibitor pictilisib and ALK inhibitor brigatinib for mechanistic studies, and I performed a xenograft experiment displaying the efficacy of these two inhibitors when used together. Here, I consider these findings in the context of previously published work and propose future directions to further develop our understanding of PI3K inhibitor resistance in HNSCC.

## Section 1: Barriers and opportunities in genetic determinants of HNSCC

Despite recent advances in cancer therapy, prognoses for HNSCC patients have not improved substantially (1, 2). Progress has been hampered at least in part by the complex array of mutations and by HPV status as well as other factors in HNSCC, which make it difficult to determine the optimal course of treatment for each patient. Interestingly, we are still uncovering the genetic landscape of HNSCC, understanding the differences between epidemiologic HNSCC cohorts, heterogeneity within individual patient tumors, interplay with the tumor environment (both immune and otherwise), and various other factors. Diversity both between and among HNSCCs has presented challenges throughout the course of my thesis and remains a significant consideration in the biology and treatment of head and neck cancer.

In the first chapter of my thesis, I review the genetic determinants of HNSCC in diverse epidemiologic cohorts. It is apparent that a variety of etiological factors play an important role in the prevention, development, and treatment of HNSCCs, and additional studies should continue to seek out these differences in order to inform patient-specific treatment protocols and improve outcomes. The incidence of HNSCC is highest in low resource settings, particularly in southeast Asia; many of these regions also are impacted by additional risk factors (such as the use of betel quid). Furthermore, mortality is correlated with incidence, such that regions with high rates of HNSCC also are characterized by poor outcomes (3). There are a host of social factors that may contribute to this association—for example, limited awareness of HNSCC and its risk factors, lack of access to health care, and delays in the initiation of treatment. Importantly, genetic factors also have potential significance. With the ever-increasing ease and ever-decreasing cost of next-generation sequencing, more and more studies will reveal important

genetic changes that may predispose patient subsets to develop HNSCC tumors of a specific subsite or severity. As an example of this, an emerging trend in HNSCC incidence is an increase in the rate of tongue tumors in young, low-risk, female patients. The factors underlying this group of oral cavity cancers remain incompletely understood, but they may be associated with changes in DNA damage response, apoptosis, cell cycle, and Fanconi anemia-related genes (4). To date, the majority of molecular studies in HNSCC have been performed in tumors from Caucasian males in developed countries (a minority group for this cancer type), but new analyses will inform better tumor characterization and clinical decision-making for individuals with a wide array of ethnic backgrounds.

In the latter chapters of my thesis, I focus on the how activation or blockade of PI3K signaling may impact response to treatment. The majority of TCGA patients display aberration in one or more PI3K pathway genes (5), but the status of any single gene or any group of genes has not, to my knowledge, been validated as a critical biomarker of response in this cancer type. Clinical trial data has not demonstrated that mutation, amplification, or loss of PI3K pathway genes is linked to sensitivity or resistance, although recent clinical trials for EGFR targeting agents have noted poorer outcomes following EGFR inhibition in patients with PI3K activation. In the phase III E2303 trial, which compared cisplatin and cisplatin plus cetuximab in recurrent and metastatic (R/M) HNSCC patients (6), *PIK3CA* mutation or *PTEN* loss was associated with poor response to EGFR targeting therapy (7). This finding was also noted in the LUX-H&N1 trial, which compared second-line treatments with afatinib and methotrexate in R/M HNSCCs (8); here, *PTEN* high tumors received greater benefit from afatinib (9). Preclinical studies have also noted that PI3K activation or *PTEN* loss may serve as a biomarker for resistance to

cetuximab (10, 11). Further studies are warranted to validate these results in larger, prospective trials.

Similarly, there is no proven biomarker for response to PI3K inhibitor treatment in HNSCC, although various factors have been proposed in cell lines, xenografts, or underpowered clinical trials. In contrast to results in other cancer types (most notably breast cancer) (12), *PIK3CA* mutation has not been associated with sensitivity to PI3K inhibition in HNSCC trials to date (13, 14). While precision medicine trials have shown a trend supporting *PIK3CA* alterations as a marker for response to PI3K inhibitors (15), these often do not reach statistical significance or have a very limited number of HNSCC patients enrolling. For example, Janku *et al.* conducted an analysis of responses to PI3K/AKT/mTOR inhibitors in tumors with H1047R *PIK3CA* mutations including 4 HNSCC patients; after inhibitor treatment, two of these patients experienced progressive disease, one had little change in tumor burden, and another had an incomplete response to therapy (16). It is possible that the difference in outcomes between tumors with and without *PIK3CA* mutations has not been noted due to an insufficient number of *PIK3CA* mutant tumors in any single clinical trial; ongoing studies of PI3K inhibitor copanlisib in HNSCC patients with *PIK3CA* mutation or amplification or *PTEN* loss will better elucidate any potential differences in response attributable to PI3K activation (NCT02822482). It is also feasible that other features predict responses to PI3K inhibitor: in the recent BERIL-1 study, a phase II trial comparing outcomes in R/M HNSCC patients treated with paclitaxel with or without pan-PI3K inhibitor buparlisib (n = 79 per group), follow-up analysis revealed that *TP53* alteration, low tumor mutation burden, HPV negativity, and high infiltration of TILs or CD8+ T-cells was associated with improved response to bupalisib. Recent preclinical work has proposed that loss of function mutations in *NOTCH1* may predict response to PI3K inhibition (17), as

discussed further below. Together these data suggest that a more nuanced understanding of tissue type specific and PI3K inhibitor response mechanisms may be required to develop clinically effective companion diagnostics for this class of inhibitors in HNSCC.

My work, consistent with previous studies, indicates that responses to PI3K inhibition (either as monotherapy or in combination with other targeted inhibitors) are complex and cannot be predicted solely based on genetic mutation, copy number alteration, or RNA expression of a single gene. Over the course of my thesis, I treated a diverse set of HNSCC cell lines with PI3K inhibitors displaying varying isoform selectivity as monotherapies. Alpha isoform targeting agents were clearly more effective than other PI3K inhibitors, but the sensitivity profiles for any individual pan- or alpha-isoform PI3K inhibitor were more difficult to stratify. This was increasingly true for drug combinations: *PIK3CA* mutation, copy number, RNA expression, and HPV status did not prove to be meaningful biomarkers for either PI3K and EGFR inhibitor dual-therapies or for other synergistic drug pairs. In the case of HS-173 and FAK inhibitor TAE226, we observed greater synergy in *PIK3CA* mutant cell lines as compared to *PIK3CA* wild type cell lines in our initial validation experiments. However, when this association was tested more rigorously with other PI3K and FAK inhibitors, dual-therapy was beneficial also in many *PIK3CA* wildtype models; this could be due to differences in selectivity or mechanism of action for individual agents (18). Thus, PI3K pathway activation (measured at the DNA level via mutation or copy number status or at the protein level via relative downstream phosphorylation) appears to be an insufficient biomarker for sensitivity in HNSCC cell lines; other cellular features, including additional alteration in PI3K pathway members (such as downstream mutations in *AKT1*) or activation of receptor tyrosine kinases (perhaps via upstream overexpression of EGFR), may contribute to signaling through the PI3K pathway and thereby

affect inhibitor responses. Indeed, multifaceted analyses, such as those considering gene sets rather than individual genetic changes, may be needed to predict sensitivity. For example, responses to EGFR or FAK inhibitor may be better stratified using gene sets assessing activation of PI3K, mTOR or other related signaling nodes instead of *PIK3CA* mutation status alone. Alternatively, an additional pathway that is changed as a result of PI3K activation (eg: epithelial to mesenchymal transition or apoptosis) may be even more effective in predicting response.

## Section 2: Improving strategies to overcome compensatory resistance through PI3K and EGFR

One of the most widely studied mechanisms of resistance to PI3K inhibition is signaling through the epidermal growth factor receptor and the downstream Ras-MEK-ERK pathway. In my thesis, I considered this resistance mechanism using a wide variety of cell lines (displaying a diverse array of genetic alterations) and a large set of ERBB family-targeting drugs. Initially, our work focused on *PIK3CA* amplified HNSCCs, demonstrating that 4/6 (67%) of cell lines with additional copies of wild-type *PIK3CA* maintained Ras-MEK-ERK pathway activity following PI3K inhibitor treatment and that two of these models also were sensitive to dual inhibition of PI3K and EGFR or MEK. Later work extended this observation to a larger panel of ERBB inhibitors and cell lines (including several with *PIK3CA* mutations). Overall, our findings mirrored those of previous studies in showing that dual-therapy with PI3K and EGFR inhibitors was often more effective than either monotherapy (19-22), but it also extended this observation to consider individual classes of ERBB-targeting agents that might result in heightened responses when used as part of combination treatments. Our work demonstrated that irreversible inhibitors of EGFR were more effective in combination with PI3K inhibitors than reversible ERBB

targeting agents in HNSCC cell lines. This represented an advance in the field as previous work had primarily considered dual-therapies that included either reversible EGFR inhibitors or EGFR-targeting antibodies such as cetuximab; a direct comparison of PI3K combination with several pharmacologies against EGFR had, to my knowledge, never been performed.

Beyond direct inhibition of the receptor tyrosine kinases PI3K and EGFR themselves, previous work has also examined drug combinations targeting PI3K and EGFR via inhibition of downstream effectors including mTOR and MEK, respectively. Several papers have noted synergy with mTOR inhibitors and EGFR agents (23-25). In one of these studies, Jimeno *et al*. used H1047R *PIK3CA* mutant Detroit 562 cells in a xenograft model and noted improved response to mTOR inhibitor temsirolimus and erlotinib. This response co-occurred with changes in MAPK and p70 S6 kinase phosphorylation (downstream of EGFR and mTOR, respectively) and in Ki67, effects that were not evidenced in less responsive xenograft models or after single-agent treatment. Our work with Detroit 562 *in vitro* showed minimal responses to PI3K inhibitor HS-173 and reversible EGFR inhibitors (including erlotinib) that could be enhanced to synergistic levels with multiple irreversible EGFR inhibitors (26). We did not specifically consider erlotinib with mTOR inhibitors (temsirolimus or otherwise); however, I would expect, based on our work in other models, that such dual-therapies might inhibit MAPK and p70 S6 kinase phosphorylation. As our ineffective reversible EGFR inhibitor combinations blocked MAPK phosphorylation (p70 S6 kinase phosphorylation was not tested), I expect that erlotinib and temsirolimus may also fail to induce significant cell death in our system. Thus, it is possible that one or more additional effectors, perhaps further downstream of MAPK/p70 S6 kinase or part of a second escape pathway, may be responsible for synergistic effects. Alternatively, *in vivo* mechanisms could be critical for responses to mTOR and EGFR agents in Detroit 562 and

potentially other HNSCCs. We have not yet tested our PI3K and irreversible EGFR inhibitor combinations in xenografts, but these experiments would allow us to better compare our responses to those in other publications and could reveal the potential of our results to translate clinically.

In light of the synergy observed following treatment with agents targeting the PI3K and EGFR pathways in preclinical models, phase I and II trials have been performed to examine these dual-therapies in HNSCC patients. Of these trials, three have been completed, all in patients receiving second-line treatment due to chemotherapy resistance, recurrence, and/or metastasis. The first of these trials examined temsirolimus with cetuximab and resulted in dose-limited toxicities in 1/3 of patients (27). The second considered another mTOR inhibitor, everolimus, with erlotinib. This combination had a reasonable toxicity profile and stopped or decreased tumor growth in several patients, but it did not result in clinical benefit as compared to previous trials considering erlotinib as a monotherapy (28). The third trial, which considered cetuximab with or without PI3K inhibitor PX-866, also did not provide evidence of improvement with the addition of PI3K inhibitor (14). Several other trials using PI3K and EGFR targeting agents, sometimes alongside of cytotoxic chemotherapy or radiotherapy, have been initiated and are in various stages of completion. Toxicity seems to be a major concern in many of these trials and may limit the use of such combinations in patients. As a result, the development of more specific combinations and/or more effective PI3K and EGFR inhibitors is warranted.

Nevertheless, previous work also suggests that the use of currently available PI3K and EGFR therapies may be optimized in other ways. For example, the sequence of combination treatments may be an important consideration. Lattanzio and colleagues showed that Cal-33 cells responded to treatment with EGFR antibody followed by PI3K inhibitor (29), while our

data showed minimal responses in this model when EGFR and PI3K targeting drugs were administered together. The type of EGFR targeting agent that was used may also explain this conflicting data: while we did not consider cetuximab or other EGFR targeting antibodies in our experiments, small molecules and biologics could have very different response profiles in combination with PI3K inhibitors.

An additional strategy to improve PI3K and EGFR inhibitor combination treatments is to combine them with radiation therapy (RT), one of the most widely used treatment modalities for HNSCC. As reviewed elsewhere (30), activation of the EGFR and PI3K pathways may lead to radiosensitivity in at least three ways: 1) increase intrinsic cell survival via activation of Ras and/or overexpression of EGFR, 2) promote cell proliferation by altering cell cycle regulation, and 3) increase hypoxia, leading to genomic instability, invasion, and metastasis. In accordance with this, blocking PI3K and EGFR signaling using BKM120 and cetuximab improved responses to radiation in Cal-27 cells (29). Bozec *et al.* also considered cetuximab, BKM120, and/or radiation in orthotopic xenograft models of Cal-33; their study showed that cetuximab followed by BKM120 was effective and that this effect was enhanced with the addition of radiotherapy (31). In contrast, Blas *et al*. recently demonstrated that BKM120 or MEK inhibitor binimetinib was more effective when administered with RT, but that the triple combination did not improve responses (32). These conflicting data clearly demonstrate that although the effects of PI3K and EGFR pathway inhibition with RT are promising, the best combination of agents in any particular model remains incompletely understood. Differential responses to treatment with targeted therapies and/or RT are expected: as such, a better understanding of the patient population of interest, the timing of RT treatment (before, after, or during targeted therapy), and the specific dosing and fractionation of radiation treatment are needed to match patients to

effective triple therapy protocols. Overall, our findings using PI3K and EGFR inhibitor combinations highlight the diversity of responses to dual-therapies that target only two signaling pathways. In the context of other work examining these agents, additional factors, including but not limited to timing and other co-treatments, require further consideration before compensation through the PI3K and EGFR pathways might be effectively exploited in a population of HNSCC patients.

## Section 3: Examining Cross-Talk Between PI3K and Notch Signaling

Recent sequencing studies have identified frequent aberrations in the PI3K and NOTCH signaling pathways as well as the importance of these pathways in HNSCC and other cancer types (5, 33-35). Molecular changes in each of these pathways have been studied separately in various preclinical models, including patient-derived cell lines and transgenic mice. For example, recent work from our laboratory has characterized a panel of UM-SCC cell lines and demonstrated hotspot *PIK3CA* mutation in one oral cavity model (UM-SCC-43) and copy number amplification of wild-type *PIK3CA* in several others (36, 37). Additionally, *NOTCH1* mutations and deletions are found in 14 and 43%, respectively, of the cell lines in the oral cavity subset (36). Transgenic mouse models have also been developed to study the role of these genes in HNSCC. Du *et al.* described a model of *PIK3CA* amplification, in which mice exhibit increased expression of wild-type PI3K driven by the K5 promoter. This resulted in increased signaling through PDK1 and accelerated tumor formation after chronic 16-week exposure to tobacco analogue 4-nitroquinoline N-oxide (4-NQO) (38). Similarly, loss of tumor suppressor *Pten* resulted in the rapid development of multiple oral tumors following 4-NQO exposure (39). Several additional studies have characterized the disparate effects of the loss of Notch signaling

in epithelial cells, including one recent publication showing that this led to head and neck carcinogenesis (40). Beyond these *in vitro* and *in vivo* analyses, HNSCC patient samples in TCGA demonstrated *NOTCH1* alterations in 21% and *PIK3CA* mutations and/or copy number changes in 35% of cases (5, 41, 42). As a whole, these research models—cell lines, transgenic mice, and tumor samples—indicate that the PI3K and NOTCH signaling pathways play an important role in HNSCC; however, the way that these pathways interact has not been fully characterized.

Taken together, at least 34/505 (6.7%) HNSCC TCGA patients exhibit both inactivation of *NOTCH1* and activation of *PIK3CA*. Interestingly, these changes may be even more frequent in the HPV positive patient subset (43) and may be associated with tobacco-associated tumors (44). Emerging data suggests cross-talk between the PI3K and NOTCH pathways. Our UM-SCC-47 *PIK3CA* knockout cell line displays differential expression of Notch pathways genes, most notably *HES2* and *DLL1*. What is more, this knockout cell line exhibits loss of ΔNp63 at the mRNA and protein levels. p63 and its transcriptional targets can be regulated by NOTCH signaling (45, 46) and also display altered expression in an *in vitro* model of *NOTCH1* knockout. Additional data from Zheng *et al.* shows that treatment with gamma secretase inhibitor PF-03084014 activated PI3K signaling in HNSCC models (47). Together, these data motivate investigation of the interaction between PI3K and NOTCH alterations in HNSCCs.

Importantly, Sambandam *et al.* recently demonstrated that cell lines with loss-of-function mutations in *NOTCH1* displayed increased sensitivity to PI3K/mTOR inhibitors (17). This is in agreement with results for a patient tumor xenograft system in which two cases with inactivating *NOTCH1* mutations responded to PI3K inhibition (11) and with a phase I study where combination mTOR inhibitor ridaforolimus and Notch inhibitor MK-0752 showed activity in

HNSCC (48). Furthermore, these data are consistent with our findings using a genetically engineered mouse model where *Notch1* and/or overexpression of H1047R mutant *Pik3ca* are driven by Cre recombinase in K14 positive epithelial cells. Following exposure to 4-NQO, we observed that double alteration (*Notch1* loss + *Pik3ca* mutation) accelerates time to endpoint as compared to single gene manipulation or K14-Cre alone. Showing that oncogenic perturbation of these pathways synergistically accelerates tumor formation suggests that mutation status for *PIK3CA*, *NOTCH1*, or related genes may affect response to targeted inhibitors of these pathways or that PI3K and NOTCH altering treatments might be synergistic. While this finding is consistent with the results of other groups, previous models of *in vitro* and *in vivo* HNSCC have suggested that PDK1 may play an important role downstream of PI3K and be responsible for synergy between PI3K inhibition and loss of NOTCH (17, 38). In contrast, we did not detect any change in PDK1 in our *Notch1*$^{c/c}$/*Pik3ca*$^{H1047R}$ SCC tumors. It is possible that PDK1-dependent mechanisms are specific to cases without aberration in NOTCH or PI3K signaling and/or that another pathway—likely outside of the canonical role of AKT in PI3K activation and potentially involving immune interactions—is an underlying factor in our observations.

Responses to EGFR targeting agents have also been linked to altered NOTCH signaling. Cetuximab interacted with NOTCH1 and HIF1α to reduce angiogenesis in a transgenic model of double *Pten* and *Tgfrb* knockout (49), while erlotinib showed synergy with PF-03084014 in cell line and xenograft HNSCC models (50). These effects have also been seen in clinical samples where NOTCH and Wnt signaling were differentially expressed in patient tumors following the cessation of cetuximab therapy. It remains to be determined if these effects are mediated by PI3K downstream of EGFR or via other signaling events (51). Recent work demonstrated that dual inhibition of EGFR and NOTCH signaling enhanced responses to pictilisib in PDX models

of breast and other epithelial tumor types by decreasing the proportion of cancer stem cells (52). While interesting, this study only considered targeting NOTCH2 and NOTCH3 and findings have yet to be validated in HNSCC. Additionally, the interplay between EGFR, PI3K and/or NOTCH may not be significant in all HNSCCs; in contrast to the findings of Zheng *et al* (50), data from our laboratory examining responses of several UM-SCC cell lines to the combination of EGFR inhibitor gefitinib and PF-03084014 did not result in drug synergy.

Loss of NOTCH signaling may also result in enhanced responses to other pharmacologic treatments—not just inhibitors of receptor tyrosine kinases like PI3K and EGFR. Marked responses to Wnt inhibitor LGK974 were observed in HNSCC models with loss of function NOTCH mutations (53), and sensitivity to DNA damage agents, including cisplatin, is heightened in cases of decreased NOTCH signaling (54-58). Increased sensitivity in the case of NOTCH inactivation may also extend to other therapies, but has not yet been shown. The shared and unique mechanisms underlying these differential treatment responses also have yet to be fully elucidated.

Ultimately, it will be important to explore how specific alterations in NOTCH and/or PI3K pathway members impact carcinogenesis and response to therapy. As mentioned above, Demehri *et al.* showed with several transgenic mouse models that severity of Notch alteration correlates with mouse lifespan and age of spontaneous tumor onset: lack of gamma secretase activity was embryonically lethal, but mice lived almost as long as wildtype littermates with other less profound alterations in Notch signaling, although skin tumors often formed in many of the Notch-deficient models (59). This study also demonstrated that NOTCH pathway members could affect survival and tumor phenotypes in disparate ways; mice lacking Notch effector *Rpbj* did not form tumors and lived for close to 4 months, while animals without *Notch1-3* lived for

similar timespans but displayed skin tumors at 3 months old (59). Other Notch altered GEMMs include those expressing the dominant-negative form of *dnMaml1*. With global expression of this transgene, mice displayed alopecia and skin cancer formation, but expression of *dnMaml1* specifically in K14 positive epithelial cells limited this phenotype and resulted in dysplasia and low-grade SCCs only after 4-NQO treatment (40). Thus, it will be informative to assess the role a diverse array of alterations in further mouse models with co-alteration of PI3K and Notch genes. Similar to the effects of various genetic changes in the NOTCH pathway, these changes could also have varying effects in combination with activating *PIK3CA* mutation. An additional layer of complexity lies in the diversity of means by which PI3K signaling might be increased: mutant *Pik3ca*, amplified *Pik3ca,* loss of *Pten*, and other PI3K pathway changes could all be considered with alterations in *Notch1* and other family members. Studying the similarities and differences in a varied selection of models with Notch loss and PI3K activation would provide further insight into the function of these pathways individually and collectively as well as inform the subset of patients that may benefit from biomarker-driven treatment paradigms in HNSCC.

## Section 4: Combination strategies to overcome PI3K inhibitor resistance

The early chapters of my thesis examined compensatory signals that may allow cell survival in the presence of PI3K inhibition by specifically evaluating pathways that were known, based on previous data, to mediate PI3K inhibitor resistance. In the fifth chapter of my dissertation, however, I profiled PI3K inhibitor resistance mechanisms in an unbiased manner using a small molecule screening approach. In doing so, I validated synergistic drug pairs including PI3K and EGFR inhibitors and identified new co-dependencies that had not been studied before in HNSCC.

We modeled our small molecule studies after the work of Garnett *et al*, who used a resazurin cell viability assay in 384-well plate format to test nearly 50,000 drug-cell line combinations (60). Our assay extended this approach to evaluate not only monotherapies, but also PI3K inhibitor combination treatments. We examined approximately 14,000 drug-cell line pairs with monotherapies, another set of 14,000 in combination with HS-173, and a third set of 14,000 in combination with BKM120. Using these experiments, some of the more novel PI3K inhibitor combinations that we identified included those targeting upstream RTKs, including ALK, IGF-1R, FAK, AURKA, and others.

Much of the previous work on compensatory resistance to PI3K inhibition has noted contributions from pathways downstream of PI3K or other co-dependent RTKs, including PDK1 (17), AKT (61), mTOR (62-64), and MEK (65, 66). In our studies, consistent with previous publications (65, 66), we observed that inhibiting PI3K and MEK was functionally similar to inhibiting PI3K and EGFR. Prior studies have also highlighted the importance of AKT in combination responses; these publications describe similar evidence of synergy when replacing PI3K inhibitors with AKT inhibition or siRNA (21) or displaying reduced AKT phosphorylation following combination treatment (19, 21, 22, 67, 68). Similarly, the work of Sambandam *et al.* demonstrated the importance of PDK1 inhibition in PI3K inhibitor responses by showing that: 1) reductions in the level of phosphorylated and total PDK1 were present in cell lines that were more sensitive to PI3K inhibition, and 2) AKT inhibitor MK-2206 and PDK1 inhibitor GSK2334470 were synergistic when used together, recapitulating or exceeding the effects of PI3K inhibitor monotherapy (17). In contrast, we observed that AKT phosphorylation was similarly reduced following treatment with PI3K monotherapy and ineffective combinations as compared to treatment with synergistic drug-pairs. This may suggest that AKT inhibition is

necessary but not sufficient for response to PI3K inhibitor therapy. PDK1 phosphorylation was also largely unchanged with PI3K mono- and dual-therapy in our models. Furthermore, we observed little benefit when adding PDK1, AKT, or mTOR inhibitors to PI3K inhibitors. Based on these findings, we can conclude that although PDK1, AKT, and mTOR are downstream effectors common to PI3K and the other RTKs involved in our synergistic drug pairs, additional mechanisms are responsible for combination effects.

The results of our small molecule screen suggest that PI3K inhibitor combinations targeting upstream rather than downstream signals may be a more effective means of blocking HNSCC proliferation. Of the top ranked combination inhibitors from our profiling experiments, 11 target RTKs, one inhibits HDACs, and three block downstream signaling molecules (AKT and Bcl-2). While individual cases may be driven by resistance through AKT, mTOR, or other similar pathways, this data may indicate that broader effects are achieved by inhibiting upstream signals. This result is not necessarily unexpected—cancer cells can compensate and bypass the inhibition of specific downstream signals more easily than they can overcome the more global changes induced by inhibition of RTKs like EGFR. Accordingly, the mechanism underlying the effects of any RTK and PI3K combination may involve a complex array of network-level changes, a decrease in several important signaling nodes simultaneously rather than a profound reduction in any one effector. If this is the case, multiple separate RTK-targeting agents may be sufficient to shift cancer cells toward response to PI3K inhibition.

Recent work has successfully implicated upstream inhibition in combination with PI3K targeting drugs to improve responses in HNSCC. For instance, based on earlier work showing that the dimerization of AXL and EGFR promotes signaling through PI3K and mTOR (but interestingly, not AKT) to limit the efficacy of PI3K inhibitors, Badarni *et al.* chose to identify

and target the transcription factors that were responsible for the increased expression of AXL in HNSCCs. They found that a c-JUN, a member of the AP-1 transcription factor (TF) complex, was likely responsible for the upregulation of AXL and that blocking the activity of this TF improved the response to PI3K inhibitor BYL719 (69). As a second example, Brand and co-authors blocked HER3 signaling as a means of reversing PI3K inhibitors resistance mediated by HPV oncoproteins E6 and E7 in HPV positive HNSCCs (70). These studies support the role of RTKs in HNSCC resistance mechanisms and validate that combination PI3K and RTK blockade may result in improved PI3K inhibitor responses.

In further support of this idea is the ability of many HNSCC cell lines to respond to multiple pairs of inhibitors rather than to just one dual-therapy. For example, UM-SCC-108 cells respond to the combination of PI3K inhibitor and EGFR inhibitor, MEK inhibitor, ALK inhibitor, IGF-1R inhibitor, FAK inhibitor, or AURKA inhibitor. Similar responses in UM-SCC-108 are also achieved with the combination of EGFR and FGFR or EGFR and IGF-1R inhibitors. This data could suggest the existence of one or two critical downstream signaling molecules that are sufficiently blocked only via multiple levels of inhibition. Alternatively, it could indicate that UM-SCC-108 cells have several RTK dependencies and that the loss of a subset of these dependencies results in cell death. The complexity of responses in this model and others lead me to favor the latter hypothesis. Under this premise, the cell would have to activate a single additional pathway (one of many possible such pathways, but likely one that has a broad effect on cell function) in order to regain the potential to grow and divide. The specific pathway responsible for recurrence is dependent on the selective pressure being applied and certainly could vary between and even within tumors from individual patients. While the effect of inhibiting PI3K and compensatory signaling may initially result in cell death and tumor

regression, the ability of other pathways to bypass even this dual-blockade should be noted. The emergence of secondary resistance mechanisms is likely and this phenomenon may be responsible for the recurrence of HNSCC and other cancer types following targeted therapy treatment.

In our HNSCC cell lines, treatment with RTK inhibitor brigatinib was one of the most effective means of sensitization to PI3K inhibition. Brigatinib is conventionally regarded an inhibitor of ALK and used clinically to treat ALK-fusion positive lung cancer patients. ALK signaling is not commonly considered as a resistance mechanism in HNSCC since fusion events are rare and ALK expression is often quite low in this cancer type. Nevertheless, previous studies have shown that EGFR inhibitors may increase the expression of ALK and display greater efficacy with ALK inhibitors (71, 72); this work demonstrates that ALK signaling is indeed important in some head and neck cancers. PI3K and ALK dual-therapy, however, has not been considered in HNSCC. The only previous studies of PI3K and ALK inhibitors examine such combinations in the context of other tumor types driven by ALK signaling due to fusion with EML4 or other genes (68, 73-75). Our work, then, may represent the first evidence of interaction between PI3K and ALK signaling in the absence of ALK gene fusion.

However, brigatinib is not a perfectly selective inhibitor of ALK—it also displays activity at IGF-1R, EGFR, and other RTKs, especially at higher concentrations (76, 77). While ALK inhibition may be an important component of the response to combinations of brigatinib and PI3K inhibitor, we cannot exclude the possibility that the blockade of IGF-1R and/or EGFR contribute at least partially to this response. Our screening data and validation show that IGF-1R inhibition can improve responses to PI3K targeting therapy, a phenomenon that has been previously observed in multiple other cancer types (78, 79). As discussed above, PI3K and

EGFR combination therapy is also well-validated in HNSCC. The genetic knockouts of *ALK* and *IGF-1R* that we generated in combination-responsive HSC-4 cells offer insight into the effect of blocking an individual RTK, mimicking a perfectly selective pharmacologic treatment. ALK knockout HSC-4 cells are more sensitive to monotherapy with AKT inhibitor GDC-0068 than wildtype HSC-4 cells. Responses to PI3K inhibition are not markedly different in the knockout model, suggests that ALK alone is not responsible for the synergy of ALK and PI3K targeting agents in HNSCC. In spite of this, we cannot conclude that ALK does not play a role in the combination response as the process of developing such a cell line may have introduced other compensatory changes (such as the upregulation of another RTK) to prevent response to single-agent PI3K inhibitor.

While the mechanistic basis for responses to pictilisib and brigatinib has not been fully elucidated, co-treatment with these agents three times per week inhibited tumor growth in a cell-line derived xenograft mouse model. However, despite the significant result observed after a three-week course with these inhibitors, tumors did progress as treatment continued for extended lengths of time. This observation is in support of the development of additional compensatory mechanisms mediating treatment resistance, as described above. Although the combination of PI3K and ALK inhibitor extended survival for weeks past what would have been observed in mice with vehicle- and brigatinib-treated tumors, our study motivates further exploration of compensatory signaling in HNSCC and the development of improved treatment paradigms including those leveraging radiation, targeted therapies (against both RTKs and other important signaling molecules), and immunotherapies.

My thesis has focused primarily on the use of targeted therapies with PI3K inhibitors, but emerging data also suggests that the PI3K pathway may interact with immune responses and

improve the efficacy of immune checkpoint receptor (ICR) blockade. One indication of the involvement of the PI3K pathway in responses to immunotherapies is based on data using models with loss of tumor suppressor *PTEN*, which acts in opposition to PI3K signaling. In multiple cancer types, increased expression of PD-L1 has been observed in models with loss of *PTEN* (80-83), and there is some evidence that this may also be the case in HNSCC (84).

The role of PI3K signaling in cellular metabolism represents one key means by which it may contribute to not only cell proliferation but also immune responses. Specifically, PI3K promotes glucose uptake and enhances glycolysis via the mTOR-AKT pathway (85). This contributes to the prioritization of the aerobic glycolysis pathway over oxidative phosphorylation, a phenomenon considered a hallmark of cancer and coined as the Warburg effect (86). As a result, cancer cells with activating mutations or amplifications of *PIK3CA* may directly compete with cytotoxic T-lymphocytes (CTLs) for the limited glucose supply in the tumor microenvironment (TME). Indeed, extracellular glucose is a key nutrient source to maintain CTL effector function. Innate immune priming expands CTLs and is ideally achieved with ICR blockade. Maintaining CTL activation entails rapid genome replication, active migration to come in proximity to target tumor cells, production of a large amount of cytokines *de novo*, and establishment of immunologic synapses—all of these processes are metabolically demanding and require bioenergetics support. Furthermore, deprivation of extracellular glucose leads to rapid CTL exhaustion (87-91). Thus, inhibiting the PI3K pathway eliminates one competing factor for extracellular glucose and reprograms cancer metabolism to favor sustained immune effector activation.

Beyond its actions to promote the Warburg effect in tumor cells, the PI3K pathway also independently enhances CTL exhaustion in HNSCCs. One potential adaptive resistance

mechanism to ICR blockade is the compensatory upregulation of other ICR members, including T-cell Ig and mucin domain-3 protein (TIM-3). Utilizing clinical HNSCC specimens, a recent study demonstrated that the ICRs PD-1 and TIM-3 are co-expressed by the most exhausted and dysfunctional CTLs. Interestingly, PD-1 blockade-treated HNSCC TILs exhibit further upregulation of TIM-3 expression, and this response is dependent on the activation of the PI3K/AKT pathway (92). Thus, targeting the PI3K pathway can also directly prevent compensatory induction of additional ICR signaling to maintain CTL activation and might mediate improved responses to ICR blockade. Additional studies are needed to further explore these interactions and determine the optimal means of combining PI3K inhibitors with immunotherapy in HNSCC.

## Section 5: Future Directions

For each project discussed in my thesis, multiple additional studies could be performed to further our understanding of the role of specific signaling pathways in PI3K inhibitor resistance. In relation to the contribution of EGFR signaling, the further work I think would be most informative would extend my findings on the efficacy of irreversible EGFR inhibitor combinations to *in vivo* models. I would like to use xenografts to evaluate PI3K and reversible or irreversible EGFR inhibitor monotherapies compared to PI3K and reversible or irreversible EGFR inhibitor combinations; I hypothesize based on my *in vitro* work that the combination of PI3K and irreversible EGFR inhibitor would be more effective in reducing tumor burden than PI3K and reversible EGFR inhibitor combination or any monotherapy treatment. Additionally, given that cetuximab has been used most widely to target EGFR in the clinic and works via another mechanism, I would be interested in comparing PI3K and irreversible EGFR

combination to PI3K and cetuximab or appropriate monotherapy treatments in mouse models. If this experiment showed that PI3K and irreversible EGFR combinations are most effective, it would support the advance of such drug pairs into further preclinical and clinical studies.

To extend my studies using our transgenic mouse model of the hotspot H1047R *Pik3ca* mutation in HNSCC, I think it would be useful to consider the effects of combining this alteration with additional transgenes. For example, we could replace the mice with *Notch1* loss that we studied with animals displaying other Notch pathway alterations (*dnMaml*, *Rpbj* KO, etc) or mutant *p53*. Evaluating the time to endpoint for mice of each of these PI3K aberrant and Notch deficient strains is warranted based on the disparate effects observed with various mechanisms of Notch inactivation in the literature (40, 59). The specific co-altered strains that display the greatest acceleration in time to tumor formation could provide insight on the subset of HNSCC patients with loss-of-function alterations in *NOTCH1* and other genes that might be most likely to respond to PI3K inhibition. Conversely, strains without accelerated tumor formation might represent genetic subsets that would not be responsive to these therapies. Furthermore, it will be informative to compare these results in Notch GEMMs to those displaying alteration in p53, the most commonly mutated gene in HNSCC. Previous preclinical work has demonstrated that PI3K inhibition may be more effective in p53 wild-type models (93); thus, I hypothesize that *K14*; *p53* mutant; *Pik3ca*$^{H1047R}$ mice might display significantly shorter time to endpoint following 4-NQO exposure as compared to *K14*; *p53* mutant, *K14*; *Pik3ca*$^{H1047R}$ strains. However, if I were to observe result—delayed time to tumor formation in *K14*; *p53* mutant; *Pik3ca*$^{H1047R}$ mice—it would provide further validation for the the results of the BERIL-1 study, which indicated improved responses to buparlisib in patients with *p53* altered tumors.

Finally, to continue my studies of PI3K and upstream RTK inhibition (including ALK, IGF-1R, etc), I would 1) perform experiments to further delineate the critical target of brigatinib and other ALK/IGF-1R inhibitors and 2) consider the mechanisms of resistance that may develop following combination treatments that initially result in synergy. The generation of HSC-4 or other combination-responsive cell lines with CRISPR/Cas9 knockout of ALK alone, IGF-1R alone, or *both* ALK and IGF-1R would could reveal the relative contributions of each of these pathways in PI3K inhibitor resistance. Furthermore, unbiased evaluation of gene expression and protein level changes (using RNA sequencing or proteomic approaches, for example) in these cell lines would suggest other compensatory signals that may drive resistance to PI3K inhibitor monotherapy. As an additional means of considering how HNSCCs might escape PI3K and ALK/IGF-1R inhibitor blockade, I could develop a model of acquired resistance to these combination treatments by culturing cells in pictilisib and brigatinib for long periods of time and isolating clones that survived this paradigm. Comparing the genetic and drug sensitivity profiles of such clones would provide further insights on secondary resistance mechanisms. Evaluation of DNA, RNA, and protein extracted from xenografts following extended treatment with the same drug combinations could also be used to evaluate these questions in the *in vivo* setting.

Strides continue to be made regarding the most effective use of PI3K inhibitors in HNSCC and other cancer types. Nevertheless, challenges remain in areas including toxicity, patient selection, and primary and secondary resistance to these agents. More work is needed to develop safer, more effective drugs, establish biomarkers for response, and elucidate and target critical resistance mechanisms. My studies serve as a contribution in these efforts. With the

combined efforts of the cancer research community, I hope that in time PI3K inhibitors will have a place among the FDA approved treatments for HNSCC.

## References

1. Leemans CR, Braakhuis BJ, Brakenhoff RH. The molecular biology of head and neck cancer. Nature reviews Cancer. 2011;11(1):9-22. Epub 2010/12/17. doi: 10.1038/nrc2982. PubMed PMID: 21160525.

2. Chinn SB, Spector ME, Bellile EL, Rozek LS, Lin T, Teknos TN, Prince ME, Bradford CR, Urba SG, Carey TE, Eisbruch A, Wolf GT, Worden FP, Chepeha DB. Efficacy of induction selection chemotherapy vs primary surgery for patients with advanced oral cavity carcinoma. JAMA otolaryngology-- head & neck surgery. 2014;140(2):134-42. Epub 2013/12/29. doi: 10.1001/jamaoto.2013.5892. PubMed PMID: 24370563; PMCID: Pmc4103099.

3. Chaturvedi P, Singhavi H, Malik A, Nair D. Outcome of Head and Neck Squamous Cell Cancers in Low-Resource Settings: Challenges and Opportunities. Otolaryngologic clinics of North America. 2018;51(3):619-29. Epub 2018/03/05. doi: 10.1016/j.otc.2018.01.008. PubMed PMID: 29501327.

4. Gingerich MA, Smith JD, Michmerhuizen NL, Ludwig M, Devenport S, Matovina C, Brenner C, Chinn SB. Comprehensive review of genetic factors contributing to head and neck squamous cell carcinoma development in low-risk, nontraditional patients. Head & neck. 2018;40(5):943-54. Epub 2018/02/11. doi: 10.1002/hed.25057. PubMed PMID: 29427520; PMCID: PMC5912962.

5. Comprehensive genomic characterization of head and neck squamous cell carcinomas. Nature. 2015;517(7536):576-82. Epub 2015/01/30. doi: 10.1038/nature14129. PubMed PMID: 25631445; PMCID: Pmc4311405.

6. Burtness B, Goldwasser MA, Flood W, Mattar B, Forastiere AA. Phase III randomized trial of cisplatin plus placebo compared with cisplatin plus cetuximab in metastatic/recurrent head and neck cancer: an Eastern Cooperative Oncology Group study. Journal of clinical oncology : official journal of the American Society of Clinical Oncology. 2005;23(34):8646-54. Epub 2005/11/30. doi: 10.1200/jco.2005.02.4646. PubMed PMID: 16314626.

7. Psyrri A, Lee JW, Pectasides E, Vassilakopoulou M, Kosmidis EK, Burtness BA, Rimm DL, Wanebo HJ, Forastiere AA. Prognostic biomarkers in phase II trial of cetuximab-containing induction and chemoradiation in resectable HNSCC: Eastern cooperative oncology group E2303. Clinical cancer research : an official journal of the American Association for Cancer Research. 2014;20(11):3023-32. Epub 2014/04/05. doi: 10.1158/1078-0432.Ccr-14-0113. PubMed PMID: 24700741; PMCID: PMC4049169.

8. Machiels JP, Haddad RI, Fayette J, Licitra LF, Tahara M, Vermorken JB, Clement PM, Gauler T, Cupissol D, Grau JJ, Guigay J, Caponigro F, de Castro G, Jr., de Souza Viana L, Keilholz U, Del Campo JM, Cong XJ, Ehrnrooth E, Cohen EE. Afatinib versus methotrexate as second-line treatment in patients with recurrent or metastatic squamous-cell carcinoma of the head and neck progressing on or after platinum-based therapy (LUX-Head & Neck 1): an open-

label, randomised phase 3 trial. The Lancet Oncology. 2015;16(5):583-94. Epub 2015/04/22. doi: 10.1016/s1470-2045(15)70124-5. PubMed PMID: 25892145.

9. Cohen EEW, Licitra LF, Burtness B, Fayette J, Gauler T, Clement PM, Grau JJ, Del Campo JM, Mailliez A, Haddad RI, Vermorken JB, Tahara M, Guigay J, Geoffrois L, Merlano MC, Dupuis N, Kramer N, Cong XJ, Gibson N, Solca F, Ehrnrooth E, Machiels JH. Biomarkers predict enhanced clinical outcomes with afatinib versus methotrexate in patients with second-line recurrent and/or metastatic head and neck cancer. Annals of oncology : official journal of the European Society for Medical Oncology. 2017;28(10):2526-32. Epub 2017/09/30. doi: 10.1093/annonc/mdx344. PubMed PMID: 28961833; PMCID: PMC5834024.

10. Eze N, Lee JW, Yang DH, Zhu F, Neumeister V, Sandoval-Schaefer T, Mehra R, Ridge JA, Forastiere A, Chung CH, Burtness B. PTEN loss is associated with resistance to cetuximab in patients with head and neck squamous cell carcinoma. Oral oncology. 2019;91:69-78. Epub 2019/03/31. doi: 10.1016/j.oraloncology.2019.02.026. PubMed PMID: 30926065.

11. Keysar SB, Astling DP, Anderson RT, Vogler BW, Bowles DW, Morton JJ, Paylor JJ, Glogowska MJ, Le PN, Eagles-Soukup JR, Kako SL, Takimoto SM, Sehrt DB, Umpierrez A, Pittman MA, Macfadden SM, Helber RM, Peterson S, Hausman DF, Said S, Leem TH, Goddard JA, Arcaroli JJ, Messersmith WA, Robinson WA, Hirsch FR, Varella-Garcia M, Raben D, Wang XJ, Song JI, Tan AC, Jimeno A. A patient tumor transplant model of squamous cell cancer identifies PI3K inhibitors as candidate therapeutics in defined molecular bins. Molecular oncology. 2013;7(4):776-90. Epub 2013/04/24. doi: 10.1016/j.molonc.2013.03.004. PubMed PMID: 23607916; PMCID: PMC3760013.

12. Andre F, Ciruelos E, Rubovszky G, Campone M, Loibl S, Rugo HS, Iwata H, Conte P, Mayer IA, Kaufman B, Yamashita T, Lu YS, Inoue K, Takahashi M, Papai Z, Longin AS, Mills D, Wilke C, Hirawat S, Juric D. Alpelisib for PIK3CA-Mutated, Hormone Receptor-Positive Advanced Breast Cancer. The New England journal of medicine. 2019;380(20):1929-40. Epub 2019/05/16. doi: 10.1056/NEJMoa1813904. PubMed PMID: 31091374.

13. Soulieres D, Licitra L, Mesia R, Remenar E, Li SH, Karpenko A, Chol M, Wang YA, Solovieff N, Bourdeau L, Sellami D, Faivre S. Molecular Alterations and Buparlisib Efficacy in Patients with Squamous Cell Carcinoma of the Head and Neck: Biomarker Analysis from BERIL-1. Clinical cancer research : an official journal of the American Association for Cancer Research. 2018;24(11):2505-16. Epub 2018/03/02. doi: 10.1158/1078-0432.Ccr-17-2644. PubMed PMID: 29490986.

14. Jimeno A, Bauman JE, Weissman C, Adkins D, Schnadig I, Beauregard P, Bowles DW, Spira A, Levy B, Seetharamu N, Hausman D, Walker L, Rudin CM, Shirai K. A randomized, phase 2 trial of docetaxel with or without PX-866, an irreversible oral phosphatidylinositol 3-kinase inhibitor, in patients with relapsed or metastatic head and neck squamous cell cancer. Oral oncology. 2015;51(4):383-8. Epub 2015/01/17. doi: 10.1016/j.oraloncology.2014.12.013. PubMed PMID: 25593016.

15. Chau NG, Li YY, Jo VY, Rabinowits G, Lorch JH, Tishler RB, Margalit DN, Schoenfeld JD, Annino DJ, Goguen LA, Thomas T, Becker H, Haddad T, Krane JF, Lindeman NI, Shapiro GI, Haddad RI, Hammerman PS. Incorporation of Next-Generation Sequencing into Routine Clinical Care to Direct Treatment of Head and Neck Squamous Cell Carcinoma. Clinical cancer research : an official journal of the American Association for Cancer Research. 2016;22(12):2939-49. Epub 2016/01/15. doi: 10.1158/1078-0432.Ccr-15-2314. PubMed PMID: 26763254.

16. Janku F, Wheler JJ, Naing A, Falchook GS, Hong DS, Stepanek VM, Fu S, Piha-Paul SA, Lee JJ, Luthra R, Tsimberidou AM, Kurzrock R. PIK3CA mutation H1047R is associated with response to PI3K/AKT/mTOR signaling pathway inhibitors in early-phase clinical trials. Cancer Res. 2013;73(1):276-84. Epub 2012/10/16. doi: 10.1158/0008-5472.can-12-1726. PubMed PMID: 23066039; PMCID: Pmc3537862.

17. Sambandam V, Frederick MJ, Shen L, Tong P, Rao X, Peng S, Singh R, Mazumdar T, Huang C, Li Q, Pickering CR, Myers JN, Wang J, Johnson FM. PDK1 mediates NOTCH1-mutated head and neck squamous carcinoma vulnerability to therapeutic PI3K/mTOR inhibition. Clinical cancer research : an official journal of the American Association for Cancer Research. 2019. Epub 2019/02/17. doi: 10.1158/1078-0432.Ccr-18-3276. PubMed PMID: 30770351.

18. Liu TJ, LaFortune T, Honda T, Ohmori O, Hatakeyama S, Meyer T, Jackson D, de Groot J, Yung WK. Inhibition of both focal adhesion kinase and insulin-like growth factor-I receptor kinase suppresses glioma proliferation in vitro and in vivo. Molecular cancer therapeutics. 2007;6(4):1357-67. Epub 2007/04/14. doi: 10.1158/1535-7163.Mct-06-0476. PubMed PMID: 17431114.

19. Rebucci M, Peixoto P, Dewitte A, Wattez N, De Nuncques MA, Rezvoy N, Vautravers-Dewas C, Buisine MP, Guerin E, Peyrat JP, Lartigau E, Lansiaux A. Mechanisms underlying resistance to cetuximab in the HNSCC cell line: role of AKT inhibition in bypassing this resistance. International journal of oncology. 2011;38(1):189-200. Epub 2010/11/27. PubMed PMID: 21109940.

20. Anisuzzaman AS, Haque A, Wang D, Rahman MA, Zhang C, Chen Z, Chen ZG, Shin DM, Amin AR. In Vitro and In Vivo Synergistic Antitumor Activity of the Combination of BKM120 and Erlotinib in Head and Neck Cancer: Mechanism of Apoptosis and Resistance. Molecular cancer therapeutics. 2017;16(4):729-38. Epub 2017/01/26. doi: 10.1158/1535-7163.Mct-16-0683. PubMed PMID: 28119490.

21. Silva-Oliveira RJ, Melendez M, Martinho O, Zanon MF, de Souza Viana L, Carvalho AL, Reis RM. AKT can modulate the in vitro response of HNSCC cells to irreversible EGFR inhibitors. Oncotarget. 2017;8(32):53288-301. Epub 2017/09/09. doi: 10.18632/oncotarget.18395. PubMed PMID: 28881811; PMCID: PMC5581110.

22. Young NR, Liu J, Pierce C, Wei TF, Grushko T, Olopade OI, Liu W, Shen C, Seiwert TY, Cohen EE. Molecular phenotype predicts sensitivity of squamous cell carcinoma of the head and neck to epidermal growth factor receptor inhibition. Molecular oncology. 2013;7(3):359-68.

Epub 2012/12/04. doi: 10.1016/j.molonc.2012.11.001. PubMed PMID: 23200321; PMCID: Pmc3661759.

23. Wang Z, Martin D, Molinolo AA, Patel V, Iglesias-Bartolome R, Degese MS, Vitale-Cross L, Chen Q, Gutkind JS. mTOR co-targeting in cetuximab resistance in head and neck cancers harboring PIK3CA and RAS mutations. Journal of the National Cancer Institute. 2014;106(9). Epub 2014/08/08. doi: 10.1093/jnci/dju215. PubMed PMID: 25099740; PMCID: PMC4133928.

24. Jimeno A, Kulesza P, Wheelhouse J, Chan A, Zhang X, Kincaid E, Chen R, Clark DP, Forastiere A, Hidalgo M. Dual EGFR and mTOR targeting in squamous cell carcinoma models, and development of early markers of efficacy. British journal of cancer. 2007;96(6):952-9. Epub 2007/03/08. doi: 10.1038/sj.bjc.6603656. PubMed PMID: 17342092; PMCID: PMC2360107.

25. Bozec A, Ebran N, Radosevic-Robin N, Sudaka A, Monteverde M, Toussan N, Etienne-Grimaldi MC, Nigro CL, Merlano M, Penault-Llorca F, Milano G. Combination of mTOR and EGFR targeting in an orthotopic xenograft model of head and neck cancer. The Laryngoscope. 2016;126(4):E156-63. Epub 2015/11/26. doi: 10.1002/lary.25754. PubMed PMID: 26597440.

26. Michmerhuizen NL, Leonard E, Matovina C, Harris M, Herbst G, Kulkarni A, Zhai J, Jiang H, Carey TE, Brenner JC. Rationale for Using Irreversible Epidermal Growth Factor Receptor Inhibitors in Combination with Phosphatidylinositol 3-Kinase Inhibitors for Advanced Head and Neck Squamous Cell Carcinoma. Molecular pharmacology. 2019;95(5):528-36. Epub 2019/03/13. doi: 10.1124/mol.118.115162. PubMed PMID: 30858165.

27. Bauman JE, Arias-Pulido H, Lee SJ, Fekrazad MH, Ozawa H, Fertig E, Howard J, Bishop J, Wang H, Olson GT, Spafford MJ, Jones DV, Chung CH. A phase II study of temsirolimus and erlotinib in patients with recurrent and/or metastatic, platinum-refractory head and neck squamous cell carcinoma. Oral oncology. 2013;49(5):461-7. Epub 2013/02/07. doi: 10.1016/j.oraloncology.2012.12.016. PubMed PMID: 23384718; PMCID: PMC3805493.

28. Massarelli E, Lin H, Ginsberg LE, Tran HT, Lee JJ, Canales JR, Williams MD, Blumenschein GR, Jr., Lu C, Heymach JV, Kies MS, Papadimitrakopoulou V. Phase II trial of everolimus and erlotinib in patients with platinum-resistant recurrent and/or metastatic head and neck squamous cell carcinoma. Annals of oncology : official journal of the European Society for Medical Oncology. 2015;26(7):1476-80. Epub 2015/05/31. doi: 10.1093/annonc/mdv194. PubMed PMID: 26025965; PMCID: PMC4855241.

29. Lattanzio L, Tonissi F, Monteverde M, Vivenza D, Russi E, Milano G, Merlano M, Lo Nigro C. Treatment effect of buparlisib, cetuximab and irradiation in wild-type or PI3KCA-mutated head and neck cancer cell lines. Investigational new drugs. 2015;33(2):310-20. Epub 2015/01/22. doi: 10.1007/s10637-015-0210-1. PubMed PMID: 25603975.

30. Bussink J, van der Kogel AJ, Kaanders JH. Activation of the PI3-K/AKT pathway and implications for radioresistance mechanisms in head and neck cancer. The Lancet Oncology.

2008;9(3):288-96. Epub 2008/03/01. doi: 10.1016/s1470-2045(08)70073-1. PubMed PMID: 18308254.

31. Bozec A, Ebran N, Radosevic-Robin N, Chamorey E, Yahia HB, Marcie S, Gautier M, Penault-Llorca F, Milano G. Combination of phosphotidylinositol-3-kinase targeting with cetuximab and irradiation: A preclinical study on an orthotopic xenograft model of head and neck cancer. Head & neck. 2017;39(1):151-9. Epub 2016/08/11. doi: 10.1002/hed.24560. PubMed PMID: 27507562.

32. Blas K, Wilson TG, Tonlaar N, Galoforo S, Hana A, Marples B, Wilson GD. Dual blockade of PI3K and MEK in combination with radiation in head and neck cancer. Clinical and translational radiation oncology. 2018;11:1-10. Epub 2018/07/18. doi: 10.1016/j.ctro.2018.04.003. PubMed PMID: 30014041; PMCID: PMC6019866.

33. Stransky N, Egloff AM, Tward AD, Kostic AD, Cibulskis K, Sivachenko A, Kryukov GV, Lawrence MS, Sougnez C, McKenna A, Shefler E, Ramos AH, Stojanov P, Carter SL, Voet D, Cortes ML, Auclair D, Berger MF, Saksena G, Guiducci C, Onofrio RC, Parkin M, Romkes M, Weissfeld JL, Seethala RR, Wang L, Rangel-Escareno C, Fernandez-Lopez JC, Hidalgo-Miranda A, Melendez-Zajgla J, Winckler W, Ardlie K, Gabriel SB, Meyerson M, Lander ES, Getz G, Golub TR, Garraway LA, Grandis JR. The mutational landscape of head and neck squamous cell carcinoma. Science (New York, NY). 2011;333(6046):1157-60. Epub 2011/07/30. doi: 10.1126/science.1208130. PubMed PMID: 21798893; PMCID: Pmc3415217.

34. Lui VW, Hedberg ML, Li H, Vangara BS, Pendleton K, Zeng Y, Lu Y, Zhang Q, Du Y, Gilbert BR, Freilino M, Sauerwein S, Peyser ND, Xiao D, Diergaarde B, Wang L, Chiosea S, Seethala R, Johnson JT, Kim S, Duvvuri U, Ferris RL, Romkes M, Nukui T, Kwok-Shing Ng P, Garraway LA, Hammerman PS, Mills GB, Grandis JR. Frequent mutation of the PI3K pathway in head and neck cancer defines predictive biomarkers. Cancer discovery. 2013;3(7):761-9. Epub 2013/04/27. doi: 10.1158/2159-8290.cd-13-0103. PubMed PMID: 23619167; PMCID: Pmc3710532.

35. Agrawal N, Frederick MJ, Pickering CR, Bettegowda C, Chang K, Li RJ, Fakhry C, Xie TX, Zhang J, Wang J, Zhang N, El-Naggar AK, Jasser SA, Weinstein JN, Trevino L, Drummond JA, Muzny DM, Wu Y, Wood LD, Hruban RH, Westra WH, Koch WM, Califano JA, Gibbs RA, Sidransky D, Vogelstein B, Velculescu VE, Papadopoulos N, Wheeler DA, Kinzler KW, Myers JN. Exome sequencing of head and neck squamous cell carcinoma reveals inactivating mutations in NOTCH1. Science (New York, NY). 2011;333(6046):1154-7. Epub 2011/07/30. doi: 10.1126/science.1206923. PubMed PMID: 21798897; PMCID: Pmc3162986.

36. Ludwig ML, Kulkarni A, Birkeland AC, Michmerhuizen NL, Foltin SK, Mann JE, Hoesli RC, Devenport SN, Jewell BM, Shuman AG, Spector ME, Carey TE, Jiang H, Brenner JC. The genomic landscape of UM-SCC oral cavity squamous cell carcinoma cell lines. Oral oncology. 2018;87:144-51. Epub 2018/12/12. doi: 10.1016/j.oraloncology.2018.10.031. PubMed PMID: 30527230; PMCID: PMC6349383.

37. Mann JE, Kulkarni A, Birkeland AC, Kafelghazal J, Eisenberg J, Jewell BM, Ludwig ML, Spector ME, Jiang H, Carey TE, Brenner JC. The molecular landscape of the University of Michigan laryngeal squamous cell carcinoma cell line panel. Head & neck. 2019. Epub 2019/05/16. doi: 10.1002/hed.25803. PubMed PMID: 31090975.

38. Du L, Chen X, Cao Y, Lu L, Zhang F, Bornstein S, Li Y, Owens P, Malkoski S, Said S, Jin F, Kulesz-Martin M, Gross N, Wang XJ, Lu SL. Overexpression of PIK3CA in murine head and neck epithelium drives tumor invasion and metastasis through PDK1 and enhanced TGFbeta signaling. Oncogene. 2016;35(35):4641-52. Epub 2016/02/16. doi: 10.1038/onc.2016.1. PubMed PMID: 26876212; PMCID: PMC4985507.

39. Squarize CH, Castilho RM, Abrahao AC, Molinolo A, Lingen MW, Gutkind JS. PTEN deficiency contributes to the development and progression of head and neck cancer. Neoplasia (New York, NY). 2013;15(5):461-71. Epub 2013/05/02. PubMed PMID: 23633918; PMCID: PMC3638349.

40. Nyman PE, Buehler D, Lambert PF. Loss of Function of Canonical Notch Signaling Drives Head and Neck Carcinogenesis. Clinical cancer research : an official journal of the American Association for Cancer Research. 2018;24(24):6308-18. Epub 2018/08/09. doi: 10.1158/1078-0432.Ccr-17-3535. PubMed PMID: 30087145; PMCID: PMC6295262.

41. Cerami E, Gao J, Dogrusoz U, Gross BE, Sumer SO, Aksoy BA, Jacobsen A, Byrne CJ, Heuer ML, Larsson E, Antipin Y, Reva B, Goldberg AP, Sander C, Schultz N. The cBio cancer genomics portal: an open platform for exploring multidimensional cancer genomics data. Cancer discovery. 2012;2(5):401-4. Epub 2012/05/17. doi: 10.1158/2159-8290.cd-12-0095. PubMed PMID: 22588877; PMCID: Pmc3956037.

42. Gao J, Aksoy BA, Dogrusoz U, Dresdner G, Gross B, Sumer SO, Sun Y, Jacobsen A, Sinha R, Larsson E, Cerami E, Sander C, Schultz N. Integrative analysis of complex cancer genomics and clinical profiles using the cBioPortal. Science signaling. 2013;6(269):pl1. Epub 2013/04/04. doi: 10.1126/scisignal.2004088. PubMed PMID: 23550210; PMCID: Pmc4160307.

43. Seiwert TY, Zuo Z, Keck MK, Khattri A, Pedamallu CS, Stricker T, Brown C, Pugh TJ, Stojanov P, Cho J, Lawrence MS, Getz G, Bragelmann J, DeBoer R, Weichselbaum RR, Langerman A, Portugal L, Blair E, Stenson K, Lingen MW, Cohen EE, Vokes EE, White KP, Hammerman PS. Integrative and comparative genomic analysis of HPV-positive and HPV-negative head and neck squamous cell carcinomas. Clinical cancer research : an official journal of the American Association for Cancer Research. 2015;21(3):632-41. Epub 2014/07/25. doi: 10.1158/1078-0432.Ccr-13-3310. PubMed PMID: 25056374; PMCID: PMC4305034.

44. Rawal RM, Joshi MN, Bhargava P, Shaikh I, Pandit AS, Patel RP, Patel S, Kothari K, Shah M, Saxena A, Bagatharia SB. Tobacco habituated and non-habituated subjects exhibit different mutational spectrums in head and neck squamous cell carcinoma. 3 Biotech. 2015;5(5):685-96. Epub 2015/01/01. doi: 10.1007/s13205-014-0267-0. PubMed PMID: 28324520; PMCID: PMC4569615.

45. Nguyen BC, Lefort K, Mandinova A, Antonini D, Devgan V, Della Gatta G, Koster MI, Zhang Z, Wang J, Tommasi di Vignano A, Kitajewski J, Chiorino G, Roop DR, Missero C, Dotto GP. Cross-regulation between Notch and p63 in keratinocyte commitment to differentiation. Genes & development. 2006;20(8):1028-42. Epub 2006/04/19. doi: 10.1101/gad.1406006. PubMed PMID: 16618808; PMCID: PMC1472299.

46. Koh LF, Ng BK, Bertrand J, Thierry F. Transcriptional control of late differentiation in human keratinocytes by TAp63 and Notch. Experimental dermatology. 2015;24(10):754-60. Epub 2015/05/28. doi: 10.1111/exd.12764. PubMed PMID: 26013684.

47. Zheng Y, Wang Z, Xiong X, Zhong Y, Zhang W, Dong Y, Li J, Zhu Z, Zhang W, Wu H, Gu W, Wu Y, Wang X, Song X. Membrane-tethered Notch1 exhibits oncogenic property via activation of EGFR-PI3K-AKT pathway in oral squamous cell carcinoma. Journal of cellular physiology. 2019;234(5):5940-52. Epub 2018/12/06. doi: 10.1002/jcp.27022. PubMed PMID: 30515785.

48. Piha-Paul SA, Munster PN, Hollebecque A, Argiles G, Dajani O, Cheng JD, Wang R, Swift A, Tosolini A, Gupta S. Results of a phase 1 trial combining ridaforolimus and MK-0752 in patients with advanced solid tumours. European journal of cancer (Oxford, England : 1990). 2015;51(14):1865-73. Epub 2015/07/23. doi: 10.1016/j.ejca.2015.06.115. PubMed PMID: 26199039; PMCID: PMC5693226.

49. Wang WM, Zhao ZL, Ma SR, Yu GT, Liu B, Zhang L, Zhang WF, Kulkarni AB, Sun ZJ, Zhao YF. Epidermal growth factor receptor inhibition reduces angiogenesis via hypoxia-inducible factor-1alpha and Notch1 in head neck squamous cell carcinoma. PloS one. 2015;10(2):e0119723. Epub 2015/02/28. doi: 10.1371/journal.pone.0119723. PubMed PMID: 25723392; PMCID: PMC4344331.

50. Zheng Y, Wang Z, Ding X, Dong Y, Zhang W, Zhang W, Zhong Y, Gu W, Wu Y, Song X. Combined Erlotinib and PF-03084014 treatment contributes to synthetic lethality in head and neck squamous cell carcinoma. Cell proliferation. 2018;51(3):e12424. Epub 2017/12/13. doi: 10.1111/cpr.12424. PubMed PMID: 29232766.

51. Schmitz S, Bindea G, Albu RI, Mlecnik B, Machiels JP. Cetuximab promotes epithelial to mesenchymal transition and cancer associated fibroblasts in patients with head and neck cancer. Oncotarget. 2015;6(33):34288-99. Epub 2015/10/06. doi: 10.18632/oncotarget.5924. PubMed PMID: 26437222; PMCID: PMC4741452.

52. Fu W, Lei C, Yu Y, Liu S, Li T, Lin F, Fan X, Shen Y, Ding M, Tang Y, Ye X, Yang Y, Hu S. EGFR/Notch Antagonists Enhance the Response to Inhibitors of the PI3K-Akt Pathway by Decreasing Tumor-Initiating Cell Frequency. Clinical cancer research : an official journal of the American Association for Cancer Research. 2019;25(9):2835-47. Epub 2019/01/24. doi: 10.1158/1078-0432.Ccr-18-2732. PubMed PMID: 30670492.

53. Liu J, Pan S, Hsieh MH, Ng N, Sun F, Wang T, Kasibhatla S, Schuller AG, Li AG, Cheng D, Li J, Tompkins C, Pferdekamper A, Steffy A, Cheng J, Kowal C, Phung V, Guo G,

Wang Y, Graham MP, Flynn S, Brenner JC, Li C, Villarroel MC, Schultz PG, Wu X, McNamara P, Sellers WR, Petruzzelli L, Boral AL, Seidel HM, McLaughlin ME, Che J, Carey TE, Vanasse G, Harris JL. Targeting Wnt-driven cancer through the inhibition of Porcupine by LGK974. Proceedings of the National Academy of Sciences of the United States of America. 2013;110(50):20224-9. Epub 2013/11/28. doi: 10.1073/pnas.1314239110. PubMed PMID: 24277854; PMCID: Pmc3864356.

54. Zhang ZP, Sun YL, Fu L, Gu F, Zhang L, Hao XS. Correlation of Notch1 expression and activation to cisplatin-sensitivity of head and neck squamous cell carcinoma. Ai zheng = Aizheng = Chinese journal of cancer. 2009;28(2):100-3. Epub 2009/06/25. PubMed PMID: 19550121.

55. Morgan KM, Fischer BS, Lee FY, Shah JJ, Bertino JR, Rosenfeld J, Singh A, Khiabanian H, Pine SR. Gamma Secretase Inhibition by BMS-906024 Enhances Efficacy of Paclitaxel in Lung Adenocarcinoma. Molecular cancer therapeutics. 2017;16(12):2759-69. Epub 2017/10/06. doi: 10.1158/1535-7163.Mct-17-0439. PubMed PMID: 28978720; PMCID: PMC5716926.

56. Li S, Ren B, Shi Y, Gao H, Wang J, Xin Y, Huang B, Liao S, Yang Y, Xu Z, Li Y, Zeng Q. Notch1 inhibition enhances DNA damage induced by cisplatin in cervical cancer. Experimental cell research. 2019;376(1):27-38. Epub 2019/01/29. doi: 10.1016/j.yexcr.2019.01.014. PubMed PMID: 30690027.

57. Chen X, Gong L, Ou R, Zheng Z, Chen J, Xie F, Huang X, Qiu J, Zhang W, Jiang Q, Yang Y, Zhu H, Shi Z, Yan X. Sequential combination therapy of ovarian cancer with cisplatin and gamma-secretase inhibitor MK-0752. Gynecologic oncology. 2016;140(3):537-44. Epub 2015/12/26. doi: 10.1016/j.ygyno.2015.12.011. PubMed PMID: 26704638.

58. Gu F, Ma Y, Zhang Z, Zhao J, Kobayashi H, Zhang L, Fu L. Expression of Stat3 and Notch1 is associated with cisplatin resistance in head and neck squamous cell carcinoma. Oncology reports. 2010;23(3):671-6. Epub 2010/02/04. doi: 10.3892/or_00000683. PubMed PMID: 20127005.

59. Demehri S, Turkoz A, Manivasagam S, Yockey LJ, Turkoz M, Kopan R. Elevated epidermal thymic stromal lymphopoietin levels establish an antitumor environment in the skin. Cancer cell. 2012;22(4):494-505. Epub 2012/10/20. doi: 10.1016/j.ccr.2012.08.017. PubMed PMID: 23079659; PMCID: PMC3480666.

60. Garnett MJ, Edelman EJ, Heidorn SJ, Greenman CD, Dastur A, Lau KW, Greninger P, Thompson IR, Luo X, Soares J, Liu Q, Iorio F, Surdez D, Chen L, Milano RJ, Bignell GR, Tam AT, Davies H, Stevenson JA, Barthorpe S, Lutz SR, Kogera F, Lawrence K, McLaren-Douglas A, Mitropoulos X, Mironenko T, Thi H, Richardson L, Zhou W, Jewitt F, Zhang T, O'Brien P, Boisvert JL, Price S, Hur W, Yang W, Deng X, Butler A, Choi HG, Chang JW, Baselga J, Stamenkovic I, Engelman JA, Sharma SV, Delattre O, Saez-Rodriguez J, Gray NS, Settleman J, Futreal PA, Haber DA, Stratton MR, Ramaswamy S, McDermott U, Benes CH. Systematic identification of genomic markers of drug sensitivity in cancer cells. Nature.

2012;483(7391):570-5. Epub 2012/03/31. doi: 10.1038/nature11005. PubMed PMID: 22460902; PMCID: Pmc3349233.

61. Erlich RB, Kherrouche Z, Rickwood D, Endo-Munoz L, Cameron S, Dahler A, Hazar-Rethinam M, de Long LM, Wooley K, Guminski A, Saunders NA. Preclinical evaluation of dual PI3K-mTOR inhibitors and histone deacetylase inhibitors in head and neck squamous cell carcinoma. British journal of cancer. 2012;106(1):107-15. Epub 2011/11/26. doi: 10.1038/bjc.2011.495. PubMed PMID: 22116303; PMCID: PMC3251846.

62. Tonlaar N, Galoforo S, Thibodeau BJ, Ahmed S, Wilson TG, Yumpo Cardenas P, Marples B, Wilson GD. Antitumor activity of the dual PI3K/MTOR inhibitor, PF-04691502, in combination with radiation in head and neck cancer. Radiotherapy and oncology : journal of the European Society for Therapeutic Radiology and Oncology. 2017;124(3):504-12. Epub 2017/08/22. doi: 10.1016/j.radonc.2017.08.001. PubMed PMID: 28823407.

63. Elkabets M, Vora S, Juric D, Morse N, Mino-Kenudson M, Muranen T, Tao J, Campos AB, Rodon J, Ibrahim YH, Serra V, Rodrik-Outmezguine V, Hazra S, Singh S, Kim P, Quadt C, Liu M, Huang A, Rosen N, Engelman JA, Scaltriti M, Baselga J. mTORC1 inhibition is required for sensitivity to PI3K p110alpha inhibitors in PIK3CA-mutant breast cancer. Science translational medicine. 2013;5(196):196ra99. Epub 2013/08/02. doi: 10.1126/scitranslmed.3005747. PubMed PMID: 23903756; PMCID: PMC3935768.

64. Ruicci KM, Pinto N, Khan MI, Yoo J, Fung K, MacNeil D, Mymryk JS, Barrett JW, Nichols AC. ERK-TSC2 signalling in constitutively-active HRAS mutant HNSCC cells promotes resistance to PI3K inhibition. Oral oncology. 2018;84:95-103. Epub 2018/08/18. doi: 10.1016/j.oraloncology.2018.07.010. PubMed PMID: 30115483.

65. Mohan S, Vander Broek R, Shah S, Eytan DF, Pierce ML, Carlson SG, Coupar JF, Zhang J, Cheng H, Chen Z, Van Waes C. MEK Inhibitor PD-0325901 Overcomes Resistance to PI3K/mTOR Inhibitor PF-5212384 and Potentiates Antitumor Effects in Human Head and Neck Squamous Cell Carcinoma. Clinical cancer research : an official journal of the American Association for Cancer Research. 2015;21(17):3946-56. Epub 2015/05/16. doi: 10.1158/1078-0432.ccr-14-3377. PubMed PMID: 25977343; PMCID: Pmc4558307.

66. Mazumdar T, Byers LA, Ng PK, Mills GB, Peng S, Diao L, Fan YH, Stemke-Hale K, Heymach JV, Myers JN, Glisson BS, Johnson FM. A comprehensive evaluation of biomarkers predictive of response to PI3K inhibitors and of resistance mechanisms in head and neck squamous cell carcinoma. Molecular cancer therapeutics. 2014;13(11):2738-50. Epub 2014/09/07. doi: 10.1158/1535-7163.Mct-13-1090. PubMed PMID: 25193510; PMCID: PMC4221385.

67. Benavente S, Huang S, Armstrong EA, Chi A, Hsu KT, Wheeler DL, Harari PM. Establishment and characterization of a model of acquired resistance to epidermal growth factor receptor targeting agents in human cancer cells. Clinical cancer research : an official journal of the American Association for Cancer Research. 2009;15(5):1585-92. Epub 2009/02/05. doi: 10.1158/1078-0432.ccr-08-2068. PubMed PMID: 19190133; PMCID: Pmc2903727.

68. Yang L, Li G, Zhao L, Pan F, Qiang J, Han S. Blocking the PI3K pathway enhances the efficacy of ALK-targeted therapy in EML4-ALK-positive nonsmall-cell lung cancer. Tumour biology : the journal of the International Society for Oncodevelopmental Biology and Medicine. 2014;35(10):9759-67. Epub 2014/06/29. doi: 10.1007/s13277-014-2252-y. PubMed PMID: 24972969.

69. Badarni M, Prasad M, Balaban N, Zorea J, Yegodayev KM, Ben-Zion J, Dinur AB, Grenman R, Rotblat B, Cohen L, Elkabets M. Repression of AXL expression by AP-1/JNK blockage overcomes resistance to PI3Ka therapy. JCI insight. 2019;5. Epub 2019/03/13. doi: 10.1172/jci.insight.125341. PubMed PMID: 30860495.

70. Brand TM, Hartmann S, Bhola NE, Li H, Zeng Y, O'Keefe RA, Ranall MV, Bandyopadhyay S, Soucheray M, Krogan NJ, Kemp C, Duvvuri U, LaVallee T, Johnson DE, Ozbun MA, Bauman JE, Grandis JR. Cross-talk Signaling between HER3 and HPV16 E6 and E7 Mediates Resistance to PI3K Inhibitors in Head and Neck Cancer. Cancer research. 2018;78(9):2383-95. Epub 2018/02/15. doi: 10.1158/0008-5472.Can-17-1672. PubMed PMID: 29440171.

71. Gonzales CB, De La Chapa JJ, Saikumar P, Singha PK, Dybdal-Hargreaves NF, Chavez J, Horning AM, Parra J, Kirma NB. Co-targeting ALK and EGFR parallel signaling in oral squamous cell carcinoma. Oral oncology. 2016;59:12-9. Epub 2016/07/18. doi: 10.1016/j.oraloncology.2016.05.007. PubMed PMID: 27424178; PMCID: PMC5460536.

72. Ouyang X, Barling A, Lesch A, Tyner JW, Choonoo G, Zheng C, Jeng S, West TM, Clayburgh D, Courtneidge SA, McWeeney SK, Kulesz-Martin M. Induction of anaplastic lymphoma kinase (ALK) as a novel mechanism of EGFR inhibitor resistance in head and neck squamous cell carcinoma patient-derived models. Cancer biology & therapy. 2018;19(10):921-33. Epub 2018/06/02. doi: 10.1080/15384047.2018.1451285. PubMed PMID: 29856687; PMCID: PMC6300392.

73. Redaelli S, Ceccon M, Zappa M, Sharma GG, Mastini C, Mauri M, Nigoghossian M, Massimino L, Cordani N, Farina F, Piazza R, Gambacorti-Passerini C, Mologni L. Lorlatinib Treatment Elicits Multiple On- and Off-Target Mechanisms of Resistance in ALK-Driven Cancer. Cancer research. 2018;78(24):6866-80. Epub 2018/10/17. doi: 10.1158/0008-5472.Can-18-1867. PubMed PMID: 30322862.

74. Tsuji T, Ozasa H, Aoki W, Aburaya S, Funazo T, Furugaki K, Yoshimura Y, Ajimizu H, Okutani R, Yasuda Y, Nomizo T, Uemasu K, Hasegawa K, Yoshida H, Yagi Y, Nagai H, Sakamori Y, Ueda M, Hirai T, Kim YH. Alectinib Resistance in ALK-Rearranged Lung Cancer by Dual Salvage Signaling in a Clinically Paired Resistance Model. Molecular cancer research : MCR. 2019;17(1):212-24. Epub 2018/09/02. doi: 10.1158/1541-7786.Mcr-18-0325. PubMed PMID: 30171175.

75. Moore NF, Azarova AM, Bhatnagar N, Ross KN, Drake LE, Frumm S, Liu QS, Christie AL, Sanda T, Chesler L, Kung AL, Gray NS, Stegmaier K, George RE. Molecular rationale for

the use of PI3K/AKT/mTOR pathway inhibitors in combination with crizotinib in ALK-mutated neuroblastoma. Oncotarget. 2014;5(18):8737-49. Epub 2014/09/18. doi: 10.18632/oncotarget.2372. PubMed PMID: 25228590; PMCID: PMC4226718.

76. Huang WS, Liu S, Zou D, Thomas M, Wang Y, Zhou T, Romero J, Kohlmann A, Li F, Qi J, Cai L, Dwight TA, Xu Y, Xu R, Dodd R, Toms A, Parillon L, Lu X, Anjum R, Zhang S, Wang F, Keats J, Wardwell SD, Ning Y, Xu Q, Moran LE, Mohemmad QK, Jang HG, Clackson T, Narasimhan NI, Rivera VM, Zhu X, Dalgarno D, Shakespeare WC. Discovery of Brigatinib (AP26113), a Phosphine Oxide-Containing, Potent, Orally Active Inhibitor of Anaplastic Lymphoma Kinase. Journal of medicinal chemistry. 2016;59(10):4948-64. Epub 2016/05/05. doi: 10.1021/acs.jmedchem.6b00306. PubMed PMID: 27144831.

77. Uchibori K, Inase N, Araki M, Kamada M, Sato S, Okuno Y, Fujita N, Katayama R. Brigatinib combined with anti-EGFR antibody overcomes osimertinib resistance in EGFR-mutated non-small-cell lung cancer. Nature communications. 2017;8:14768. Epub 2017/03/14. doi: 10.1038/ncomms14768. PubMed PMID: 28287083; PMCID: PMC5355811.

78. Zorea J, Prasad M, Cohen L, Li N, Schefzik R, Ghosh S, Rotblat B, Brors B, Elkabets M. IGF1R upregulation confers resistance to isoform-specific inhibitors of PI3K in PIK3CA-driven ovarian cancer. Cell death & disease. 2018;9(10):944. Epub 2018/09/22. doi: 10.1038/s41419-018-1025-8. PubMed PMID: 30237504; PMCID: PMC6148236.

79. Leroy C, Ramos P, Cornille K, Bonenfant D, Fritsch C, Voshol H, Bentires-Alj M. Activation of IGF1R/p110beta/AKT/mTOR confers resistance to alpha-specific PI3K inhibition. Breast cancer research : BCR. 2016;18(1):41. Epub 2016/04/07. doi: 10.1186/s13058-016-0697-1. PubMed PMID: 27048245; PMCID: PMC4820873.

80. Xu C, Fillmore CM, Koyama S, Wu H, Zhao Y, Chen Z, Herter-Sprie GS, Akbay EA, Tchaicha JH, Altabef A, Reibel JB, Walton Z, Ji H, Watanabe H, Janne PA, Castrillon DH, Rustgi AK, Bass AJ, Freeman GJ, Padera RF, Dranoff G, Hammerman PS, Kim CF, Wong KK. Loss of Lkb1 and Pten leads to lung squamous cell carcinoma with elevated PD-L1 expression. Cancer cell. 2014;25(5):590-604. Epub 2014/05/06. doi: 10.1016/j.ccr.2014.03.033. PubMed PMID: 24794706; PMCID: PMC4112370.

81. Zhu J, Chen L, Zou L, Yang P, Wu R, Mao Y, Zhou H, Li R, Wang K, Wang W, Hua D, Zhang X. MiR-20b, -21, and -130b inhibit PTEN expression resulting in B7-H1 over-expression in advanced colorectal cancer. Human immunology. 2014;75(4):348-53. Epub 2014/01/29. doi: 10.1016/j.humimm.2014.01.006. PubMed PMID: 24468585.

82. Zhang Y, Zhang J, Xu K, Xiao Z, Sun J, Xu J, Wang J, Tang Q. PTEN/PI3K/mTOR/B7-H1 signaling pathway regulates cell progression and immuno-resistance in pancreatic cancer. Hepato-gastroenterology. 2013;60(127):1766-72. Epub 2014/03/14. PubMed PMID: 24624456.

83. Parsa AT, Waldron JS, Panner A, Crane CA, Parney IF, Barry JJ, Cachola KE, Murray JC, Tihan T, Jensen MC, Mischel PS, Stokoe D, Pieper RO. Loss of tumor suppressor PTEN

function increases B7-H1 expression and immunoresistance in glioma. Nature medicine. 2007;13(1):84-8. Epub 2006/12/13. doi: 10.1038/nm1517. PubMed PMID: 17159987.

84. Lyford-Pike S, Peng S, Young GD, Taube JM, Westra WH, Akpeng B, Bruno TC, Richmon JD, Wang H, Bishop JA, Chen L, Drake CG, Topalian SL, Pardoll DM, Pai SI. Evidence for a role of the PD-1:PD-L1 pathway in immune resistance of HPV-associated head and neck squamous cell carcinoma. Cancer research. 2013;73(6):1733-41. Epub 2013/01/05. doi: 10.1158/0008-5472.Can-12-2384. PubMed PMID: 23288508; PMCID: PMC3602406.

85. Courtnay R, Ngo DC, Malik N, Ververis K, Tortorella SM, Karagiannis TC. Cancer metabolism and the Warburg effect: the role of HIF-1 and PI3K. Mol Biol Rep. 2015;42(4):841-51. Epub 2015/02/19. doi: 10.1007/s11033-015-3858-x. PubMed PMID: 25689954.

86. Hanahan D, Weinberg RA. Hallmarks of cancer: the next generation. Cell. 2011;144(5):646-74. Epub 2011/03/08. doi: 10.1016/j.cell.2011.02.013. PubMed PMID: 21376230.

87. Sugiura A, Rathmell JC. Metabolic Barriers to T Cell Function in Tumors. J Immunol. 2018;200(2):400-7. doi: 10.4049/jimmunol.1701041. PubMed PMID: 29311381; PMCID: PMC5777533.

88. Siska PJ, Rathmell JC. T cell metabolic fitness in antitumor immunity. Trends in immunology. 2015;36(4):257-64. doi: 10.1016/j.it.2015.02.007. PubMed PMID: 25773310; PMCID: PMC4393792.

89. Delgoffe GM, Powell JD. Feeding an army: The metabolism of T cells in activation, anergy, and exhaustion. Molecular immunology. 2015;68(2 Pt C):492-6. doi: 10.1016/j.molimm.2015.07.026. PubMed PMID: 26256793; PMCID: PMC4837657.

90. Topalian SL, Taube JM, Anders RA, Pardoll DM. Mechanism-driven biomarkers to guide immune checkpoint blockade in cancer therapy. Nature reviews Cancer. 2016;16(5):275-87. doi: 10.1038/nrc.2016.36. PubMed PMID: 27079802; PMCID: PMC5381938.

91. Palucka AK, Coussens LM. The Basis of Oncoimmunology. Cell. 2016;164(6):1233-47. doi: 10.1016/j.cell.2016.01.049. PubMed PMID: 26967289; PMCID: PMC4788788.

92. Shayan G, Srivastava R, Li J, Schmitt N, Kane LP, Ferris RL. Adaptive resistance to anti-PD1 therapy by Tim-3 upregulation is mediated by the PI3K-Akt pathway in head and neck cancer. Oncoimmunology. 2017;6(1):e1261779. Epub 2017/02/16. doi: 10.1080/2162402X.2016.1261779. PubMed PMID: 28197389; PMCID: PMC5283618.

93. Herzog A, Bian Y, Vander Broek R, Hall B, Coupar J, Cheng H, Sowers AL, Cook JD, Mitchell JB, Chen Z, Kulkarni AB, Van Waes C. PI3K/mTOR inhibitor PF-04691502 antitumor activity is enhanced with induction of wild-type TP53 in human xenograft and murine knockout models of head and neck cancer. Clinical cancer research : an official journal of the American

Association for Cancer Research. 2013;19(14):3808-19. Epub 2013/05/04. doi: 10.1158/1078-0432.Ccr-12-2716. PubMed PMID: 23640975; PMCID: PMC3715575.

# Appendix

## Table A.1. Inhibitor Library Used in Small Molecule Profiling

1406 inhibitors were purchased (most as part of the Selleckchem inhibitor library) and were used in small molecule profiling studies as described in Chapter 5. The catalog number, product name, pathway, and molecular target for each inhibitor are listed below.

| Cat No | Product Name | Pathway | Targets |
|---|---|---|---|
| S1001 | ABT-263 (Navitoclax) | Apoptosis | Bcl-2 |
| S1002 | ABT-737 | Apoptosis | Bcl-2,Autophagy |
| S1003 | Linifanib (ABT-869) | Protein Tyrosine Kinase | VEGFR,PDGFR,CSF-1R |
| S1004 | Veliparib (ABT-888) | DNA Damage | PARP |
| S1005 | Axitinib | Protein Tyrosine Kinase | c-Kit,PDGFR,VEGFR |
| S1006 | Saracatinib (AZD0530) | Angiogenesis | Bcr-Abl,Src |
| S1007 | FG-4592 | Angiogenesis | HIF |
| S1008 | Selumetinib (AZD6244) | MAPK | MEK |
| S1010 | Nintedanib (BIBF 1120) | Protein Tyrosine Kinase | VEGFR,PDGFR,FGFR |
| S1011 | Afatinib (BIBW2992) | Protein Tyrosine Kinase | EGFR,HER2 |
| S1012 | BMS-536924 | Protein Tyrosine Kinase | IGF-1R |
| S1013 | Bortezomib (PS-341) | Proteases | Proteasome |
| S1014 | Bosutinib (SKI-606) | Angiogenesis | Src |
| S1017 | Cediranib (AZD2171) | Protein Tyrosine Kinase | VEGFR |
| S1018 | Dovitinib (TKI-258, CHIR-258) | Angiogenesis | FLT3,VEGFR,FGFR,c-Kit,PDGFR |
| S1020 | PD184352 (CI-1040) | MAPK | MEK |
| S1021 | Dasatinib | Angiogenesis | Bcr-Abl,Src,c-Kit |
| S1023 | Erlotinib HCl (OSI-744) | Protein Tyrosine Kinase | EGFR,Autophagy |
| S1025 | Gefitinib (ZD1839) | Protein Tyrosine Kinase | EGFR |
| S1026 | Imatinib Mesylate (STI571) | Protein Tyrosine Kinase | c-Kit,Bcr-Abl,PDGFR |
| S1028 | Lapatinib (GW-572016) Ditosylate | Protein Tyrosine Kinase | EGFR,HER2 |
| S1029 | Lenalidomide (CC-5013) | Apoptosis | TNF-alpha |
| S1030 | Panobinostat (LBH589) | Epigenetics | HDAC |
| S1032 | Motesanib Diphosphate (AMG-706) | Protein Tyrosine Kinase | PDGFR,VEGFR,c-Kit |
| S1033 | Nilotinib (AMN-107) | Angiogenesis | Bcr-Abl |
| S1034 | NVP-AEW541 | Protein Tyrosine Kinase | IGF-1R |
| S1035 | Pazopanib HCl (GW786034 HCl) | Protein Tyrosine Kinase | PDGFR,VEGFR,c-Kit |
| S1036 | PD0325901 | MAPK | MEK |
| S1038 | PI-103 | PI3K/Akt/mTOR | PI3K,DNA-PK,Autophagy,mTOR |
| S1039 | Rapamycin (Sirolimus) | PI3K/Akt/mTOR | mTOR,Autophagy |
| S1040 | Sorafenib Tosylate | MAPK | VEGFR,Raf,PDGFR |
| S1044 | Temsirolimus (CCI-779, NSC 683864) | PI3K/Akt/mTOR | mTOR |
| S1045 | Trichostatin A (TSA) | Epigenetics | HDAC |
| S1046 | Vandetanib (ZD6474) | Protein Tyrosine Kinase | VEGFR |
| S1047 | Vorinostat (SAHA, MK0683) | Epigenetics | HDAC,Autophagy |
| S1048 | VX-680 (Tozasertib, MK-0457) | Cell Cycle | Aurora Kinase |
| S1049 | Y-27632 2HCl | Cell Cycle | ROCK,Autophagy |
| S1052 | Elesclomol (STA-4783) | Cytoskeletal Signaling | HSP (e.g. HSP90) |
| S1053 | Entinostat (MS-275) | Epigenetics | HDAC |
| S1055 | Enzastaurin (LY317615) | TGF-beta/Smad | PKC |
| S1056 | AC480 (BMS-599626) | Protein Tyrosine Kinase | HER2,EGFR |
| S1057 | Obatoclax Mesylate (GX15-070) | Apoptosis | Autophagy,Bcl-2 |
| S1060 | Olaparib (AZD2281, Ku-0059436) | DNA Damage | PARP |
| S1061 | Nutlin-3 | Apoptosis | E3 Ligase ,Mdm2 |
| S1064 | Masitinib (AB1010) | Protein Tyrosine Kinase | PDGFR,c-Kit |
| S1065 | GDC-0941 | PI3K/Akt/mTOR | PI3K |
| S1066 | SL-327 | MAPK | MEK |
| S1067 | SB431542 | TGF-beta/Smad | TGF-beta/Smad |
| S1068 | Crizotinib (PF-02341066) | Protein Tyrosine Kinase | ALK,c-Met |
| S1069 | AUY922 (NVP-AUY922) | Cytoskeletal Signaling | HSP (e.g. HSP90) |
| S1070 | PHA-665752 | Protein Tyrosine Kinase | c-Met |

| | | | |
|---|---|---|---|
| S1071 | HA14-1 | Apoptosis | Bcl-2 |
| S1072 | ZSTK474 | PI3K/Akt/mTOR | PI3K |
| S1075 | SB216763 | PI3K/Akt/mTOR | GSK-3 |
| S1076 | SB203580 | MAPK | p38 MAPK |
| S1077 | SB202190 (FHPI) | MAPK | p38 MAPK |
| S1078 | MK-2206 2HCl | PI3K/Akt/mTOR | Akt |
| S1080 | SU11274 | Protein Tyrosine Kinase | c-Met |
| S1082 | Vismodegib (GDC-0449) | Stem Cells & Wnt | Hedgehog/Smoothened |
| S1084 | Brivanib (BMS-540215) | Protein Tyrosine Kinase | VEGFR,FGFR |
| S1085 | Belinostat (PXD101) | Epigenetics | HDAC |
| S1087 | Iniparib (BSI-201) | DNA Damage | PARP |
| S1088 | NVP-ADW742 | Protein Tyrosine Kinase | IGF-1R |
| S1089 | Refametinib (RDEA119, Bay 86-9766) | MAPK | MEK |
| S1090 | PCI-24781 (Abexinostat) | Cytoskeletal Signaling | HDAC |
| S1091 | OSI-906 (Linsitinib) | Protein Tyrosine Kinase | IGF-1R |
| S1092 | KU-55933 (ATM Kinase Inhibitor) | DNA Damage | ATM/ATR |
| S1093 | GSK1904529A | Protein Tyrosine Kinase | IGF-1R |
| S1094 | PF-04217903 | Protein Tyrosine Kinase | c-Met |
| S1095 | LAQ824 (Dacinostat) | Epigenetics | HDAC |
| S1096 | Quisinostat (JNJ-26481585) | Epigenetics | HDAC |
| S1098 | Rucaparib (AG-014699,PF-01367338) | DNA Damage | PARP |
| S1100 | MLN8054 | Cell Cycle | Aurora Kinase |
| S1101 | Vatalanib (PTK787) 2HCl | Protein Tyrosine Kinase | c-Kit,VEGFR |
| S1102 | U0126-EtOH | MAPK | MEK |
| S1103 | ZM 447439 | Cell Cycle | Aurora Kinase |
| S1104 | GDC-0879 | MAPK | Raf |
| S1105 | LY294002 | PI3K/Akt/mTOR | Autophagy,PI3K |
| S1106 | OSU-03012 (AR-12) | PI3K/Akt/mTOR | PDK-1 |
| S1107 | Danusertib (PHA-739358) | Cell Cycle | FGFR,Aurora Kinase,c-RET,Bcr-Abl |
| S1109 | BI 2536 | Cell Cycle | PLK |
| S1110 | Varespladib (LY315920) | Metabolism | Phospholipase (e.g. PLA) |
| S1111 | Foretinib (GSK1363089) | Protein Tyrosine Kinase | VEGFR,c-Met |
| S1112 | SGX-523 | Protein Tyrosine Kinase | c-Met |
| S1113 | GSK690693 | PI3K/Akt/mTOR | Akt |
| S1114 | JNJ-38877605 | Protein Tyrosine Kinase | c-Met |
| S1115 | Odanacatib (MK-0822) | Others | Cysteine Protease |
| S1116 | Palbociclib (PD-0332991) HCl | Cell Cycle | CDK |
| S1117 | Triciribine | PI3K/Akt/mTOR | Akt |
| S1118 | XL147 | PI3K/Akt/mTOR | PI3K |
| S1119 | Cabozantinib (XL184, BMS-907351) | Protein Tyrosine Kinase | Tie-2,TAM Receptor,FLT3,VEGFR,c-Met,c-Kit |
| S1120 | Everolimus (RAD001) | PI3K/Akt/mTOR | mTOR |
| S1121 | TW-37 | Apoptosis | Bcl-2 |
| S1122 | Mocetinostat (MGCD0103) | Epigenetics | HDAC |
| S1124 | BMS-754807 | Protein Tyrosine Kinase | IGF-1R,Trk receptor,c-Met |
| S1129 | SRT1720 | Epigenetics | Sirtuin |
| S1130 | YM155 (Sepantronium Bromide) | Apoptosis | Survivin |
| S1132 | INO-1001 | DNA Damage | PARP |
| S1133 | Alisertib (MLN8237) | Cell Cycle | Aurora Kinase |
| S1134 | AT9283 | JAK/STAT | Aurora Kinase,JAK,Bcr-Abl |
| S1138 | Brivanib Alaninate (BMS-582664) | Protein Tyrosine Kinase | VEGFR,FGFR |
| S1139 | ADL5859 HCl | Neuronal Signaling | Opioid Receptor |
| S1140 | Andarine | Endocrinology & Hormones | Androgen Receptor |
| S1141 | 17-AAG (Tanespimycin) | Cytoskeletal Signaling | HSP (e.g. HSP90) |
| S1142 | 17-DMAG (Alvespimycin) HCl | Cytoskeletal Signaling | HSP (e.g. HSP90) |
| S1143 | AG-490 (Tyrphostin B42) | Protein Tyrosine Kinase | JAK,EGFR |
| S1144 | Ivacaftor (VX-770) | Transmembrane Transporters | CFTR |
| S1145 | SNS-032 (BMS-387032) | Cell Cycle | CDK |
| S1147 | Barasertib (AZD1152-HQPA) | Cell Cycle | Aurora Kinase |
| S1148 | Docetaxel | Others | |
| S1150 | Paclitaxel | Others | |
| S1152 | PLX-4720 | MAPK | Raf |
| S1153 | Roscovitine (Seliciclib,CYC202) | Cell Cycle | CDK |
| S1154 | SNS-314 Mesylate | Cell Cycle | Aurora Kinase |
| S1155 | S3I-201 | JAK/STAT | STAT |
| S1157 | CEP-18770 (Delanzomib) | Proteases | Proteasome |
| S1159 | Ganetespib (STA-9090) | Cytoskeletal Signaling | HSP (e.g. HSP90) |
| S1163 | AT13387 | Cytoskeletal Signaling | HSP (e.g. HSP90) |
| S1164 | Lenvatinib (E7080) | Protein Tyrosine Kinase | VEGFR |
| S1166 | Cisplatin | Others | |
| S1167 | CP-724714 | Protein Tyrosine Kinase | EGFR,HER2 |
| S1168 | Valproic acid sodium salt (Sodium valproate) | Neuronal Signaling | GABA Receptor,HDAC,Autophagy |
| S1169 | TGX-221 | PI3K/Akt/mTOR | PI3K |
| S1170 | WZ3146 | Protein Tyrosine Kinase | EGFR |
| S1171 | CYC116 | Cell Cycle | VEGFR,Aurora Kinase |
| S1172 | JNJ-26854165 (Serdemetan) | Apoptosis | E3 Ligase ,p53 |
| S1173 | WZ4002 | Protein Tyrosine Kinase | EGFR |

| | | | |
|---|---|---|---|
| S1174 | MK-2866 (GTx-024) | Endocrinology & Hormones | Androgen Receptor |
| S1175 | BIIB021 | Cytoskeletal Signaling | HSP (e.g. HSP90) |
| S1176 | Plinabulin (NPI-2358) | Angiogenesis | VDA |
| S1177 | PD98059 | MAPK | MEK |
| S1178 | Regorafenib (BAY 73-4506) | Protein Tyrosine Kinase | c-RET,VEGFR |
| S1179 | WZ8040 | Protein Tyrosine Kinase | EGFR |
| S1180 | XAV-939 | Stem Cells & Wnt | Wnt/beta-catenin |
| S1181 | ENMD-2076 | Angiogenesis | Aurora Kinase,FLT3,VEGFR |
| S1183 | Danoprevir (ITMN-191) | Proteases | HCV Protease |
| S1185 | Ritonavir | Proteases | HIV Protease |
| S1186 | BIBR 1532 | DNA Damage | Telomerase |
| S1188 | Anastrozole | Endocrinology & Hormones | Aromatase |
| S1189 | Aprepitant | Others | Substance P |
| S1190 | Bicalutamide | Endocrinology & Hormones | Androgen Receptor |
| S1191 | Fulvestrant | Endocrinology & Hormones | Estrogen/progestogen Receptor |
| S1193 | Thalidomide | Apoptosis | E3 Ligase ,TNF-alpha |
| S1194 | CUDC-101 | Epigenetics | EGFR,HER2,HDAC |
| S1195 | TAK-700 (Orteronel) | Metabolism | P450 (e.g. CYP17) |
| S1196 | Exemestane | Endocrinology & Hormones | Aromatase |
| S1197 | Finasteride | Endocrinology & Hormones | 5-alpha Reductase |
| S1198 | Irinotecan | DNA Damage | Topoisomerase |
| S1200 | Decitabine | Epigenetics | DNA Methyltransferase |
| S1202 | Dutasteride | Endocrinology & Hormones | 5-alpha Reductase |
| S1205 | PIK-75 | PI3K/Akt/mTOR | DNA-PK,PI3K |
| S1207 | Tivozanib (AV-951) | Protein Tyrosine Kinase | PDGFR,c-Kit,VEGFR |
| S1208 | Doxorubicin (Adriamycin) | DNA Damage | Autophagy,Topoisomerase |
| S1210 | Methotrexate | Metabolism | DHFR |
| S1216 | PFI-1 (PF-6405761) | Epigenetics | Epigenetic Reader Domain |
| S1219 | YM201636 | PI3K/Akt/mTOR | PI3K |
| S1220 | OSI-930 | Protein Tyrosine Kinase | CSF-1R,VEGFR,c-Kit |
| S1225 | Etoposide | DNA Damage | Topoisomerase |
| S1226 | KU-0063794 | PI3K/Akt/mTOR | mTOR |
| S1227 | Raloxifene HCl | Endocrinology & Hormones | Estrogen/progestogen Receptor |
| S1228 | Idarubicin HCl | DNA Damage | Topoisomerase |
| S1230 | Flavopiridol (Alvocidib) | Cell Cycle | CDK |
| S1231 | Topotecan HCl | DNA Damage | Topoisomerase |
| S1233 | 2-Methoxyestradiol (2-MeOE2) | Angiogenesis | HIF |
| S1234 | AG-1024 | Protein Tyrosine Kinase | IGF-1R |
| S1235 | Letrozole | Endocrinology & Hormones | Aromatase |
| S1237 | Temozolomide | Ubiquitin | Autophagy |
| S1244 | Amuvatinib (MP-470) | Protein Tyrosine Kinase | FLT3,PDGFR,c-Kit |
| S1249 | JNJ-7706621 | Cell Cycle | Aurora Kinase,CDK |
| S1250 | Enzalutamide (MDV3100) | Endocrinology & Hormones | Androgen Receptor |
| S1251 | Dienogest | Endocrinology & Hormones | Estrogen/progestogen Receptor |
| S1256 | Rufinamide | Transmembrane Transporters | Sodium Channel |
| S1258 | Prasugrel | Neuronal Signaling | P2 Receptor |
| S1259 | Ramelteon | GPCR & G Protein | MT Receptor |
| S1260 | Cinacalcet HCl | GPCR & G Protein | CaSR |
| S1261 | Celecoxib | Neuronal Signaling | COX |
| S1262 | Avagacestat (BMS-708163) | Proteases | Beta Amyloid,Gamma-secretase |
| S1263 | CHIR-99021 (CT99021) | PI3K/Akt/mTOR | GSK-3 |
| S1264 | PD173074 | Angiogenesis | VEGFR,FGFR |
| S1266 | WYE-354 | PI3K/Akt/mTOR | mTOR |
| S1267 | Vemurafenib (PLX4032, RG7204) | MAPK | Raf |
| S1274 | BX-795 | PI3K/Akt/mTOR | IκB/IKK,PDK-1 |
| S1275 | BX-912 | PI3K/Akt/mTOR | PDK-1 |
| S1280 | Amisulpride | Neuronal Signaling | Dopamine Receptor |
| S1281 | Aniracetam | Neuronal Signaling | AMPA Receptor-kainate Receptor-NMDA Receptor |
| S1283 | Asenapine | Neuronal Signaling | Adrenergic Receptor,5-HT Receptor |
| S1284 | Benazepril HCl | Endocrinology & Hormones | RAAS |
| S1288 | Camptothecin | DNA Damage | Topoisomerase |
| S1290 | Celastrol | Proteases | Proteasome |
| S1291 | Cetirizine DiHCl | Neuronal Signaling | Histamine Receptor |
| S1293 | Cilnidipine | Transmembrane Transporters | Calcium Channel |
| S1294 | Cilostazol | Metabolism | PDE |
| S1304 | Megestrol Acetate | Endocrinology & Hormones | Androgen Receptor,Estrogen/progestogen Receptor |
| S1315 | Ki16425 | GPCR & G Protein | LPA Receptor |
| S1319 | Costunolide | DNA Damage | Telomerase |
| S1322 | Dexamethasone (DHAP) | Others | IL Receptor,Autophagy |
| S1324 | Doxazosin Mesylate | Neuronal Signaling | Adrenergic Receptor |
| S1328 | Etodolac | Neuronal Signaling | COX |
| S1329 | Etomidate | Neuronal Signaling | GABA Receptor |
| S1332 | Flumazenil | Neuronal Signaling | GABA Receptor |
| S1333 | Fluoxetine HCl | Neuronal Signaling | 5-HT Receptor |
| S1336 | Fluvoxamine maleate | Neuronal Signaling | 5-HT Receptor |
| S1342 | Genistein | Protein Tyrosine Kinase | EGFR,Topoisomerase |

| | | | |
|---|---|---|---|
| S1343 | Ginkgolide B | Others | PAFR |
| S1344 | Glimepiride | Proteases | Potassium Channel |
| S1352 | TG100-115 | PI3K/Akt/mTOR | PI3K |
| S1353 | Ketoconazole | Metabolism | P450 (e.g. CYP17) |
| S1354 | Lansoprazole | Transmembrane Transporters | Proton Pump |
| S1357 | Lidocaine | Neuronal Signaling | Histamine Receptor |
| S1358 | Loratadine | Neuronal Signaling | Histamine Receptor |
| S1359 | Losartan Potassium (DuP 753) | Endocrinology & Hormones | RAAS |
| S1360 | GSK1059615 | PI3K/Akt/mTOR | mTOR,PI3K |
| S1361 | MGCD-265 | Protein Tyrosine Kinase | c-Met,Tie-2,VEGFR |
| S1362 | Rigosertib (ON-01910) | Cell Cycle | PLK |
| S1363 | Ki8751 | Protein Tyrosine Kinase | c-Kit,VEGFR,PDGFR |
| S1366 | BMS-707035 | Microbiology | Integrase |
| S1367 | Amonafide | DNA Damage | Topoisomerase |
| S1376 | Gestodene | Endocrinology & Hormones | Estrogen/progestogen Receptor |
| S1377 | Drospirenone | Endocrinology & Hormones | Estrogen/progestogen Receptor |
| S1378 | Ruxolitinib (INCB018424) | JAK/STAT | JAK |
| S1379 | Isotretinoin | Metabolism | Hydroxylase |
| S1380 | Lopinavir | Proteases | HIV Protease |
| S1382 | Mianserin HCl | Neuronal Signaling | Histamine Receptor |
| S1385 | Mosapride Citrate | Neuronal Signaling | 5-HT Receptor |
| S1386 | Nafamostat Mesylate | Proteases | Serine Protease |
| S1387 | Naftopidil DiHCl | Neuronal Signaling | Adrenergic Receptor |
| S1389 | Omeprazole | Transmembrane Transporters | Autophagy,Proton Pump |
| S1390 | Ondansetron HCl | Neuronal Signaling | 5-HT Receptor |
| S1391 | Oxcarbazepine | Transmembrane Transporters | Sodium Channel |
| S1392 | Pelitinib (EKB-569) | Protein Tyrosine Kinase | EGFR |
| S1396 | Resveratrol | Epigenetics | Sirtuin,Autophagy |
| S1397 | Rocuronium Bromide | Neuronal Signaling | AChR |
| S1398 | Stavudine (d4T) | Microbiology | Reverse Transcriptase |
| S1401 | Tenofovir | Microbiology | Reverse Transcriptase |
| S1404 | Trilostane | Metabolism | Dehydrogenase |
| S1409 | Alfuzosin HCl | Neuronal Signaling | Adrenergic Receptor |
| S1415 | Clopidogrel | Neuronal Signaling | P2 Receptor |
| S1421 | Staurosporine | TGF-beta/Smad | PKC |
| S1422 | Droxinostat | Cytoskeletal Signaling | HDAC |
| S1425 | Ranolazine 2HCl | Transmembrane Transporters | Calcium Channel |
| S1426 | Repaglinide | Transmembrane Transporters | Potassium Channel |
| S1430 | Rolipram | Metabolism | PDE |
| S1431 | Sildenafil Citrate | Metabolism | PDE |
| S1432 | Sumatriptan Succinate | Neuronal Signaling | 5-HT Receptor |
| S1436 | Tianeptine sodium | Neuronal Signaling | 5-HT Receptor |
| S1437 | Tizanidine HCl | Neuronal Signaling | Adrenergic Receptor |
| S1438 | Topiramate | Metabolism | Carbonic Anhydrase |
| S1441 | Venlafaxine | Neuronal Signaling | 5-HT Receptor |
| S1442 | Voriconazole | Metabolism | P450 (e.g. CYP17) |
| S1451 | Aurora A Inhibitor I | Cell Cycle | Aurora Kinase |
| S1452 | Ispinesib (SB-715992) | Cytoskeletal Signaling | Kinesin |
| S1453 | Tipifarnib | Metabolism | Transferase |
| S1454 | PHA-680632 | Cell Cycle | Aurora Kinase |
| S1455 | Cilomilast | Metabolism | PDE |
| S1456 | Zibotentan (ZD4054) | GPCR & G Protein | Endothelin Receptor |
| S1457 | Atazanavir Sulfate | Proteases | HIV Protease |
| S1458 | VX-745 | MAPK | p38 MAPK |
| S1459 | Thiazovivin | Cell Cycle | ROCK |
| S1460 | SP600125 | MAPK | JNK |
| S1462 | AZD6482 | PI3K/Akt/mTOR | PI3K |
| S1465 | Moxifloxacin HCl | DNA Damage | Topoisomerase |
| S1470 | TSU-68 (SU6668, Orantinib) | Protein Tyrosine Kinase | PDGFR,FGFR,VEGFR |
| S1472 | Safinamide Mesylate | Metabolism | MAO |
| S1474 | GSK429286A | Cell Cycle | ROCK |
| S1475 | Pimasertib (AS-703026) | MAPK | MEK |
| S1476 | SB525334 | TGF-beta/Smad | TGF-beta/Smad |
| S1478 | Oligomycin A | Transmembrane Transporters | ATPase |
| S1480 | VX-222 (VCH-222, Lomibuvir) | Proteases | HCV Protease |
| S1481 | Zosuquidar (LY335979) 3HCl | Transmembrane Transporters | P-gp |
| S1482 | Daclatasvir (BMS-790052) | Proteases | HCV Protease |
| S1484 | MC1568 | Cytoskeletal Signaling | HDAC |
| S1485 | HMN-214 | Cell Cycle | PLK |
| S1486 | AEE788 (NVP-AEE788) | Protein Tyrosine Kinase | VEGFR,EGFR,HER2 |
| S1487 | PHA-793887 | Cell Cycle | CDK |
| S1488 | Naratriptan | Neuronal Signaling | 5-HT Receptor |
| S1489 | PIK-93 | PI3K/Akt/mTOR | PI3K |
| S1490 | Ponatinib (AP24534) | Angiogenesis | Bcr-Abl,PDGFR,VEGFR,FGFR |
| S1491 | Fludarabine | JAK/STAT | STAT,DNA/RNA Synthesis |
| S1494 | LY2228820 | MAPK | p38 MAPK |

| | | | |
|---|---|---|---|
| S1497 | Pralatrexate | Metabolism | DHFR |
| S1501 | Mycophenolate Mofetil | Metabolism | Dehydrogenase |
| S1504 | Dyphylline | Metabolism | PDE |
| S1512 | Tadalafil | Metabolism | PDE |
| S1515 | Pracinostat (SB939) | Cytoskeletal Signaling | HDAC |
| S1519 | CCT129202 | Cell Cycle | Aurora Kinase |
| S1523 | SAR245409 (XL765) | PI3K/Akt/mTOR | PI3K,mTOR |
| S1524 | AT7519 | Cell Cycle | CDK |
| S1525 | MK-1775 | Cell Cycle | Wee1 |
| S1526 | Quizartinib (AC220) | Angiogenesis | FLT3 |
| S1528 | LY2811376 | Proteases | Beta Amyloid,BACE |
| S1529 | Hesperadin | Cell Cycle | Aurora Kinase |
| S1530 | BIX 02188 | MAPK | MEK |
| S1531 | BIX 02189 | MAPK | MEK |
| S1532 | AZD7762 | Cell Cycle | Chk |
| S1533 | R406 (free base) | Angiogenesis | Syk |
| S1534 | Org 27569 | GPCR & G Protein | Cannabinoid Receptor |
| S1536 | CP-673451 | Protein Tyrosine Kinase | PDGFR |
| S1537 | DMXAA (Vadimezan) | Angiogenesis | VDA |
| S1538 | Telaprevir (VX-950) | Proteases | HCV Protease |
| S1540 | Saxagliptin | Proteases | DPP-4 |
| S1541 | EX 527 (Selisistat) | Epigenetics | Sirtuin |
| S1544 | AM1241 | GPCR & G Protein | Cannabinoid Receptor |
| S1545 | SB408124 | GPCR & G Protein | OX Receptor |
| S1548 | Dapagliflozin | GPCR & G Protein | SGLT |
| S1549 | Nebivolol | Neuronal Signaling | Adrenergic Receptor |
| S1550 | Pimobendan | Metabolism | PDE |
| S1555 | AZD8055 | PI3K/Akt/mTOR | mTOR |
| S1556 | PHT-427 | PI3K/Akt/mTOR | Akt,PDK-1 |
| S1557 | KRN 633 | Protein Tyrosine Kinase | VEGFR,PDGFR |
| S1558 | AT7867 | PI3K/Akt/mTOR | S6 Kinase,Akt |
| S1561 | BMS-777607 | Protein Tyrosine Kinase | c-Met,TAM Receptor |
| S1565 | VX-809 (Lumacaftor) | Transmembrane Transporters | CFTR |
| S1567 | Pomalidomide | Apoptosis | TNF-alpha |
| S1568 | PD318088 | MAPK | MEK |
| S1570 | KU-60019 | DNA Damage | ATM/ATR |
| S1572 | BS-181 HCl | Cell Cycle | CDK |
| S1573 | Fasudil (HA-1077) HCl | Cell Cycle | ROCK,Autophagy |
| S1574 | BIRB 796 (Doramapimod) | MAPK | p38 MAPK |
| S1575 | RO4929097 | Proteases | Gamma-secretase,Beta Amyloid |
| S1577 | Tie2 kinase inhibitor | Protein Tyrosine Kinase | Tie-2 |
| S1578 | Candesartan | Endocrinology & Hormones | RAAS |
| S1582 | H 89 2HCl | PI3K/Akt/mTOR | PKA,S6 Kinase |
| S1590 | TWS119 | PI3K/Akt/mTOR | GSK-3 |
| S1593 | Apixaban | Metabolism | Factor Xa |
| S1594 | Semagacestat (LY450139) | Proteases | Gamma-secretase |
| S1604 | Olmesartan Medoxomil | Endocrinology & Hormones | RAAS |
| S1608 | Pyridostigmine Bromide | Neuronal Signaling | AChR |
| S1613 | Silodosin | Neuronal Signaling | Adrenergic Receptor |
| S1614 | Riluzole | Transmembrane Transporters | Sodium Channel,GluR |
| S1615 | Risperidone | Neuronal Signaling | 5-HT Receptor |
| S1620 | Darunavir Ethanolate | Proteases | HIV Protease |
| S1623 | Acetylcysteine | Others | Others |
| S1626 | Naproxen | Neuronal Signaling | COX |
| S1630 | Allopurinol | GPCR & G Protein | Others |
| S1638 | Ibuprofen | Neuronal Signaling | COX |
| S1639 | Amprenavir | Proteases | HIV Protease |
| S1645 | Ketoprofen | Neuronal Signaling | COX |
| S1646 | Ketorolac | Neuronal Signaling | COX |
| S1649 | Zolmitriptan | Neuronal Signaling | 5-HT Receptor |
| S1657 | Enalaprilat Dihydrate | Endocrinology & Hormones | RAAS |
| S1662 | Isradipine | Transmembrane Transporters | Calcium Channel |
| S1665 | Estrone | Endocrinology & Hormones | Estrogen/progestogen Receptor |
| S1672 | Aminoglutethimide | Endocrinology & Hormones | Aromatase |
| S1673 | Aminophylline | Metabolism | PDE |
| S1693 | Carbamazepine | Transmembrane Transporters | Sodium Channel,Autophagy |
| S1702 | Didanosine | Microbiology | Reverse Transcriptase |
| S1703 | Divalproex Sodium | Ubiquitin | Autophagy |
| S1704 | Emtricitabine | Microbiology | Reverse Transcriptase |
| S1706 | Lamivudine | Microbiology | Reverse Transcriptase |
| S1713 | Piroxicam | Neuronal Signaling | COX |
| S1714 | Gemcitabine | DNA Damage | DNA/RNA Synthesis,Autophagy |
| S1718 | Adefovir Dipivoxil | Microbiology | Reverse Transcriptase |
| S1719 | Zalcitabine | Microbiology | Reverse Transcriptase |
| S1738 | Telmisartan | Endocrinology & Hormones | RAAS |
| S1742 | Nevirapine | Microbiology | Reverse Transcriptase |

| | | | |
|---|---|---|---|
| S1747 | Nimodipine | Transmembrane Transporters | Autophagy,Calcium Channel |
| S1763 | Quetiapine Fumarate | Neuronal Signaling | Dopamine Receptor |
| S1771 | Chlorprothixene | Neuronal Signaling | Dopamine Receptor |
| S1776 | Toremifene Citrate | Endocrinology & Hormones | Estrogen/progestogen Receptor |
| S1782 | Azacitidine | DNA Damage | DNA Methyltransferase |
| S1793 | Ramipril | Endocrinology & Hormones | RAAS |
| S1801 | Ranitidine | Neuronal Signaling | Histamine Receptor |
| S1802 | Acadesine | PI3K/Akt/mTOR | AMPK |
| S1805 | Acetylcholine Chloride | Neuronal Signaling | AChR |
| S1813 | Amlodipine Besylate | Transmembrane Transporters | Calcium Channel |
| S1816 | Chlorpheniramine Maleate | Neuronal Signaling | Histamine Receptor |
| S1828 | Proparacaine HCl | Transmembrane Transporters | Sodium Channel |
| S1831 | Carvedilol | Neuronal Signaling | Adrenergic Receptor |
| S1835 | Azithromycin | Ubiquitin | Autophagy |
| S1845 | Cimetidine | Neuronal Signaling | Histamine Receptor |
| S1847 | Clemastine Fumarate | Neuronal Signaling | Histamine Receptor |
| S1856 | Metoprolol Tartrate | Neuronal Signaling | Adrenergic Receptor |
| S1869 | Dapoxetine HCl | Neuronal Signaling | 5-HT Receptor |
| S1880 | Roxatidine Acetate HCl | Neuronal Signaling | Histamine Receptor |
| S1885 | Felodipine | Transmembrane Transporters | Calcium Channel |
| S1890 | Nizatidine | Neuronal Signaling | Histamine Receptor |
| S1894 | Valsartan | Endocrinology & Hormones | RAAS |
| S1898 | Tropisetron | Neuronal Signaling | 5-HT Receptor |
| S1903 | Diclofenac Sodium | Neuronal Signaling | COX |
| S1905 | Amlodipine | Transmembrane Transporters | Calcium Channel |
| S1908 | Flutamide | Endocrinology & Hormones | Androgen Receptor |
| S1909 | Fluvastatin Sodium | Metabolism | HMG-CoA Reductase |
| S1913 | Tropicamide | Neuronal Signaling | AChR |
| S1914 | Pregnenolone | Endocrinology & Hormones | Estrogen/progestogen Receptor |
| S1929 | Irsogladine | Metabolism | AChR,PDE |
| S1941 | Enalapril Maleate | Endocrinology & Hormones | RAAS |
| S1959 | Tolfenamic Acid | Neuronal Signaling | COX |
| S1969 | Nefiracetam | Neuronal Signaling | GABA Receptor |
| S1971 | Nicorandil | Transmembrane Transporters | Potassium Channel |
| S1972 | Tamoxifen Citrate | Endocrinology & Hormones | Autophagy,Estrogen/progestogen Receptor |
| S1975 | Aripiprazole | Neuronal Signaling | 5-HT Receptor |
| S1978 | Methscopolamine | Neuronal Signaling | AChR |
| S1979 | Amiodarone HCl | Transmembrane Transporters | Potassium Channel,Autophagy |
| S1994 | Lacidipine | Transmembrane Transporters | Calcium Channel |
| S2001 | Elvitegravir (GS-9137, JTK-303) | Microbiology | Integrase |
| S2003 | Maraviroc | Microbiology | CCR |
| S2005 | Raltegravir (MK-0518) | Microbiology | Integrase |
| S2006 | Pyrimethamine | Metabolism | DHFR |
| S2012 | PCI-34051 | Epigenetics | HDAC |
| S2013 | PF-573228 | Angiogenesis | FAK |
| S2014 | BMS-265246 | Cell Cycle | CDK |
| S2017 | Benidipine HCl | Transmembrane Transporters | Calcium Channel |
| S2020 | Formoterol Hemifumarate | Neuronal Signaling | Adrenergic Receptor |
| S2024 | Ketotifen Fumarate | Neuronal Signaling | Histamine Receptor |
| S2025 | Urapidil HCl | Neuronal Signaling | 5-HT Receptor |
| S2026 | Ginkgolide A | Neuronal Signaling | GABA Receptor |
| S2030 | Flunarizine 2HCl | Transmembrane Transporters | Calcium Channel |
| S2037 | Candesartan Cilexetil | Endocrinology & Hormones | RAAS |
| S2038 | Phentolamine Mesylate | Neuronal Signaling | Adrenergic Receptor |
| S2040 | Nimesulide | Neuronal Signaling | COX |
| S2042 | Cyproterone Acetate | Endocrinology & Hormones | Androgen Receptor |
| S2043 | Memantine HCl | Neuronal Signaling | AMPA Receptor-kainate Receptor-NMDA Receptor |
| S2044 | Cyproheptadine HCl | Neuronal Signaling | Histamine Receptor |
| S2046 | Pioglitazone HCl | Metabolism | P450 (e.g. CYP17) |
| S2047 | Lornoxicam | Neuronal Signaling | COX |
| S2051 | Captopril | Endocrinology & Hormones | RAAS |
| S2054 | Orphenadrine Citrate | Neuronal Signaling | AChR |
| S2055 | Gimeracil | Metabolism | Dehydrogenase |
| S2059 | Terazosin HCl | Neuronal Signaling | Adrenergic Receptor |
| S2061 | Lovastatin | Metabolism | HMG-CoA Reductase |
| S2065 | Lafutidine | Neuronal Signaling | Histamine Receptor |
| S2077 | Atorvastatin Calcium | Metabolism | HMG-CoA Reductase |
| S2078 | Famotidine | Neuronal Signaling | Histamine Receptor |
| S2079 | Moexipril HCl | Endocrinology & Hormones | RAAS |
| S2080 | Clevidipine Butyrate | Transmembrane Transporters | Calcium Channel |
| S2084 | Duloxetine HCl | Neuronal Signaling | 5-HT Receptor |
| S2085 | Trimebutine | Neuronal Signaling | Opioid Receptor |
| S2086 | Ivabradine HCl | Neuronal Signaling | Adrenergic Receptor |
| S2087 | Rivastigmine Tartrate | Neuronal Signaling | AChR |
| S2091 | Betaxolol | Neuronal Signaling | Adrenergic Receptor |
| S2092 | Detomidine HCl | Neuronal Signaling | Adrenergic Receptor |

| | | | |
|---|---|---|---|
| S2096 | Almotriptan Malate | Neuronal Signaling | 5-HT Receptor |
| S2099 | Temocapril HCl | Endocrinology & Hormones | RAAS |
| S2101 | Gabexate Mesylate | Proteases | Serine Protease |
| S2102 | Rasagiline Mesylate | Metabolism | MAO |
| S2103 | Naltrexone HCl | Neuronal Signaling | Opioid Receptor |
| S2104 | Levosulpiride | Neuronal Signaling | Dopamine Receptor |
| S2108 | Flunixin Meglumin | Neuronal Signaling | COX |
| S2109 | Imidapril HCl | Endocrinology & Hormones | RAAS |
| S2113 | Cisatracurium Besylate | Neuronal Signaling | Adrenergic Receptor |
| S2118 | Ibutilide Fumarate | Transmembrane Transporters | Sodium Channel |
| S2126 | Naftopidil | Neuronal Signaling | Adrenergic Receptor |
| S2127 | S- (+)-Rolipram | Metabolism | PDE |
| S2128 | Bazedoxifene HCl | Endocrinology & Hormones | Estrogen/progestogen Receptor |
| S2130 | Atropine | Neuronal Signaling | AChR |
| S2131 | Roflumilast | Metabolism | PDE |
| S2134 | AZD8330 | MAPK | MEK |
| S2149 | GSK1292263 | Endocrinology & Hormones | GPR |
| S2151 | LDE225 (NVP-LDE225,Erismodegib) | Stem Cells & Wnt | Hedgehog/Smoothened |
| S2153 | CGS 21680 HCl | Angiogenesis | Adenosine Receptor |
| S2158 | KW-2449 | Angiogenesis | Bcr-Abl,Aurora Kinase,FLT3 |
| S2160 | Almorexant HCl | GPCR & G Protein | OX Receptor |
| S2161 | RAF265 (CHIR-265) | MAPK | VEGFR,Raf |
| S2162 | AZD1480 | JAK/STAT | JAK |
| S2163 | PF-4708671 | PI3K/Akt/mTOR | S6 Kinase |
| S2168 | PD128907 HCl | Neuronal Signaling | Dopamine Receptor |
| S2169 | Rosuvastatin Calcium | Endocrinology & Hormones | HMG-CoA Reductase |
| S2170 | Givinostat (ITF2357) | Cytoskeletal Signaling | HDAC |
| S2173 | Telotristat Etiprate (LX 1606 Hippurate) | Metabolism | Hydroxylase |
| S2178 | AG-14361 | DNA Damage | PARP |
| S2179 | LY2784544 | JAK/STAT | JAK |
| S2180 | MLN2238 | Proteases | Proteasome |
| S2181 | MLN9708 | Proteases | Proteasome |
| S2183 | BGJ398 (NVP-BGJ398) | Angiogenesis | FGFR |
| S2185 | AST-1306 | Protein Tyrosine Kinase | EGFR |
| S2186 | SB505124 | TGF-beta/Smad | TGF-beta/Smad |
| S2187 | Avasimibe | Metabolism | P450 (e.g. CYP17) |
| S2192 | AZD8931 (Sapitinib) | Protein Tyrosine Kinase | EGFR,HER2 |
| S2193 | GSK461364 | Cell Cycle | PLK |
| S2194 | R406 | Angiogenesis | FLT3,Syk |
| S2195 | CYT997 (Lexibulin) | Cytoskeletal Signaling | Microtubule Associated |
| S2197 | A-966492 | DNA Damage | PARP |
| S2198 | SGI-1776 free base | JAK/STAT | Pim |
| S2199 | Aliskiren Hemifumarate | Endocrinology & Hormones | RAAS |
| S2201 | BMS-794833 | Protein Tyrosine Kinase | VEGFR,c-Met |
| S2202 | NVP-BHG712 | Protein Tyrosine Kinase | Raf,Bcr-Abl,Src,Ephrin receptor |
| S2205 | OSI-420 | Protein Tyrosine Kinase | EGFR |
| S2207 | PIK-293 | PI3K/Akt/mTOR | PI3K |
| S2208 | Formestane | Endocrinology & Hormones | Aromatase |
| S2209 | Vinflunine Tartrate | Cytoskeletal Signaling | Microtubule Associated |
| S2214 | AZ 960 | JAK/STAT | JAK |
| S2215 | DAPT (GSI-IX) | Proteases | Gamma-secretase,Beta Amyloid |
| S2216 | Mubritinib (TAK 165) | Protein Tyrosine Kinase | HER2 |
| S2217 | Irinotecan HCl Trihydrate | DNA Damage | Topoisomerase |
| S2218 | PP242 | PI3K/Akt/mTOR | mTOR,Autophagy |
| S2219 | CYT387 | JAK/STAT | JAK |
| S2220 | SB590885 | MAPK | Raf |
| S2221 | Apatinib | Protein Tyrosine Kinase | VEGFR |
| S2224 | UK 383367 | Metabolism | Procollagen C Proteinase |
| S2225 | TAME | Cell Cycle | APC,E3 Ligase |
| S2226 | CAL-101 (Idelalisib, GS-1101) | PI3K/Akt/mTOR | PI3K |
| S2227 | PIK-294 | PI3K/Akt/mTOR | PI3K |
| S2228 | VX-765 | Apoptosis | Caspase |
| S2230 | LY2157299 | TGF-beta/Smad | TGF-beta/Smad |
| S2231 | Telatinib | Protein Tyrosine Kinase | VEGFR,PDGFR,c-Kit |
| S2232 | Ketanserin | Neuronal Signaling | 5-HT Receptor |
| S2233 | Esomeprazole Sodium | Transmembrane Transporters | ATPase |
| S2235 | Volasertib (BI 6727) | Cell Cycle | PLK |
| S2239 | Tubacin | Cytoskeletal Signaling | HDAC |
| S2240 | Fesoterodine Fumarate | Neuronal Signaling | AChR |
| S2243 | Degrasyn (WP1130) | Angiogenesis | Bcr-Abl,DUB |
| S2247 | BKM120 (NVP-BKM120, Buparlisib) | PI3K/Akt/mTOR | PI3K |
| S2262 | Apigenin | Metabolism | P450 (e.g. CYP17) |
| S2266 | Asiatic Acid | MAPK | p38 MAPK |
| S2268 | Baicalein | Metabolism | P450 (e.g. CYP17) |
| S2285 | Cryptotanshinone | JAK/STAT | STAT |
| S2308 | Hesperetin | TGF-beta/Smad | TGF-beta/Smad,Histamine Receptor |

| | | | |
|---|---|---|---|
| S2310 | Honokiol | PI3K/Akt/mTOR | MEK,Akt |
| S2312 | Icariin | Metabolism | PDE |
| S2320 | Luteolin | Metabolism | PDE |
| S2322 | (+)-Matrine | Neuronal Signaling | Opioid Receptor |
| S2341 | (-)-Parthenolide | Ubiquitin | E3 Ligase |
| S2362 | Synephrine | GPCR & G Protein | Adrenergic Receptor |
| S2386 | Indirubin | PI3K/Akt/mTOR | GSK-3 |
| S2391 | Quercetin | Epigenetics | Sirtuin,PI3K,Src,PKC |
| S2394 | Naringenin | Metabolism | P450 (e.g. CYP17) |
| S2401 | Sodium Danshensu | Others | P450 (e.g. CYP17) |
| S2406 | Chrysophanic Acid | Protein Tyrosine Kinase | EGFR,mTOR |
| S2415 | Astragaloside A | TGF-beta/Smad | Others |
| S2423 | (S)-10-Hydroxycamptothecin | DNA Damage | Topoisomerase |
| S2437 | Rotundine | Neuronal Signaling | Dopamine Receptor |
| S2438 | Synephrine HCl | Neuronal Signaling | Adrenergic Receptor |
| S2443 | Tolbutamide | Transmembrane Transporters | Potassium Channel |
| S2448 | Gambogic Acid | Apoptosis | Caspase,Bcl-2 |
| S2449 | Forskolin | GPCR & G Protein | cAMP |
| S2450 | Equol | Endocrinology & Hormones | Estrogen/progestogen Receptor |
| S2451 | Amantadine HCl | Neuronal Signaling | Dopamine Receptor |
| S2452 | Amfebutamone HCl | Neuronal Signaling | AChR,Dopamine Receptor |
| S2453 | Benserazide HCl | Others | Others |
| S2454 | Bupivacaine HCl | GPCR & G Protein | Sodium Channel |
| S2455 | Bethanechol chloride | Neuronal Signaling | AChR |
| S2456 | Chlorpromazine HCl | Neuronal Signaling | Dopamine Receptor,Potassium Channel |
| S2458 | Clonidine HCl | Neuronal Signaling | Autophagy,Adrenergic Receptor |
| S2459 | Clozapine | Neuronal Signaling | 5-HT Receptor |
| S2460 | Pramipexole | Neuronal Signaling | Dopamine Receptor |
| S2461 | Domperidone | Neuronal Signaling | Dopamine Receptor |
| S2466 | Estriol | Endocrinology & Hormones | Estrogen/progestogen Receptor |
| S2471 | Gallamine Triethiodide | Neuronal Signaling | AChR |
| S2473 | Hexestrol | Endocrinology & Hormones | Estrogen/progestogen Receptor |
| S2475 | Imatinib (STI571) | Protein Tyrosine Kinase | PDGFR |
| S2480 | Loperamide HCl | Neuronal Signaling | Autophagy,Opioid Receptor |
| S2481 | Manidipine | Transmembrane Transporters | Calcium Channel |
| S2482 | Manidipine 2HCl | Transmembrane Transporters | Calcium Channel |
| S2484 | Milrinone | Metabolism | ATPase,PDE |
| S2489 | Nateglinide | Transmembrane Transporters | Potassium Channel |
| S2491 | Nitrendipine | Transmembrane Transporters | Calcium Channel,Autophagy |
| S2493 | Olanzapine | Neuronal Signaling | 5-HT Receptor,Dopamine Receptor |
| S2494 | Olopatadine HCl | Neuronal Signaling | Histamine Receptor |
| S2495 | Oxymetazoline HCl | Neuronal Signaling | Adrenergic Receptor |
| S2496 | Ozagrel | Metabolism | P450 (e.g. CYP17) |
| S2497 | Pancuronium dibromide | Neuronal Signaling | AChR |
| S2499 | Phenoxybenzamine HCl | GPCR & G Protein | Adrenergic Receptor |
| S2500 | Propafenone HCl | Transmembrane Transporters | Sodium Channel |
| S2503 | Racecadotril | Neuronal Signaling | Opioid Receptor |
| S2508 | Scopolamine HBr | Neuronal Signaling | AChR |
| S2509 | Sotalol | Neuronal Signaling | Adrenergic Receptor |
| S2515 | Vardenafil HCl Trihydrate | Metabolism | PDE |
| S2516 | Xylazine HCl | Neuronal Signaling | Adrenergic Receptor |
| S2517 | Maprotiline HCl | Neuronal Signaling | Adrenergic Receptor |
| S2519 | Naphazoline HCl | Neuronal Signaling | Adrenergic Receptor |
| S2521 | Epinephrine Bitartrate | GPCR & G Protein | Adrenergic Receptor |
| S2522 | L-Adrenaline | Neuronal Signaling | Adrenergic Receptor |
| S2524 | Phenytoin sodium | Transmembrane Transporters | Sodium Channel |
| S2525 | Phenytoin | Transmembrane Transporters | Sodium Channel |
| S2526 | Alizarin | Metabolism | P450 (e.g. CYP17) |
| S2529 | Dopamine HCl | Neuronal Signaling | Dopamine Receptor |
| S2531 | Asaraldehyde | Neuronal Signaling | COX |
| S2533 | Ritodrine HCl | Neuronal Signaling | Adrenergic Receptor |
| S2542 | Phenformin HCl | PI3K/Akt/mTOR | AMPK |
| S2545 | Scopine | Neuronal Signaling | Adrenergic Receptor |
| S2547 | Tiotropium Bromide hydrate | Neuronal Signaling | AChR |
| S2549 | Trospium chloride | Neuronal Signaling | AChR |
| S2550 | Tolterodine tartrate | Neuronal Signaling | AChR |
| S2552 | Azelastine HCl | Neuronal Signaling | Histamine Receptor |
| S2555 | Clarithromycin | Metabolism | P450 (e.g. CYP17) |
| S2556 | Rosiglitazone | DNA Damage | PPAR |
| S2561 | Clomifene citrate | Endocrinology & Hormones | Estrogen/progestogen Receptor |
| S2566 | Isoprenaline HCl | Neuronal Signaling | Adrenergic Receptor |
| S2567 | Medroxyprogesterone acetate | Endocrinology & Hormones | Estrogen/progestogen Receptor |
| S2569 | Phenylephrine HCl | GPCR & G Protein | Adrenergic Receptor |
| S2573 | Tetracaine HCl | Transmembrane Transporters | Calcium Channel |
| S2577 | Phenacetin | Neuronal Signaling | COX |
| S2579 | Zidovudine | Microbiology | Reverse Transcriptase |

| | | | |
|---|---|---|---|
| S2581 | Quinapril HCl | Endocrinology & Hormones | RAAS |
| S2585 | Brompheniramine hydrogen maleate | Neuronal Signaling | Histamine Receptor |
| S2593 | Tolvaptan | GPCR & G Protein | Vasopressin Receptor |
| S2601 | Gliclazide | Transmembrane Transporters | Potassium Channel |
| S2602 | Acemetacin | Neuronal Signaling | COX |
| S2603 | Tioxolone | Metabolism | Carbonic Anhydrase |
| S2604 | Dehydroepiandrosterone (DHEA) | Endocrinology & Hormones | Estrogen/progestogen Receptor,Androgen Receptor |
| S2606 | Mifepristone | Endocrinology & Hormones | Estrogen/progestogen Receptor |
| S2614 | Arecoline | Neuronal Signaling | AChR |
| S2617 | TAK-733 | MAPK | MEK |
| S2619 | MG-132 | Proteases | Proteasome |
| S2620 | GSK256066 | Metabolism | PDE |
| S2621 | AZD5438 | Cell Cycle | CDK |
| S2622 | PP121 | Protein Tyrosine Kinase | PDGFR,mTOR,DNA-PK |
| S2623 | Omecamtiv mecarbil (CK-1827452) | Transmembrane Transporters | ATPase |
| S2624 | OSI-027 | PI3K/Akt/mTOR | mTOR |
| S2625 | Fostamatinib (R788) | Angiogenesis | Syk |
| S2626 | LY2603618 | Cell Cycle | Chk |
| S2627 | Tubastatin A HCl | Epigenetics | HDAC |
| S2629 | PNU-120596 | Neuronal Signaling | AChR |
| S2630 | GW3965 HCl | Others | Liver X Receptor |
| S2631 | URB597 | Metabolism | FAAH |
| S2633 | NPS-2143 | GPCR & G Protein | CaSR |
| S2634 | DCC-2036 (Rebastinib) | Angiogenesis | Bcr-Abl |
| S2635 | CCT128930 | PI3K/Akt/mTOR | Akt |
| S2636 | A66 | PI3K/Akt/mTOR | PI3K |
| S2637 | TAK-875 | Endocrinology & Hormones | GPR |
| S2638 | NU7441 (KU-57788) | DNA Damage | DNA-PK,PI3K |
| S2639 | SNX-2112 (PF-04928473) | Cytoskeletal Signaling | HSP (e.g. HSP90) |
| S2656 | PF-04929113 (SNX-5422) | Cytoskeletal Signaling | HSP (e.g. HSP90) |
| S2658 | GSK2126458 (GSK458) | PI3K/Akt/mTOR | mTOR,PI3K |
| S2659 | 5-hydroxymethyl Tolterodine (PNU 200577, 5-HMT, 5-HM) | Neuronal Signaling | AChR |
| S2660 | MK-0752 | Proteases | Gamma-secretase,Beta Amyloid |
| S2661 | WYE-125132 (WYE-132) | PI3K/Akt/mTOR | mTOR |
| S2662 | ICG-001 | Stem Cells & Wnt | Wnt/beta-catenin |
| S2663 | WAY-100635 Maleate | Neuronal Signaling | 5-HT Receptor |
| S2664 | Clinofibrate | Endocrinology & Hormones | HMG-CoA Reductase |
| S2665 | Ciprofibrate | DNA Damage | PPAR |
| S2666 | PF-3845 | Metabolism | FAAH |
| S2667 | Dolutegravir (GSK1349572) | Microbiology | Integrase |
| S2670 | A-674563 | PI3K/Akt/mTOR | PKA,Akt,CDK |
| S2671 | AS-252424 | PI3K/Akt/mTOR | PI3K |
| S2672 | PF-00562271 | Angiogenesis | FAK |
| S2673 | Trametinib (GSK1120212) | MAPK | MEK |
| S2674 | A922500 | Metabolism | Transferase |
| S2677 | BRL-15572 | Neuronal Signaling | 5-HT Receptor |
| S2679 | Flavopiridol HCl | Cell Cycle | CDK |
| S2680 | Ibrutinib (PCI-32765) | Angiogenesis | BTK |
| S2681 | AS-604850 | PI3K/Akt/mTOR | PI3K |
| S2683 | CHIR-124 | Cell Cycle | Chk |
| S2685 | KW-2478 | Cytoskeletal Signaling | HSP (e.g. HSP90) |
| S2686 | NVP-BSK805 2HCl | JAK/STAT | JAK |
| S2687 | PF-2545920 | Metabolism | PDE |
| S2688 | R547 | Cell Cycle | CDK |
| S2689 | WAY-600 | PI3K/Akt/mTOR | mTOR |
| S2690 | ADX-47273 | Neuronal Signaling | GluR |
| S2691 | BMY 7378 | Neuronal Signaling | 5-HT Receptor,Adrenergic Receptor |
| S2692 | TG101209 | JAK/STAT | JAK,FLT3,c-RET |
| S2693 | Resminostat | Epigenetics | HDAC |
| S2694 | XL335 | Others | FXR |
| S2695 | Nepicastat (SYN-117) HCl | Metabolism | Hydroxylase |
| S2696 | GDC-0980 (RG7422) | PI3K/Akt/mTOR | mTOR,PI3K |
| S2697 | A-769662 | PI3K/Akt/mTOR | AMPK |
| S2698 | RS-127445 | Neuronal Signaling | 5-HT Receptor |
| S2699 | CH5132799 | PI3K/Akt/mTOR | mTOR,PI3K |
| S2700 | KX2-391 | Angiogenesis | Src |
| S2703 | GSK1838705A | Protein Tyrosine Kinase | ALK,IGF-1R |
| S2711 | YO-01027 | Proteases | Gamma-secretase |
| S2713 | Geldanamycin | Cytoskeletal Signaling | HSP (e.g. HSP90),Autophagy |
| S2714 | LY411575 | Proteases | Gamma-secretase |
| S2717 | CP-91149 | Metabolism | Phosphorylase |
| S2718 | TAK-901 | Cell Cycle | Aurora Kinase |
| S2719 | AMG-900 | Cell Cycle | Aurora Kinase |
| S2720 | ZM 336372 | MAPK | Raf |
| S2721 | Nilvadipine | Transmembrane Transporters | Calcium Channel |
| S2722 | JTC-801 | Neuronal Signaling | Opioid Receptor |

| | | | |
|---|---|---|---|
| S2726 | PH-797804 | MAPK | p38 MAPK |
| S2727 | Dacomitinib (PF299804, PF299) | Protein Tyrosine Kinase | EGFR |
| S2728 | AG-1478 (Tyrphostin AG-1478) | Protein Tyrosine Kinase | EGFR |
| S2729 | SB415286 | PI3K/Akt/mTOR | GSK-3 |
| S2730 | Crenolanib (CP-868596) | Protein Tyrosine Kinase | PDGFR |
| S2731 | AZ 3146 | Cytoskeletal Signaling | Kinesin |
| S2735 | MK-8776 (SCH 900776) | Cell Cycle | Chk,CDK |
| S2736 | TG101348 (SAR302503) | JAK/STAT | JAK |
| S2738 | PAC-1 | Apoptosis | Caspase |
| S2742 | PHA-767491 | Cell Cycle | CDK |
| S2743 | PF-04691502 | PI3K/Akt/mTOR | mTOR,Akt,PI3K |
| S2744 | CCT137690 | Cell Cycle | Aurora Kinase |
| S2745 | CHIR-98014 | PI3K/Akt/mTOR | GSK-3 |
| S2746 | AZ 628 | MAPK | Raf |
| S2747 | AMG-458 | Protein Tyrosine Kinase | c-Met |
| S2749 | BGT226 (NVP-BGT226) | PI3K/Akt/mTOR | mTOR,PI3K |
| S2750 | GW788388 | TGF-beta/Smad | TGF-beta/Smad |
| S2751 | Milciclib (PHA-848125) | Cell Cycle | CDK |
| S2753 | Tivantinib (ARQ 197) | Protein Tyrosine Kinase | c-Met |
| S2755 | Varlitinib | Protein Tyrosine Kinase | EGFR |
| S2757 | TH-302 | Others | Others |
| S2758 | Wortmannin | PI3K/Akt/mTOR | PI3K,ATM/ATR,Autophagy |
| S2759 | CUDC-907 | Cytoskeletal Signaling | PI3K,HDAC |
| S2760 | Canagliflozin | GPCR & G Protein | SGLT |
| S2761 | NVP-BVU972 | Protein Tyrosine Kinase | c-Met |
| S2765 | MK-2048 | Microbiology | Integrase |
| S2767 | 3-Methyladenine | PI3K/Akt/mTOR | PI3K,Autophagy |
| S2768 | Dinaciclib (SCH727965) | Cell Cycle | CDK |
| S2769 | Dovitinib (TKI-258) Dilactic Acid | Angiogenesis | FGFR,PDGFR,VEGFR,c-Kit,FLT3 |
| S2770 | MK-5108 (VX-689) | Cell Cycle | Aurora Kinase |
| S2772 | Dalcetrapib (JTT-705, RO4607381) | Metabolism | CETP |
| S2773 | SB705498 | Others | TRPV |
| S2774 | MK-2461 | Protein Tyrosine Kinase | FGFR,PDGFR,c-Met |
| S2775 | Nocodazole | cytoskeletal signaling | Autophagy,Microtubule Associated |
| S2776 | CPI-613 | Metabolism | Dehydrogenase |
| S2778 | GW842166X | GPCR & G Protein | Cannabinoid Receptor |
| S2779 | M344 | Cytoskeletal Signaling | HDAC |
| S2781 | RITA (NSC 652287) | Apoptosis | E3 Ligase ,p53 |
| S2782 | GW4064 | Others | FXR |
| S2783 | AZD2014 | PI3K/Akt/mTOR | mTOR |
| S2784 | TAK-285 | Protein Tyrosine Kinase | HER2,EGFR |
| S2785 | A-803467 | Transmembrane Transporters | Sodium Channel |
| S2787 | Laquinimod | Others | Others |
| S2789 | Tofacitinib (CP-690550,Tasocitinib) | JAK/STAT | JAK |
| S2791 | Sotrastaurin | TGF-beta/Smad | PKC |
| S2792 | Torcetrapib | Metabolism | CETP |
| S2794 | Sofosbuvir (PSI-7977, GS-7977) | DNA Damage | DNA/RNA Synthesis |
| S2795 | VU 0357121 | Neuronal Signaling | GluR |
| S2796 | WP1066 | JAK/STAT | JAK |
| S2797 | Lonafarnib | Metabolism | Transferase |
| S2801 | AZD4547 | Angiogenesis | FGFR |
| S2803 | Galeterone | Endocrinology & Hormones | P450 (e.g. CYP17),Androgen Receptor |
| S2804 | Sirtinol | Epigenetics | Sirtuin |
| S2806 | CEP-33779 | JAK/STAT | JAK |
| S2807 | Dabrafenib (GSK2118436) | MAPK | Raf |
| S2808 | GDC-0068 | PI3K/Akt/mTOR | Akt |
| S2809 | MPEP | Neuronal Signaling | GluR |
| S2811 | INK 128 (MLN0128) | PI3K/Akt/mTOR | mTOR |
| S2812 | AT101 | Apoptosis | Bcl-2 |
| S2813 | Ciproxifan | Neuronal Signaling | Histamine Receptor |
| S2814 | BYL719 | PI3K/Akt/mTOR | PI3K |
| S2816 | Tyrphostin AG 879 | Protein Tyrosine Kinase | HER2 |
| S2817 | Torin 2 | PI3K/Akt/mTOR | mTOR,ATM/ATR |
| S2818 | CI994 (Tacedinaline) | Epigenetics | HDAC |
| S2819 | AM251 | GPCR & G Protein | Cannabinoid Receptor |
| S2820 | TAE226 (NVP-TAE226) | Angiogenesis | FAK |
| S2821 | RG108 | Epigenetics | Transferase,DNA Methyltransferase |
| S2822 | OC000459 | Endocrinology & Hormones | GPR |
| S2824 | TPCA-1 | NF-κB | IκB/IKK |
| S2825 | ML133 HCl | Transmembrane Transporters | Potassium Channel |
| S2828 | JNJ-1661010 | Metabolism | FAAH |
| S2832 | Epiandrosterone | Endocrinology & Hormones | Androgen Receptor,Estrogen/progestogen Receptor |
| S2840 | ARN-509 | Endocrinology & Hormones | Androgen Receptor |
| S2841 | R428 (BGB324) | Protein Tyrosine Kinase | TAM Receptor |
| S2843 | BI-D1870 | PI3K/Akt/mTOR | S6 Kinase |
| S2845 | Semaxanib (SU5416) | Protein Tyrosine Kinase | VEGFR |

| | | | |
|---|---|---|---|
| S2849 | SB269970 HCl | Neuronal Signaling | 5-HT Receptor |
| S2851 | Baricitinib (LY3009104, INCB028050) | Epigenetics | JAK |
| S2852 | BRL-54443 | Neuronal Signaling | 5-HT Receptor |
| S2853 | Carfilzomib (PR-171) | Proteases | Proteasome |
| S2854 | BML-190 | GPCR & G Protein | Cannabinoid Receptor |
| S2855 | MRS 2578 | Neuronal Signaling | P2 Receptor |
| S2856 | SB271046 | Neuronal Signaling | 5-HT Receptor |
| S2857 | MK-801 (Dizocilpine) | Neuronal Signaling | GluR |
| S2859 | Golvatinib (E7050) | Protein Tyrosine Kinase | VEGFR,c-Met |
| S2860 | IEM 1754 dihydrobroMide | Neuronal Signaling | GluR |
| S2861 | CTEP (RO4956371) | Neuronal Signaling | GluR |
| S2862 | VU 0364770 | Neuronal Signaling | GluR |
| S2863 | ML130 (Nodinitib-1) | NF-κB | NOD1 |
| S2864 | IMD 0354 | NF-κB | IκB/IKK |
| S2865 | VUF 10166 | Neuronal Signaling | 5-HT Receptor |
| S2866 | U-104 | Metabolism | Carbonic Anhydrase |
| S2867 | WHI-P154 | JAK/STAT | JAK,EGFR |
| S2868 | Alogliptin | Proteases | DPP-4 |
| S2870 | TG100713 | PI3K/Akt/mTOR | PI3K |
| S2871 | T0070907 | DNA Damage | PPAR |
| S2872 | GW5074 | MAPK | Raf |
| S2875 | Prucalopride | Neuronal Signaling | 5-HT Receptor |
| S2876 | (-)-MK 801 Maleate | Neuronal Signaling | GluR |
| S2882 | IKK-16 (IKK Inhibitor VII) | NF-κB | IκB/IKK |
| S2890 | PF-562271 | Angiogenesis | FAK |
| S2891 | GW441756 | Protein Tyrosine Kinase | Trk receptor |
| S2892 | VU 0361737 | Neuronal Signaling | GluR |
| S2894 | SB742457 | Neuronal Signaling | 5-HT Receptor |
| S2895 | Tyrphostin 9 | Protein Tyrosine Kinase | EGFR |
| S2896 | ZM 323881 HCl | Protein Tyrosine Kinase | VEGFR |
| S2897 | ZM 306416 | Protein Tyrosine Kinase | VEGFR |
| S2898 | MLN0905 | Cell Cycle | PLK |
| S2899 | GNF-2 | Angiogenesis | Bcr-Abl |
| S2900 | Cobicistat (GS-9350) | Metabolism | P450 (e.g. CYP17) |
| S2902 | S-Ruxolitinib (INCB018424) | JAK/STAT | JAK |
| S2903 | Lumiracoxib | Neuronal Signaling | COX |
| S2904 | PF-477736 | Cell Cycle | Chk |
| S2905 | JNJ-7777120 | Neuronal Signaling | Histamine Receptor |
| S2906 | Ki16198 | GPCR & G Protein | LPA Receptor |
| S2907 | Pirfenidone | TGF-beta/Smad | TGF-beta/Smad |
| S2911 | Go 6983 | TGF-beta/Smad | PKC |
| S2912 | WZ811 | GPCR & G Protein | CXCR |
| S2913 | BAY 11-7082 | NF-κB | E2 conjugating,IκB/IKK |
| S2914 | Dapivirine (TMC120) | Microbiology | Reverse Transcriptase |
| S2915 | GW9662 | DNA Damage | PPAR |
| S2919 | IOX2 | Angiogenesis | HIF |
| S2921 | PF-4981517 | Metabolism | P450 (e.g. CYP17) |
| S2922 | Icotinib | Protein Tyrosine Kinase | EGFR |
| S2925 | Evacetrapib (LY2484595) | Metabolism | CETP |
| S2926 | TDZD-8 | PI3K/Akt/mTOR | GSK-3 |
| S2927 | Apoptosis Activator 2 | Apoptosis | Caspase |
| S2928 | TAK-715 | MAPK | p38 MAPK |
| S2929 | Pifithrin-α (PFTα) | Apoptosis | Autophagy,p53 |
| S2930 | Pifithrin-μ | Apoptosis | p53 |
| S3002 | Rivaroxaban | Metabolism | Factor Xa |
| S3005 | Paroxetine HCl | Neuronal Signaling | 5-HT Receptor,AChR |
| S3008 | Zaltoprofen | Neuronal Signaling | COX |
| S3012 | Pazopanib | Protein Tyrosine Kinase | PDGFR,VEGFR,c-Kit |
| S3017 | Aspirin | Proteases | COX |
| S3018 | Niflumic acid | Neuronal Signaling | GABA Receptor,COX |
| S3019 | Ciclopirox ethanolamine | Transmembrane Transporters | ATPase |
| S3021 | Rimonabant | GPCR & G Protein | Cannabinoid Receptor |
| S3023 | Bufexamac | Neuronal Signaling | COX |
| S3024 | Lamotrigine | Transmembrane Transporters | 5-HT Receptor,Sodium Channel |
| S3026 | Piceatannol | Angiogenesis | Syk |
| S3031 | Linagliptin | Proteases | DPP-4 |
| S3033 | Vildagliptin (LAF-237) | Proteases | DPP-4 |
| S3035 | Daunorubicin HCl | DNA Damage | Topoisomerase |
| S3036 | Pravastatin sodium | Metabolism | HMG-CoA Reductase |
| S3037 | Bepotastine Besilate | Neuronal Signaling | Histamine Receptor |
| S3042 | Purmorphamine | Stem Cells & Wnt | Hedgehog/Smoothened |
| S3043 | Rofecoxib | Neuronal Signaling | COX |
| S3046 | Azilsartan | Endocrinology & Hormones | RAAS |
| S3047 | Otilonium Bromide | Neuronal Signaling | AChR |
| S3048 | Solifenacin succinate | Neuronal Signaling | AChR |
| S3051 | Bosentan Hydrate | GPCR & G Protein | Endothelin Receptor |

| | | | |
|---|---|---|---|
| S3052 | Rupatadine Fumarate | Neuronal Signaling | Histamine Receptor |
| S3053 | Azelnidipine | Transmembrane Transporters | Calcium Channel |
| S3057 | Azilsartan Medoxomil | Endocrinology & Hormones | RAAS |
| S3060 | Medetomidine HCl | Neuronal Signaling | Adrenergic Receptor |
| S3061 | Epinephrine HCl | Neuronal Signaling | Adrenergic Receptor |
| S3064 | Ambroxol HCl | Transmembrane Transporters | Sodium Channel |
| S3066 | Naloxone HCl | Neuronal Signaling | Opioid Receptor |
| S3075 | Dexmedetomidine | Neuronal Signaling | Adrenergic Receptor |
| S3080 | Etravirine (TMC125) | Microbiology | Reverse Transcriptase |
| S3083 | Indacaterol Maleate | Neuronal Signaling | Adrenergic Receptor |
| S3117 | Oxybutynin chloride | Neuronal Signaling | AChR |
| S3144 | Darifenacin HBr | Neuronal Signaling | AChR |
| S3146 | Tripelennamine HCl | Neuronal Signaling | Histamine Receptor |
| S3147 | Entacapone | Epigenetics | Histone Methyltransferase |
| S3149 | Estradiol valerate | Endocrinology & Hormones | Estrogen/progestogen Receptor |
| S3151 | Gliquidone | Transmembrane Transporters | Potassium Channel |
| S3160 | Ethynodiol diacetate | Endocrinology & Hormones | Estrogen/progestogen Receptor |
| S3163 | Benztropine mesylate | Neuronal Signaling | Dopamine Receptor |
| S3167 | Altrenogest | Endocrinology & Hormones | Estrogen/progestogen Receptor |
| S3172 | Anagrelide HCl | Metabolism | PDE |
| S3175 | Atomoxetine HCl | Neuronal Signaling | 5-HT Receptor |
| S3178 | Brinzolamide | Metabolism | Carbonic Anhydrase |
| S3180 | Eletriptan HBr | Neuronal Signaling | 5-HT Receptor |
| S3181 | Flumequine | DNA Damage | Topoisomerase |
| S3183 | Amitriptyline HCl | Neuronal Signaling | 5-HT Receptor |
| S3185 | Adrenalone HCl | Neuronal Signaling | Adrenergic Receptor |
| S3186 | Azatadine dimaleate | Neuronal Signaling | Histamine Receptor |
| S3200 | Triflusal | Neuronal Signaling | COX |
| S3201 | Trifluoperazine 2HCl | Ubiquitin | Autophagy |
| S3208 | Fexofenadine HCl | Neuronal Signaling | Histamine Receptor |
| S3212 | Moclobemide (Ro 111163) | Metabolism | MAO |
| S3603 | Betulinic acid | DNA Damage | Topoisomerase |
| S4000 | Pergolide mesylate | Neuronal Signaling | Dopamine Receptor |
| S4001 | Cabozantinib malate (XL184) | Protein Tyrosine Kinase | VEGFR,TAM Receptor |
| S4002 | Sitagliptin phosphate monohydrate | Proteases | DPP-4 |
| S4009 | Mirabegron | Neuronal Signaling | Adrenergic Receptor |
| S4010 | Acebutolol HCl | Neuronal Signaling | Adrenergic Receptor |
| S4011 | Ampiroxicam | Neuronal Signaling | COX |
| S4012 | Desloratadine | Neuronal Signaling | Histamine Receptor |
| S4014 | Hyoscyamine | Neuronal Signaling | AChR |
| S4016 | Ouabain | Transmembrane Transporters | Sodium Channel |
| S4019 | Avanafil | Metabolism | PDE |
| S4021 | Tolcapone | Metabolism | Transferase |
| S4023 | Procaine HCl | Transmembrane Transporters | Sodium Channel |
| S4024 | Homatropine Methylbromide | Neuronal Signaling | AChR |
| S4025 | Homatropine Bromide | Neuronal Signaling | AChR |
| S4026 | Hydroxyzine 2HCl | Neuronal Signaling | Histamine Receptor |
| S4027 | Flavoxate HCl | Neuronal Signaling | AChR |
| S4031 | Aclidinium Bromide | Neuronal Signaling | AChR |
| S4034 | Diphemanil Methylsulfate | Neuronal Signaling | AChR |
| S4038 | Dibucaine HCl | Transmembrane Transporters | Sodium Channel |
| S4039 | Methazolamide | Metabolism | Carbonic Anhydrase |
| S4043 | Tetrahydrozoline HCl | Neuronal Signaling | Adrenergic Receptor |
| S4046 | Estradiol Cypionate | Endocrinology & Hormones | Estrogen/progestogen Receptor |
| S4049 | Valdecoxib | Neuronal Signaling | COX |
| S4051 | Nabumetone | Neuronal Signaling | COX |
| S4053 | Sertraline HCl | Neuronal Signaling | 5-HT Receptor |
| S4054 | Spironolactone | Endocrinology & Hormones | Androgen Receptor |
| S4061 | Levobupivacaine HCl | Transmembrane Transporters | Sodium Channel |
| S4064 | Escitalopram Oxalate | Neuronal Signaling | 5-HT Receptor |
| S4065 | Guanabenz Acetate | Neuronal Signaling | Adrenergic Receptor |
| S4072 | Decamethonium Bromide | Neuronal Signaling | AChR |
| S4073 | Sodium 4-Aminosalicylate | NF-κB | NF-κB |
| S4075 | Zinc Pyrithione | Transmembrane Transporters | Proton Pump |
| S4076 | Propranolol HCl | GPCR & G Protein | Adrenergic Receptor |
| S4078 | Mefenamic Acid | Neuronal Signaling | COX |
| S4079 | Ticagrelor | Neuronal Signaling | P2 Receptor |
| S4080 | Triamterene | Transmembrane Transporters | Sodium Channel |
| S4081 | Sulfacetamide Sodium | Ubiquitin | Autophagy |
| S4091 | Ifenprodil Tartrate | Neuronal Signaling | GluR |
| S4109 | Lorcaserin HCl | Neuronal Signaling | 5-HT Receptor |
| S4110 | Estradiol Benzoate | Others | Estrogen/progestogen Receptor |
| S4112 | Desvenlafaxine Succinate | Neuronal Signaling | 5-HT Receptor |
| S4113 | Desvenlafaxine | Neuronal Signaling | 5-HT Receptor |
| S4118 | Histamine 2HCl | Neuronal Signaling | Histamine Receptor |
| S4119 | Pefloxacin Mesylate Dihydrate | DNA Damage | Topoisomerase |

| | | | |
|---|---|---|---|
| S4123 | Timolol Maleate | Neuronal Signaling | Adrenergic Receptor |
| S4124 | Tolazoline HCl | Neuronal Signaling | Adrenergic Receptor |
| S4125 | Sodium Phenylbutyrate | DNA Damage | HDAC |
| S4131 | Levodropropizine | Neuronal Signaling | Histamine Receptor |
| S4139 | Cyclizine 2HCl | Neuronal Signaling | Histamine Receptor |
| S4212 | Tenatoprazole | Transmembrane Transporters | Proton Pump |
| S4220 | Bosentan | GPCR & G Protein | Endothelin Receptor |
| S4246 | Tranylcypromine (2-PCPA) HCl | Epigenetics | MAO |
| S4261 | EUK 134 | Neuronal Signaling | Beta Amyloid |
| S4269 | Vinorelbine Tartrate | Cytoskeletal Signaling | Microtubule Associated |
| S4270 | Oxiracetam | Others | Others |
| S4274 | Rotigotine | Neuronal Signaling | Dopamine Receptor |
| S4276 | Etizolam | Others | Others |
| S4277 | Bambuterol HCl | GPCR & G Protein | Adrenergic Receptor |
| S4278 | Carteolol HCl | GPCR & G Protein | Adrenergic Receptor |
| S4279 | Demeclocycline HCl | Others | Others |
| S4282 | Nelfinavir Mesylate | Proteases | HIV Protease |
| S4283 | Cyclobenzaprine HCl | Others | Others |
| S4285 | Ospemifene | Endocrinology & Hormones | Estrogen/progestogen Receptor |
| S4286 | Anidulafungin (LY303366) | Others | Others |
| S4288 | Chloroambucil | DNA Damage | DNA/RNA Synthesis |
| S4289 | MetoclopraMide HCl | Neuronal Signaling | Dopamine Receptor |
| S4290 | Digoxin | Transmembrane Transporters | Sodium Channel |
| S4291 | Labetalol HCl | GPCR & G Protein | Adrenergic Receptor |
| S4292 | Diphenidol HCl | Neuronal Signaling | AChR |
| S4293 | Promethazine HCl | Neuronal Signaling | Histamine Receptor |
| S4294 | Procainamide HCl | Transmembrane Transporters | DNA Methyltransferase,Sodium Channel |
| S4295 | Meclofenamate Sodium | Neuronal Signaling | COX |
| S4297 | Mupirocin | DNA Damage | DNA/RNA Synthesis |
| S4299 | Dicoumarol | Others | Others |
| S4420 | Mefloquine HCl | Others | Others |
| S4504 | 6-Mercaptopurine (6-MP) Monohydrate | DNA Damage | DNA/RNA Synthesis |
| S4900 | Tenovin-6 | Apoptosis | p53,Sirtuin |
| S4901 | JNK-IN-8 | MAPK | JNK |
| S4902 | QNZ (EVP4593) | NF-κB | NF-κB,TNF-alpha |
| S4907 | SC-514 | NF-κB | IκB/IKK |
| S4908 | SN-38 | DNA Damage | Topoisomerase |
| S4920 | b-AP15 | Ubiquitin | DUB |
| S4921 | MNS (3,4-Methylenedioxy-β-nitrostyrene, MDBN) | Ubiquitin | p97 |
| S4926 | (R)-Nepicastat HCl | Metabolism | Hydroxylase |
| S5001 | Tofacitinib (CP-690550) Citrate | JAK/STAT | JAK |
| S5002 | Fingolimod (FTY720) HCl | GPCR & G Protein | S1P Receptor |
| S6003 | Ataluren (PTC124) | Transmembrane Transporters | CFTR |
| S6005 | VX-702 | MAPK | p38 MAPK |
| S7000 | AP26113 | Protein Tyrosine Kinase | ALK |
| S7003 | AZD2932 | Protein Tyrosine Kinase | VEGFR,c-Kit,PDGFR,FLT3 |
| S7007 | MEK162 (ARRY-162, ARRY-438162) | MAPK | MEK |
| S7008 | PP2 | Angiogenesis | Src |
| S7009 | LCL161 | Apoptosis | IAP |
| S7010 | GDC-0152 | Apoptosis | IAP |
| S7015 | Birinapant | Apoptosis | IAP |
| S7016 | VS-5584 (SB2343) | PI3K/Akt/mTOR | PI3K |
| S7018 | CZC24832 | PI3K/Akt/mTOR | PI3K |
| S7023 | Z-VAD-FMK | Apoptosis | Caspase |
| S7024 | Stattic | JAK/STAT | STAT |
| S7025 | Embelin | Apoptosis | IAP |
| S7028 | IPI-145 (INK1197) | Angiogenesis | PI3K |
| S7029 | AZD2461 | DNA Damage | PARP |
| S7030 | RG-7112 | Apoptosis | Mdm2 |
| S7033 | GSK2656157 | Apoptosis | PERK |
| S7035 | XL388 | PI3K/Akt/mTOR | mTOR |
| S7036 | XL019 | JAK/STAT | JAK |
| S7037 | Wnt-C59 (C59) | Stem Cells & Wnt | Wnt/beta-catenin |
| S7039 | PD168393 | Protein Tyrosine Kinase | EGFR |
| S7040 | AZD3514 | Endocrinology & Hormones | Androgen Receptor |
| S7041 | CX-6258 HCl | JAK/STAT | Pim |
| S7046 | Brefeldin A | Transmembrane Transporters | ATPase,Autophagy |
| S7048 | BMN 673 | Epigenetics | PARP |
| S7049 | Oprozomib (ONX 0912) | Proteases | Proteasome |
| S7050 | AZ20 | PI3K/Akt/mTOR | ATM/ATR |
| S7051 | CGI1746 | Angiogenesis | BTK |
| S7057 | LY2874455 | Protein Tyrosine Kinase | VEGFR,FGFR |
| S7059 | VX-661 | Transmembrane Transporters | CFTR |
| S7060 | PP1 | Angiogenesis | Src |
| S7061 | GSK126 | Epigenetics | Histone Methyltransferase |
| S7062 | EPZ5676 | Epigenetics | Histone Methyltransferase |

| | | | |
|---|---|---|---|
| S7063 | LY2090314 | PI3K/Akt/mTOR | GSK-3 |
| S7065 | MK-8745 | Cell Cycle | Aurora Kinase |
| S7067 | Tepotinib (EMD 1214063) | Protein Tyrosine Kinase | c-Met |
| S7070 | GSK J4 HCl | Epigenetics | Histone Demethylase |
| S7072 | NMDA (N-Methyl-D-aspartic acid) | Neuronal Signaling | GluR |
| S7076 | T0901317 | Others | Liver X Receptor |
| S7077 | Cilengitide | Others | Integrin |
| S7079 | SGC 0946 | Epigenetics | Histone Methyltransferase |
| S7080 | RN486 | Angiogenesis | BTK |
| S7083 | LDK378 | Protein Tyrosine Kinase | ALK |
| S7085 | IWP-2 | Stem Cells & Wnt | Wnt/beta-catenin |
| S7086 | IWR-1-endo | Stem Cells & Wnt | Wnt/beta-catenin |
| S7087 | GSK2334470 | PI3K/Akt/mTOR | PDK-1 |
| S7088 | UNC1215 | Epigenetics | Epigenetic Reader Domain |
| S7090 | GSK923295 | Cytoskeletal Signaling | Kinesin |
| S7091 | Zotarolimus(ABT-578) | PI3K/Akt/mTOR | mTOR |
| S7092 | SANT-1 | Stem Cells & Wnt | Hedgehog/Smoothened |
| S7093 | IPA-3 | Cytoskeletal Signaling | PAK |
| S7094 | PF-3758309 | Cytoskeletal Signaling | PAK |
| S7096 | KY02111 | Stem Cells & Wnt | Wnt/beta-catenin |
| S7097 | HSP990 (NVP-HSP990) | Cytoskeletal Signaling | HSP (e.g. HSP90) |
| S7098 | PD123319 | Endocrinology & Hormones | RAAS |
| S7099 | (-)-Blebbistatin | Transmembrane Transporters | ATPase |
| S7102 | VE-822 | PI3K/Akt/mTOR | ATM/ATR |
| S7103 | GDC-0032 | PI3K/Akt/mTOR | PI3K |
| S7104 | AZD1208 | JAK/STAT | Pim |
| S7106 | AZD3463 | Protein Tyrosine Kinase | ALK |
| S7108 | LGX818 | MAPK | Raf |
| S7110 | (+)-JQ1 | Epigenetics | Epigenetic Reader Domain |
| S7111 | NLG919 | Metabolism | IDO |
| S7113 | Zebularine | Epigenetics | DNA Methyltransferase |
| S7114 | NU6027 | Cell Cycle | CDK |
| S7115 | AMG-517 | Others | TRPV |
| S7119 | Go6976 | TGF-beta/Smad | JAK,FLT3,PKC |
| S7120 | 3-Deazaneplanocin A (DZNeP) | Epigenetics | Histone Methyltransferase |
| S7122 | XL888 | Cytoskeletal Signaling | HSP (e.g. HSP90) |
| S7125 | KPT-185 | Transmembrane Transporters | CRM1 |
| S7127 | TIC10 | PI3K/Akt/mTOR | Akt |
| S7128 | EPZ-6438 | Epigenetics | Histone Methyltransferase |
| S7129 | PYR-41 | Ubiquitin | E1 Activating |
| S7130 | PR-619 | Ubiquitin | DUB |
| S7132 | P5091 (P005091) | Ubiquitin | DUB |
| S7133 | P22077 | Ubiquitin | DUB |
| S7134 | IU1 | Proteases | DUB |
| S7135 | LDN-57444 | Proteases | DUB |
| S7136 | CGK 733 | DNA Damage | ATM/ATR |
| S7138 | BMS-833923 | GPCR & G Protein | Hedgehog/Smoothened |
| S7139 | CFTRinh-172 | Transmembrane Transporters | CFTR |
| S7140 | TCID | Ubiquitin | DUB |
| S7142 | NSC697923 | Ubiquitin | E2 conjugating |
| S7143 | LGK-974 | Stem Cells & Wnt | Wnt/beta-catenin |
| S7145 | AZD1080 | PI3K/Akt/mTOR | GSK-3 |
| S7146 | DMH1 | TGF-beta/Smad | TGF-beta/Smad |
| S7147 | LDN-212854 | TGF-beta/Smad | TGF-beta/Smad |
| S7148 | ML347 | TGF-beta/Smad | TGF-beta/Smad |
| S7149 | NSC 319726 | Apoptosis | p53 |
| S7152 | C646 | Epigenetics | Histone Acetyltransferase |
| S7153 | 10058-F4 | Cell Cycle | c-Myc |
| S7155 | Batimastat (BB-94) | Proteases | MMP |
| S7156 | Marimastat(BB-2516) | Proteases | MMP |
| S7158 | LY2835219 | Cell Cycle | CDK |
| S7162 | Mdivi-1 | Cytoskeletal Signaling | Dynamin |
| S7163 | Dyngo-4a | Cytoskeletal Signaling | Dynamin |
| S7165 | UNC1999 | Epigenetics | Histone Methyltransferase |
| S7167 | SSR128129E | Angiogenesis | FGFR |
| S7170 | RO5126766 (CH5126766) | MAPK | Raf |
| S7171 | GKT137831 | Others | Others |
| S7172 | ONX-0914 (PR-957) | Proteases | Proteasome |
| S7173 | AVL-292 | Angiogenesis | BTK |
| S7174 | ABC294640 | GPCR & G Protein | S1P Receptor |
| S7176 | SKI II | GPCR & G Protein | S1P Receptor |
| S7177 | PF-543 | GPCR & G Protein | S1P Receptor |
| S7185 | AGI-5198 | Metabolism | Dehydrogenase |
| S7188 | CID755673 | Others | Others |
| S7189 | I-BET-762 | Epigenetics | Epigenetic Reader Domain |
| S7192 | PF-04620110 | Metabolism | Transferase |

| | | | |
|---|---|---|---|
| S7193 | 1-Azakenpaullone | PI3K/Akt/mTOR | GSK-3 |
| S7194 | GZD824 | Angiogenesis | Bcr-Abl |
| S7195 | RKI-1447 | Cell Cycle | ROCK |
| S7198 | BIO | PI3K/Akt/mTOR | GSK-3 |
| S7199 | DBeQ | Ubiquitin | p97 |
| S7205 | Idasanutlin (RG-7388) | Apoptosis | Mdm2 |
| S7206 | CNX-2006 | Protein Tyrosine Kinase | EGFR |
| S7208 | GF109203X | TGF-beta/Smad | PKC |
| S7214 | Skepinone-L | MAPK | p38 MAPK |
| S7215 | Losmapimod (GW856553X) | MAPK | p38 MAPK |
| S7218 | Alvelestat (AZD9668) | Proteases | Serine Protease |
| S7223 | RepSox | TGF-beta/Smad | TGF-beta/Smad |
| S7224 | Deltarasin | Metabolism | PDE |
| S7229 | RGFP966 | Epigenetics | HDAC |
| S7231 | GSK2801 | Epigenetics | Epigenetic Reader Domain |
| S7233 | Bromosporine | Epigenetics | Epigenetic Reader Domain |
| S7234 | IOX1 | Epigenetics | Histone Demethylase |
| S7237 | OG-L002 | Epigenetics | Histone Demethylase |
| S7239 | G007-LK | DNA Damage | PARP |
| S7241 | AGI-6780 | Metabolism | Dehydrogenase |
| S7242 | Erastin | Metabolism | Ferroptosis |
| S7243 | Ferrostatin-1 (Fer-1) | Metabolism | Ferroptosis |
| S7248 | Ro3280 | Cell Cycle | PLK |
| S7251 | KPT-276 | Transmembrane Transporters | CRM1 |
| S7252 | KPT-330 | Transmembrane Transporters | CRM1 |
| S7253 | AZD2858 | PI3K/Akt/mTOR | GSK-3 |
| S7256 | SGC-CBP30 | Epigenetics | Epigenetic Reader Domain |
| S7257 | CNX-774 | Angiogenesis | BTK |
| S7258 | SKLB1002 | Protein Tyrosine Kinase | VEGFR |
| S7259 | FLLL32 | JAK/STAT | JAK |
| S7261 | Beta-Lapachone | DNA Damage | Topoisomerase |
| S7262 | Vidofludimus | Metabolism | Dehydrogenase |
| S7263 | AZD1981 | Endocrinology & Hormones | GPR |
| S7265 | MM-102 | Epigenetics | Histone Methyltransferase |
| S7266 | Golgicide A | Transmembrane Transporters | ATPase |
| S7269 | PD173955 | Angiogenesis | Bcr-Abl |
| S7271 | FRAX597 | Cytoskeletal Signaling | PAK |
| S7273 | SC75741 | NF-κB | NF-κB |
| S7276 | SGI-1027 | Epigenetics | DNA Methyltransferase |
| S7278 | HPOB | Cytoskeletal Signaling | HDAC |
| S7279 | Suvorexant (MK-4305) | GPCR & G Protein | OX Receptor |
| S7280 | Edoxaban | Metabolism | Factor Xa |
| S7281 | JIB-04 | Epigenetics | Histone Demethylase |
| S7282 | NMS-E973 | Cytoskeletal Signaling | HSP (e.g. HSP90) |
| S7284 | CO-1686 (AVL-301) | Protein Tyrosine Kinase | EGFR |
| S7285 | NMS-873 | Ubiquitin | p97 |
| S7289 | PFK15 | Others | Others |
| S7291 | TAK-632 | MAPK | Raf |
| S7292 | RG2833 (RGFP109) | Epigenetics | HDAC |
| S7293 | ZCL278 | Cell Cycle | Rho |
| S7294 | PFI-2 | Epigenetics | Histone Methyltransferase |
| S7295 | RVX-208 | Epigenetics | Epigenetic Reader Domain |
| S7296 | ML324 | Epigenetics | Histone Demethylase |
| S7297 | AZD9291 | Protein Tyrosine Kinase | EGFR |
| S7298 | AZ5104 | Protein Tyrosine Kinase | EGFR |
| S7300 | PJ34 HCl | DNA Damage | PARP |
| S7301 | IWP-L6 | Stem Cells & Wnt | Wnt/beta-catenin |
| S7303 | Rilpivirine | Microbiology | Reverse Transcriptase |
| S7304 | CPI-203 | Epigenetics | Epigenetic Reader Domain |
| S7305 | MS436 | Epigenetics | Epigenetic Reader Domain |
| S7307 | GSK2606414 | Apoptosis | PERK |
| S7310 | SF1670 | Others | Others |
| S7315 | PFI-3 | Epigenetics | Epigenetic Reader Domain |
| S7317 | WZ4003 | PI3K/Akt/mTOR | AMPK |
| S7318 | HTH-01-015 | PI3K/Akt/mTOR | AMPK |
| S7319 | EHop-016 | Cell Cycle | Rho |
| S7320 | TG003 | Cell Cycle | CDK |
| S7324 | TMP269 | Epigenetics | HDAC |
| S7325 | UNC2881 | Others | TAM Receptor |
| S7326 | Tasisulam | Apoptosis | Caspase |
| S7329 | IOWH032 | Transmembrane Transporters | CFTR |
| S7330 | 6H05 | Cell Cycle | Rho |
| S7331 | K-Ras(G12C) inhibitor 12 | Cell Cycle | Rho |
| S7332 | K-Ras(G12C) inhibitor 9 | Cell Cycle | Rho |
| S7333 | K-Ras(G12C) inhibitor 6 | Cell Cycle | Rho |
| S7334 | ERK5-IN-1 | MAPK | ERK |

| | | | |
|---|---|---|---|
| S7336 | CW069 | Cytoskeletal Signaling | Microtubule Associated |
| S7337 | SH-4-54 | JAK/STAT | STAT |
| S7340 | CH5138303 | Cytoskeletal Signaling | HSP (e.g. HSP90) |
| S7343 | URMC-099 | Others | MLK,LRRK,Abl,VEGFR/FLT |
| S7351 | JSH-23 | NF-κB | NF-κB |
| S7352 | Bay 11-7085 | NF-κB | IκB/IKK |
| S7353 | EPZ004777 | Epigenetics | Histone Methyltransferase |
| S7355 | ARQ 621 | Cytoskeletal Signaling | Kinesin |
| S7356 | HS-173 | PI3K/Akt/mTOR | PI3K |
| S7357 | PF-562271 HCl | Angiogenesis | FAK |
| S7358 | Poziotinib (HM781-36B) | Protein Tyrosine Kinase | EGFR |
| S7359 | K02288 | TGF-beta/Smad | TGF-beta/Smad |
| S7360 | OTX015 | Epigenetics | Epigenetic Reader Domain |
| S7364 | Atglistatin | Others | Others |
| S7367 | GNE-0877 | Autophagy | LRRK2 |
| S7368 | GNE-9605 | Autophagy | LRRK2 |
| S7369 | 4EGI-1 | Others | Others |
| S7370 | 4E1RCat | Others | Others |
| S7372 | PTC-209 | Others | Others |
| S7373 | UNC669 | Epigenetics | Epigenetic Reader Domain |
| S7378 | AEBSF HCl | Proteases | Serine Protease |
| S7379 | E-64 | Proteases | Cysteine Protease |
| S7382 | Phosphoramidon Disodium Salt | Others | Others |
| S7383 | (-)-p-Bromotetramisole Oxalate | Others | Others |
| S7386 | MG-101 (ALLN) | Proteases | Cysteine Protease |
| S7391 | Z-FA-FMK | Proteases | Cysteine Protease |
| S7392 | Loxistatin Acid (E-64C) | Proteases | Cysteine Protease |
| S7393 | Aloxistatin | Proteases | Cysteine Protease |
| S7396 | Calpeptin | Proteases | Cysteine Protease |
| S7397 | Sorafenib | MAPK | Raf |
| S7399 | FLI-06 | Stem Cells & Wnt | Gamma-secretase |
| S7400 | ISRIB (trans-isomer) | Apoptosis | PERK |
| S7409 | Anisomycin | MAPK | JNK |
| S7414 | Caffeic Acid Phenethyl Ester | NF-κB | NF-κB |
| S7421 | CGP 57380 | Others | Others |
| S7422 | KN-62 | Others | CaMK |
| S7423 | KN-93 Phosphate | Others | CaMK |
| S7424 | PD 151746 | Proteases | Cysteine Protease |
| S7429 | MI-2 (MALT1 inhibitor) | Others | Others |
| S7430 | SB-3CT | Proteases | MMP |
| S7434 | TAPI-1 | Others | Others |
| S7435 | AR-A014418 | PI3K/Akt/mTOR | GSK-3 |
| S7436 | NH125 | Others | CaMK |
| S7437 | Sal003 | Others | Others |
| S7438 | ME0328 | Epigenetics | PARP |
| S7440 | LEE011 | Cell Cycle | CDK |
| S7441 | WS3 | NF-κB | IκB/IKK |
| S7442 | WS6 | NF-κB | IκB/IKK |
| S7445 | E3330 | DNA Damage | DNA/RNA Synthesis |
| S7448 | CORM-3 | Others | Others |
| S7449 | CRT0044876 | DNA Damage | DNA/RNA Synthesis |
| S7452 | FPH2 (BRD-9424) | Others | Others |
| S7457 | XEN445 | Others | Others |
| S7458 | VER-49009 | Cytoskeletal Signaling | HSP (e.g. HSP90) |
| S7459 | VER-50589 | Cytoskeletal Signaling | HSP (e.g. HSP90) |
| S7460 | BTB06584 | Transmembrane Transporters | ATPase |
| S7461 | LDC000067 | Cell Cycle | CDK |
| S7462 | PI-1840 | Proteases | Proteasome |
| S7465 | FTI 277 HCl | Metabolism | Transferase |
| S7467 | LB42708 | Metabolism | Transferase |
| S7470 | Triapine | DNA Damage | DNA/RNA Synthesis |
| S7473 | Nexturastat A | Epigenetics | HDAC |
| S7476 | MG149 | Epigenetics | Histone Acetyltransferase |
| S7482 | EHT 1864 | Cell Cycle | Rho |
| S7484 | FH535 | Stem Cells & Wnt | Wnt/beta-catenin,PPAR |
| S7488 | MPI-0479605 | Cytoskeletal Signaling | Kinesin |
| S7489 | YH239-EE | Apoptosis | Mdm2 |
| S7490 | WIKI4 | Stem Cells & Wnt | Wnt/beta-catenin |
| S7493 | INH1 | Cytoskeletal Signaling | Microtubule Associated |
| S7494 | INH6 | Cytoskeletal Signaling | Microtubule Associated |
| S7495 | TAI-1 | Cytoskeletal Signaling | Microtubule Associated |
| S7497 | CK-636 | Cytoskeletal Signaling | Microtubule Associated |
| S7498 | DDR1-IN-1 | Others | Others |
| S7499 | ESI-09 | Others | Others |
| S7500 | HJC0350 | Others | Others |
| S7501 | HO-3867 | JAK/STAT | STAT |

| | | | |
|---|---|---|---|
| S7505 | (S)-crizotinib | Others | Others |
| S7508 | JNK Inhibitor IX | MAPK | JNK |
| S7509 | ML167 | Cell Cycle | CDK |
| S7513 | Trelagliptin | Proteases | DPP-4 |
| S7517 | AZD7545 | Others | Others |
| S7518 | Voreloxin (SNS-595) | DNA Damage | Topoisomerase |
| S7519 | GNF-5837 | Protein Tyrosine Kinase | Trk receptor |
| S7520 | Darapladib (SB-480848) | Metabolism | Phospholipase (e.g. PLA) |
| S7521 | Afuresertib (GSK2110183) | PI3K/Akt/mTOR | Akt |
| S7523 | GS-9973 | Angiogenesis | Syk |
| S7524 | FR 180204 | MAPK | ERK |
| S7525 | XMD8-92 | MAPK | ERK |
| S7526 | GNF-5 | Angiogenesis | Bcr-Abl |
| S7528 | GNE-7915 | Autophagy | LRRK2 |
| S7529 | ML323 | Ubiquitin | DUB |
| S7530 | EW-7197 | TGF-beta/Smad | TGF-beta/Smad |
| S7531 | UMI-77 | Apoptosis | Bcl-2 |
| S7534 | BAPTA-AM | Others | Others |
| S7536 | PF-06463922 | Protein Tyrosine Kinase | ALK |
| S7539 | PTC-209 HBr | Others | Others |
| S7540 | SB273005 | Cytoskeletal Signaling | Integrin |
| S7545 | G-749 | Angiogenesis | FLT3 |
| S7546 | Pritelivir (BAY 57-1293) | Others | Others |
| S7553 | GDC-0623 | MAPK | MEK |
| S7554 | GDC-0994 | MAPK | ERK |
| S7555 | 4SC-202 | Epigenetics | HDAC |
| S7557 | CL-387785 (EKI-785) | Protein Tyrosine Kinase | EGFR |
| S7563 | AT13148 | PI3K/Akt/mTOR | Akt,ROCK,PKA,S6 Kinase |
| S7565 | WH-4-023 | Angiogenesis | Src |
| S7566 | IM-12 | PI3K/Akt/mTOR | GSK-3 |
| S7569 | LMK-235 | DNA Damage | HDAC |
| S7570 | UNC0379 | Epigenetics | Histone Methyltransferase |
| S7573 | GSK2830371 | Angiogenesis | Wip1 phosphatase |
| S7574 | GSK-LSD1 2HCl | Epigenetics | Histone Demethylase |
| S7576 | UNC-2025 | Protein Tyrosine Kinase | TAM Receptor,FLT3 |
| S7577 | AGK2 | Cytoskeletal Signaling | Sirtuin |
| S7579 | Ledipasvir (GS5885) | Microbiology | HCV Protease |
| S7581 | GSK J1 | Epigenetics | Histone Demethylase |
| S7582 | Anacardic Acid | Epigenetics | Histone Acetyltransferase |
| S7584 | LRRK2-IN-1 | Autophagy | LRRK2 |
| S7587 | INCB024360 | Metabolism | IDO |
| S7589 | N6022 | Others | Others |
| S7591 | BRD4770 | Epigenetics | Histone Methyltransferase |
| S7593 | Splitomicin | Cytoskeletal Signaling | Sirtuin |
| S7595 | Santacruzamate A (CAY10683) | DNA Damage | HDAC |
| S7596 | CAY10603 | DNA Damage | HDAC |
| S7597 | BV-6 | Apoptosis | IAP |
| S7605 | Filgotinib (GLPG0634) | JAK/STAT | JAK |
| S7606 | RBC8 | Others | GTPases RalA/RalB |
| S7607 | BQU57 | Others | Others |
| S7610 | UNC0631 | Epigenetics | Histone Methyltransferase |
| S7611 | EI1 | Epigenetics | Histone Methyltransferase |
| S7612 | PX-478 2HCl | Angiogenesis | HIF |
| S7616 | CPI-169 | Epigenetics | Histone Methyltransferase |
| S7617 | Tasquinimod | Angiogenesis | HDAC |
| S7618 | MI-2 (Menin-MLL Inhibitor) | Epigenetics | Histone Methyltransferase |
| S7619 | MI-3 (Menin-MLL Inhibitor) | Epigenetics | Histone Methyltransferase |
| S7620 | GSK1324726A (I-BET726) | Epigenetics | Epigenetic Reader Domain |
| S7623 | PI-3065 | PI3K/Akt/mTOR | PI3K |
| S7624 | SD-208 | TGF-beta/Smad | TGF-beta/Smad |
| S7627 | LDN-214117 | TGF-beta/Smad | TGF-beta/Smad |
| S7631 | TH287 | Others | Others |
| S7634 | Cerdulatinib (PRT062070, PRT2070) | JAK/STAT | JAK |
| S7636 | SU9516 | Cell Cycle | CDK |
| S7637 | DTP3 | MAPK | JNK |
| S7638 | LDC1267 | Protein Tyrosine Kinase | TAM Receptor |
| S7641 | Remodelin | Epigenetics | Histone Acetyltransferase |
| S7642 | D 4476 | Metabolism | Casein Kinase |
| S7644 | PF-431396 | Angiogenesis | FAK |
| S7645 | Pilaralisib (XL147) | PI3K/Akt/mTOR | PI3K |
| S7650 | Peficitinb (ASP015K, JNJ-54781532) | JAK/STAT | JAK |
| S7653 | PND-1186 (VS-4718) | Angiogenesis | FAK |
| S7654 | Defactinib (VS-6063, PF-04554878) | Angiogenesis | FAK |
| S7655 | CB-839 | Others | Others |
| S7656 | CPI-360 | Epigenetics | Histone Methyltransferase |
| S7664 | GSK2578215A | Autophagy | LRRK2 |

| | | | |
|---|---|---|---|
| S7665 | CH5183284 (Debio-1347) | Angiogenesis | FGFR |
| S7667 | SU5402 | Protein Tyrosine Kinase | FGFR,VEGFR |
| S7668 | Picropodophyllin (PPP) | Protein Tyrosine Kinase | IGF-1R |
| S7669 | NPS-1034 | Protein Tyrosine Kinase | TAM Receptor,c-Met |
| S7672 | Omaveloxolone (RTA-408) | Others | Others |
| S7673 | L-685,458 | Neuronal Signaling | Gamma-secretase |
| S7675 | PF-4989216 | PI3K/Akt/mTOR | PI3K |
| S7678 | LCZ696 | Endocrinology & Hormones | RAAS |
| S7679 | YK-4-279 | Cell Cycle | DNA/RNA Synthesis |
| S7680 | SP2509 | Epigenetics | Histone Demethylase |
| S7681 | OF-1 | Epigenetics | Epigenetic Reader Domain |
| S7685 | SecinH3 | Others | hCyh,drosophila steppke,yGea2-S7 |
| S7686 | ML141 | Cell Cycle | Rho |
| S7689 | BG45 | DNA Damage | HDAC |
| S7693 | AZD6738 | PI3K/Akt/mTOR | ATM/ATR |
| S7694 | AZD8186 | PI3K/Akt/mTOR | PI3K |
| S7697 | LY2409881 | NF-κB | IκB/IKK |
| S7699 | Liproxstatin-1 | Metabolism | Ferroptosis |
| S7704 | LY2584702 Tosylate | PI3K/Akt/mTOR | S6 Kinase |
| S7707 | Verdinexor (KPT-335) | Transmembrane Transporters | CRM1 |
| S7714 | FIIN-2 | Protein Tyrosine Kinase | FGFR |
| S7718 | BMH-21 | DNA Damage | DNA/RNA Synthesis |
| S7719 | CCG-1423 | Cell Cycle | Rho |
| S7720 | SBE 13 HCl | Cell Cycle | PLK |
| S7722 | Bikinin | PI3K/Akt/mTOR | GSK-3 |
| S7725 | BLZ945 | Protein Tyrosine Kinase | CSF-1R |
| S7726 | BRD73954 | DNA Damage | HDAC |
| S7730 | NU1025 | DNA Damage | PARP |
| S7731 | AZD3839 | Neuronal Signaling | BACE |
| S7734 | LFM-A13 | Angiogenesis | BTK |
| S7741 | SB239063 | MAPK | p38 MAPK |
| S7742 | SCR7 | DNA Damage | DNA/RNA Synthesis |
| S7747 | Ro-3306 | Cell Cycle | CDK |
| S7748 | EPZ015666 | Epigenetics | Histone Methyltransferase |
| S7750 | KNK437 | Cell Cycle | HSP (e.g. HSP90) |
| S7751 | VER155008 | Cytoskeletal Signaling | HSP (e.g. HSP90) |
| S7753 | BPTES | Others | Others |
| S7765 | Dovitinib (TKI258) Lactate | Angiogenesis | FGFR,VEGFR,c-Kit,PDGFR,FLT3 |
| S7766 | Cabotegravir (GSK744, GSK1265744) | Microbiology | Integrase |
| S7771 | STF-083010 | Others | Others |
| S7772 | Elacridar (GF120918) | Transmembrane Transporters | P-gp |
| S7774 | SU6656 | Angiogenesis | Src |
| S7776 | Akti-1/2 | PI3K/Akt/mTOR | Akt |
| S7781 | Sunitinib | Protein Tyrosine Kinase | VEGFR,PDGFR,c-Kit |
| S7783 | Combretastatin A4 | Cytoskeletal Signaling | Microtubule Associated |
| S7786 | Erlotinib | Protein Tyrosine Kinase | EGFR |
| S7787 | Docetaxel Trihydrate | Cytoskeletal Signaling | Microtubule Associated |
| S7790 | A-1210477 | Apoptosis | Bcl-2 |
| S7793 | Purvalanol A | Cell Cycle | CDK |
| S7795 | ORY-1001 (RG-6016) | Epigenetics | Histone Demethylase |
| S7798 | GNE-317 | PI3K/Akt/mTOR | PI3K |
| S7799 | Pexmetinib (ARRY-614) | MAPK | Tie-2,p38 MAPK |
| S7804 | GSK503 | Epigenetics | Histone Methyltransferase |
| S7808 | AT7519 HCl | Cell Cycle | CDK |
| S7810 | Afatinib (BIBW2992) Dimaleate | Protein Tyrosine Kinase | HER2,EGFR |
| S7811 | MHY1485 | PI3K/Akt/mTOR | mTOR,Autophagy |
| S7813 | AMG319 | PI3K/Akt/mTOR | PI3K |
| S7818 | Pexidartinib (PLX3397) | Protein Tyrosine Kinase | CSF-1R,c-Kit |
| S7819 | BLU9931 | Angiogenesis | FGFR |
| S7834 | Cyclo (-RGDfK) | Cytoskeletal Signaling | Integrin |
| S7840 | Dorsomorphin (Compound C) | PI3K/Akt/mTOR | AMPK |
| S7842 | LY3009120 | MAPK | Raf |
| S7843 | BI-847325 | MAPK | MEK,Aurora Kinase |
| S7844 | Cyclo(RGDyK) | Cytoskeletal Signaling | Integrin |
| S7845 | SirReal2 | Epigenetics | Sirtuin |
| S7846 | TP-0903 | Protein Tyrosine Kinase | TAM Receptor |
| S7851 | AZD3264 | NF-κB | IκB/IKK |
| S7854 | Ulixertinib (BVD-523, VRT752271) | MAPK | ERK |
| S7856 | Tenofovir Alafenamide (GS-7340) | Microbiology | Reverse Transcriptase |
| S7863 | SC79 | PI3K/Akt/mTOR | Akt |
| S7877 | ONO-4059 | Angiogenesis | BTK |
| S7884 | AMI-1 | Epigenetics | Histone Methyltransferase |
| S7885 | SBI-0206965 | Autophagy | Autophagy |
| S7888 | Spautin-1 | Autophagy | Autophagy |
| S7889 | Xanthohumol | Metabolism | COX |
| S7906 | PFI-4 | Epigenetics | Epigenetic Reader Domain |

| | | | |
|---|---|---|---|
| S7910 | Epacadostat (INCB024360) | Metabolism | IDO |
| S7912 | PD-1/PD-L1 inhibitor 2 | Apoptosis | PD-1/PD-L1 |
| S7915 | BIO-acetoxime | PI3K/Akt/mTOR | GSK-3 |
| S7918 | Bromodeoxyuridine (BrdU) | DNA Damage | DNA/RNA Synthesis |
| S7921 | DEL-22379 | MAPK | ERK |
| S7922 | Tiplaxtinin (PAI-039) | Others | Others |
| S7931 | STF-31 | Others | Others |
| S7933 | VR23 | Proteases | Proteasome |
| S7946 | KC7F2 | Angiogenesis | HIF |
| S7963 | TIC10 | PI3K/Akt/mTOR | Akt |
| S7975 | Favipiravir (T-705) | DNA Damage | DNA/RNA Synthesis |
| S7998 | Entrectinib (RXDX-101) | Protein Tyrosine Kinase | ALK,Trk receptor |
| S8000 | Tenovin-1 | Apoptosis | E3 Ligase ,p53 |
| S8001 | Rocilinostat (ACY-1215) | Epigenetics | HDAC |
| S8002 | GSK2636771 | PI3K/Akt/mTOR | PI3K |
| S8003 | PQ 401 | Protein Tyrosine Kinase | IGF-1R |
| S8004 | ZM 39923 HCl | JAK/STAT | JAK |
| S8005 | SMI-4a | JAK/STAT | Pim |
| S8006 | BIX 01294 | Epigenetics | Histone Methyltransferase |
| S8007 | VE-821 | DNA Damage | ATM/ATR |
| S8009 | AG-18 | Protein Tyrosine Kinase | EGFR |
| S8010 | PRX-08066 Maleic acid | Neuronal Signaling | 5-HT Receptor |
| S8011 | U73122 | Metabolism | Phospholipase (e.g. PLA) |
| S8014 | GW9508 | Endocrinology & Hormones | GPR |
| S8015 | CEP-32496 | MAPK | CSF-1R,Raf |
| S8016 | TAK-438 | Transmembrane Transporters | Potassium Channel |
| S8018 | PF-03084014 (PF-3084014) | Neuronal Signaling | Gamma-secretase |
| S8019 | AZD5363 | PI3K/Akt/mTOR | Akt |
| S8020 | GW0742 | Metabolism | PPAR |
| S8021 | Vortioxetine (Lu AA21004) HBr | Neuronal Signaling | 5-HT Receptor |
| S8022 | Empagliflozin (BI 10773) | GPCR & G Protein | SGLT |
| S8023 | TCS 359 | Angiogenesis | FLT3 |
| S8024 | Tyrphostin AG 1296 | Protein Tyrosine Kinase | PDGFR,FGFR,c-Kit |
| S8025 | GSK3787 | Metabolism | PPAR |
| S8028 | Tariquidar | Transmembrane Transporters | P-gp |
| S8029 | WY-14643 (Pirinixic Acid) | Metabolism | PPAR |
| S8031 | NSC 23766 | Cell Cycle | Rho |
| S8032 | PRT062607 (P505-15, BIIB057) HCl | Angiogenesis | Syk |
| S8034 | Apremilast (CC-10004) | Metabolism | PDE |
| S8035 | VU 0364439 | Neuronal Signaling | GluR |
| S8036 | Butein | Protein Tyrosine Kinase | EGFR |
| S8037 | Necrostatin-1 | Apoptosis | TNF-alpha |
| S8038 | UPF 1069 | DNA Damage | PARP |
| S8039 | PU-H71 | Cytoskeletal Signaling | HSP (e.g. HSP90) |
| S8040 | GDC-0349 | PI3K/Akt/mTOR | mTOR |
| S8041 | Cobimetinib (GDC-0973, RG7420) | MAPK | MEK |
| S8042 | GW2580 | Protein Tyrosine Kinase | CSF-1R |
| S8043 | Scriptaid | DNA Damage | HDAC |
| S8044 | BMS-345541 | NF-κB | IκB/IKK |
| S8047 | Dynasore | Others | Dynamin |
| S8048 | ABT-199 (GDC-0199) | Apoptosis | Bcl-2 |
| S8049 | Tubastatin A | Epigenetics | HDAC |
| S8050 | ETP-46464 | PI3K/Akt/mTOR | ATM/ATR,mTOR |
| S8051 | Macitentan | GPCR & G Protein | Endothelin Receptor |
| S8056 | Lomeguatrib | Epigenetics | DNA Methyltransferase |
| S8057 | Pacritinib (SB1518) | JAK/STAT | FLT3,JAK |
| S8058 | P276-00 | Cell Cycle | CDK |
| S8059 | Nutlin-3a | Apoptosis | Mdm2 |
| S8065 | Nutlin-3b | Apoptosis | Mdm2 |
| S8072 | NSC 405020 | Proteases | MMP |
| S8073 | Optovin | Others | Others |
| S8076 | PluriSIn #1 (NSC 14613) | Metabolism | Dehydrogenase |
| S8103 | Sotagliflozin (LX4211) | GPCR & G Protein | SGLT |